Alireza Azmoudeh-Ardalan

High Resolution Regional Geoid Computation
in The World Geodetic Datum 2000

based upon collocation of
linearized observational functionals of the type GPS,
gravity potential and gravity intensity

Dissertationen

High Resolution Regional Geoid Computation in The World Geodetic Datum 2000 based upon collocation of linearized observational functionals of the type GPS, gravity potential and gravity intensity

Von der Fakultät für
Bauingenieur- und Vermessungswessen
der Universität Stuttgart
zur Erlangung der Würde eines
Doktor-Ingenieurs (Dr. –Ing.)
genehmigte Abhandlung

vorgelegt von

M. Sc. Alireza Azmoudeh-Ardalan

aus Tehran/Iran

November 99

Hauptberichter: o. Prof. Dr.-Ing. habil, Dr. tech. h.c. mult., Dr.-Ing. E.h. mult E.W. Grafarend

Mitberichter: o. Prof. Dr.-Ing. D. Fritsch
o. Prof. Dr.-Ing. E. Groten

Tag der mündlichen Prüfung: 29.02.2000

ISBN: 3-00-006457-5

Abstract

New methods for high-resolution regional geoid and quasi-geoid determination based on ellipsoidal approximation in geometry and gravity space are developed and tested.

Deterministic collocation of linearized observational functionals of type *(i)* gravity potential and *(ii)* gravity intensity at GPS positioned stations is used to compute a high resolution regional *Gauss-Listing Geoid* as well as *Molodensky Quasi-Geoid*. The *Gauss-Listing Geoid* is solved via fixed-free two-boundary value problem of *Physical Geodesy*. The solution technique produces a harmonic incremental potential field by means of *remove-restore methodology* for the centrifugal potential, for the topographic masses (terrain effect), and for the higher order (degree/order 360/360) ellipsoidal harmonic expansion. The incremental (or reduced) observational functionals of type (i) and (ii) are downward continued by means of a *Tikhonov-Phillips* regularised inversion of the *ellipsoidal Abel-Poisson integral*. The downward continued incremental potential data on the surface of the *International Reference Ellipsoid* $\mathbb{E}^2_{a,b}$ – the *World Geodetic Datum 2000* – are converted into geoidal undulations by means of the nonlinear, ellipsoidal *Bruns transform* (*Bruns formula*). The innovative method is tested numerically by presenting a high resolution regional geoid for the *State of Baden-Württemberg* /Germany/ and is compared to *European Gravimetric Quasi-Geoid 97* (*EGG97*). The advantages of the new methodology for high resolution geoid computation are as follows: (i) a higher order ellipsoidal reference potential field with respect to the *World Geodetic Datum 2000* is implemented avoiding any datum bias with respect to the traditional spherical approach, (ii) in contrast to the *Stokes boundary value problem* incremental potential data (gravimetric levelling) as well as incremental gravity data (National Gravity Survey) given on the (GPS) topographic surface of the Earth are directly converted via regularised downward continuation *to* the incremental potential on the *International Reference Ellipsoid* $\mathbb{E}^2_{a,b}$.

The problem of global geoid computation is presented as an application of the soft *Implicit Function Theorem*: *Given* the level datum of the geoid $W_0 = U_0(\lambda, \phi, u)$ with respect to (i) a reference gravitational potential $U(\lambda, \phi, u)$ at level datum U_0 *and* (ii) spheroidal / ellipsoidal coordinates of type {longitude λ, latitude ϕ, “height u”}, we solve for $u = u(\lambda, \phi, W_0)$

as a representative of the *shape of the geoid* with respect to the reference ellipsoid / *World Geodetic Datum 2000*. The analysis is based on a set of coefficients ("spheroidal moments") of a spheroidal / ellipsoidal harmonic expansion of the terrestrial gravity potential up to degree/order 360/360. Wavelength signatures of the order of 50-60 km are resolved, sufficient for a global geoid representation. A numerical evaluation of the spheroidal geoid computation based upon the s*pheroidal Bruns formula*, namely for 23 benchmarks of the *Baltic Level Project*, has documented a level of accuracy of the order of $\pm 0.18cm$.

Minimum-distance mapping is applied to determine a potential type *Molodensky telluroid* and *Quasi-Geoid*. With respect to a *reference potential* field of *Somigliana-Pizzetti type* which relates to the *World Geodetic Datum 2000* it is shown that a point-wise minimum distance mapping of the topographical surface of the Earth onto the telluroid surface, constrained to the *gauge* $W(P) = u(p)$, leads to a system of four nonlinear normal equations. Those normal equations are solved by a fast *Newton-Raphson* iteration. The method is tested numerically by presenting the quasi-geoid for the *East Germany* and the *State of Baden-Württemberg* /Germany/ which are compared to *European Gravimetric Quasi-Geoid 97* (*EGG97*).

Acknowledgements

This dissertation has been prepared in the Department of Geodesy and GeoInformatics, University of Stuttgart, Germany. The financial support by the *Ministry of Culture and Higher Education of Iran*, in terms of a scholarship to study at the Department of Geodesy and GeoInformatics of the University of Stuttgart is gratefully acknowledged.

I wish to express my sincere thanks to my supervisor *Herr o.Prof. Dr. –Ing. habil. Dr. tech. h.c. mult. Dr.-Ing. E.h. Erik W. Grafarend* without whose permanent support and guidance this work would have never succeeded. His overall guidance in the research work, readiness for discussion, and encouragement are highly acknowledged.

Herr o.Prof. Dr. –Ing. habil D. Fritsch, and *Herr Professor Dr.-Ing. E. Groten* are highly acknowledged for their interest in reviewing the Ph.D. thesis and their constructive comments.

I would like to thank *Herr Professor Dr.-Ing. W. Keller* and *Herr Professor Dr.-Ing. A. Kleusberg* for their scientific supports and readiness for discussion.

Special thanks to *Herr Dr.-Ing Friedhelm Krumm* whose door was always open to help with various academic problems.

My gratitude is awarded to *Herr Dr.-Ing Johannes Engels*, who was always whole heartedly ready for discussions and giving constructive guidelines.

I would like to express my sincere thanks to the entire members of Institute of Geodesy and GeoInformatics of the University of Stuttgart, for their friendship and support, which inspired my study.

Last, but not least, I wish to acknowledge the patience, understanding, and love of my wife *Dr. Effat Shohadaei*, my daughter *Parisa A. Ardalan*, and my parents *Yalollah A. Ardalan* and *Vahideh Ghiasi*.

Contents

List of Notations

Symbols	Definition
$\mathbb{M}_e^2$	2-dimensional Riemannian manifold of the earth surface
$\mathbb{M}_g^2$	2-dimensional Riemannian manifold of the geoid surface
$\cdot / \cdot$	Difference
ω	Angular velocity of the earth
$\partial\mathcal{G}_e^-$	Approach to the Earth surface from inside
$\partial\mathcal{G}_e^+$	Approach to the Earth surface from the outside
$\mathcal{D}$	Domain of the massive Earth
$\langle \cdot \mid \cdot \rangle$	Inner or scalar product operator
$\rho(\mathbf{x})$	Mass density of the earth
gm	Product of Newton gravitational constant and mass of the Earth
$\Vert \cdot \Vert$	Norm operator
$\mathbf{x}$	Placement/Position vector of a point on the physical surface of the earth or geoid
$\mathbf{X}$	Placement/Position vector of a point on the surface of reference ellipsoid or telluroid
$\mathcal{D} \cup \partial\mathcal{G}_e^-$	Surface of the Earth and domain of the massive Earth (approach to the surface from inside)
$\mathcal{D} \cup \partial\mathcal{G}_e^+$	Surface of the Earth and the domain of the massive Earth (approach to surface from outside)
CAPITAL LETTERS	Reference quantities
lower case letters	Actual quantities
$\wedge$	And
$\cup$	Union
$\varepsilon = \sqrt{a^2 - b^2}$	Linear eccentricity
a	Semi-major axis of reference ellipsoid
b	Semi-minor axis of reference ellipsoid
w_0	geoid's potential
$D_u U$	Partial derivative of U with respect to u
$\nabla_{\mathbf{e}_u} U$	Directional derivative of U along the unit normal vector $\mathbf{e}_u$

0 Introduction

Geoid as a particular *level surface* (*equipotential surface*) of the gravity field of the earth, which fits to the surface of the oceans in an *optimum* way, has been the centre of interest in geodesy for decades. *C. Gauss* was first who introduced the aforementioned definition in 1828 as the *mathematical surface of the earth*. In his famous historical publication (*C. Gauss*, 1828 p. 49) he writes:

> "What we call in the geometric sense the surface of the earth is nothing else but that surface which intersects the direction of gravity at right angles and from which the surface of the world's ocean is a part."

J. Listing in 1872 introduced the term *geoid* to the *mathematical surface of the earth* in *C. Gauss's* terminology. He wrote (*J. Listing* 1873 p.45):

> "We shall call the previously defined mathematical surface of the earth, of which the ocean surface is a part, <u>geoidal surface</u> of the earth or the <u>geoid</u>"

Here we remain faithful to the definition of geoid according to *C. Gauss* and *J. Listing*. Let us explain the term "optimum fit to the oceans surface" in the definition of geoid. In practice by the "optimum fit to the oceans surface" we mean that the average separation between geoid and mean oceans surface is zero.

If w_0 be the *actual gravity potential* at the geoid's surface, then in terms of *Cartesian coordinates* (x,y,z), geoid can be defined as the lattice of points for which the following formula holds

$$w(x,y,z) = w_0. \tag{0.1}$$

However in practice instead of Cartesian coordinates, geoid is presented in terms of surface normal heights of a reference equipotential surface which can be derived by gauging a reference potential to the geoid potential value w_0. As is shown in *Figure 0-1* the minimum distance mapping of the geoid onto the surface of reference equipotential surface can be established via the *Bruns formula*. Having selected a reference gravity field and determined the incremental potential $\delta W(\mathbf{X}) = w_0 - w(\mathbf{X})$ (geoid's potential w_0 minus actual potential $w(\mathbf{X})$ at the reference equipotential surface) Bruns *formula* provides us with transformation equation of the incremental potential $\delta W(\mathbf{X})$ in gravity space, into surface normal heights h, in geometry space. For example, if we select a reference field of *Somigliana-Pizzetti* type, then we will end up with an ellipsoid of revolution as the reference equipotential surface, e.g. *International Reference Ellipsoid WGD2000* (*E. Grafarend and A. Ardalan* 1999) (see Box 0-1 and *Figure*

0-2) and the Bruns formula as introduced in *Box 0-2* provides us with minimum distance mapping of geoid onto the surface of reference ellipsoid $\mathbb{E}^2_{a,b}$ of WGD2000.

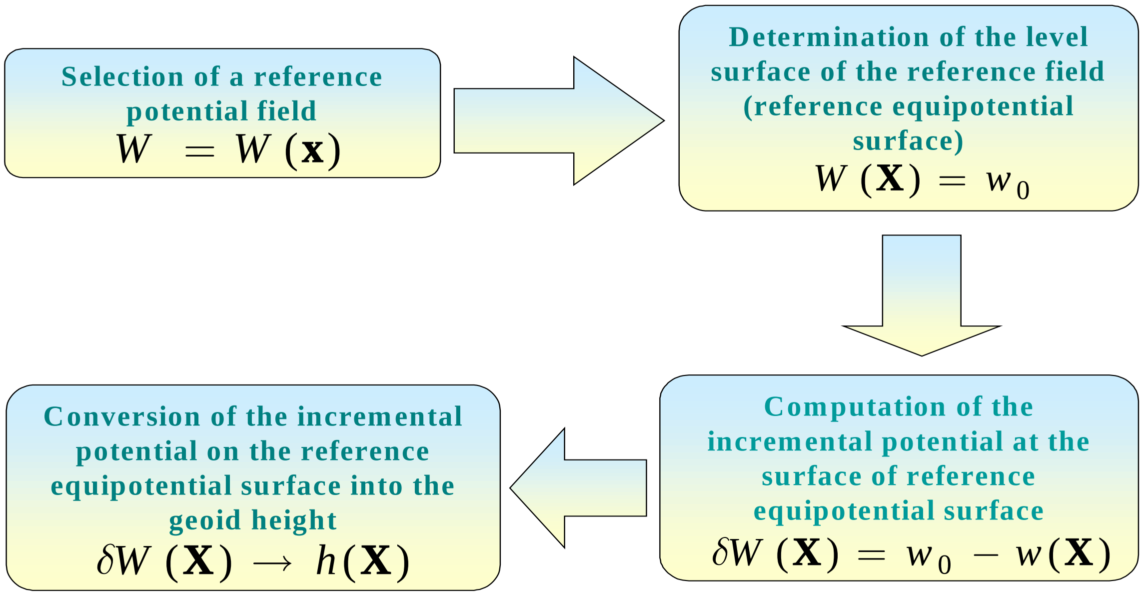

Figure 0-1: The steps of geoid computation at-large.

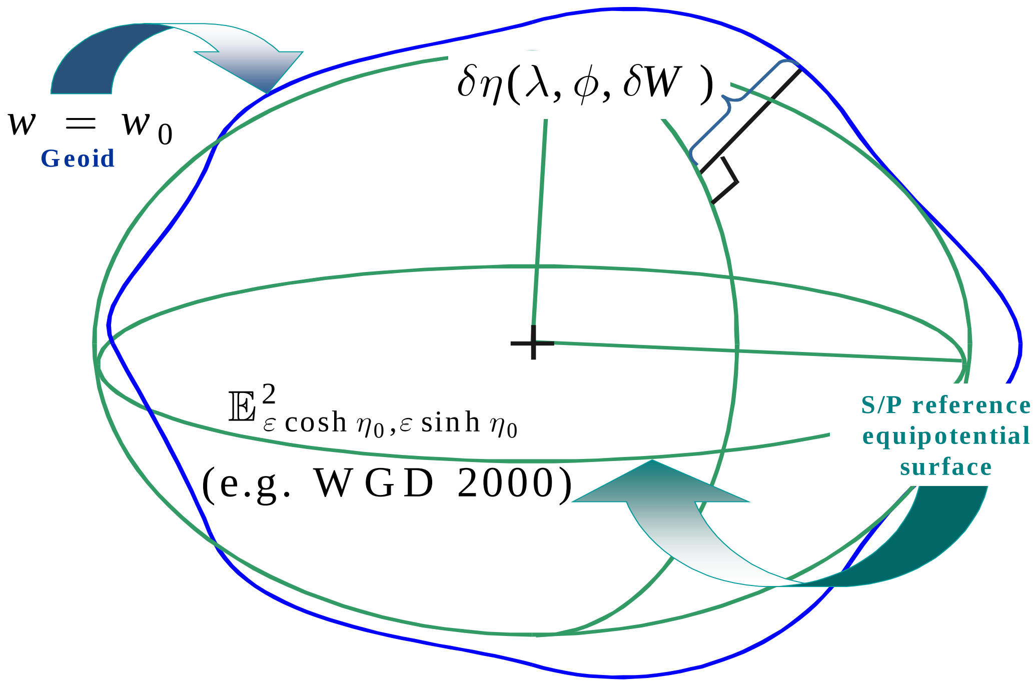

Figure 0-2: minimum distance mapping of the geoid onto the reference equipotential surface of the ellipsoidal type.

Box 0-1: Minimum-distance mapping of the geoid onto the reference equipotential surface of Somigliana-Pizzetti type (e.g. WGD2000).

- **Reference potential field**

$$W(\phi,\eta) = \frac{GM}{\varepsilon}\operatorname{arc\,cot}(\sinh\eta)$$
$$+\frac{1}{6}\Omega^2 a^2 \frac{(3\sinh^2\eta + 1)\operatorname{arc\,cot}(\sinh\eta) - 3\sinh\eta}{(3\sinh^2\eta_0 + 1)\operatorname{arc\,cot}(\sinh\eta_0) - 3\sinh\eta_0}(3\sin^2\phi - 1)$$
$$+\frac{1}{2}\Omega^2(u^2+\varepsilon^2)\cos^2\phi$$

- **Level surface of the reference potential field (*reference equipotential surface*)**

$$W(\phi,\eta) = w_0 \Rightarrow \mathbb{E}^2_{\varepsilon\cosh\eta_0,\varepsilon\sinh\eta_0} \quad \text{(e.g. WGD 2000)}$$

- **Incremental potential on surface of *reference equipotential surface***

$$\delta W(\Lambda,\Phi,\eta=\eta_0) = w_0 - w(\Lambda,\Phi,\eta=\eta_0)$$

- **Bruns formula**

$$\delta W(\Lambda,\Phi,\eta=\eta_0) \xrightarrow{\text{Bruns Formula}} \delta\eta(\Lambda,\Phi,w_0)$$

Minimum Distance Mapping of the *geoid* onto the *reference equipotential surface*

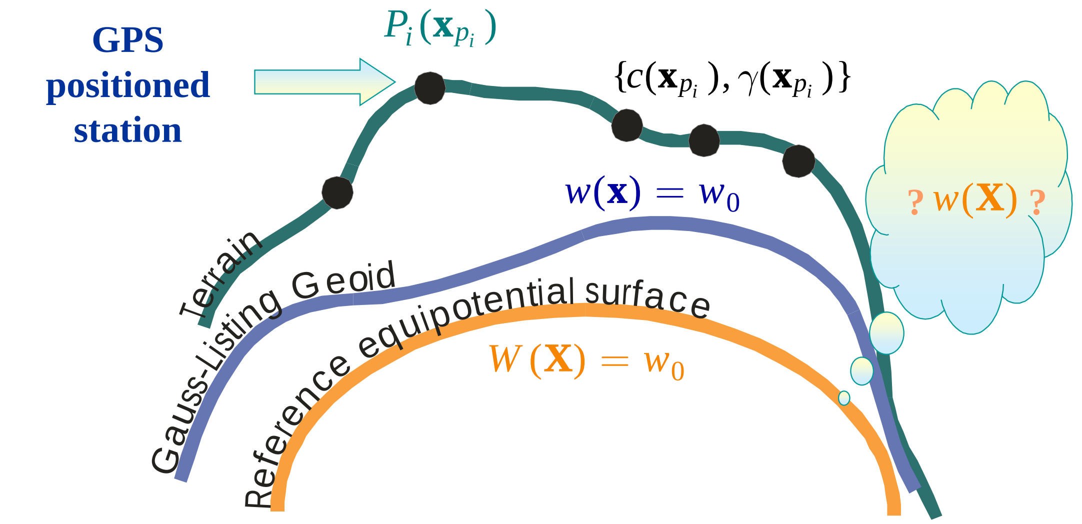

Figure 0-3: The required gravity potential $w(\mathbf{X})$ on the surface of the reference equipotential surface versus the observations of the type geopotential numbers $c(\mathbf{x}_{p_i})$, and gravity intensity $\gamma(\mathbf{x}_{p_i})$ at GPS positioned stations on the surface of the earth.

Box 0-2: Bruns formula as the transformation relation between geometry and gravity space.

- **Expand geoid's potential into Taylor series.**

$$w_0 = w(\mathbf{x}) = w(\mathbf{X}) + \frac{1}{1!}(\nabla_N w(\mathbf{X}))h + \frac{1}{2!}(\nabla_N \nabla_N w(\mathbf{X}))h^2 + \mathcal{O}_W(h^3)$$

$$\delta W(\mathbf{X}) = W(X) - w(\mathbf{X}) = \frac{1}{1!}(\nabla_N w(\mathbf{X}))h + \frac{1}{2!}(\nabla_N \nabla_N w(\mathbf{X}))h^2 + \mathcal{O}_W(h^3)$$

$$= \sum_{n=0}^{\infty} a_{1n} h^n$$

Hom. Pol.

- **Solve for "h" through series inversion**

$$h = \sum_{n=0}^{\infty} b_{1n} \delta W^n$$

Bruns Formula

- **For example if we assume** $w(\mathbf{X}) = \frac{GM}{\varepsilon} \operatorname{arc}\cot(\sinh\eta)$ **then**

$$h = \delta W(\mathbf{X}) \frac{\varepsilon^2 \cosh\eta(\cosh^2\eta - \cos^2\phi)^{1/2}}{gm} - (\delta W(\mathbf{X}))^2 \left(\frac{\varepsilon^2 \cosh\eta(\cosh^2\eta - \cos^2\phi)^{1/2}}{gm}\right)^3$$

$$\times\left(\frac{1}{2} gm \frac{\sinh\eta\left(2\cosh^2\eta - \cos^2\phi\right)}{\varepsilon^3 \cosh^2\eta(\cosh^2\eta - \cos^2\phi)^2}\right) + \mathcal{O}(\delta W(\mathbf{X})^3)$$

However, as shown in *Figure 0-3*, the geoid and its best fitting ellipsoid (e.g. *WGD2000*) is partially within the earth and as such is not accessible to direct potential observations. Therefore, we have to determine the required potential on the surface of reference equipotential surface, as the solution of a boundary value problem. The common gravity observables of the boundary value problems of the geoid determination are:

(i) *Gravity potential* (or zero order derivative of the gravity potential) measured by means of gravimetric levelling (*E. Groten*, 1979)

(ii) *Modulus of gravity intensity* (or vertical derivative of the gravity potential) measured by means of relative or absolute gravimetry (*E. Groten*, 1984)

(iii) Components of deflection of vertical (horizontal derivatives of the gravity potential) measured by means of astrogeodetic or GPS-LPS levelling (*E. Grafarend*, 1988a, 1991)

(iv) Higher order derivatives of gravity potential, measured via gradiometry

Besides the above listed observables, any geodetic observation can be used as an information source of the gravity field of the earth. Since all the geodetic observations are made under the influence of the earth gravity field, they are in one way or the another related to gravity field of the earth. *E. Grafarend* (1980) has shown that all the geodetic observation equations can be equivalently set up in geometry or gravity space.

Any measured gravity field quantity must always be accompanied with position and time information. In other words, we must know where in 3-D space and at which time the gravity observation has been made. The time information is necessary since the gravity field of the earth is a function of time. Especially, due to of gravitational force of external celestial bodies, deformation of the earth, and the movement of the interior masses of the earth. The required accuracy for the positional of the gravity stations depends on the accuracy or resolution of the gravity observation itself. If 0.1mGal (1 milli-Gal is equal to $10^{-5} m^2/s^2$) be the average resolution of the currently available gravity data, then one readily can determine that 100m horizontal movement in geometry space can hardly produce a variation more than 0.1mGal in gravity space. It is even true for the most mountainous areas! In contrast, 0.1mGal change in gravity space is equivalent to 0.3m movement in vertical direction. Therefore, if we consider 0.1mGal as the accuracy of the currently available gravity data, the horizontal position of the gravity stations must be given to a few meters accuracy. However, the height component should be accurate to a few centimetres to meet the same accuracy level in the gravity space. *F. Sansó* (1995) has a complete review on accuracy requirements in the boundary value problems of the geoid determination.

The boundary value problems for geoid determination can be classified according to:

(i) Type of the input data

- Classical or Stokes boundary value problem, where the modulus of the gravity intensity vector on the boundary (earth's surface $\mathbb{M}_h^2$), as well as the orthometric heights of the points on $\mathbb{M}_h^2$ are given.
- Non-Classical, where other sources of data are given.

(ii) Redundancy of the data

- Over-determined boundary value problem, where the input data are more than the minimum necessary.
- Just determined, where exactly the minimum necessary amount of data and/or conditions to solve the boundary value problem are available.

(iii) The boundary on which the input gravity data are given

- Fixed boundary-value problem, where the gravity data are given on a known surface of the earth.
- Free boundary-value problem where the gravity data are given on a surface which we are searching for (say the geoid $\mathbb{M}_g^2$).
- Weakly known, where the estimated position vector of the boundary $\mathbf{x}$ and its corresponding variance-covariance matrix $\boldsymbol{\Sigma}_x$ are known.

(iv) The resolution of the solution

- Global, with about 50-100km resolution, determined based on spherical/ellipsoidal harmonic expansion of the gravity field of the earth.
- Marine geoid, nowadays with maximum resolution of 6km, based on satellite altimetry (see for example *D. Chambers*, 1998).
- Continental geoid, with accuracy demand of decimetre, based on the gravimetric boundary value problems, the geopotential models, and the Digital Terrain Models (DTM's).

- Local/regional geoid, with highest accuracy, nowadays centimetre accuracy level is the target, to specifically support the GPS derived heights in order to compute orthometric heights (*H. Euler et al.*, 1986, *T. Kling et al.*, 1987, *E. Groten*, 1996).

If instead of the surface of the earth we stick to the *telluroid* and instead of geoid to *quasi-geoid* then, we are walking in the realm of *Molodensky boundary value problem*, where the modulus of gravitational intensity vector and the gravitational potential on the *telluroid* $\mathbb{M}^2_H$ are given.

Here, for our boundary value problem, we assume that the gravity observables of the type *modulus of gravity intensity* $\gamma(\mathbf{x})$, and *gravity potential* $w(\mathbf{x})$ are given on the known surface of the earth, e.g., positioned by GPS observations. These observables build up the data on the fixed boundary. Whereas, geoid's potential w_0 provides the boundary data on the geoid, which is geometrically unknown (the free boundary). The two-boundary value problem for the observable of the kind *modulus of gravity intensity* has already been studied by *E. Grafarend and F. Sansó* (1984), *M. Mihelcic* (1972) and recently by *Z. Martinec* (1998a). Here in contrast to the previous studies, we present the fixed free two-boundary value problem for two types of observables, namely, *modulus of gravity intensity* $\gamma(\mathbf{x})$ and *gravity potential* $w(\mathbf{x})$, both given on the outer boundary. Consequently, we are left with an over-determined boundary value problem.

The highlight of our approach is ellipsoidal approximation, which is maintained throughout the computations. It has been revealed by the great early 18th century expeditions that the earth is *not* geometrically a sphere, but nearly an oblate ellipsoid-of-revolution $\mathbb{E}^2_{a,b}$. Historical review of the progress in the determination of the shape of the earth is well documented in *J. Kakkuri et al.* (1986), *J. Smith* (1986, 1987) and *E. Tobé* (1986) *J. L. Greenberg* (1995). Due to the closeness of the figure of the earth to an oblate ellipsoid-of-revolution, gravity field of the type *Somigliana-Pizzetti*, developed separately by *P. Pizzetti* (1894) and *C. Somigliana* (1930) and extensively analysed by *E. Grafarend et al.* (1977) and recently, by *E. Grafarend and A. Ardalan* (1999a, 1999b), has been introduced as the standard gravity field in the Geodesist's Handbook 2000 (edited by *H. Moritz*, 2000). Here for completeness let us also mention the *World Geodetic Datum* developed by *B. Eitschberger and E. Grafarend* (1974), and *World Geodetic Datum 2000* developed by *E. Grafarend and A. Ardalan* (1999a, 1999b), which are based on the gravity field of the *Somigliana-Pizzetti* type. Therefore, in order to be close to the earth's reality, both in geometry and gravity spaces, we shall use a reference ellipsoidal gravity field, and remain at the level of ellipsoidal approximation for all computations.

The reference / normal gravity field plays an important role in the set up of a boundary value problem. The reference gravity field contains the modelled part of the gravity field of the earth. The reference gravity field is normally used to remove the major known part of the gravity signal from the gravity observations. If the modelled gravity be close to the *actual* gravity field it can remove the high frequency part of the signal and make the remaining *incremental* part fairly smooth. Which is the needed property for the linearization of a non-linear boundary value problem.

The boundary value problems, which are based on the *Laplace* partial differential equation, all require harmonic data on the boundary. A proper choice of the reference field beside the smoothing role can be a tool to produce the surface *incremental* quantities which are harmonic on the surface of the earth, and down to the geoid's surface (usually approximated by reference ellipsoid $\mathbb{E}^2_{a,b}$). This property is injected in to our solution, by considering a high degree/order reference field and including the terrain correction, which corrects for the remaining high frequency part of the signal, emitted from the local topographic masses.

0.1 Objectives of the Study

The goal of this work is to study the local high-resolution geoid determination with the support of GPS positions, gravity, and potential data. As the by-products of the study, methods for geoid determination with global details as well as quasi-geoid determination with support of GPS observations will be presented.

Improvements in the accuracy of the gravity observation and positioning, thanks to GPS, demand the revision of geoid determination techniques. Especially to provide theories compatible with accuracy of the modern observations. It is now a clear fact that the classical geoid-determination based on spherical approximations cannot produce the required accuracy demanded by observations / input data. As a contribution towards the refinement of the theory of geoid determination, we will present methodologies for (i) local/ regional high-resolution geoid computation, (ii) global geoid computation, and (iii) quasi-geoid determination, all at the level of *ellipsoidal approximation*. The feasibility of the derived methods is also verified by numerical studies. The methods that will be presented are comprised of

(i) *Fixed-free two-boundary value problem* based on ellipsoidal approximation as a contribution towards high-resolution local geoid determination.

(ii) Application of global geopotential models and n*on-linear ellipsoidal Bruns formula*, as the realisation of soft implicit-function theorem, for geoid determination with global details.

(iii) *Minimum distance mapping* of the physical surface of the earth into the *Molodensky telluroid*, as the fast and accurate technique for quasi-geoid determination with support of GPS positions.

Let us now briefly highlight the main features of the first technique, which is the *heart* of this study. The fixed-free two-boundary value problem in ellipsoidal approximation is a boundary value problem tailored to the gravity observables of the type *modulus of gravity intensity* $\gamma(\mathbf{x})$ (from gravimetry) and *gravity potential* $w(\mathbf{x})$ or *geopotential numbers* $c(\mathbf{x})$ (from precise levelling), both with GPS derived positions. These observables satisfy the *non-linear Poisson equation*. By taking advantage of a *normal / reference gravity field*, the surface gravity observations can be converted into *disturbing* quantities of the kind $\delta\gamma(\mathbf{x})$ and $\delta w(\mathbf{x})$.

By a proper choice of *reference* gravity field, which synthesises the *actual* gravity field of the earth very closely, the *Laplace-Poisson equation* for the *disturbing* quantities can be linearized in *gravity* space. In summary, the linearization process leads to "*linearized fixed-free two-boundary value problem*". Our choice of reference field is ellipsoidal eigenvalue/eigenfunction expansion of the external gravity field of the Earth up to degree/order 360/360.

To remain as close as possible to the *actual* geometry of the Earth, which in global sense resembles an *oblate spheroid /ellipsoid of revolution,* we have chosen *ellipsoidal coordinates* and *ellipsoidal Laplace-Poisson equation*. In other words, we are using *ellipsoidal fixed-free two-boundary value problem* to tackle the problem of local high-resolution geoid determination.

By eliminating the effect of *topographical masses* between the surface of the earth and the reference ellipsoid, we will be left with disturbing quantities which are harmonic at the surface of the earth down to the level of reference ellipsoid. This process can be referred to as "*terrain reduction*". Indeed, in the global sense the *Newton Potential* generated by topographical masses has to be computed in ellipsoidal coordinates. However, once the effect of global and regional masses is removed, i.e. by means of a reference field of ellipsoidal harmonic expansion of degree/order 360/360, the remaining effect of the local topographical masses can be successfully modelled in planar approximation, extended to a radius of 50km around the computational points. We refer to this step as the "*remove step*" of topographic masses.

For the *downward continuation*, we will use the *ellipsoidal Abel-Poisson* integral. The downward continuation is need to transfer the surface disturbing quantities of the type *modulus of gravity intensity* and *gravity potential* form the surface of the earth to *disturbing gravity potential* down at the level of reference ellipsoid of *World Geodetic Datum 2000*. The *downward continuation*, via the *ellipsoidal Abel-Poisson* integral, is an improperly posed problem and can be stabilised by means of *Phillips-Tikhonov* regularisation procedure among the others.

The downward continuation is finally followed by the *restore step*. In this step on the level of reference ellipsoid $\mathbb{E}^2_{a,b}$, we restore the impact of the topographic masses and the effect of the removed reference field.

Finally, the potential at the surface of geoid derived from the restore process can be subtracted from the geoid's potential w_0 to produce disturbing potential which can be converted to geoidal undulation via *Bruns formula* (we will use non-linear ellipsoidal *Bruns formula*).

The whole procedure described above can be summarised in terms of a flowchart as shown in *Figure 0-4*.

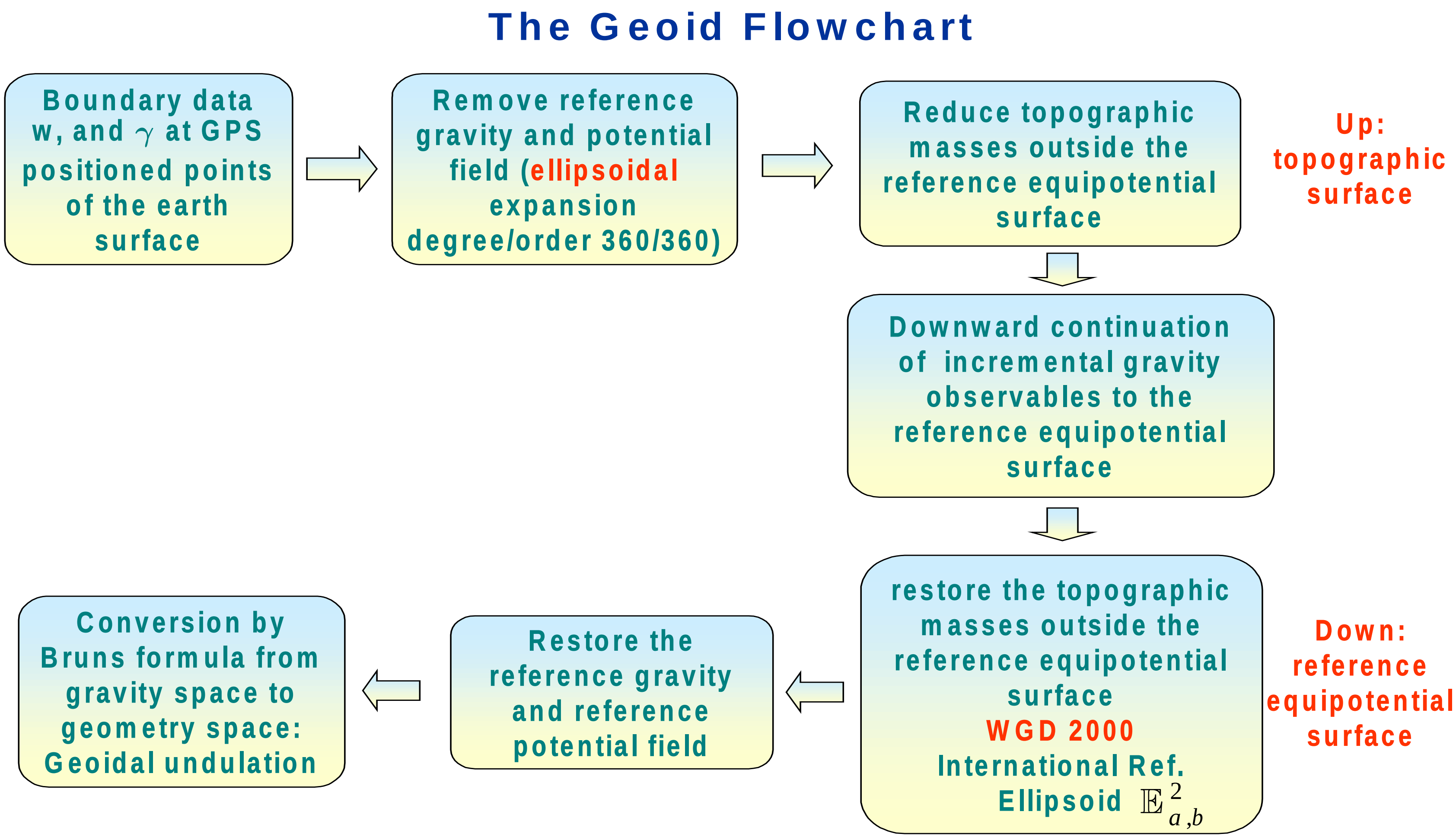

Figure 0-4: Flowchart of geoid determination.

1 Fixed-free two-boundary value problem—mathematical set-up

In this chapter, a new methodology for precise geoid determination with finest local details based on ellipsoidal approximation is presented. This methodology is formulated through the "*fixed-free two boundary-value problem*" based on the observables of the type *modulus of gravity intensity /gravity acceleration /* and *gravity potential* at the GPS positioned stations, with support of the known geoid's potential value, w_0. The solution of the boundary value problem is obtained through the following steps:

(i) Removal of the reference gravity potential, and gravity intensity fields, as the additive combination of
  (a) ellipsoidal harmonic expansion of degree/order 360/360, including the mass of the atmosphere, and,
  (b) centrifugal field.

(ii) Removal of gravitational potential and gravitational intensity of the topographical masses between the physical surface of the earth and the reference ellipsoid $\mathbb{E}^2_{a,b}$ (i.e. *World Geodetic Datum 2000, WGD2000*) up to 50km around the computational points, in planar approximation.

(iii) Downward continuation of the surface disturbing quantities of the type *gravitational potential* and *gravitational intensity* from the surface of the earth into *disturbing potential* on the surface of reference ellipsoid (World Geodetic Datum 2000, *WGD 2000*), through inverse solution of *ellipsoidal Abel-Poisson integral*.

(iv) Restoration of the removed gravitational potential of the topographical masses and the gravitational potential of the reference fields both for the computational points on the surface of the reference ellipsoid (*WGD2000*), to produce finally the gravity potential at the surface of the reference ellipsoid.

(v) Transformation of obtained gravity potential values at the surface of the reference ellipsoidal into *geoidal heights /geoidal undulations/* with respect to the reference ellipsoid *(WGD2000)* via nonlinear ellipsoidal Bruns formula.

The practical feasibility of the procedure is tested numerically by computing a high-resolution geoid for the state of *Baden Württemberg / Germany*.

The *two-boundary value problem* of the observables of the type *modulus of the gravity intensity* has already been studied by *E. Grafarend and F. Sansó* (1984), *M. Mihelcic* (1972) and recently by *Z. Martinec* (1998a pages 6-7). Here in contrast, we will apply the fixed free two-boundary value problem to observables of the type *modulus of gravity intensity* $\gamma(\mathbf{x})$ <u>and</u> *gravity potential* $w(\mathbf{x})$, given on the physical surface of the earth (the outer boundary). Such a boundary value problem is *over-determined*!

In this chapter, the theoretical details of the fixed-free two-boundary value problem and its solution will be explained. The numerical example, i.e., the case study of "the high-resolution *potential-geoid* and *gravity-geoid* of the state of *Baden-Württemberg*" is left to the next chapter.

1.1 Over-determined, non-linear, fixed-free two-boundary value problem

The fixed-free two-boundary value problem, is the problem of solving the Laplace-Poisson partial differential equation for the boundary data of the type *modulus of gravity intensity* /gravity acceleration/ $\gamma(\mathbf{x})$, and the *gravity potential* $w(\mathbf{x})$ on the surface of the earth. The surface of the earth $\mathbb{M}_h^2$ is further assumed be positioned point-wise, for example by GPS (Global Positioning system), and therefore is a fixed boundary. The gauge value of the geoid w_0, comprises the boundary data on the free boundary, the geoid $\mathbb{M}_g^2$. A summary of the definition of the fixed-free two-boundary value problem is given in *Box 1-1*.

The fixed-free two-boundary value problem, is an *over determined*, *non-linear*, *oblique* boundary value problem. It is an *over determined* boundary value problem since we have two boundary data of the type modulus of *gravity intensity* and *gravity potential* on the fixed boundary. In a fixed boundary value problem, *one* scalar type observable /boundary data/ is sufficient to obtain a unique solution of the unknown potential function for the whole $\mathbb{R}^3$ space. The fixed-free two-boundary value problem is *non-linear* since the norm operator, introduced by the modulus of gravity intensity, is a non-linear operator. It is also an *oblique boundary value problem* since the direction of gravity vector, in general, is not perpendicular to the boundary, i.e. the earth surface.

Box 1-1: Over determine, non-linear fixed-free two-boundary value problem.

$$\left.\begin{array}{l}\operatorname{div}\operatorname{grad}W(\mathbf{x}) = 2\omega^2 \qquad \forall \mathbf{x} \in \mathbb{R}^3 / \mathcal{D} \cup \partial\mathcal{G}_e^+ \\ \operatorname{div}\operatorname{grad}W(\mathbf{x}) = -4\pi g\rho(\mathbf{x}) + 2\omega^2 \;\forall \mathbf{x} \in \mathcal{D} \cup \partial\mathcal{G}_e^-\end{array}\right\} \text{Field Diff. Equ.}$$

$$\left.\begin{array}{l}\left\| grad\, W(\mathbf{x}) \right\|_2 = \gamma(\mathbf{x}), \qquad \forall \mathbf{x} \in \partial\mathcal{G}_e =: \mathbb{M}_h^2 \\ W(\mathbf{x}) = w(\mathbf{x}) \qquad \forall \mathbf{x} \in \partial\mathcal{G}_e =: \mathbb{M}_h^2 \\ W(\mathbf{x}) = w_0 \qquad \forall \mathbf{x} \in \partial\mathcal{G}_i =: \mathbb{M}_g^2\end{array}\right\} \text{Boundary Values}$$

$$\left. W(\mathbf{x}) = \frac{1}{2}\omega^2 \|\mathbf{x} - \langle \mathbf{x} | \mathbf{e}_\omega \rangle \mathbf{e}_\omega\|_2^2 + \frac{gm}{\|\mathbf{x}\|_2} + \mathcal{O}_w\!\left(\frac{1}{\|\mathbf{x}\|_2^3}\right) \text{ for } \|\mathbf{x}\|_2 \to \infty \right\} \text{Regularity at inf.}$$

Since we are interested in the solution of an ellipsoidal boundary value problem, the most suitable coordinate system is the one, which has an ellipsoid of revolution as one of its coordinate surfaces. This property can be fulfilled by six ellipsoidal coordinates introduced in the *Appendix A* (*page 205*). However, amongst those six ellipsoidal coordinates, *Jacobi ellipsoidal coordinates* are the only ones, allowing for the separation of *three-dimensional Laplace partial differential equation*. As a thorough study on the separation of the *Laplace partial differential equation* in terms of different ellipsoidal coordinates, the contribution by *E. Grafarend* (1989) is notable. *Appendix A* has a brief introduction into six different types of ellipsoidal coordinates.

Our solution technique to tackle the stated boundary value problem is base on the *inversion of ellipsoidal Abel-Poisson integral*. For this reason in *Appendix A* we have started with a brief review of *ellipsoidal coordinates* and then in *Appendix B* we have formulated *ellipsoidal eigenvalue/eigenfunction solution* of the three-dimensional *Laplace partial differential equation* in terms of two *Jacobi ellipsoidal coordinates* $\{\lambda, \phi, \eta\}$ and $\{\lambda, \phi, u\}$. Further, in *Appendix D* we have shown how a particular solution of the *Laplace partial differential equation* can lead to the *ellipsoidal Abel-Poisson integral*. That is done in terms of two types of *Jacobi ellipsoidal coordinates* $\{\lambda, \phi, \eta\}$ and $\{\lambda, \phi, u\}$ in *Appendix D.1* and *D.2*, respectively. In the next section, we will formulate the *ellipsoidal Abel-Poisson integral* as the sum of well know *spherical Abel-Poisson kernel* and some further terms showing the ellipticity of the field.

1.2 Abel-Poisson integral for the gravitational potential

Appendix B introduces the eigenspace solution of 3-D Laplace differential equation. Indeed, the *ellipsoidal Abel-Poisson integral*, as derived in *Appendix D*, is nothing else but the solution of external *Dirichlet* problem value problem of the *Laplace* equation, with boundary data on an ellipsoid of revolution, which is outlined in *Appendix B* (*page 225*). *Box 1-2* below starts with the rigorous presentation of *Abel-Poisson integral* and goes further to present an approximate form of the *Abel-Poisson integral* which is correct up to the order of relative eccentricity cubed, $\mathcal{O}(e^4)$.

Box 1-2: Ellipsoidal *Abel-Poisson integral* for the gravitational potential "$\mathcal{O}(e^4)$ approximation".

(i) Ellipsoidal Abel-Poisson integral (c.f. *Appendix B.1*)

$$\begin{aligned} U(\lambda,\phi,\eta) &= \int_{E^2_{a,b}} dS'(\frac{w(\phi')}{S}\sum_{n=0}^{\infty}\sum_{m=-n}^{n}\frac{Q_{n|m|}(i\sinh\eta)}{Q_{n|m|}(i\sinh\eta_0)} \\ &\quad\times e_{nm}(\lambda',\phi')e_{nm}(\lambda,\phi))f(\lambda',\phi') \qquad (1.1)\\ &= \frac{1}{S}\int_{E^2_{a,b}} dS'w(\phi')K(\lambda,\phi,\eta;\lambda',\phi',\eta_0)f(\lambda',\phi') \end{aligned}$$

(ii) Abel-Poisson Kernel

$$K(\lambda,\phi,\eta;\lambda',\phi',\eta_0) = \sum_{n=0}^{\infty}\sum_{m=-n}^{n}\frac{Q_{n|m|}(i\sinh\eta)}{Q_{n|m|}(i\sinh\eta_0)}e_{nm}(\lambda',\phi')e_{nm}(\lambda,\phi) \qquad (1.2)$$

(iii) Power series expansion of $Q_{nm}(i\sinh\eta)/Q_{nm}(i\sinh\eta_0)$ according to *N. Thong* (1993) and *Z. Martinec and E. Grafarend* (1997b)

$$\begin{aligned} \frac{Q_{nm}(i\sinh\eta)}{Q_{nm}(i\sinh\eta_0)} &= \left(\frac{\cosh\eta_0}{\cosh\eta}\right)^{n+1}\frac{1+\sum_{k=1}^{\infty}A_{nmk}e^{2k}}{1+\sum_{k=1}^{\infty}A_{nmk}e_0^{2k}} \\ &= \left(\frac{\cosh\eta_0}{\cosh\eta}\right)^{n+1}\frac{1+A_{nm1}e^2}{1+A_{nm1}e_0^2}+\mathcal{O}(e^4,e_0^4) \end{aligned}$$

$$= \left(\frac{\cosh\eta_0}{\cosh\eta}\right)^{n+1}\left[1 + A_{nm1}(e^2 - e_0^2)\right] + \mathcal{O}(e^4, e_0^4) \tag{1.3}$$

$a_0 = \varepsilon\cosh\eta_0$ is major semi-axis of the reference ellipsoid $\mathbb{E}^2_{a_0,b_0}$ and $a = \varepsilon\cosh\eta$ is the minor semi-axis of the ellipsoid passing through the computational point and A_{nm1} is as defined below.

$$A_{nm1} = \frac{1}{4}\frac{(n+m+1)(n-m+1)}{\frac{2n+1}{4}} = \frac{(n+1)^2 - m^2}{2(2n+3)} \tag{1.4}$$

(iv) Ellipsoidal *Abel-Poisson integral* for the gravitational potential up to the level of approximation $\mathcal{O}(e^4)$.

$$\begin{aligned} U(\lambda,\phi,\eta) &= \frac{1}{S}\int\limits_{\mathbb{E}^2_{a,b}} dS'w(\phi')\{\sum_{n=0}^{\infty}\sum_{m=-n}^{n}\left(\frac{\cosh\eta_0}{\cosh\eta}\right)^{n+1} \\ &\times\left[1 + (e^2 - e_0^2)A_{nm1}\right]e_{nm}(\lambda',\phi')e_{nm}(\lambda,\phi)\}U(\lambda',\phi') \\ &= \frac{1}{S}\int\limits_{\mathbb{E}^2_{a,b}} dS'w(\phi')K_{ellpsoidal}(\lambda,\phi,\eta;\lambda',\phi',\eta_0)U(\lambda',\phi') + \mathcal{O}(e^4) \end{aligned} \tag{1.5}$$

where

$$\begin{aligned} K_{ellipsoidal}(\lambda,\phi,\eta;\lambda',\phi',\eta_0) = {} & K_0(\lambda,\phi,\eta;\lambda',\phi',\eta_0) \\ & + K_1(\lambda,\phi,\eta;\lambda',\phi',\eta_0) \\ & + K_2(\lambda,\phi,\eta;\lambda',\phi',\eta_0) + \mathcal{O}(e^4) \end{aligned} \tag{1.6}$$

$$K_0(\lambda,\phi,\eta;\lambda',\phi',\eta_0) = \sum_{n=0}^{\infty}\left(\frac{\cosh\eta_0}{\cosh\eta}\right)^{n+1}(2n+1)P_n(\cos\psi) \tag{1.7}$$

$$K_1(\lambda,\phi,\eta;\lambda',\phi',\eta_0) = \sum_{n=0}^{\infty}\left(\frac{\cosh\eta_0}{\cosh\eta}\right)^{n+1}\frac{(n+1)^2}{2(2n+3)}(2n+1)P_n(\cos\psi) \tag{1.8}$$

$$\begin{aligned} K_2(\lambda,\phi,\eta;\lambda',\phi',\eta_0) &= \sum_{n=0}^{\infty}\sum_{m=-n}^{n}\left(\frac{\cosh\eta_0}{\cosh\eta}\right)^{n+1} \\ &\times\frac{m^2}{2(2n+3)}e_{nm}(\lambda',\phi')e_{nm}(\lambda,\phi) \end{aligned} \tag{1.9}$$

subject to

$$\cos\psi = \sin\phi\sin\phi' + \cos\phi\cos\phi'\cos(\lambda - \lambda') \tag{1.10}$$

Putting $\cosh\eta = r/\varepsilon$ and $\cosh\eta_0 = R/\varepsilon$, reduce the equation (1.7) to

$$K_0(\lambda,\phi,\eta;\lambda',\phi',\eta_0) = \sum_{n=0}^{\infty}(\frac{R}{r})^{n+1}(2n+1)P_n(\cos\psi) \\ = K_{spherical}(\lambda,\phi,r;\lambda',\phi',R) \tag{1.11}$$

which is the well-known *spherical Abel-Poisson kernel* (*Kellogg*, 1929). For *spherical Abel-Poisson kernel* following closed-form formula exists.

$$k_{spherical}(\lambda,\phi,r;\lambda',\phi',R) = R\frac{r-R^2}{\|\mathbf{x}-\mathbf{x}'\|^3} \tag{1.12}$$

Therefore, in Box 1-2 we succeeded in splitting the ellipsoidal Abel-Poisson kernel into spherical Abel-Poisson kernel $K_{spherical}(\lambda,\phi,\eta;\lambda',\phi',\eta_0)$ and ellipsoidal corrections being introduced here up to the order of $\mathcal{O}(e^4)$ via $K_1(\lambda,\phi,\eta;\lambda',\phi',\eta_0)$ and $K_2(\lambda,\phi,\eta;\lambda',\phi',\eta_0)$.

Equation (1.5) provides us with the observation equation for observables of the type gravitational potential. Indeed, given the harmonic gravitational potentials $U(\lambda,\phi,\eta)$, integral equation (1.5) can be solved for $U(\lambda,\phi,\eta=\eta_0)$. More on this to come in Section 1.13.

Z. Martinec and E. Grafarend (1998b) have offered a closed form formula for $K_1(\lambda,\phi,\eta;\eta_0)$, which is correct up to the order of accuracy of first eccentricity squared $\mathcal{O}(e_0^2)$. They have also shown that $K_1(\lambda,\phi,\eta;\ \lambda',\phi',\eta_0) < K_0(\lambda,\phi,\eta;\lambda',\phi',\eta_0)$, and that $K_1(\lambda,\phi,\eta;\lambda',\phi',\eta_0)$ has the same degree of singularity as $K_0(\lambda,\phi,\eta;\lambda',\phi',\eta_0)$. The closed form of the *ellipsoidal Abel-Poisson kernel*, i.e. $K_{ellipsoidal}(\lambda,\phi,\eta;\lambda',\phi',\eta_0)$, is represented in *Box 1-3*. *Figure 1-1* shows the variation of the *ellipsoidal Abel-Poisson kernel* $K_{ellipsoidal}(\lambda,\phi,\eta;\lambda',\phi',\eta_0)$, the *spherical Abel-Poisson kernel* $K_{spherical}(\lambda,\phi,\eta;\lambda',\phi',\eta_0)$, and the *ellipsoidal correction to spherical Abel-Poisson kernel* $dK_{ellipsoidal}(\lambda,\phi,\eta;\ \lambda',\phi',\eta_0)$ against the space angle ψ, while *Figure 1-2* represents the ellipsoidal Abel-Poisson kernel $K_{ellipsoidal}(\lambda,\phi,\eta;\lambda',\phi',\eta_0)$ calculated for the same point but for different azimuths at the space angle $\psi = 1^\circ$. *Figure 1-3* represents the variation of ellipsoidal Abel-Poisson kernel $K_{ellipsoidal}(\lambda,\phi,\eta;\lambda',\phi',\eta_0)$ of *Figure 1-2* but in terms of the percentage of the kernel's value for $\alpha = 0^\circ$. From a study of the *Figure 1-1* to *Figure 1-3* following conclusions can be made:

(i) Ellipsoidal correction term of the Abel-Poisson kernel vanishes rather faster than spherical part of the kernel.

(ii) Dependency of the ellipsoidal Abel-Poisson kernel on azimuth is quite minute. In fact, as is shown in *Figure 1-3* the dependency on azimuth is not exceeding 0.3 percent of the whole kernel value at $\alpha = 0^\circ$.

Box 1-3: Closed form solution of the *ellipsoidal Abel-Poisson kernel*

"$K_{ellipsoidal}\ (\lambda, \phi, \eta; \lambda', \phi', \eta_0)$"

(i) Ellipsoidal Abel-Poisson kernel

$$K_{ellipsoidal}(\lambda, \phi, \eta; \lambda', \phi', \eta_0) = K_{spherical}(\lambda, \phi, \eta; \lambda', \phi', \eta_0) + dK_{ellipsoidal}(\lambda, \phi, \eta; \lambda', \phi', \eta_0) \tag{1.13}$$

(ii) spherical Abel-Poisson kernel

$$\begin{aligned} & K_{spherical}(\lambda, \phi, \eta; \lambda', \phi', \eta_0) \\ &= \cosh \eta_0 \frac{\cosh^2 \eta - \cosh^2 \eta_0}{(\cosh^2 \eta + \cosh^2 \eta_0 - 2\cosh \eta \cosh \eta_0 \cos \psi)^{3/2}} \\ &= K_{spherical}(\lambda, \phi, r; \lambda', \phi', R) = R \frac{r - R^2}{\|\mathbf{x} - \mathbf{x}'\|^3} \end{aligned} \tag{1.14}$$

(iii) ellipsoidal correction to spherical Abel-Poisson kernel

$$\begin{aligned} & dK_{ellipsoidal}(\lambda, \phi, \eta; \lambda', \phi', \eta_0) \\ &= \frac{t^2 - 1}{2\cosh^2 \eta_0} \Big\{ \frac{\cos \phi \cos \alpha}{\sin \psi} (\sin \phi - \sin \phi' \cos \psi)[\cos \psi L_1 - L_2] \\ &\quad + \cos \phi (\cos \phi - \sin \phi' \sin \psi \cos \alpha) L_1 \\ &\quad + (1 - \cos^2 \phi \sin^2 \alpha) L_3 + \sin \phi \sin \phi' L_4 \Big\} + \mathcal{O}(e^2) \end{aligned} \tag{1.15}$$

(iv) isotropic parts of the ellipsoidal correction

$$\begin{aligned} L_1 &= \frac{t}{g^3} - \frac{15}{8} \frac{t(g+1)}{g(g+1-t\cos\psi)} \\ &\quad + \frac{5}{4}\left(\frac{t}{g} - t + \frac{t^2 \cos\psi (g+1)}{g(g+1-t\cos\psi)} - t\ln\left(\frac{g+1-t\cos\psi}{2}\right)\right) \\ &\quad - \frac{3}{8}\left(\begin{aligned} & t - \frac{7t^2\cos\psi}{2} + \frac{t}{2g}(1+3t\cos\psi) - \frac{3tg}{2} \\ & + \frac{t^3(3\cos^2\psi - 1)(g+1)}{2g(g+1-t\cos\psi)} - 3t^2\cos\psi \ln\left(\frac{g+1-t\cos\psi}{2}\right) \end{aligned} \right) \\ &\quad + \frac{29}{24} t - \frac{171}{80} t^2 \cos\psi \end{aligned} \tag{1.16}$$

$$L_2 = \frac{t(t+\cos\psi)}{g^3} - \frac{3t^2(1-\cos^2\psi)}{g^5} - \frac{1}{2}\left(\frac{1}{g}-1\right) - \frac{1}{4}\ln\left(\frac{g+1-t\cos\psi}{2}\right) \tag{1.17}$$

$$L_3 = (1-\cos^2\psi)\left[\frac{t}{g^3} - \frac{3t^2(t-\cos\psi)}{g^5} - \frac{1}{2}\frac{t}{g^3} - \frac{1}{2}L_1\right] \tag{1.18}$$

$$L_4 = 2\left(\frac{t(t+\cos\psi)}{g^3} - \frac{3t^2(1-\cos^2\psi)}{g^5}\right) + \frac{t(t-\cos\psi)}{g^3} - L_2 \tag{1.19}$$

subject to

$$\psi = \cos^{-1}\left(\sin\phi\sin\phi' + \cos\phi\cos\phi'\cos(\lambda-\lambda')\right),$$

$$\alpha = \cos^{-1}\left(\frac{\sin\phi' - \cos\psi\sin\phi}{\sin\psi\cos\phi}\right),$$

$$t = \frac{\cosh\eta_0}{\cosh\eta},$$

and

$$g \coloneqq \frac{\sqrt{\cosh^2\eta + \cosh^2\eta_0 - 2\cosh\eta\cosh\eta_0\cos\psi}}{\cosh\eta}.$$

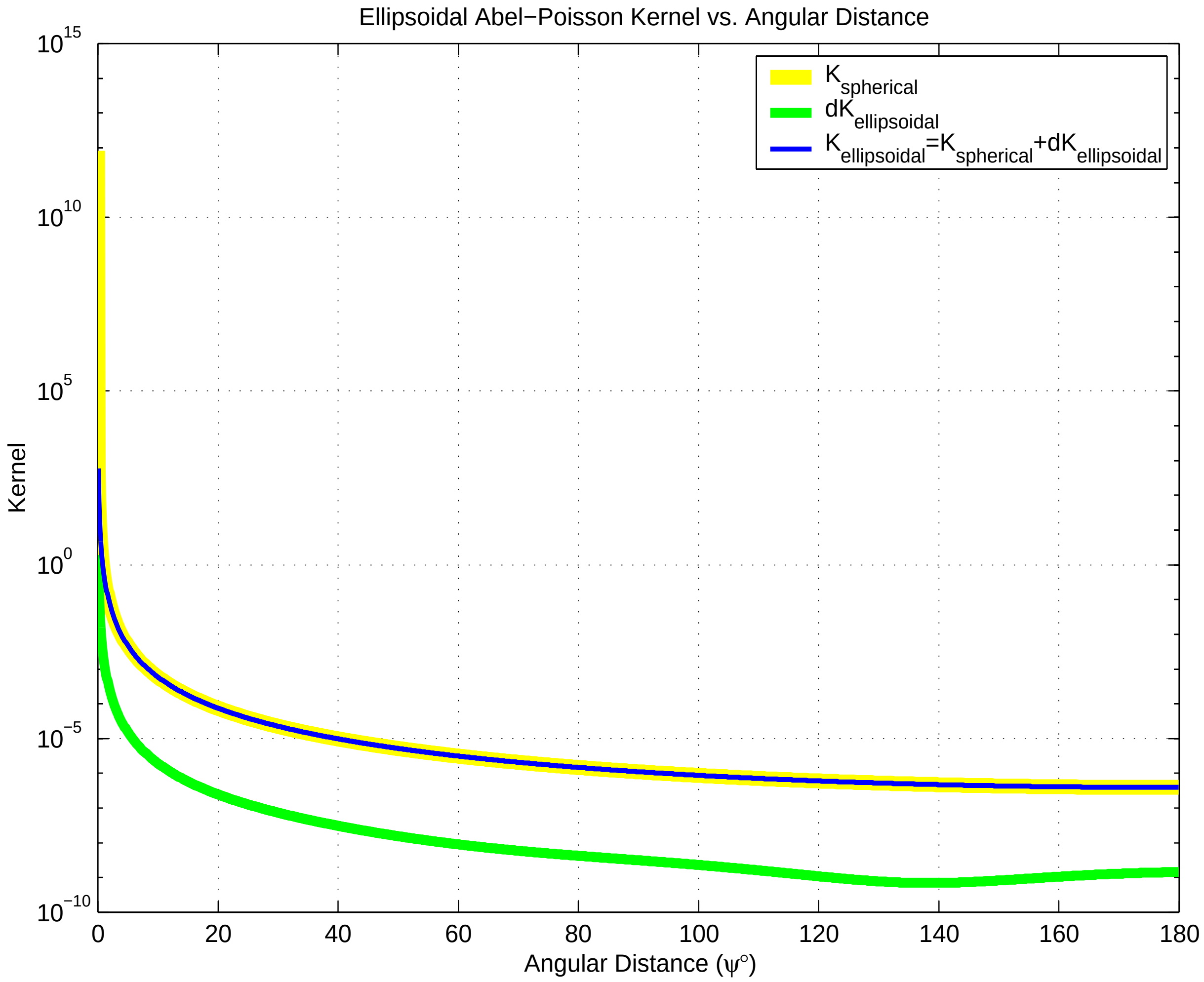

Figure 1-1: Ellipsoidal Abel-Poisson kernel $K_{ellip}(\lambda,\phi,\eta;\lambda',\phi',\eta_0)$, spherical Abel-Poisson kernel $K_{sph}(\lambda,\phi,\eta;\lambda',\phi',\eta_0)$, and ellipsoidal correction to spherical Abel-Poisson kernel $dK_{ellip}(\lambda,\phi,\eta;\lambda',\phi',\eta_0)$ versus angular distance ψ. Calculated for the point $\{\lambda,\phi,\eta\} = \{9.6174328693^\circ, 49.703934050^\circ, 3.19471515096\}$ with respect to the reference ellipsoid $\eta_0 = 3.1947135814$ (WGD2000) along the azimuth $\alpha = 10^\circ$. The scale on the vertical axis is logarithmic.

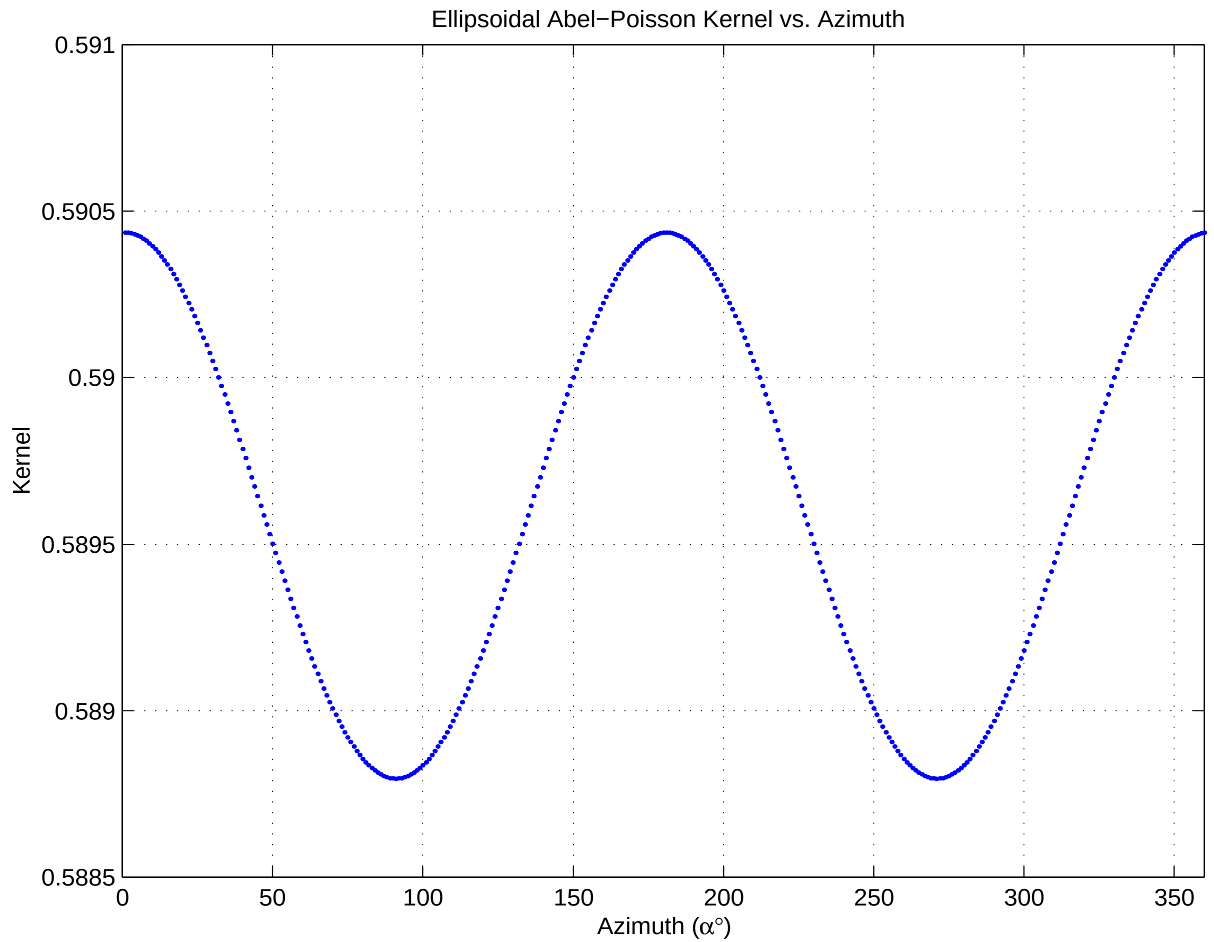

Figure 1-2: Ellipsoidal Abel-Poisson kernel $K_{ellipsoidal}(\lambda, \phi, \eta; \lambda', \phi', \eta_0)$ versus azimuth α. Calculated for the point $\{\lambda, \phi, \eta\} = \{9.617432869327196^\circ, 49.70393405021537^\circ, 3.194715150960513\}$, at the space angle $\psi = 1^\circ$, with respect to the reference ellipsoid $\eta_0 = 3.194713581$.

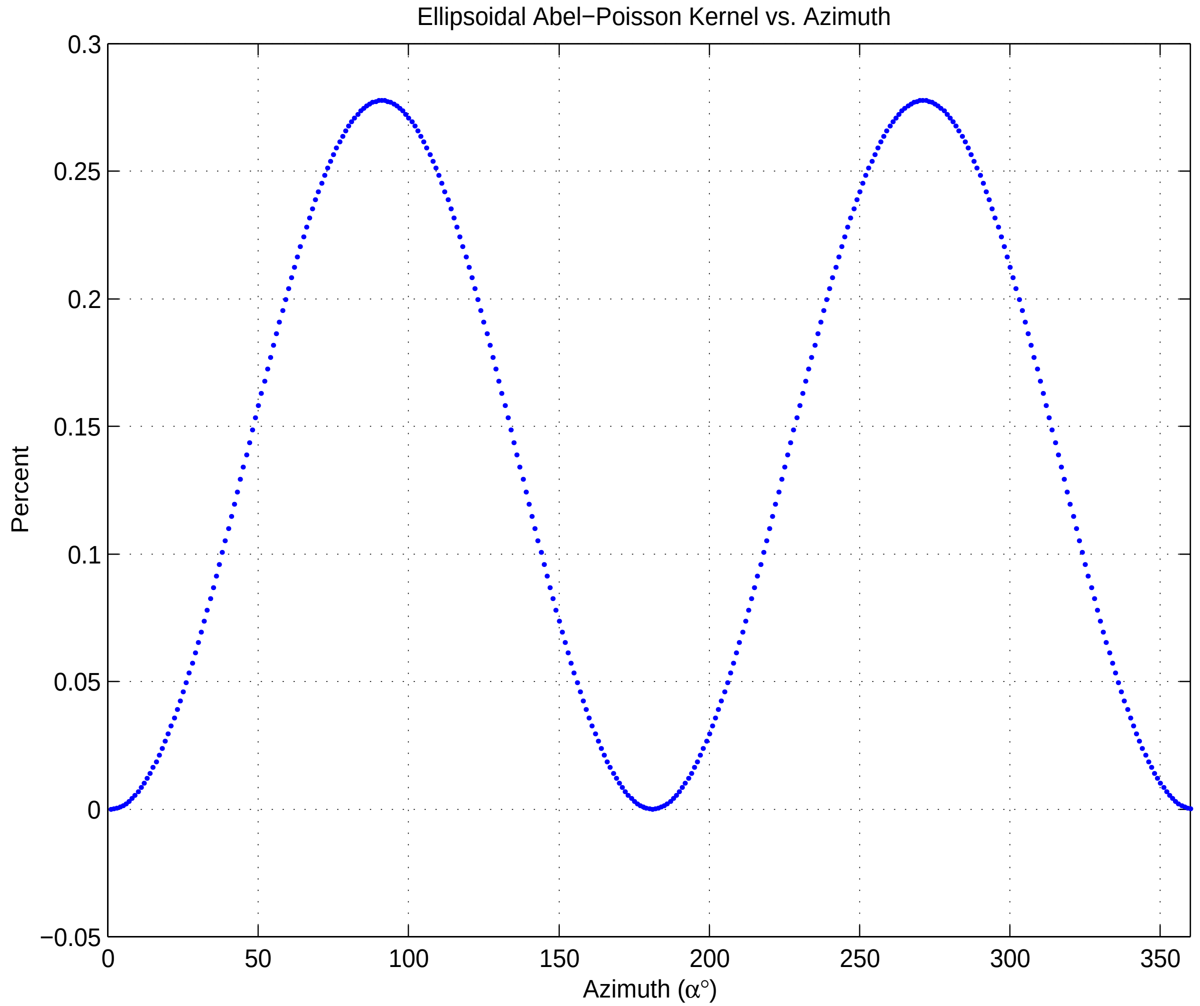

Figure 1-3: Variation of ellipsoidal Abel-Poisson kernel $K_{ellipsoidal}(\lambda, \phi, \eta; \lambda', \phi', \eta_0)$ versus azimuth α, in terms of percentage of the value of the kernel at $\alpha = 0^\circ$. Calculations are for the point $\{\lambda, \phi, \eta\} = \{9.617432869327196^\circ, 49.70393405021537^\circ, 3.194715150960513\}$ with respect to the reference ellipsoid $\eta_0 = 3.194713581445341$ at the space angle $\psi = 1^\circ$.

1.3 Euler δ-increment

It is clear that *Abel-Poisson integral* and its inverse solution is valid only for external space of the earth where there are no masses. However, in the space between the surface of the earth and the reference ellipsoid, the region where we want to apply the *inverse Abel-Poisson integral*, there are topographical masses. Therefore, before applying the *inverse Abel-Poisson integral* to our problem, the effect of topographical masses must be removed from the observed gravity quantities (i.e. $\gamma(\mathbf{x})$ and $w(\mathbf{x})$). If besides the effect of topographical masses we remove the global gravity potential and gravity intensity, by using a global geopotential model, we get such a smooth incremental / disturbing / quantities which can be satisfactorily linearized. *Disturbing quantities* / *Euler* δ*-increments* / can be introduced for the various quantities involved in our boundary value problem. *Box 1-4* has a list of those *Euler* δ*-increments*.

To generate the smooth incremental boundary data, we will use the ellipsoidal harmonic expansion of the external gravitational field of the earth up to degree/order 360/360, as the *normal / reference gravitational field*.

Box 1-4: Euler δ-increments

(i) observables of the type modulus of gravity intensity

$$\delta\Gamma(\mathbf{x}) := \|\boldsymbol{\delta\Gamma}\| = \|\boldsymbol{\gamma}(\mathbf{x}) - \boldsymbol{\Gamma}(\mathbf{x})\| = \|\boldsymbol{\gamma}(\mathbf{x}) - \boldsymbol{\Gamma}(\mathbf{x})\| \tag{1.20}$$

(ii) observables of the type potential

$$\delta W(\mathbf{x}) = w(\mathbf{x}) - W(\mathbf{x}) \tag{1.21}$$

(iii) mass density

$$\delta \mathrm{P} = \rho - \mathrm{P} \tag{1.22}$$

(iv) angular velocity of the earth

$$\delta\Omega = \| \boldsymbol{\delta\Omega} \| = \| \boldsymbol{\omega} - \boldsymbol{\Omega} \| \tag{1.23}$$

Figure 1-4 illustrates the decomposition scheme for the three different gravity field quantities of the type potential $w(\mathbf{x})$, gravity intensity vector $\boldsymbol{\Gamma}(\mathbf{X})$ and modulus of gravity intensity $\|\boldsymbol{\Gamma}(\mathbf{x})\|_2 = \gamma$, which are some times confusing.

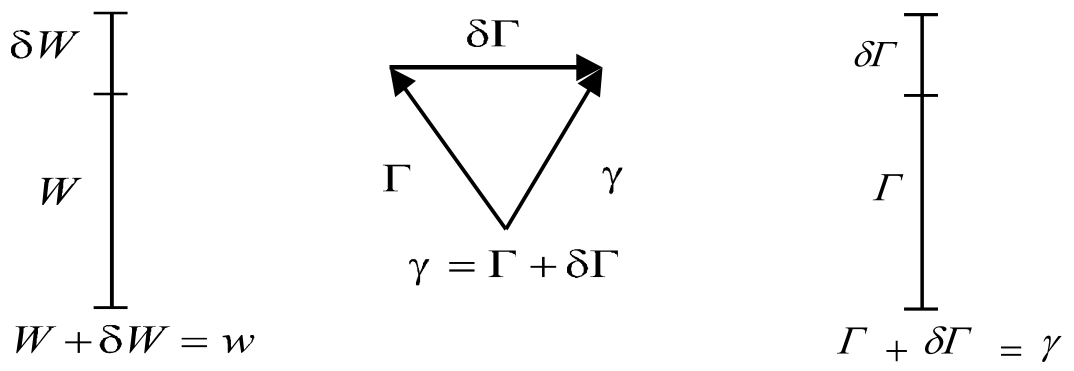

Figure 1-4: Decomposition of the scalar valued *gravity potential* $w(\mathbf{x})$, of the vector-valued gravity intensity $\mathbf{\Gamma}(\mathbf{x})$ and of the scalar-valued modulus of gravity intensity $\|\mathbf{\Gamma}(\mathbf{x})\|_2 = \gamma$.

We refer to the step whereby the domain of *Laplace differential equation* is extended to the space between the surface of the earth and the surface of reference ellipsoid as *remove step*. *Box 1-5* bellow summarises the remove step.

Box 1-5: The remove step

(i) Subtraction of the reference ellipsoidal gravity field comprised of gravitational potential and gravitational intensity of ellipsoidal harmonic expansion up to degree/order 360/360, and the centrifugal part (including the effect of atmospheric masses, and the permanent tide) from the observations of the type *modulus of gravity intensity* $\Gamma(\mathbf{x})$ and gravity potential $W(\mathbf{x})$.

(ii) Removal of the effect of local topographical masses between observation point and the reference ellipsoid WGD2000 in a radius of 50km around the computational point.

Note that in our remove step thanks to the application of ellipsoidal harmonic expansion up to degree/order 360/360 there is no need to include the effect of balancing isostatic masses, they are included in the high degree/order ellipsoidal harmonic model. In summary, the *remove step* will lead to disturbing quantities, $\delta\Gamma(\mathbf{x})$ and $\delta W(\mathbf{x})$, which are harmonic outside the reference ellipsoid $\mathbb{E}^2_{a,b}$ and which are free from high frequency variations.

In the next section, we shall introduce the linearized fixed-free two-boundary value problem.

1.4 Over-determined, linear, fixed-free two-boundary value problem

The boundary operator for the observables of the type *modulus of gravity intensity* $\|\boldsymbol{\Gamma}(\mathbf{x})\|_2 = \gamma$ is a non-linear. In *Box 1-6* we have a résumé of *Taylor* expansion of the boundary operator $\|\boldsymbol{\Gamma}(\mathbf{x})\|_2 = \gamma$ up to the order of five in $\delta\Gamma$, (i.e. $\mathcal{O}(\delta\Gamma^5)$). Based on the linear part of this expansion, collected in *Box 1-7*, the *over-determined, linear fixed-free two-boundary value problem* can be constructed. *Box 1-8* is devoted to the definition of linear fixed-free two-boundary value problem, based on incremental quantities $\delta\Gamma$, δW, and $\delta \mathrm{P}$.

Box 1-6: expansion of non-linear boundary operator $\gamma(\mathbf{x})$ up to the order five in $\delta\Gamma$

(i) *Non-linear boundary operator:*

$$\begin{aligned}\gamma(\mathbf{x}) &= \left\|\operatorname{grad} w(\mathbf{x})\right\| = \left\|\operatorname{grad} W(\mathbf{x}) + \operatorname{grad}\delta W(\mathbf{x})\right\| \\ &= \sqrt{\left\langle \operatorname{grad} W(\mathbf{x}) + \operatorname{grad}\delta W(\mathbf{x}) \middle| \operatorname{grad} W(\mathbf{x}) + \operatorname{grad}\delta W(\mathbf{x})\right\rangle} \\ &= \left(\left\|\operatorname{grad} W(\mathbf{x})\right\|^2 + \left\|\operatorname{grad}\delta W(\mathbf{x})\right\|^2 + 2\left\langle \operatorname{grad} W(\mathbf{x}) \middle| \operatorname{grad}\delta W(\mathbf{x})\right\rangle\right)^{1/2} \\ &= \Gamma(\mathbf{x})\left(1 + \frac{2}{\Gamma^2}\langle \boldsymbol{\Gamma} | \boldsymbol{\delta\Gamma}\rangle + \frac{1}{\Gamma^2}\delta\Gamma^2\right)^{1/2}\end{aligned} \tag{1.24}$$

subject to *B. Taylor expansion of* $(1+x)^{1/2}$ where $|\, x \,| < 0$, i.e.,

$$(1+x)^{1/2} = 1 + \frac{1}{2}x - \frac{1}{8}x^2 + \frac{1}{16}x^3 + \mathcal{O}(x^4) \tag{1.25}$$

we have:

(ii) Expansion of non-linear boundary operator $\gamma(\mathbf{x})$

$$\begin{aligned}\gamma(\mathbf{x}) = \Gamma(\mathbf{x}) &+ \frac{1}{\Gamma}\langle \boldsymbol{\Gamma} | \boldsymbol{\delta\Gamma}\rangle + \frac{1}{2\Gamma}\delta\Gamma^2 \\ &- \frac{1}{2\Gamma^3}\langle \boldsymbol{\Gamma} | \boldsymbol{\delta\Gamma}\rangle^2 - \frac{1}{2\Gamma^3}\langle \boldsymbol{\Gamma} | \boldsymbol{\delta\Gamma}\rangle\delta\Gamma^2 - \frac{1}{8\Gamma^3}\delta\Gamma^4 \\ &+ \mathcal{O}_\gamma\{\delta\Gamma^5\}\end{aligned} \tag{1.26}$$

(iii) Expansion of non-linear boundary operator $\delta\Gamma(\mathbf{x})$

$$\Rightarrow \begin{cases} \delta\Gamma(\mathbf{x}) = \gamma(\mathbf{x}) - \Gamma(\mathbf{x}) = \dfrac{1}{\Gamma}\langle \mathbf{\Gamma} | \boldsymbol{\delta\Gamma}\rangle + \dfrac{1}{2\Gamma}\delta\Gamma^2 \\ \quad -\dfrac{1}{2\Gamma^3}\langle \mathbf{\Gamma} | \boldsymbol{\delta\Gamma}\rangle^2 - \dfrac{1}{2\Gamma^3}\langle \mathbf{\Gamma} | \boldsymbol{\delta\Gamma}\rangle \delta\Gamma^2 - \dfrac{1}{8\Gamma^3}\delta\Gamma^4 \\ \quad +\mathcal{O}_\gamma\{\delta\Gamma^5\} \end{cases} \tag{1.27}$$

Box 1-7: linearized boundary operator $\delta\Gamma$

According to *Box 1-6*, the linearized boundary operator $\delta\Gamma$ can be constructed as follows:

$$\begin{aligned} \delta\Gamma(\mathbf{x}) &= \gamma(\mathbf{x}) - \Gamma(\mathbf{x}) = \frac{1}{\Gamma}\langle \mathbf{\Gamma} | \boldsymbol{\delta\Gamma}\rangle + \mathcal{O}(\delta\Gamma^2) \\ &= \left\langle \frac{\mathbf{\Gamma}}{\Gamma} \middle| \boldsymbol{\delta\Gamma} \right\rangle + \mathcal{O}(\delta\Gamma^2) \\ &= \langle \mathbf{e}_\Gamma | \boldsymbol{\delta\Gamma}\rangle + \mathcal{O}(\delta\Gamma^2) \end{aligned} \tag{1.28}$$

where $\langle \mathbf{e}_\Gamma | \boldsymbol{\delta\Gamma}\rangle$ in (1.28) is the directional derivative of $\boldsymbol{\delta\Gamma}$ in the direction of reference gravity vector $\mathbf{\Gamma}$.

Box 1-8: Over determine, linear fixed-free two-boundary value problem.

$$\left.\begin{aligned} &\operatorname{div}\operatorname{grad}\delta W(\mathbf{x}) = 0 \qquad \forall \mathbf{x} \in \mathbb{R}^3 / \mathcal{D} \cup \partial\mathcal{G}_g \\ &\operatorname{div}\operatorname{grad}\delta W(\mathbf{x}) = -4\pi\delta P(\mathbf{x}) \qquad \forall \mathbf{x} \in \mathcal{D} \cup \partial\mathcal{G}_g \end{aligned}\right\} \text{Field Diff. Equ.}$$

$$\left.\begin{aligned} &\delta\Gamma(\mathbf{x}) = \nabla_{\boldsymbol{\delta\Gamma}}\delta W(\mathbf{x}) + \mathcal{O}(\delta\Gamma^2) = \left\langle \frac{\mathbf{\Gamma}}{\Gamma} \middle| \boldsymbol{\delta\Gamma} \right\rangle + \mathcal{O}(\delta\Gamma^2)\ \forall \mathbf{x} \in \mathbb{R}^3 / \mathcal{D} \cup \partial\mathcal{G}_e^- \\ &\delta W(\mathbf{x}) = \delta W \\ &w_0 = W(\mathbf{x}) + \delta W(\mathbf{x}) \qquad \forall \mathbf{x} \in \partial\mathcal{G}_i =: \mathbb{M}_g^2 \end{aligned}\right\} \text{Boundary Values}$$

$$\left.\delta W(\mathbf{x}) = \frac{gm}{\|\mathbf{x}\|_2} + \mathcal{O}_{\delta w}\left(\frac{1}{\|\mathbf{x}\|_2^3}\right) \qquad \text{for } \|\mathbf{x}\|_2 \to \infty \right\} \text{Regularity at Infinity}$$

For the space where there are no masses, the boundary values of the type δW , and $\delta\Gamma$, satisfy the *Abel-Poisson integral*, as the *special solution* of the *Laplace partial differential equation*. Therefore, if we are looking for the *incremental gravitational potential* on the surface of reference ellipsoid $\mathbb{E}^2_{a,b}$, the Abel-Poisson integral can be used as the observation equation. That is, given the harmonic *incremental gravitational potential* $\delta W(\mathbf{x})$, and modulus of *incremental* gravitational intensity $\delta\Gamma(\mathbf{x})$ on the surface of the earth $\mathbb{M}_h^2$, the *incremental* gravitational potential $\delta\Gamma(\mathbf{X})$ on the reference ellipsoid $\mathbb{E}_{a,b}^2$ can the derived as the inverse solution of the *Poisson-Abel integral*. More on the inverse solution of an integral equation will come later in this chapter.

Let us now present the *Abel-Poisson integral* equation for the linearized harmonic boundary values of the types modulus of *incremental* gravitational intensity $\delta\Gamma$ and *incremental* gravitational potential δW . It is clear that the *Abel-Poisson integral* (1.1) is true for any harmonic function $f(\lambda,\phi)$. Therefore, if we assume that the *incremental* gravitational potential δW is free from the effect of the masses outside the reference ellipsoid, it satisfies the *Abel-Poisson integral* as is presented in *Box 1-9*.

Box 1-9: *Abel-Poisson integral* for *incremental* gravitational potential δW .

$$\begin{aligned}\delta W(\lambda,\phi,\eta) = &\int_{\mathbb{E}_{a,b}^2} dS'[\frac{w(\phi')}{S} \\ &\sum_{n=0}^{\infty}\sum_{m=-n}^{n}\frac{Q_{n|m|}(i\sinh\eta)}{Q_{n|m|}(i\sinh\eta_0)} \\ &\times e_{nm}(\lambda',\phi')e_{nm}(\lambda,\phi)]\delta W(\lambda',\phi') \\ = &\frac{1}{S}\int_{\mathbb{E}_{a,b}^2} dS' w(\phi')K(\lambda,\phi,\eta;\lambda',\phi',\eta_0)\delta W(\lambda',\phi')\end{aligned} \tag{1.29}$$

Where the Abel-Poisson Kernel in spectral form is given by

$$\begin{aligned}K(\lambda,\phi,\eta;\lambda',\phi',\eta_0) = &\sum_{n=0}^{\infty}\sum_{m=-n}^{n}\frac{Q_{n|m|}(i\sinh\eta)}{Q_{n|m|}(i\sinh\eta_0)} \\ &\times e_{nm}(\lambda',\phi')e_{nm}(\lambda,\phi)\end{aligned} \tag{1.30}$$

In order to obtain an *Abel-Poisson integral* structure for the modulus of *incremental* gravitational intensity $\delta\Gamma$, one can set off from the linearized relation given in (1.28). *Box 1-10* and *Box 1-11* have the details of the derivation.

Box 1-10: Abel Poisson integral for the modulus of *incremental* gravitational intensity $\delta\Gamma$

(i) the linearized boundary operator $\delta\Gamma$

$$\delta\Gamma(\mathbf{x}) = \gamma(\mathbf{x}) - \Gamma(\mathbf{x}) = \langle \mathbf{e}_\Gamma | \boldsymbol{\delta\Gamma}\rangle + \mathcal{O}(\delta\Gamma^2) \tag{1.31}$$

(ii) the unit reference gravity vector $\mathbf{e}_{\boldsymbol{\Gamma}}$

$$\mathbf{e}_{\boldsymbol{\Gamma}} = \frac{\boldsymbol{\Gamma}}{\|\boldsymbol{\Gamma}\|} \tag{1.32}$$

(iii) the vector of incremental gravitational intensity

$$\begin{aligned}
\boldsymbol{\delta\Gamma}(\lambda,\phi,\eta) &= \mathrm{Grad}(\delta W(\lambda,\phi,\eta)) \\
&= \mathrm{Grad}\left(\frac{1}{S}\int_{\mathbb{E}^2_{a,b}} dS\,'w(\phi')K(\lambda,\phi,\eta;\lambda',\phi',\eta_0)\delta W(\lambda',\phi')\right) \\
= \frac{1}{\sqrt{g_{11}}}\frac{\partial}{\partial\lambda}&\left(\frac{1}{S}\int_{\mathbb{E}^2_{a,b}} dS\,'w(\phi')K(\lambda,\phi,\eta;\lambda',\phi',\eta_0)\delta W(\lambda',\phi')\right)\mathbf{e}_\lambda \\
&+\frac{1}{\sqrt{g_{22}}}\frac{\partial}{\partial\phi}\left(\frac{1}{S}\int_{\mathbb{E}^2_{a,b}} dS\,'w(\phi')K(\lambda,\phi,\eta;\lambda',\phi',\eta_0)\delta W(\lambda',\phi')\right)\mathbf{e}_\phi \\
&+\frac{1}{\sqrt{g_{33}}}\frac{\partial}{\partial\eta}\left(\frac{1}{S}\int_{\mathbb{E}^2_{a,b}} dS\,'w(\phi')K(\lambda,\phi,\eta;\lambda',\phi',\eta_0)\delta W(\lambda',\phi')\right)\mathbf{e}_\eta
\end{aligned} \tag{1.33}$$

(iv) Ellipsoidal Abel-Poisson integral for incremental gravitational intensity $\delta\Gamma$

$$\begin{aligned}
\delta\Gamma(\mathbf{x}) &= \gamma(\mathbf{x}) - \Gamma(\mathbf{x}) = \langle \mathbf{e}_{\boldsymbol{\Gamma}} | \boldsymbol{\delta\Gamma}\rangle \\
&= \frac{1}{\sqrt{g_{11}}}\frac{\Gamma_\lambda}{\|\boldsymbol{\Gamma}\|}\frac{1}{S}\int_{\mathbb{E}^2_{a,b}} dS\,'w(\phi')\frac{\partial K(\lambda,\phi,\eta;\lambda',\phi',\eta_0)}{\partial\lambda}\delta W(\lambda',\phi') \\
&+\frac{1}{\sqrt{g_{22}}}\frac{\Gamma_\phi}{\|\boldsymbol{\Gamma}\|}\frac{1}{S}\int_{\mathbb{E}^2_{a,b}} dS\,'w(\phi')\frac{\partial K(\lambda,\phi,\eta;\lambda',\phi',\eta_0)}{\partial\phi}\delta W(\lambda',\phi') \\
&+\frac{1}{\sqrt{g_{33}}}\frac{\Gamma_\eta}{\|\boldsymbol{\Gamma}\|}\frac{1}{S}\int_{\mathbb{E}^2_{a,b}} dS\,'w(\phi')\frac{\partial K(\lambda,\phi,\eta;\lambda',\phi',\eta_0)}{\partial\eta}\delta W(\lambda',\phi')
\end{aligned} \tag{1.34}$$

Box 1-11: First derivatives of ellipsoidal Abel-Poisson kernel, in closed form.

$$\begin{aligned}
\frac{\partial K(\lambda,\phi,\eta;\lambda',\phi',\eta_0)}{\partial\lambda} &= \frac{\partial K_{sph}(\lambda,\phi,\eta;\lambda',\phi',\eta_0)}{\partial\lambda} \\
&+\frac{\partial dK_{ellip}(\lambda,\phi,\eta;\lambda',\phi',\eta_0)}{\partial\lambda}
\end{aligned} \tag{1.35}$$

(i) $\partial K_{spherical}(\lambda,\phi,\eta;\lambda',\phi',\eta_0)\ /\ \partial\lambda$

$$\frac{\partial K_{sph}(\lambda,\phi,\eta;\lambda',\phi',\eta_0)}{\partial\lambda} = -3\frac{\cosh^2\eta_0\cos\phi\cos\phi'\sin\lambda\cos\lambda'}{f_\lambda^{5/2}\cosh^2\eta}$$

$$+3\frac{\cosh^2\eta_0\cos\phi\cos\phi'\cos\lambda\sin\lambda'}{f_\lambda^{5/2}\cosh^2\eta}$$

$$+3\frac{\cosh^4\eta_0\cos\phi\cos\phi'\sin\lambda\cos\lambda'}{f_\lambda^{5/2}\cosh^4\eta} \tag{1.36}$$

$$-3\frac{\cosh^4\eta_0\cos\phi\cos\phi'\cos\lambda\sin\lambda'}{f_\lambda^{5/2}\cosh^4\eta}$$

subject to

$$f_\phi = 1+\frac{\cosh^2\eta_0}{\cosh^2\eta}-\frac{\cosh\eta_0\sin\phi\sin\phi'}{\cosh\eta}$$

$$-2\frac{\cosh\eta_0\cos\phi\cos\phi'\cos\lambda\cos\lambda'}{\cosh\eta} \tag{1.37}$$

$$-2\frac{\cosh\eta_0\cos\phi\cos\phi'\sin\lambda\sin\lambda'}{\cosh\eta}$$

$$\frac{\partial K(\lambda,\phi,\eta;\lambda',\phi',\eta_0)}{\partial\phi} = \frac{\partial K_{spherical}(\lambda,\phi,\eta;\lambda',\phi',\eta_0)}{\partial\phi} + \frac{\partial dK_{ellipsoidal}(\lambda,\phi,\eta;\lambda',\phi',\eta_0)}{\partial\phi} \tag{1.38}$$

(i) $\partial K_{spherical}(\lambda,\phi,\eta;\lambda',\phi',\eta_0)\ /\ \partial\phi$

$$\frac{\partial K_{sph}(\lambda,\phi,\eta;\lambda',\phi',\eta_0)}{\partial\phi} = 3\frac{\cosh^2\eta_0\cos\phi\sin\phi'}{f_\phi^{5/2}\cosh^2\eta}$$

$$-3\frac{\cosh^2\eta_0\sin\phi\cos\phi'\cos\lambda\cos\lambda'}{f_\phi^{5/2}\cosh^2\eta}$$

$$-3\frac{\cosh^2\eta_0\sin\phi\cos\phi'\sin\lambda\sin\lambda'}{f_\phi^{5/2}\cosh^2\eta}$$

$$-3\frac{\cosh^4\eta_0\cos\phi\sin\phi'}{f_\phi^{5/2}\cosh^4\eta}$$

$$+3\frac{\cosh^4\eta_0\sin\phi\cos\phi'\cos\lambda\cos\lambda'}{f_\phi^{5/2}\cosh^4\eta}$$

$$+3\frac{\cosh^4\eta_0\sin\phi\cos\phi'\sin\lambda\sin\lambda'}{f_\phi^{5/2}\cosh^4\eta}$$

subject to

$$f_\phi=1+\frac{\cosh^2\eta_0}{\cosh^2\eta}-2\frac{\cosh\eta_0\sin\phi\sin\phi'}{\cosh\eta}$$
$$-2\frac{\cosh\eta_0\cos\phi\cos\phi'\cos\lambda\cos\lambda'}{\cosh\eta} \tag{1.39}$$
$$-2\frac{\cosh\eta_0\cos\phi\cos\phi'\sin\lambda\sin\lambda'}{\cosh\eta}$$

$$\frac{\partial K(\lambda,\phi,\eta;\lambda',\phi',\eta_0)}{\partial\eta}=\frac{\partial K_{sph}(\lambda,\phi,\eta;\lambda',\phi',\eta_0)}{\partial\eta}+\frac{\partial dK_{ellip}(\lambda,\phi,\eta;\lambda',\phi',\eta_0)}{\partial\eta} \tag{1.40}$$

(i) $\partial K_{spherical}(\lambda,\phi,\eta;\lambda',\phi',\eta_0)\ /\ \partial\eta$

$$\frac{\partial K_{sph}(\lambda,\phi,\eta;\lambda',\phi',\eta_0)}{\partial\eta}$$
$$=-\frac{\cos\eta_0\sinh\eta}{f_\eta^{3/2}\cosh^2\eta}+3\frac{\cos^3\eta_0\sinh\eta}{f_\eta^{3/2}\cosh^4\eta}$$
$$+3\frac{\cos^3\eta_0\sinh\eta}{f_\eta^{5/2}\cosh^4\eta}-3\frac{\cos^2\eta_0\sinh\eta\sin\phi\sin\phi'}{f_\eta^{5/2}\cosh^3\eta}$$
$$-3\frac{\cos^2\eta_0\sinh\eta\cos\phi\cos\phi'\cos\lambda\cos\lambda'}{f_\eta^{5/2}\cosh^3\eta}$$
$$-3\frac{\cos^2\eta_0\sinh\eta\cos\phi\cos\phi'\sin\lambda\sin\lambda'}{f_\eta^{5/2}\cosh^3\eta}$$
$$-3\frac{\cos^5\eta_0\sinh\eta}{f_\eta^{5/2}\cosh^6\eta}+3\frac{\cos^4\eta_0\sinh\eta\sin\phi\sin\phi'}{f_\eta^{5/2}\cosh^5\eta}$$
$$+3\frac{\cos^4\eta_0\sinh\eta\cos\phi\cos\phi'\cos\lambda\cos\lambda'}{f_\eta^{5/2}\cosh^5\eta} \tag{1.41}$$
$$+3\frac{\cos^4\eta_0\sinh\eta\cos\phi\cos\phi'\sin\lambda\sin\lambda'}{f_\eta^{5/2}\cosh^5\eta}$$

subject to

$$f_\eta = 1 + \frac{\cosh^2\eta_0}{\cosh^2\eta} - 2\frac{\cosh\eta_0 \sin\phi \sin\phi'}{\cosh\eta}$$
$$-2\frac{\cosh\eta_0 \cos\phi \cos\phi' \cos\lambda \cos\lambda'}{\cosh\eta}$$
$$-2\frac{\cosh\eta_0 \cos\phi \cos\phi' \sin\lambda \sin\lambda'}{\cosh\eta} \quad (1.42)$$

Note that the derivatives of the ellipsoidal correction-part of the kernel are not presented here!

1.5 Modified ellipsoidal Abel-Poisson kernel

The closed form solution of the *Abel-Poisson kernel* presented in the previous section contains the effect of harmonics of all degree and order. However, since in preparation of the *incremental* quantities (δW , $\delta\Gamma$) we remove the effect of a reference field made up of ellipsoidal harmonic expansion up to degree/order 360/360, naturally the effect of these harmonics must also be removed from the *Abel-Poisson kernel*. However, the most dominant parts are coming from the zero and first. degree/order harmonics. Those harmonics are reflecting the effects originated from the mass of the earth GM , and the origin of the coordinate system. The *modified Abel-Poisson kernel* after removal of the zero and first-degree harmonics is given in *Box 1-12*.

Box 1-12: Removal of the *zero* and *first-degree* harmonics form the *Abel-Poisson integral*.

(i) *Spectral form of the ellipsoidal Abel-Poisson kernel*

$$K(\lambda,\phi,\eta;\lambda',\phi',\eta_0) = \sum_{n=0}^{\infty}\sum_{m=-n}^{n} \frac{Q_{n|m|}(i\sinh\eta)}{Q_{n|m|}(i\sinh\eta_0)} e_{nm}(\lambda',\phi') e_{nm}(\lambda,\phi)$$
$$= \sum_{n=0}^{\infty}\sum_{m=-n}^{n} \frac{Q^*_{n|m|}(\sinh\eta)}{Q^*_{n|m|}(\sinh\eta_0)} e_{nm}(\lambda',\phi') e_{nm}(\lambda,\phi)$$
$$= \sum_{n=0}^{\infty}\sum_{m=-n}^{n} K_{n,m}$$

Subject to

$$Q^*_{nm}(\sinh\eta) = i^{n+1} Q_{nm}(i\sinh\eta) \quad (1.44)$$

(ii) zero-degree term of the ellipsoidal Abel-Poisson kernel

$$K_{0,0}(\lambda,\phi,\eta;\lambda',\phi',\eta_0)=\frac{Q_{0,0}(i\sinh\eta)}{Q_{0,0}(i\sinh\eta_0)}=\frac{\cot^{-1}(\sinh\eta)}{\cot^{-1}(\sinh\eta_0)} \tag{1.45}$$

(iii) first-degree term of the ellipsoidal Abel-Poisson kernel

$$\begin{aligned}K_{1,0}(\lambda,\phi,\eta;\lambda',\phi',\eta_0)&=\frac{Q^*_{1,0}(\sinh\eta)}{Q^*_{1,0}(\sinh\eta_0)}P^*_{10}(\sin\phi)P^*_{10}(\sin\phi')\\&=3\frac{1-\sinh\eta\cot^{-1}(\sinh\eta)}{1-\sinh\eta_0\cot^{-1}(\sinh\eta_0)}\sin\phi\sin\phi'\end{aligned} \tag{1.46}$$

Subject to

$$\begin{aligned}P^*_{10}(\sin\phi)&=\sqrt{3}\sin\phi\\P^*_{11}(\sin\phi)&=\sqrt{3}\cos\phi\end{aligned} \tag{1.47}$$

$$\begin{aligned}Q^*_{00}(i\sinh\eta)&=\cot^{-1}(\sinh\eta)\\Q^*_{10}(i\sinh\eta)&=1-\sinh\eta\cot^{-1}(\sinh\eta)\\Q^*_{11}(i\sinh\eta)&=\tanh\eta-\cosh\eta\cot^{-1}(\sinh\eta)\end{aligned} \tag{1.48}$$

(iv) Modified ellipsoidal Abel-Poisson kernel

$$\begin{aligned}K^*_{ellipsoidal}(\lambda,\phi,\eta;\lambda',\phi',\eta_0)=K_{spherical}&(\lambda,\phi,\eta;\lambda',\phi',\eta_0)\\&+dK_{ellipsoidal}(\lambda,\phi,\eta;\lambda',\phi',\eta_0)\\&-K_{00}-K_{10}\end{aligned} \tag{1.49}$$

Let us now have a look at the shape of the modified *Poisson kernel* $K^*_{ellipsoidal}$ as derived in *Box 1-12*. *Figure 1-5* illustrates the variation of the modified ellipsoidal Abel-Poisson kernel $K_{ellipsoidal}(\lambda,\phi,\eta;\lambda',\phi',\eta_0)$ versus angular distance ψ. This figure is plotted for variations of the kernel at the point $\{\lambda,\phi,\eta\}=\{9.617432869327^\circ,\ 49.7039340502^\circ,\ 3.19471515096\}$, with respect to the reference ellipsoid $\eta_0=3.194713581445341$ along the azimuth $\alpha=10^\circ$. *Figure 1-6* shows the variation of the modified ellipsoidal Abel-Poisson kernel $K_{ellipsoidal}(\lambda,\phi,\eta;\lambda',\phi',\eta_0)$ versus azimuth α, calculated for the same point, when the running point of integral is fixed along the space angle $\psi=1^\circ$. *Figure 1-7* is the same as *Figure 1-6*, except that it is plotted in percentage of the value of the kernel at $\alpha=0^\circ$. As it is shown in *Figure 1-7* dependency of the modified ellipsoidal Abel-Poisson kernel on azimuth is not exceeding 0.3 percent of the whole kernel's value at $\alpha=0^\circ$.

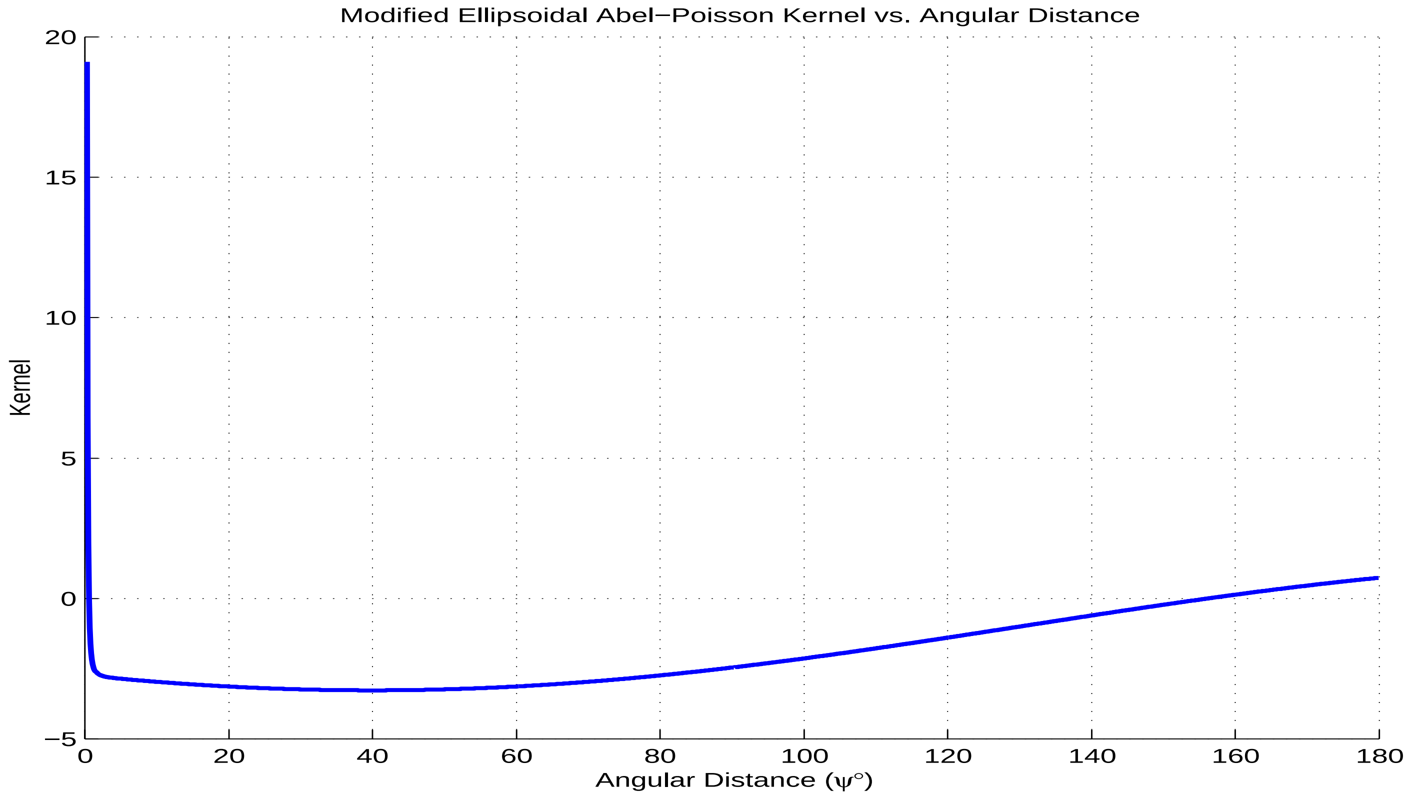

Figure 1-5: Variation of the Modified ellipsoidal Abel-Poisson kernel $K_{ellipsoidal}(\lambda, \phi, \eta; \lambda', \phi', \eta_0)$ versus angular distance ψ. Calculated for the point $\{\lambda, \phi, \eta\} = \{9.617432869327196^\circ, 49.70393405021537^\circ, 3.194715150960513\}$, with respect to the reference ellipsoid $\eta_0 = 3.194713581445341$ along the azimuth $\alpha = 10^\circ$.

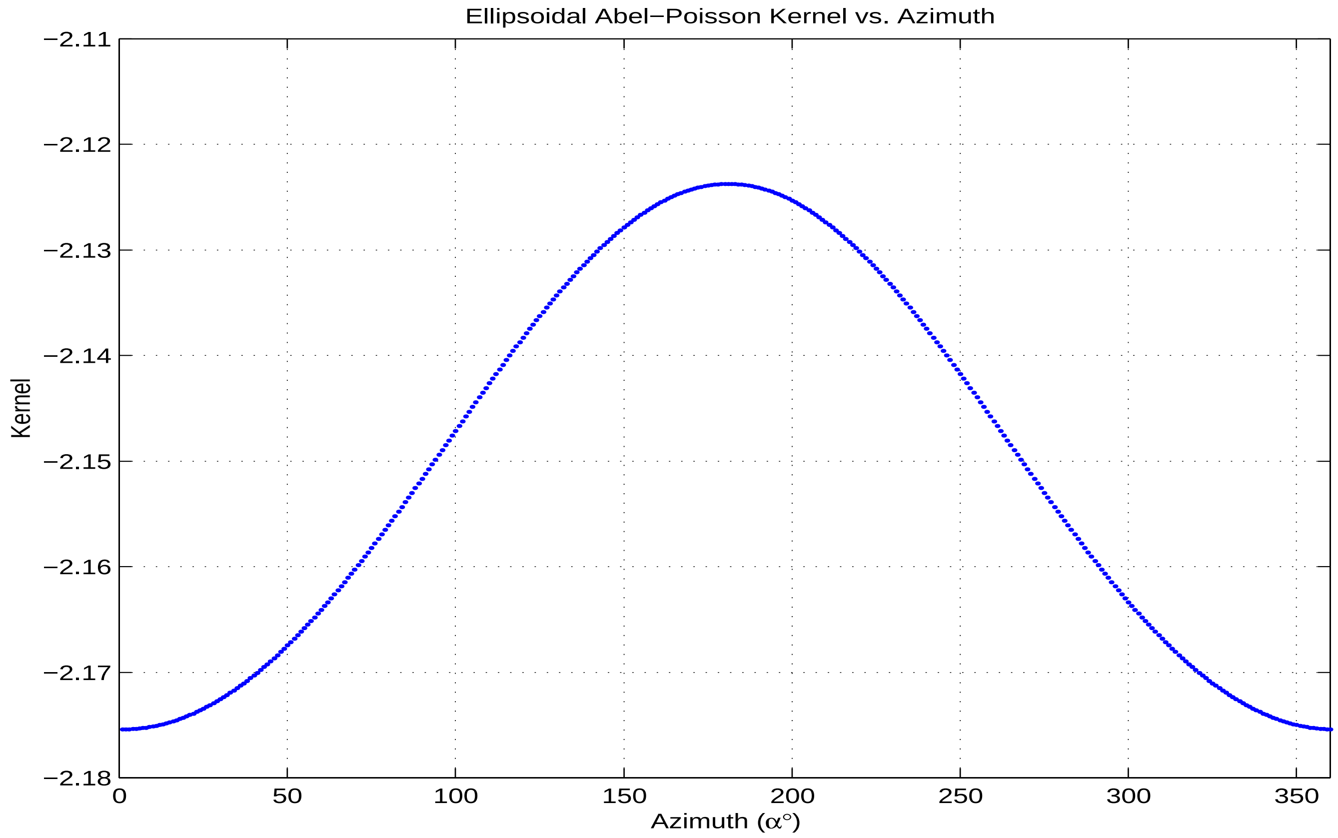

Figure 1-6: Variation of the modified ellipsoidal Abel-Poisson kernel $K_{ellipsoidal}(\lambda,\phi,\eta;\lambda',\phi',\eta_0)$ versus azimuth α. Calculated for the point $\{\lambda,\phi,\eta\} = \{9.617432869327196^{\circ},\ 49.70393405021537^{\circ},\ 3.194715150960513\}$ with respect to the reference ellipsoid $\eta_0 = 3.194713581445341$ at the space angle $\psi = 1^{\circ}$.

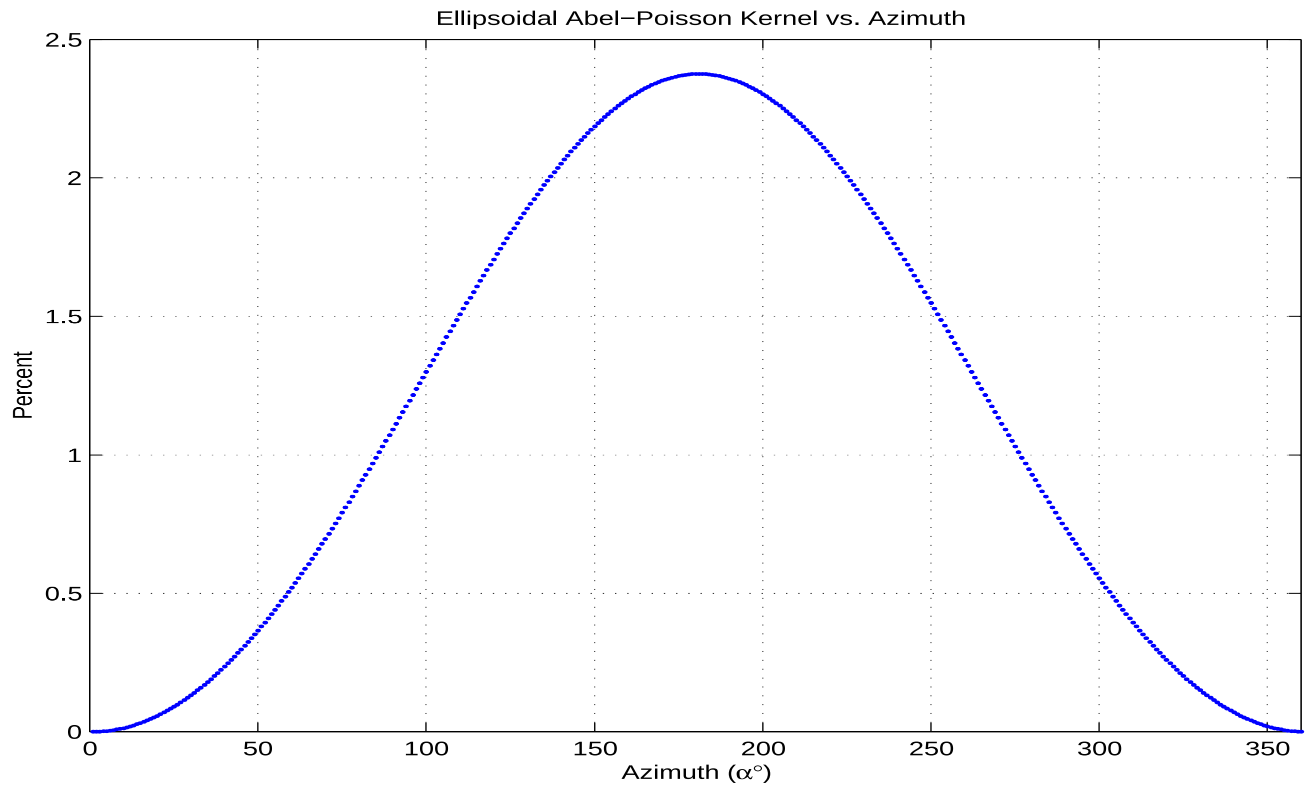

Figure 1-7: Variation of the Modified ellipsoidal Abel-Poisson kernel $K_{ellipsoidal}(\lambda, \phi, \eta; \lambda', \phi', \eta_0)$ versus azimuth α, in terms of percentage of the value of the kernel at $\alpha = 0^\circ$. Calculations are for the point $\{\lambda, \phi, \eta\} = \{9.617432869327196^\circ, 49.70393405021537^\circ, 3.194715150960513\}$ with respect to the reference ellipsoid $\eta_0 = 3.194713581445341$ at the space angle $\psi = 1^\circ$.

Similar modified kernel can also be derived for the kernel of e*llipsoidal Abel-Poisson integral of* the *incremental* gravitational intensity $\delta\Gamma$. Indeed, what we have to do is to remove the derivatives of the zero and first terms of the kernel of e*llipsoidal Abel-Poisson integral for incremental* gravitational intensity $\delta\Gamma$ of *Box 1-10*. Those derivatives are collected in *Box 1-13*.

Box 1-13: First derivatives of zero order and first terms of ellipsoidal Abel-Poisson kernel.

$$\begin{cases} \dfrac{\partial K_{00}}{\partial \lambda} = 0 \\ \dfrac{\partial K_{00}}{\partial \phi} = 0 \\ \dfrac{\partial K_{00}}{\partial \eta} = -\dfrac{1}{\cosh\eta \cot^{-1}(\sinh\eta_0)} \end{cases} \tag{1.50}$$

$$\begin{cases} \dfrac{\partial K_{10}}{\partial \lambda} = 0 \\ \dfrac{\partial K_{10}}{\partial \phi} = \dfrac{\left[3 - 3\sinh\eta \cot^{-1}(\sinh\eta)\right]\cos\phi \sin\phi'}{1 - \sinh\eta_0 \cot^{-1}(\sinh\eta_0)} \\ \dfrac{\partial K_{10}}{\partial \eta} = 3\dfrac{\left[\cosh^2\eta \cot^{-1}(\sinh\eta) - \sinh\eta\right]\sin\phi \sin\phi'}{\left[-1 + \sinh\eta_0 \cot^{-1}(\sinh\eta_0)\right]\cosh\eta} \end{cases} \tag{1.51}$$

In the next section, we shall be concentrating on the determination of general form of the *Bruns formula*. Such a study is quite necessary since the *Bruns formula* plays a crucial role in our geoid calculation. Indeed, it provides us with the transformation relation between the *incremental* gravity potential at the surface of reference ellipsoid of the *Somigliana-Pizzetti* type and the geoidal undulation.

1.6 General Bruns transformation

The result of the remove, downward continuation, and restore is the gravity potential $w(\lambda, \phi, \eta_0)$ at the surface of reference ellipsoid $\mathbb{E}^2_{a,b}$. As was mentioned before the gravity potential on the surface of the reference ellipsoid $\mathbb{E}^2_{a,b}$ can be converted into the geoidal undulations h via the *Bruns formula*. Such a transformation requires the reference ellipsoid

$\mathbb{E}^2_{a,b}$, be a reference level surface /equipotential surface/ with the gauge value w_0, i.e. $W(\lambda, \phi, \eta) = w_0$.

A summary of the derivation of the most general form of *Bruns formula /Bruns transformation/* is given in *Box 1-14*. The derivation starts with the decomposition of the actual *gravity potential* $w(\mathbf{x})$ at the geoid surface $\mathbf{x} \in \partial\mathcal{G}_i =: \mathbb{M}^2_g$, into *reference gravity potential* $W(\mathbf{x})$ and *incremental* potential $\delta W(\mathbf{x})$, within equation (1.52). In the second step the reference potential $W(\mathbf{x})$ at the geoid and incremental gravity potential at the geoid $\delta W(\mathbf{x})$ are represented by a *Taylor* series expansion for the expansion point on the surface of the reference equipotential surface $\mathbf{X} \in \mathbb{M}^2_G$, through equations (1.53)-(1.54). Remarkable issues related to the *Taylor* expansion here are:

(i) The directional derivative $\nabla_N W(\mathbf{X})$, which is along the normal to the surface of the ellipsoid $\mathbb{E}^2_{a,b}$ (see *Appendix F*, *page 236* for the advantage of presenting the Taylor series expansion in terms of directional derivative operator).

(ii) The height *h*, which due to the type of directional derivatives applied, is of *isozenithal* type.

The *Taylor* expansion leads to forward transformation equation from geometry space into gravity space, shown in power series of isozenithal height *h*, equation in (1.56). It is important to note that here we have given way to different potential values on the geoid and reference ellipsoid $w_0 - W_0 =: \Delta W(\mathbf{x}, \mathbf{X})$, see equation (1.56). This will keep the *Bruns transformation* at its most general form. The series (1.56) is a *homogeneous polynomial* and can be inverted according to the series inversion developed by *E. Grafarend et al.* (1996) to backward transformation from gravity space into geometry space, according to equation (1.57). The first few coefficients of inverse series expansion according to *E. Grafarend et al.* (1996) are collected in *Box 1-15*. In connection with the *Non-linear Bruns transformation* related contributions by *E. Grafarend and W. Niemeier* (1971) and *E. Grafarend et al.* (1999) can be acknowledged. *Box 1-16* covers the highlights of the *directional derivative* $\nabla_{\mathbf{Y}}\mathbf{X} := \langle \nabla\mathbf{X} | \mathbf{Y} \rangle$.

Box 1-14: General form of the *Bruns* transformation.

(i) Decomposition of the actual *gravity potential* $w(\mathbf{x})$ into reference potential $W(\mathbf{x})$ and *incremental* potential $\delta W(\mathbf{x})$

$$w(\mathbf{x}) = W(\mathbf{x}) + \delta W(\mathbf{x}) \tag{1.52}$$

$$\forall\ \mathbf{x} \in \partial\mathcal{G}_i =: \mathbb{M}_g^2 \text{ and } \mathbf{X} \in \mathbb{M}_G^2 \text{ e.g. } \mathbb{E}_{a,b}^2$$

$\mathbb{M}_g^2$ presents the geoid's surface, and $\mathbb{M}_G^2$ presents the surface of a reference equipotential surface .

(ii) *Taylor* series expansion of the *reference gravity potential* and *incremental gravity potential* reads as

$$W(\mathbf{x}) = W(\mathbf{X}) + \frac{1}{1!}(\nabla_N W(\mathbf{X}))h + \frac{1}{2!}(\nabla_N \nabla_N W(\mathbf{X}))h^2 + \mathcal{O}_W(h^3) \tag{1.53}$$

$$\delta W(\mathbf{x}) = \delta W(\mathbf{X}) + \frac{1}{1!}(\nabla_N \delta W(\mathbf{X}))h + \frac{1}{2!}(\nabla_N \nabla_N \delta W(\mathbf{X}))h^2 + \mathcal{O}_{\delta W}(h^3) \tag{1.54}$$

Where directional derivatives ∇_N are along the normal to the equipotential surfaces $\mathbb{M}_G^2$, i.e. reference ellipsoid $\mathbb{E}_{a,b}^2$. h is called *normal isozenithal height.*

(iii) Forward transformation from geometry space into gravity space

$$\begin{aligned} w_0 = w(\mathbf{x}) = W(\mathbf{x}) + \delta W(\mathbf{x}) &= W(\mathbf{X}) + \sum_{n=1}^{\infty} a_{1n} h^n + \delta W(\mathbf{X}) \\ &= W_0 + \sum_{n=1}^{\infty} a_{1n} h^n + \delta W(\mathbf{X}) \end{aligned} \tag{1.55}$$

$$\Leftrightarrow$$

$$-\delta W(\mathbf{X}) + w_0 - W_0 = -\delta W(\mathbf{X}) + \Delta W(\mathbf{x}, \mathbf{X}) = \sum_{n=1}^{\infty} a_{1n} h^n \tag{1.56}$$

$$\forall \mathbf{x} \in \partial G := \mathbb{M}_g^2 \text{ and } \mathbf{X} \in \mathbb{M}_G^2 \text{ e.g. } \mathbb{E}_{a,b}^2$$

subject to

$$a_{11} := \frac{1}{1!}\nabla_N W(\mathbf{X}) + \frac{1}{1!}\nabla_N \delta W(\mathbf{X}),$$

$$a_{12} = \frac{1}{2!}\nabla_N \nabla_N W(\mathbf{X}) + \frac{1}{2!}\nabla_N \nabla_N \delta W(\mathbf{X}),$$

$$\dots$$

$$a_{1n} := \frac{1}{n!}\underbrace{\nabla_N \dots \nabla_N}_{\text{n times}} W(\mathbf{X}) + \frac{1}{n!}\underbrace{\nabla_N \dots \nabla_N}_{\text{n times}} \delta W(\mathbf{X})$$

(iv) Backward transformation from gravity space into geometry space

$$h = \sum_{n=1}^{\infty} b_{1n} [-\delta W(\mathbf{X}) + \Delta W(\mathbf{x}, \mathbf{X})]^n \tag{1.57}$$

subject to

$$b_{11} := \frac{1}{\nabla_N W(\mathbf{X}) + \nabla_N \delta W(\mathbf{X})}$$

$$b_{12} := -\frac{1}{(\nabla_N W(\mathbf{X}) + \nabla_N \delta W(\mathbf{X}))^3}\left(\frac{1}{2!}\nabla_N\nabla_N W(\mathbf{X}) + \frac{1}{2!}\nabla_N\nabla_N \delta W(\mathbf{X})\right)$$

$$b_{13} := \frac{(\nabla_N\nabla_N W(\mathbf{X}) + \nabla_N\nabla_N \delta W(\mathbf{X}))^2}{2(\nabla_N W(\mathbf{X})\nabla_N \delta W(\mathbf{X}))^6} - \frac{\nabla_N\nabla_N\nabla_N W(\mathbf{X}) + \nabla_N\nabla_N\nabla_N \delta W(\mathbf{X})}{6(\nabla_N W(\mathbf{X}) + \nabla_N \delta W(\mathbf{X}))^4}$$

$$\ldots$$

The two-point function $\Delta W(\mathbf{x}, \mathbf{X})$, called *Laplace* Δ- *increments*, is defined as follows

$$\Delta W(\mathbf{x}, \mathbf{X}) := w(\mathbf{x}) - W(\mathbf{X}) \tag{1.58}$$

Box 1-15: Inversion of a *homogeneous polynomial*

$$y(x) = a_{11}x + a_{12}x^2 + \cdots + a_{1n}x^n \tag{1.59}$$

versus

$$x(y) = b_{11}y + b_{12}y^2 + \cdots + b_{1n}y^n \tag{1.60}$$

subject to

$$b_{11} = a_{11}^{-1}$$
$$b_{12} = a_{11}^{-3}a_{12}$$
$$b_{13} = 2a_{11}^{-6}a_{12}^2 - a_{11}^{-4}a_{13}$$
$$\ldots$$

Box 1-16: Directional derivative $\nabla_v w$

(i) *Directional derivative* $\nabla_v w$ of a function w from a vector space $w \in \mathbb{V}$ equipped with a canonical differential structure

$$\nabla_v w := \langle dw | v \rangle = \left\langle \operatorname{grad} w \middle| v \right\rangle \tag{1.61}$$

(ii) the properties of the directional derivative

(1) $\nabla_v(w_1 + w_2) = \nabla_v w_1 + \nabla_v w_2$

(2) $\nabla_v(\tau w) = \tau\nabla_v w + (\nabla_v \tau)w$

(3) $\nabla_{v_1+v_2} w = \nabla_{v_1} w + \nabla_{v_2} w$

(4) $\nabla_{\tau v} w = \tau \nabla_v w$;

where $\tau \in \mathbb{R}$ and $(w_1, w_2, \nu_1, \nu_2) \in \mathbb{V}$.

In the next section, we shall restrict the general representation of the *Bruns formula*, derived in *Box 1-14*, to the *Jacobi ellipsoidal coordinates*

$\{\lambda, \phi, \eta\}$ and to the reference ellipsoidal field of the first order term of ellipsoidal harmonic expansion.

1.7 Non-linear ellipsoidal Bruns transformation

In the previous section, we derived the most general form of the *Bruns transformation.* Here, we derive an especial *non-linear ellipsoidal* form of it in terms of *Jacobi ellipsoidal coordinates* $\{\lambda, \phi, \eta\}$. If we limit ourselves to the order of accuracy of first eccentricity squared $\mathcal{O}(e^2)$ ($e^2 = (a^2 - b^2)/a^2$) then the first term of ellipsoidal harmonic expansion, $U(\lambda, \phi, \eta) = gm/\varepsilon \operatorname{arc}\cot(\sinh \eta)$, can be used as the reference gravitational field. The order of accuracy of $\mathcal{O}(e^2)$ is enough for the geoid determination at centimetre accuracy level (see e.g. *Z. Martinec* 1998a, and *Z. Martinec and Grafarend* 1997a, 1997b). Such a reference field besides its simple form has the property of having ellipsoidal level surfaces (see *Box 1-20* for the proof). Since we want to present the deviation /the disturbance/ of the actual equipotential field of the earth from reference field of an ellipsoid of revolution this model is the correct choice.

Box 1-17 presents the definition of the gradient of the scalar function $U(\lambda, \phi, \eta)$ as the covariant derivative $D_\mu U$ of the function $U(\lambda, \phi, \eta)$ with respect to contravariant base vectors $\boldsymbol{\mu}^\mu$. The contravariant base vectors are replaced by $g^{\mu\nu}\boldsymbol{\mu}_\nu$, the transformation relation of covariant base vectors into contravariant ones. The non-normalised covariant base vectors $\boldsymbol{\mu}_\nu$ are further written in terms of normalised base vectors $\mathbf{e}_\nu$ multiplied by the norm of $\boldsymbol{\mu}_\nu$ ($\boldsymbol{\mu}_\nu = \sqrt{g_{\nu\nu}}\mathbf{e}_\nu$). Finally the orthogonality of the *Jacobi ellipsoidal* base vectors has led to special representations of (1.63) and (1.64). *Box 1-18* provides us with the directional derivative along the surface-normals of reference ellipsoid $\mathbb{E}^2_{a,b}$, while *Box 1-19* presents the application of the directional derivatives to the reference gravitational potential field $U(\lambda, \phi, \eta) = gm/\varepsilon \operatorname{arc}\cot(\sinh \eta)$. We have to mention that in *Box 1-19* we have gone up to directional *second order* derivatives. Finally, under the assumptions and approximations collected in *Box 1-21*, *non-linear ellipsoidal Bruns transformation formula* of *Box 1-22* is derived.

Box 1-17: Gradient of a scalar function $U(\lambda, \phi, \eta)$

(i) General definition of the gradient of a scalar function in terms of a curvilinear coordinate system

$$\begin{aligned} \operatorname{grad} U &= \mathbf{m}^{\mu} D_{\mu} U = g^{\mu\nu} \mathbf{m}_{\nu} D_{\mu} U \\ &= g^{\mu\nu} \| \mathbf{m}_{\nu} \| \mathbf{e}_{\nu} D_{\mu} U = g^{\mu\nu} \sqrt{g_{\nu\nu}} \mathbf{e}_{\nu} D_{\mu} U \end{aligned} \tag{1.62}$$

(ii) Gradient of the scalar function U in terms of orthogonal Jacobi ellipsoidal coordinates $\{\lambda, \phi, \eta\}$

$$\operatorname{grad} U = \mathbf{E}_{\lambda} \frac{1}{\sqrt{g_{\lambda\lambda}}} D_{\lambda} U + \mathbf{E}_{\phi} \frac{1}{\sqrt{g_{\phi\phi}}} D_{\phi} U + \mathbf{E}_{\eta} \frac{1}{\sqrt{g_{\eta\eta}}} D_{\eta} U \tag{1.63}$$

$$\Rightarrow$$

$$\begin{aligned} \operatorname{grad} U = {} & \mathbf{E}_{\lambda} \frac{1}{\varepsilon \cosh \eta \cos \phi} D_{\lambda} U + \mathbf{E}_{\phi} \frac{1}{\varepsilon \sqrt{\cosh^2 \eta - \cos^2 \phi}} D_{\phi} U \\ & + \mathbf{E}_{\eta} \frac{1}{\varepsilon \sqrt{\cosh^2 \eta - \cos^2 \phi}} D_{\eta} U \end{aligned} \tag{1.64}$$

Box 1-18: Directional derivative along the surface normal of the reference ellipsoid $\mathbb{E}^2_{a,b}$

$$\langle \operatorname{grad} U | \mathbf{E}_{\eta} \rangle = \nabla_{\mathbf{E}_{\eta}} U = \frac{1}{\varepsilon \sqrt{\cosh^2 \eta - \cos^2 \phi}} D_{\eta} U = \frac{1}{\sqrt{g_{\eta\eta}}} \partial_{\eta} U \tag{1.65}$$

Box 1-19: Reference ellipsoidal gravitational field and its directional derivatives along the surface normals of reference ellipsoid $\mathbb{E}^2_{a,b}$

(i) Reference ellipsoidal field of the first order

$$U(\lambda, \phi, \eta) = \frac{gm}{\varepsilon} \operatorname{arc} \cot(\sinh \eta) \tag{1.66}$$

(ii) Directional derivative along the surface normals of $\mathbb{E}^2_{a,b}$

$$\begin{aligned} \nabla_N U &= \nabla_{\mathbf{E}_{\eta}} U = \frac{1}{\sqrt{g_{\eta\eta}}} \partial_{\eta} U = \frac{1}{\varepsilon \sqrt{\cosh^2 \eta - \cos^2 \phi}} D_{\eta} U \\ &= -\frac{gm}{\varepsilon^2 \cosh \eta (\cosh^2 \eta - \cos^2 \phi)^{1/2}} \end{aligned} \tag{1.67}$$

$$
\begin{aligned}
\nabla_N \nabla_N U = \nabla_{\mathbf{E}_\eta} \nabla_{\mathbf{E}_\eta} U = \frac{1}{\sqrt{g_{\eta\eta}}} \partial_\eta \nabla_{\mathbf{E}_\eta} U = \frac{1}{\varepsilon\sqrt{\cosh^2\eta - \cos^2\phi}} D_\eta \nabla_{\mathbf{E}_\eta} U \\
= gm \frac{\sinh\eta\left(2\cosh^2\eta - \cos^2\phi\right)}{\varepsilon^3 \cosh^2\eta(\cosh^2\eta - \cos^2\phi)^2}
\end{aligned}
\tag{1.68}
$$

Box 1-20: Geometrical interpretation of the reference equipotential surface $U(\lambda,\phi,\eta) = gm/\varepsilon \operatorname{arc\,cot}(\sinh\eta) = w_0$.

from the reference equipotential surface

$$U(\lambda,\phi,\eta) = \frac{gm}{\varepsilon} \operatorname{arc\,cot}(\sinh\eta) = w_0 \tag{1.69}$$

one can imply that the only varying parameter, i.e., η must be constant

$$\eta = \eta_0 \tag{1.70}$$

from the inverse transformation of Cartesian coordinates $\{x,y,z\}$ into Jacobi ellipsoidal coordinate η (cf. *Appendix A.1.2* (*page 209*)) we have

$$
\begin{aligned}
\eta &= \operatorname{arccosh}\{\frac{1}{2\varepsilon^2}[x^2+y^2+z^2+\varepsilon^2 \\
&+\sqrt{(x^2+y^2+z^2+\varepsilon^2)^2 - 4\varepsilon^2(x^2+y^2)}]\}^{1/2} \\
&= \eta_0 \\
&\Leftrightarrow \{\frac{1}{2\varepsilon^2}[x^2+y^2+z^2+\varepsilon^2 \\
&+\sqrt{(x^2+y^2+z^2+\varepsilon^2)^2 - 4\varepsilon^2(x^2+y^2)}]\}^{1/2} \\
&= \cosh\eta_0 \\
&\Leftrightarrow \frac{1}{2\varepsilon^2}[x^2+y^2+z^2+\varepsilon^2 \\
&+\sqrt{(x^2+y^2+z^2+\varepsilon^2)^2 - 4\varepsilon^2(x^2+y^2)}] \\
&= \cosh^2\eta_0 \\
&\Leftrightarrow \sqrt{(x^2+y^2+z^2+\varepsilon^2)^2 - 4\varepsilon^2(x^2+y^2)} \\
&= 2\varepsilon^2\cosh^2\eta_0 - \left(x^2+y^2+z^2+\varepsilon^2\right) \\
&\Leftrightarrow (x^2+y^2+z^2+\varepsilon^2)^2 - 4\varepsilon^2(x^2+y^2) \\
&= 4\varepsilon^4\cosh^4\eta_0 - 4\varepsilon^2\left(x^2+y^2+z^2+\varepsilon^2\right)\cosh^2\eta_0 \\
&+\left(x^2+y^2+z^2+\varepsilon^2\right)^2 \\
&\Leftrightarrow \left(-4\varepsilon^2 + 4\varepsilon^2\cosh^2\eta_0\right)(x^2+y^2) \\
&+\left(4\varepsilon^2\cosh^2\eta_0\right)z^2 \\
&= 4\varepsilon^4\cosh^4\eta_0 - 4\varepsilon^4\cosh^2\eta_0
\end{aligned}
\tag{1.71}
$$

$$\Leftrightarrow (\sinh^2 \eta_0)(x^2 + y^2) + (\cosh^2 \eta_0) z^2$$
$$= \varepsilon^2 \cosh^2 \eta_0 \sinh^2 \eta_0$$
$$\Leftrightarrow \frac{x^2 + y^2}{\varepsilon^2 \cosh^2 \eta_0} + \frac{z^2}{\varepsilon^2 \sinh^2 \eta_0} = 1$$

which is the equation of the reference ellipsoid $\mathbb{E}^2_{\varepsilon \cosh \eta_0, \varepsilon \sinh \eta_0}$.

Box 1-21: Assumptions and approximations used in the derivation of non-linear ellipsoidal Bruns transformation formula of *Box 1-22*.

(i) Equality of the actual gravity potential on the geoid to the reference potential on the reference ellipsoid $\mathbb{E}^2_{a,b}$

$$w(\mathbf{x}) = W(\mathbf{X}) \quad \forall \mathbf{x} \in \partial \mathcal{G}_i := \mathbb{M}^2_g \quad \text{and} \quad \mathbf{X} \in \mathbb{M}^2_G, \text{ i.e. } \mathbb{E}^2_{a,b} \tag{1.72}$$

$$\Rightarrow \Delta W(\mathbf{x}, \mathbf{X}) := w(\mathbf{x}) - W(\mathbf{X}) = 0 \tag{1.73}$$

(ii) Directional derivatives of the incremental potential

$$\nabla_N \delta W(\mathbf{X}) = \nabla_N \nabla_N \delta W(\mathbf{X}) = \cdots = \underbrace{\nabla_N \ldots \nabla_N}_{\text{n times}} \delta W(\mathbf{X}) = 0 + \mathcal{O}(e^2)$$

(iii) Reference gravity potential field

$$W(\mathbf{x}) = \sum_{n=0}^{360} \sum_{m=-n}^{+n} u_{nm} \frac{Q^*_{n|m|}(\sinh \eta)}{Q^*_{n|m|}(\sinh \eta_0)} e_{nm}(\lambda, \phi) + \frac{1}{2} \omega^2 \varepsilon^2 \cosh^2 \eta \cos^2 \phi \tag{1.75}$$

(iv) Reference gravitational potential field

$$U(\lambda, \phi, \eta) = \frac{gm}{\varepsilon} \operatorname{arc\,cot}(\sinh \eta) \tag{1.76}$$

Box 1-22: *Non-linear ellipsoidal Bruns transformation*

$$h = \sum_{n=1}^{\infty} b_{1n} [-\delta W(\mathbf{X}) + \Delta W(\mathbf{x}, \mathbf{X})]^n \underset{w(\mathbf{x}) = W(\mathbf{X})}{=} \sum_{n=1}^{\infty} b_{1n} [-\delta W(\mathbf{X})]^n$$

subject to

$$
\begin{aligned}
b_{11} &:= \frac{1}{\nabla_N W(\mathbf{X}) + \nabla_N \delta W(\mathbf{X})} \underset{\nabla_N \delta W(\mathbf{X})=0+\mathcal{O}(e^2)}{=} \frac{1}{\nabla_N W(\mathbf{X})} + \mathcal{O}(e^2) \\
&= \frac{1}{\nabla_{\mathbf{E}_\eta} U} + \mathcal{O}(e^2) = (\frac{1}{\sqrt{g_{\eta\eta}}} \partial_\eta U)^{-1} + \mathcal{O}(e^2) \\
&= (\frac{1}{\varepsilon\sqrt{\cosh^2\eta - \cos^2\phi}} D_\eta U)^{-1} + \mathcal{O}(e^2) \\
&= -\frac{\varepsilon^2 \cosh\eta (\cosh^2\eta - \cos^2\phi)^{1/2}}{gm} + \mathcal{O}(e^2)
\end{aligned} \tag{1.78}
$$

$$
\begin{aligned}
b_{12} &:= -\frac{1}{(\nabla_N W(\mathbf{X}) + \nabla_N \delta W(\mathbf{X}))^3}\left(\frac{1}{2!}\nabla_N\nabla_N W(\mathbf{X}) + \frac{1}{2!}\nabla_N\nabla_N \delta W(\mathbf{X})\right) \\
&\underset{\nabla_N\nabla_N \delta W(\mathbf{X})=0+\mathcal{O}(e^2)}{=} -\frac{1}{(\nabla_N W(\mathbf{X}))^3}\left(\frac{1}{2!}\nabla_N\nabla_N W(\mathbf{X})\right) + \mathcal{O}(e^2) \\
&= -(\frac{\varepsilon^2 \cosh\eta (\cosh^2\eta - \cos^2\phi)^{1/2}}{gm})^3 \\
&\quad \times(\frac{1}{2} gm \, \frac{\sinh\eta\left(2\cosh^2\eta - \cos^2\phi\right)}{\varepsilon^3 \cosh^2\eta (\cosh^2\eta - \cos^2\phi)^2}) + \mathcal{O}(e^2)
\end{aligned} \tag{1.79}
$$

$$\cdots$$

$$
\Rightarrow \begin{cases}
h = \delta W(\mathbf{X}) \dfrac{\varepsilon^2 \cosh\eta (\cosh^2\eta - \cos^2\phi)^{1/2}}{gm} \\
\quad -(\delta W(\mathbf{X}))^2 (\dfrac{\varepsilon^2 \cosh\eta (\cosh^2\eta - \cos^2\phi)^{1/2}}{gm})^3 \\
\quad \times(\dfrac{1}{2} gm \, \dfrac{\sinh\eta\left(2\cosh^2\eta - \cos^2\phi\right)}{\varepsilon^3 \cosh^2\eta (\cosh^2\eta - \cos^2\phi)^2}) + \mathcal{O}(e^2)
\end{cases} \tag{1.80}
$$

1.8 The reference field

As was mentioned in *Section 1.4*, our geoid determination requires quantities of the type *gravity potential* and *modulus of gravity intensity* which are harmonic at the surface of the earth down to the surface of the reference ellipsoid $\mathbb{E}^2_{a,b}$. However, the observed *modulus of gravity intensity* and *gravity potential* /geopotential numbers/ at the surface of the earth due to the centrifugal field, the retained permanent tide effects, and the gravitation of atmospheric masses are not harmonic. To tackle this problem we shift form the *actual* observation space into *incremental* space by adopting a suitable reference field. In other words, we adopt a reference field, which includes the effects of all sources of non-harmonicity of the boundary data on the surface of the earth. Apart from this necessary condition, the adopted reference field must also behave like a low-pass filter to remove the high frequency spatial variations of the observations. Of course, such a goal can only be achieved if we a reference field which is as close as possible to the actual gravity intensity and gravity potential fields.

Consequently, before deciding upon the type of the reference field, we must be aware of all type of reductions which are applied to the observations of the type *modulus of gravity intensity* and *gravity potential*. For example, the gravity data of the state Baden-Württemberg are given in the *IGSN71* (IAG, 1974) system. This means that the direct and indirect effects of the permanent tide according to specifications of IGSN71 are retained in the gravity data. Besides, the gravity observations are under the effect of the attraction of the atmospheric masses, with average gravitation of 0.87 mGal on the earth's surface (*M. Vermeer* and *M. Poutanen*, 1997). Therefore, the reference field of our choice, besides the centrifugal field, must include the effect of the gravitation of the atmospheric masses, and should be in mean-tide permanent tide system. Clearly, it must also include the gravitational effect of the masses between the surface of the earth and the reference ellipsoid.

As the reference gravitational field, we will use the ellipsoidal harmonic expansion of the earth's gravitational potential and its gradient field up to degree/order 360/360 in mean-tide permanent tide system (see *Section 1.12* for the definition of different permanent tide systems). We also include the effect of the atmospheric masses in our ellipsoidal reference field by using a gravitational constant, GM, value which includes the mass of the earth's atmosphere (*J. C. Ries*, 1992, and *E. Groten*, 1997). Such a reference field can take care of the global and regional masses as well as isostasy balancing masses up to features of 50-60 km. The effect of remaining topographical masses between the computation point at the surface of the earth and the reference ellipsoid $\mathbb{E}^2_{a,b}$ will be determined by Newton's integral. In the following sections, the ellipsoidal expansion of the external gravitational field of the earth and the reference centrifugal field will be described in details.

1.8.1 Reference potential field of the external gravity field of the earth

For a rigid uniformly rotating earth, the *gravity potential* field $w(\lambda, \phi, \eta)$ can be additively decomposed into the gravitational potential field $u(\lambda, \phi, \eta)$ and the centrifugal potential field $v(\lambda, \phi, \eta)$, namely

$$w(\lambda, \phi, \eta) = u(\lambda, \phi, \eta) + v(\lambda, \phi, \eta). \tag{1.81}$$

See *Appendix A.1.2 Page 209*, for the definition of ellipsoidal coordinates $\{\lambda, \phi, \eta\}$. The multiplicative decomposition of the gravitational potential field into separable functions $u(\lambda, \phi, \eta) = \Lambda(\lambda)\Phi(\phi)H(\eta)$ generates the following eigenvalue solution of the three dimensional *Laplace* partial differential equation.

$$u(\lambda, \phi, \eta) = \sum_{n=0}^{\infty} \sum_{m=-n}^{+n} u_{nm} \frac{Q^*_{n|m|}(\sinh \eta)}{Q^*_{n|m|}(\sinh \eta_0)} e_{nm}(\lambda, \phi) \tag{1.82}$$

where $e_{nm}(\lambda, \phi)$ are surface ellipsoidal harmonic functions

$$e_{nm}(\lambda, \phi) = P^*_{n|m|}(\sin \phi) \left[\begin{array}{l} \cos m\lambda \quad \forall m \geq 0 \\ \sin \mid m \mid \lambda \quad \forall m < 0 \end{array} \right. \tag{1.83}$$

(1.82) is valid for the space $\{\mathbb{R}^3 / \mathbb{E}^2_{a,b}\}$ which is external to the reference ellipsoid of $(x^2 + y^2)/\varepsilon^2 \cosh^2 \eta_0 + z^2 / \varepsilon^2 \sinh^2 \eta_0 = 1$. The normalised associated Legendre functions of the first kind $P^*_{nm}(\sin \phi)$ and of the second kind $Q^*_{nm}(\sinh \eta)$ are defined in *Appendix C*. The surface ellipsoidal harmonic functions $e_{nm}(\lambda, \phi)$ are orthonormal with respect to the weighted scalar product

$$\begin{aligned} &\langle e_{pq}(\lambda, \phi) | e_{nm}(\lambda, \phi) \rangle_w \\ &:= \frac{1}{S} \int\limits_{\mathbb{E}^2_{\varepsilon \cosh \eta, \varepsilon \sinh \eta}} dS\, w(\phi) e_{pq}(\lambda, \phi) e_{nm}(\lambda, \phi) = \delta_{pn} \delta_{qm}, \end{aligned} \tag{1.84}$$

where the weight function is defined by

$$w(\phi) := \frac{a}{\sqrt{b^2 + \varepsilon^2 \sin^2 \phi}} \left(\frac{1}{2} + \frac{1}{4} \frac{b^2}{a\varepsilon} \cdot \ln \frac{a + \varepsilon}{a - \varepsilon}\right), \tag{1.85}$$

S is the area of the surface of the reference ellipsoid $\mathbb{E}^2_{a,b}$

$$S = \text{area } (\mathbb{E}^2_{a,b}) = 4\pi a \cdot \left\{ \frac{1}{2} + \frac{1}{4} \frac{b^2}{a\varepsilon} \ln \frac{a + \varepsilon}{a - \varepsilon} \right\}. \tag{1.86}$$

The representation of the centrifugal potential in terms of *(i)* Cartesian coordinates $\{x,y,z\}$, *(ii)* ellipsoidal coordinates $\{\lambda,\phi,\eta\}$ and *(iii)* surface ellipsoidal harmonic functions $e_{nm}(\lambda,\phi)$ are as follows.

$$\text{(i)}\ \ v(x,y) = \frac{1}{2}\omega^2(x^2+y^2) \tag{1.87}$$

$$\text{(ii)}\ \ v(\phi,\eta) = \frac{1}{2}\omega^2\varepsilon^2\cosh^2\eta\cos^2\phi \tag{1.88}$$

$$\text{(iii)}\ \begin{cases} v(\phi,\eta) = \frac{1}{3}\omega^2\left(P^*_{20}(\sinh\eta)+\varepsilon^2\right)\cos^2\phi \\ \quad = \frac{2}{9}\omega^2\left(P^*_{20}(\sinh\eta)+\varepsilon^2\right)P^*_{00}(\sin\phi) \\ \quad -\frac{2}{9\sqrt{5}}\omega^2\left(P^*_{20}(\sinh\eta)+\varepsilon^2\right)P^*_{20}(\sin\phi) \\ \quad = \frac{2}{9}\omega^2\left(P^*_{20}(\sinh\eta)+\varepsilon^2\right)e_{00} \\ \quad -\frac{2}{9\sqrt{5}}\omega^2\left(P^*_{20}(\sinh\eta)+\varepsilon^2\right)e_{20} \end{cases} \tag{1.89}$$

where to derive (1.89) we have used the following relations

$$\cos^2\phi = \frac{2}{3}(P^*_{00}(\sin\phi)-\frac{1}{\sqrt{5}}P^*_{20}(\sin\phi) \tag{1.90}$$

$$u^2+\varepsilon^2 = \frac{2}{3}\left(P^*_{20}(\sinh\eta)+\varepsilon^2\right) \tag{1.91}$$

If the series of ellipsoidal harmonic expansion of the earth be extended up to a limited degree and order, one arrives at an approximate representation for the external gravitational potential field of the earth, which can be used as a reference gravitational field. For example if we expand the ellipsoidal harmonic expansion of the external gravitational field of the earth up to degree/order 360/360 we have

$$U(\lambda,\phi,\eta) = \sum_{n=0}^{360}\sum_{m=-n}^{+n} u_{nm}\frac{Q^*_{n|m|}(\sinh\eta)}{Q^*_{n|m|}(\sinh\eta_0)}e_{nm}(\lambda,\phi) \tag{1.92}$$

with

$$e_{nm}(\lambda,\phi) = P^*_{n|m|}(\sin\phi)\begin{bmatrix}\cos m\lambda & \forall m\geq 0 \\ \sin\mid m\mid\lambda & \forall m<0\end{bmatrix} \tag{1.93}$$

which is an approximate solution of the actual eigen-value problem of the three dimensional *Laplace* partial differential equation. The ellipsoidal harmonic coefficients u_{nm} appearing in (1.92) can be determined either, through an ellipsoidal harmonic analysis of the external gravitational field of the earth, or by an exact transformation of spherical harmonic coefficients into ellipsoidal harmonic coefficients. In the *Section 2.2*, we will see the numerical details of exact transformation of spherical harmonic coefficients into ellipsoidal ones.

1.8.2 Reference gravity intensity field of the external gravity field of the earth

In the preceding section the following formulation was presented for external gravitational field of the earth

$$u(\lambda,\phi,\eta) = \sum_{n=0}^{\infty}\sum_{m=-n}^{+n} u_{nm}\,\frac{Q^{*}_{n|m|}(\sinh\eta)}{Q^{*}_{n|m|}(\sinh\eta_0)}e_{nm}(\lambda,\phi)\,. \tag{1.94}$$

Gradient of formula (1.94) can provide us with a presentation for gravitational intensity field for the external space of the earth.

$$\begin{aligned}\mathrm{Grad}\left(u(\lambda,\phi,\eta)\right) &= \mathrm{Grad}\left(\sum_{n=0}^{\infty}\sum_{m=-n}^{+n} u_{nm}\,\frac{Q^{*}_{n|m|}(\sinh\eta)}{Q^{*}_{n|m|}(\sinh\eta_0)}e_{nm}(\lambda,\phi)\right)\\ &= \frac{1}{\sqrt{g_{11}}}\frac{\partial u(\lambda,\phi,\eta)}{\partial\lambda}\mathbf{e}_{\lambda} + \frac{1}{\sqrt{g_{22}}}\frac{\partial u(\lambda,\phi,\eta)}{\partial\phi}\mathbf{e}_{\underline{\phi}} + \frac{1}{\sqrt{g_{33}}}\frac{\partial u(\lambda,\phi,\eta)}{\partial\eta}\mathbf{e}_{\eta}\end{aligned} \tag{1.95}$$

where the metric tensor coefficients are as follows

$$g_{11} = \varepsilon^2\cosh^2\eta\cos^2\phi \tag{1.96}$$

$$g_{22} = g_{33} = \varepsilon^2(\cosh^2\eta - \cos^2\phi) \tag{1.97}$$

Box 1-23. presents the partial derivatives used in (1.95) while *Box 1-24* provides us with some *non-recursive* formulas for computation of first derivatives of the *Legendre functions of the first kind* as well as *second kind*.

Box 1-23: Partial derivatives of the gravitational potential of the external gravitational field of the earth.

$$\begin{aligned}\frac{\partial u(\lambda,\phi,\eta)}{\partial\lambda} &= \frac{\partial\left(\sum_{n=0}^{\infty}\sum_{m=-n}^{+n} u_{nm}\,\frac{Q^{*}_{n|m|}(\sinh\eta)}{Q^{*}_{n|m|}(\sinh\eta_0)}e_{nm}(\lambda,\phi)\right)}{\partial\lambda}\\ &= \sum_{n=0}^{\infty}\sum_{m=-n}^{+n} u_{nm}\,\frac{Q^{*}_{n|m|}(\sinh\eta)}{Q^{*}_{n|m|}(\sinh\eta_0)}\frac{\partial e_{nm}(\lambda,\phi)}{\partial\lambda}\end{aligned} \tag{1.98}$$

$$\frac{\partial u(\lambda,\phi,\eta)}{\partial \phi} = \frac{\partial \left(\sum_{n=0}^{\infty} \sum_{m=-n}^{+n} u_{nm} \frac{Q^*_{n|m|}(\sinh \eta)}{Q^*_{n|m|}(\sinh \eta_0)} e_{nm}(\lambda,\phi) \right)}{\partial \phi}$$
$$= \sum_{n=0}^{\infty} \sum_{m=-n}^{+n} u_{nm} \frac{Q^*_{n|m|}(\sinh \eta)}{Q^*_{n|m|}(\sinh \eta_0)} \frac{\partial e_{nm}(\lambda,\phi)}{\partial \phi} \tag{1.99}$$

$$\frac{\partial u(\lambda,\phi,\eta)}{\partial \eta} = \frac{\partial \left(\sum_{n=0}^{\infty} \sum_{m=-n}^{+n} u_{nm} \frac{Q^*_{n|m|}(\sinh \eta)}{Q^*_{n|m|}(\sinh \eta_0)} e_{nm}(\lambda,\phi) \right)}{\partial \eta}$$
$$= \sum_{n=0}^{\infty} \sum_{m=-n}^{+n} u_{nm} \frac{\frac{dQ^*_{n|m|}(\sinh \eta)}{d\eta}}{Q^*_{n|m|}(\sinh \eta_0)} e_{nm}(\lambda,\phi) \tag{1.100}$$

subject to

$$\frac{\partial e_{nm}(\lambda,\phi)}{\partial \lambda} = P^*_{n|m|}(\sin \phi) \begin{bmatrix} -m \sin m\lambda & \forall m \geq 0 \\ |\ m\ | \cos |\ m\ | \lambda & \forall m < 0 \end{bmatrix} \tag{1.101}$$

$$\frac{\partial e_{nm}(\lambda,\phi)}{\partial \phi} = \frac{dP^*_{n|m|}(\sin \phi)}{d\phi} \begin{bmatrix} \cos m\lambda & \forall m \geq 0 \\ \sin |\ m\ | \lambda & \forall m < 0 \end{bmatrix} \tag{1.102}$$

Box 1-24: First order derivatives of the Legendre functions of the first kind and the Legendre functions of second kind (Thong 1989).

(i) *Non-recursive* formulas for computations of the first order derivatives of the Legendre functions of the first kind.

$$\frac{dP^*_{0,0}(\sin \phi)}{d\phi} = 0,$$
$$\frac{dP^*_{n,0}(\sin \phi)}{d\phi} = -\sqrt{\frac{n(n+1)}{2}} P^*_{n,1}(\sin \phi) \qquad \forall n > 1 \tag{1.103}$$
$$\frac{dP^*_{1,1}(\sin \phi)}{d\phi} = P^*_{1,0}(\sin \phi) = \sqrt{3} \sin \phi$$

(ii) *Non-recursive* formulas for computations of the first order derivatives of the Legendre functions of the second kind.

$$\frac{dQ^*_{0,0}(\sinh\eta)}{d\eta} = -\frac{\cosh\eta_0}{\cosh\eta}$$

$$\frac{dQ^*_{n,0}(\sinh\eta)}{d\eta} = n\tanh\eta Q^*_{n,0}(\sinh\eta)$$

$$-(2n+1)\frac{\cosh\eta_0}{\cosh\eta}Q^*_{n-1,0}(\sinh\eta)$$

$$\frac{dQ^*_{n,m}(\sinh\eta)}{d\eta} = -(n-m+1)Q^*_{n,m-1}(\sinh\eta)$$

$$-m\tanh\eta Q^*_{n,m}(\sinh\eta) \quad \forall m \in [1,n]$$

$$\frac{dQ^*_{0,0}(\sinh\eta)}{d\eta} = -\frac{\cosh\eta_0}{\cosh\eta}$$

$$\frac{dQ^*_{n,0}(\sinh\eta)}{d\eta} = n\tanh\eta Q^*_{n,0}(\sinh\eta)$$

$$-(2n+1)\frac{\cosh\eta_0}{\cosh\eta}Q^*_{n-1,0}(\sinh\eta)$$

$$\frac{dQ^*_{n,m}(\sinh\eta)}{d\eta} = -(n-m+1)Q^*_{n,m-1}(\sinh\eta)$$

$$-m\tanh\eta Q^*_{n,m}(\sinh\eta) \quad \forall m \in [1,n]$$

$$\frac{dP^*_{n,n}(\sin\phi)}{d\phi} = \frac{\sqrt{n(n+1)-n(n-1)}}{2}P^*_{n,n-1}(\sin\phi) \qquad \forall n > 2$$

$$\frac{dP^*_{n,n}(\sin\phi)}{d\phi} = \frac{\sqrt{n(n+1)-n(n-1)}}{2}P^*_{n,n-1}(\sin\phi) \qquad \forall n > 2$$

$$\frac{dP^*_{n,1}(\sin\phi)}{d\phi} = \sqrt{\frac{n(n+1)}{2}}P^*_{n,0}(\sin\phi)$$
$$-\frac{\sqrt{n(n+1)-2}}{2}P^*_{n,2}(\sin\phi) \qquad \forall n > 2$$
$$\frac{dP^*_{n,m}(\sin\phi)}{d\phi} = \frac{\sqrt{n(n+1)-m(m-1)}}{2}P^*_{n,m-1}(\sin\phi) \tag{1.104}$$
$$-\frac{\sqrt{n(n+1)-m(m+1)}}{2}P^*_{n,m+1}(\sin\phi)$$
$$\forall n, m > 2 \text{ and } m \leq n-1$$

In the same way, the centrifugal intensity can be determined from the gradient of the centrifugal potential.

$$\begin{aligned} \mathrm{Grad}(v(\phi,\eta)) &= \mathrm{Grad}(\frac{1}{2}\omega^2\varepsilon^2\cosh^2\eta\cos^2\phi) \\ &= \frac{1}{\sqrt{g_{22}}}\frac{\partial v(\lambda,\phi,\eta)}{\partial\phi}\mathbf{e}_\phi + \frac{1}{\sqrt{g_{33}}}\frac{\partial v(\lambda,\phi,\eta)}{\partial\eta}\mathbf{e}_\eta, \end{aligned} \tag{1.105}$$

The partial derivatives of the centrifugal potential with respect to ϕ and λ are given in *Box 1-25* bellow.

Box 1-25: Partial derivatives of the centrifugal potential.

$$\frac{\partial v(\lambda,\phi,\eta)}{\partial\phi} = -\omega^2\varepsilon^2\cosh^2\eta\cos\phi\sin\phi \tag{1.106}$$
$$\frac{\partial v(\lambda,\phi,\eta)}{\partial\eta} = \omega^2\varepsilon^2\cosh\eta\sinh\eta\cos^2\phi \tag{1.107}$$

Finally, the sum of the gravitational intensity and centrifugal intensity produces the gravity intensity vector $\gamma(\lambda,\phi,\eta)$ as follows.

$$\gamma(\lambda,\phi,\eta) = \mathrm{Grad}\big(u(\lambda,\phi,\eta)\big) + \mathrm{Grad}(v(\phi,\eta)) \tag{1.108}$$

where $\mathrm{Grad}\big(u(\lambda,\phi,\eta)\big)$ and $\mathrm{Grad}(v(\phi,\eta))$ are given by (1.95) and (1.105), respectively.

If the summation (1.95) is continued up to some finite degree/order one arrives at an approximate representation of the external gravitational intensity vector field of the earth.

1.9 Terrain correction

So far, we modelled the effect of global and regional masses of the earth by ellipsoidal harmonic expansion of the earth's gravitational potential up to degree/order 360/360. We will supply the ellipsoidal harmonic coefficients needed for such an expansion by the exact transformation of spherical harmonic coefficients of EGM96 geopotential model (*F. Lemoine et al.*, 1996) into ellipsoidal harmonic coefficients (see *Section 2.2 page 79*). According to *F. Lemoine et al.* (1996) the EGM96 geopotential model has the maximum resolution of about 55km. That is, the removal of the reference field of ellipsoidal harmonic expansion of gravitational potential up to degree/order 360/360, with support of EGM96 global geopotential model, will remove the effect of the global and regional masses up to 55 km wave length. The same is true for reference gravitational intensity field. The effect of remaining local masses, i.e. the effect of the features smaller than 55 km, especially the gravitation of those masses between the evaluation point and reference ellipsoid can be removed by the *Newton integral* over the local topographical masses. In literature, such a correction is known as *terrain reduction*.

If one be interested in computation of the global topographical masses the most accurately modelled is of *ellipsoidal* type. Such an ellipsoidal model can be obtained by expressing the *Newton integral*, in terms of for example *Jacobi coordinates* $\{\lambda, \phi, u\}$. However, in the case of local near zone topographical masses one can obtain satisfactory results even in terms of planar approximation. The *Planar or flat approximation* is obtained by presenting the Newton integral in terms of *local Cartesian coordinate system* centred at the calculation point, with x, y axes in the tangent plane and z along the local normal. The name "planar" comes form the fact that such a formulation is based on the assumption that earth or geoid is flat! This is of course wrong for the case of global topographic reduction.

However, we shouldn't forget that in our cases, after removal of the reference field of degree/order 360/360, we are left with only some very small and localised topographical effects. Therefore, planar approximation can provide reasonable accuracy for terrain reduction. *E. Grafarend and S. Hanke* (2000) have made an analytical study over the classical planar approximation and have shown that the error of planar approximation grows exponentially as we go away from the calculation point.

The planar terrain reduction has become very popular especially for the construction of a convolution kernel and application of *Fast Fourier Transformation* (*FFT*) techniques and wavelet algorithms, see for example contributions by *Y. Li and M. Sideris* (1992, 1994), *K. Schwarz et al.* (1990), *M. Sideris and Y. Li* (1993), *M. Peng, et al.* (1994), *R. Forsberg* (1984, 1985, 1994), and *M. Sideris* (1995) *G. Papp and J. Benedek* (2000) for planar terrain reduction and/or application of FFF technique. Somewhere between the ellipsoidal approximation and planar approximation, we have the spherical terrain reduction, which assumes a spherical model for the earth or geoid. In this respect we can refer to contributions by *H. Abd-Elmotaal* (1995), *R. Rummel et al.* (1988) *L. Sjoeberg* (1998, 2000), *H. Nahavandchi* (1996), *H. Nahavandchi and L. Sjoeberg* (1998), *J. Engels and E. Grafarend* (1993), *J. Engels et al.* (1993).

Though we will use the planar approximation for the terrain reduction let us for completeness give the outlines of the ellipsoidal approximation for the topographic reduction.

1.9.1 Newton gravitational potential and gravitational intensity in terms of the Jacobi ellipsoidal coordinates {λ,ϕ,u}

At point p in three-dimensional space $\mathbb{R}^3$, located by position vector $\mathbf{x}$, the gravitational potential of a mass body V can be derived via the *Newton's gravitational law*

$$U(\mathbf{x}) = G\int_V \frac{dm^*}{\left\|\mathbf{x}-\mathbf{x}^*\right\|} \tag{1.109}$$

where $U(\mathbf{x})$ is the gravitational potential of the mass body V, dm^* is the differential mass element at the running point of the integral $\mathbf{x}^*$, and G is the *Newton* gravitational constant. In terms of *Cartesian coordinates*, *Newton potential* (1.109) may be written as

$$U(\mathbf{x}) = G\int_V \frac{\rho^* dx^* dy^* dz^*}{\sqrt{(x-x^*)^2+(y-y^*)^2+(z-z^*)^2}}, \tag{1.110}$$

where ρ^* is the mass density at the running point of integral, i.e. $\mathbf{x}^* = \{x^*, y^*, z^*\}$.

The *Jacobi ellipsoidal coordinates* $\{\lambda, \phi, u\}$ are generated by intersection of three coordinate surfaces from three families of surfaces, namely: *(i)* the family of confocal oblate spheroids, *(ii)* the family of confocal half hyperboloids, and *(iii)* the family of half planes. *Jacobi ellipsoidal coordinates* $\{\lambda, \phi, u\}$ are related to *Cartesian coordinates* $\{x, y, z\}$ as follows

$$\begin{aligned} x &= \sqrt{u^2 + \varepsilon^2} \cos\phi \cos\lambda \\ y &= \sqrt{u^2 + \varepsilon^2} \cos\phi \sin\lambda \\ z &= u \sin\phi \end{aligned} \tag{1.111}$$

with the *Jacobi matrix*

$$J = \begin{bmatrix} -\sqrt{u^2 + \varepsilon^2} \cos\phi \sin\lambda & -\sqrt{u^2 + \varepsilon^2} \sin\phi \cos\lambda & \dfrac{u}{\sqrt{u^2 + \varepsilon^2}} \cos\phi \cos\lambda \\ \sqrt{u^2 + \varepsilon^2} \cos\phi \cos\lambda & -\sqrt{u^2 + \varepsilon^2} \sin\phi \sin\lambda & \dfrac{u}{\sqrt{u^2 + \varepsilon^2}} \cos\phi \sin\lambda \\ 0 & u \cos\phi & \sin\phi. \end{bmatrix} \tag{1.112}$$

and the matrix of metrics

$$G := J^* J \begin{bmatrix} (u^2 + \varepsilon^2)\cos^2\phi & 0 & 0 \\ 0 & u^2 + \varepsilon^2 \sin^2\phi & 0 \\ 0 & 0 & \dfrac{u^2 + \varepsilon^2 \sin^2\phi}{u^2 + \varepsilon^2} \end{bmatrix}$$

$$:= g_{nm} \ \forall \quad n, m = 1, 2, 3. \tag{1.113}$$

Using equations (1.111) to (1.113) we can formulate the *Newton's gravitational law* in terms of ellipsoidal coordinates $\{\lambda, \phi, u\}$ as is done in *Box 1-26*.

Box 1-26: Newton gravitational integral in terms of ellipsoidal coordinates $\{\lambda, \phi, u\}$

(i) *Newton kernel in terms of Jacobi ellipsoidal coordinates* $\{\lambda, \phi, u\}$

$$\frac{1}{\left\| \mathbf{x} - \mathbf{x}^* \right\|} = \frac{1}{\sqrt{(x - x^*)^2 + (y - y^*)^2 + (z - z^*)^2}}$$

$$
\begin{aligned}
&= (-2\sqrt{u^2+\varepsilon^2}\cos\phi\cos\lambda\sqrt{u^{*2}+\varepsilon^2}\cos\phi^*\cos\lambda^* \\
&\quad +\varepsilon^2\cos^2\phi - 2\sqrt{u^2+\varepsilon^2}\cos\phi\sin\lambda\sqrt{u^{*2}+\varepsilon^2}\cos\phi^*\sin\lambda^* \\
&\quad +\varepsilon^2\cos^2\phi^* - 2(u\sin\phi)(u^*\sin\phi^*) + u^2 + u^{*2})^{-1/2}
\end{aligned}
\tag{1.114}
$$

subject to

$$
\begin{aligned}
\left\|\mathbf{x}-\mathbf{x}^*\right\|^2 &= (\sqrt{u^2+\varepsilon^2}\cos\phi\cos\lambda - \sqrt{u^{*2}+\varepsilon^2}\cos\phi^*\cos\lambda^*)^2 \\
&\quad +(\sqrt{u^2+\varepsilon^2}\cos\phi\sin\lambda - \sqrt{u^{*2}+\varepsilon^2}\cos\phi^*\sin\lambda^*)^2 \\
&\quad +(u\sin\phi - u^*\sin\phi^*)^2 \\
&= -2\sqrt{u^2+\varepsilon^2}\cos\phi\cos\lambda\sqrt{u^{*2}+\varepsilon^2}\cos\phi^*\cos\lambda^* \\
&\quad +\varepsilon^2\cos^2\phi - 2\sqrt{u^2+\varepsilon^2}\cos\phi\sin\lambda\sqrt{u^{*2}+\varepsilon^2}\cos\phi^*\sin\lambda^* \\
&\quad +\varepsilon^2\cos^2\phi^* - 2(u\sin\phi)(u^*\sin\phi^*) + u^2 + u^{*2}
\end{aligned}
\tag{1.115}
$$

(ii) The volume element

$$
\begin{aligned}
\mathrm{d}x\,\mathrm{d}y\,\mathrm{d}z &= (g_{11}g_{22}g_{33})^{1/2}\,\mathrm{d}\lambda\,\mathrm{d}\phi\,\mathrm{d}u \\
&= (u^2+\varepsilon^2\sin^2\phi)\cos\phi\,\mathrm{d}\lambda\,\mathrm{d}\phi\,\mathrm{d}u
\end{aligned}
\tag{1.116}
$$

(iii) The Newton's gravitational law in terms of ellipsoidal coordinates $\{\lambda,\phi,u\}$

$$
\begin{aligned}
U_T(\mathbf{x}) &= G\int_{\lambda^*=0}^{2\pi}\int_{\phi^*=-\frac{\pi}{2}}^{+\frac{\pi}{2}}\int_{u^*=0}^{u(\lambda^*,\phi^*)} \rho^*\{[(-2\sqrt{u^2+\varepsilon^2}\cos\phi\cos\lambda) \\
&\quad \times(\sqrt{u^{*2}+\varepsilon^2}\cos\phi^*\cos\lambda^*) \\
&\quad +\varepsilon^2\cos^2\phi - 2(\sqrt{u^2+\varepsilon^2}\cos\phi\sin\lambda)(\sqrt{u^{*2}+\varepsilon^2}\cos\phi^*\sin\lambda^*) \\
&\quad +\varepsilon^2\cos^2\phi^* - 2(u\sin\phi)(u^*\sin\phi^*) + u^2 + u^{*2}]^{-1/2} \\
&\quad \times(u^{*2}+\varepsilon^2\sin^2\phi^*)\cos\phi^*\}\,\mathrm{d}\lambda^*\,\mathrm{d}\phi^*\,\mathrm{d}u^*
\end{aligned}
\tag{1.117}
$$

where in (1.117) $u(\lambda^*,\phi^*)$ is the representation of topographical surface of the earth in terms of *Jacobi height* u.

The Newton integral (1.117) is extended over the whole topographical masses of the earth. However, one may be interested in the gravitational potential of local masses between the computational point and the reference ellipsoid in some limited radial distance from the calculation point, therefore, (1.117) can be written as

$$
\begin{aligned}
U_T(\mathbf{x}) = G \int_{\lambda^*=\lambda_1}^{\lambda_2} \int_{\phi^*=\phi_1}^{\phi_2} \int_{u^*=b}^{b+\delta u(\lambda^*,\phi^*)} & \rho^* \{[(-2\sqrt{u^2+\varepsilon^2}\cos\phi\cos\lambda) \\
& \times(\sqrt{u^{*2}+\varepsilon^2}\cos\phi^*\cos\lambda^*) \\
& +\varepsilon^2\cos^2\phi - 2(\sqrt{u^2+\varepsilon^2}\cos\phi\sin\lambda)(\sqrt{u^{*2}+\varepsilon^2}\cos\phi^*\sin\lambda^*) \\
& +\varepsilon^2\cos^2\phi^* - 2(u\sin\phi)(u^*\sin\phi^*) + u^2 + u^{*2}]^{-1/2} \\
& \times(u^{*2}+\varepsilon^2\sin^2\phi^*)\cos\phi^*\}\mathrm{d}\lambda^*\,\mathrm{d}\phi^*\,\mathrm{d}u^*
\end{aligned}
\tag{1.118}
$$

1.9.2 Planar approximation of terrain reduction

An exact terrain reduction in the local Cartesian coordinate system, can be obtained by equi-areal map projection of the surface of the reference ellipsoid $\mathbb{E}^2_{a,b}$ into local tangent plane. However, according to *E. Grafarend and S. Hanke* (2000), the classical planar approximation is still of reasonable accuracy if it is applied to the topographical masses in a radius of shorter than 100km around the computation point. Therefore, in our case where we are talking about the terrain reduction in a radius of 50km around the computational point the classical planar approximation is of sufficient accuracy.

Let us now briefly explain planar approximation and planar terrain reduction. In planar approximation the masses of the local-terrain is divided into rectangular prisms and the total potential of the local-terrain masses, are calculated by summing up the contributions of individual prisms. In this method, the earth is regarded as a plane surface and the Newton integral is formulated at the local Cartesian coordinate system in the tangent plane at the computation point. This three-dimensional Cartesian coordinate system $\{x,y,z\}$ is built at the calculation point as follows (see *Figure 1-8*):

1. The origin located at the calculation point
2. The z axis along the local vertical of the computation point

3. The x and y coordinates in the tangent plane at the calculation point
4. The x axis pointing towards North
5. The y axis completes the right-handed system

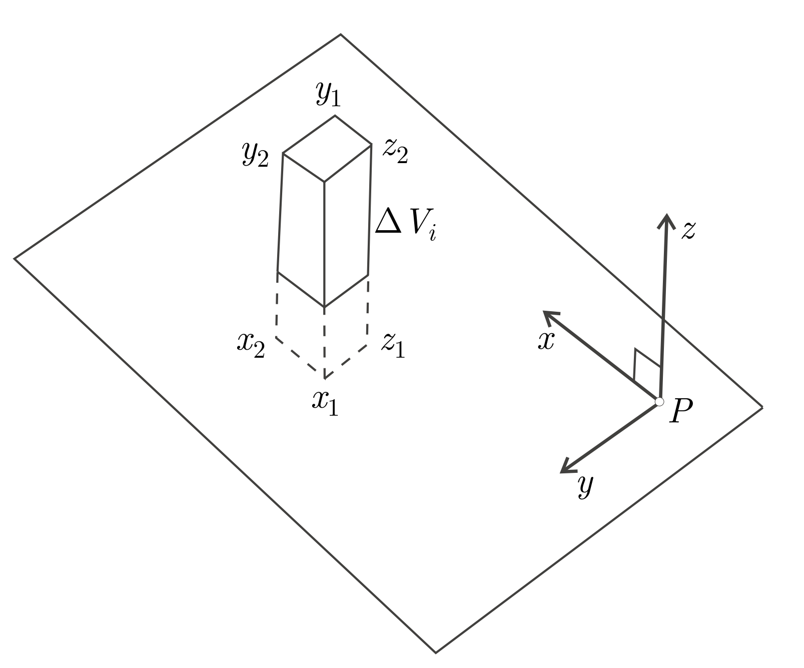

Figure 1-8: The Cartesian coordinate system $\{x,y,z\}$ in local tangent plane and the mass prism ΔV_i.

The Newton integral equation in terms of local Cartesian coordinate system for one rectangular prism can be written as follows.

$$U(\mathbf{x}) = G\int_V \frac{dm^*}{\left\|\mathbf{x}-\mathbf{x}^*\right\|} = G\int_V \frac{dm^*}{\sqrt{(x-x^*)^2+(y-y^*)^2+(z-z^*)^2}}$$

$$= G\int_{z=z_1}^{z_2}\int_{y=y_1}^{y_2}\int_{x=x_1}^{x_2} \frac{\rho(x^*,y^*,z^*)dx^*dy^*dz^*}{\sqrt{(x-x^*)^2+(y-y^*)^2+(z-z^*)^2}} \tag{1.119}$$

Assuming a constant density ρ, and putting the centre of coordinate system at the computational point p, the volume integral (1.119) can be solved analytically.

$$U(\mathbf{x}) = G\rho\int_{z=z_1}^{z_2}\int_{y=y_1}^{y_2}\int_{x=x_1}^{x_2} \frac{dx^*dy^*dz^*}{\sqrt{x^{*2}+y^{*2}+z^{*2}}} \tag{1.120}$$

$$=G\rho[\frac{z_1^2}{2}\arctan\frac{x_1y_1}{z_1\sqrt{x_1^2+y_1^2+z_1^2}}+\frac{y_1^2}{2}\arctan\frac{x_1z_1}{y_1\sqrt{x_1^2+y_1^2+z_1^2}}$$

$$+\frac{x_1^2}{2}\arctan\frac{y_1z_1}{x_1\sqrt{x_1^2+y_1^2+z_1^2}}-\frac{z_1^2}{2}\arctan\frac{x_2y_1}{z_1\sqrt{x_2^2+y_1^2+z_1^2}}$$

$$-\frac{y_1^2}{2}\arctan\frac{x_2 z_1}{y_1\sqrt{x_2^2 + y_1^2 + z_1^2}} - \frac{x_2^2}{2}\arctan\frac{y_1 z_1}{x_2\sqrt{x_2^2 + y_1^2 + z_1^2}}$$
$$-\frac{z_1^2}{2}\arctan\frac{x_1 y_2}{z_1\sqrt{x_1^2 + y_2^2 + z_1^2}} - \frac{y_2^2}{2}\arctan\frac{x_1 z_1}{y_2\sqrt{x_1^2 + y_2^2 + z_1^2}}$$
$$-\frac{x_1^2}{2}\arctan\frac{y_2 z_1}{x_1\sqrt{x_1^2 + y_2^2 + z_1^2}} + \frac{z_1^2}{2}\arctan\frac{x_2 y_2}{z_1\sqrt{x_2^2 + y_2^2 + z_1^2}}$$
$$+\frac{y_2^2}{2}\arctan\frac{x_2 z_1}{y_2\sqrt{x_2^2 + y_2^2 + z_1^2}} + \frac{x_2^2}{2}\arctan\frac{y_2 z_1}{x_2\sqrt{x_2^2 + y_2^2 + z_1^2}}$$
$$-\frac{z_2^2}{2}\arctan\frac{x_1 y_1}{z_2\sqrt{x_1^2 + y_1^2 + z_2^2}} - \frac{y_1^2}{2}\arctan\frac{x_1 z_2}{y_1\sqrt{x_1^2 + y_1^2 + z_2^2}}$$
$$-\frac{x_1^2}{2}\arctan\frac{y_1 z_2}{x_1\sqrt{x_1^2 + y_1^2 + z_2^2}} + \frac{z_2^2}{2}\arctan\frac{x_2 y_1}{z_2\sqrt{x_2^2 + y_1^2 + z_2^2}}$$
$$+\frac{y_1^2}{2}\arctan\frac{x_2 z_2}{y_1\sqrt{x_2^2 + y_1^2 + z_2^2}} + \frac{x_2^2}{2}\arctan\frac{y_1 z_2}{x_2\sqrt{x_2^2 + y_1^2 + z_2^2}}$$
$$+\frac{z_2^2}{2}\arctan\frac{x_1 y_2}{z_2\sqrt{x_1^2 + y_2^2 + z_2^2}} + \frac{y_2^2}{2}\arctan\frac{x_1 z_2}{y_2\sqrt{x_1^2 + y_2^2 + z_2^2}}$$
$$+\frac{x_1^2}{2}\arctan\frac{y_2 z_2}{x_1\sqrt{x_1^2 + y_2^2 + z_2^2}} - \frac{z_2^2}{2}\arctan\frac{x_2 y_2}{z_2\sqrt{x_2^2 + y_2^2 + z_2^2}}$$
$$-\frac{y_2^2}{2}\arctan\frac{x_2 z_2}{y_2\sqrt{x_2^2 + y_2^2 + z_2^2}} - \frac{x_2^2}{2}\arctan\frac{y_2 z_2}{x_2\sqrt{x_2^2 + y_2^2 + z_2^2}}$$
$$-y_1 z_1 \ln(x_1 + \sqrt{x_1^2 + y_1^2 + z_1^2})$$
$$-x_1 z_1 \ln(y_1 + \sqrt{x_1^2 + y_1^2 + z_1^2})$$
$$-x_1 y_1 \ln(z_1 + \sqrt{x_1^2 + y_1^2 + z_1^2})$$
$$+y_1 z_1 \ln(x_2 + \sqrt{x_2^2 + y_1^2 + z_1^2})$$
$$+x_2 z_1 \ln(y_1 + \sqrt{x_2^2 + y_1^2 + z_1^2})$$
$$+x_2 y_1 \ln(z_1 + \sqrt{x_2^2 + y_1^2 + z_1^2})$$
$$+y_2 z_1 \ln(x_1 + \sqrt{x_1^2 + y_2^2 + z_1^2})$$
$$+x_1 z_1 \ln(y_2 + \sqrt{x_1^2 + y_2^2 + z_1^2})$$
$$+x_1 y_2 \ln(z_1 + \sqrt{x_1^2 + y_2^2 + z_1^2})$$
$$-y_2 z_1 \ln(x_2 + \sqrt{x_2^2 + y_2^2 + z_1^2})$$
$$-x_2 z_1 \ln(y_2 + \sqrt{x_2^2 + y_2^2 + z_1^2})$$
$$+y_1 z_2 \ln(x_1 + \sqrt{x_1^2 + y_1^2 + z_2^2})$$
$$+x_1 z_2 \ln(y_1 + \sqrt{x_1^2 + y_1^2 + z_2^2})$$
$$+x_1 y_1 \ln(z_2 + \sqrt{x_1^2 + y_1^2 + z_2^2})$$
$$-y_1 z_2 \ln(x_2 + \sqrt{x_2^2 + y_1^2 + z_2^2})$$
$$-x_2 z_2 \ln(y_1 + \sqrt{x_2^2 + y_1^2 + z_2^2})$$

$$-x_2 y_1 \ln(z_2 + \sqrt{x_2^2 + y_1^2 + z_2^2})$$
$$-y_2 z_2 \ln(x_1 + \sqrt{x_1^2 + y_2^2 + z_2^2})$$
$$-x_1 z_2 \ln(y_2 + \sqrt{x_1^2 + y_2^2 + z_2^2})$$
$$-x_1 y_2 \ln(z_2 + \sqrt{x_1^2 + y_2^2 + z_2^2})$$
$$+y_2 z_2 \ln(x_2 + \sqrt{x_2^2 + y_2^2 + z_2^2})$$
$$+x_2 z_2 \ln(y_2 + \sqrt{x_2^2 + y_2^2 + z_2^2})$$
$$+x_2 y_2 \ln(z_2 + \sqrt{x_2^2 + y_2^2 + z_2^2})]$$

Since we are also going to employ the observations of the type modulus of gravitational intensity in our geoid computations let us, also derive the gravitational intensity of a rectangular prism shown in *Figure 1-8*. For a differential mass element dM , the gravitational intensity can be derived from the gradient of the gravitational potential as follows.

$$\begin{aligned} d\mathbf{\Gamma} &= \mathrm{Grad}(dU) \\ &= \rho G[-\frac{x}{(x^2+y^2+z^2)^{3/2}}\mathbf{e_x} - \frac{y}{(x^2+y^2+z^2)^{3/2}}\mathbf{e_y} \\ &\quad -\frac{z}{(x^2+y^2+z^2)^{3/2}}\mathbf{e_z}] \end{aligned} \tag{1.121}$$

Therefore, for a mass prism shown in *Figure 1-8* one can write

$$\begin{aligned} \mathbf{\Gamma}(\mathbf{x}) &= G\rho \int_{z=z_1}^{z_2} \int_{y=y_1}^{y_2} \int_{x=x_1}^{x_2} \mathrm{Grad}(dU) \\ &= -G\rho \int_{z=z_1}^{z_2} \int_{y=y_1}^{y_2} \int_{x=x_1}^{x_2} [\frac{x}{(x^2+y^2+z^2)^{3/2}}\mathbf{e_x} \\ &\quad +\frac{y}{(x^2+y^2+z^2)^{3/2}}\mathbf{e_y} + \frac{z}{(x^2+y^2+z^2)^{3/2}}\mathbf{e_z}] \\ &= \Gamma_x \mathbf{e_x} + \Gamma_y \mathbf{e_y} + \Gamma_z \mathbf{e_z} \end{aligned} \tag{1.122}$$

where

$$\Gamma_x = G\rho[\, x_1 \arctan\frac{y_1 z_1}{x_1\sqrt{x_1^2 + y_1^2 + z_1^2}}$$
$$-x_2 \arctan\frac{y_1 z_1}{x_2\sqrt{x_2^2 + y_1^2 + z_1^2}} - x_1 \arctan\frac{y_2 z_1}{x_1\sqrt{x_1^2 + y_2^2 + z_1^2}}$$
$$+x_2 \arctan\frac{y_2 z_1}{x_2\sqrt{x_2^2 + y_2^2 + z_1^2}} - x_1 \arctan\frac{y_1 z_2}{x_1\sqrt{x_1^2 + y_1^2 + z_2^2}} +$$
$$x_2 \arctan\frac{y_1 z_2}{x_2\sqrt{x_2^2 + y_1^2 + z_2^2}} + x_1 \arctan\frac{y_2 z_2}{x_1\sqrt{x_1^2 + y_2^2 + z_2^2}}$$
$$-x_2 \arctan\frac{y_2 z_2}{x_2\sqrt{x_2^2 + y_2^2 + z_2^2}} - z_1 \ln(y_1 + \sqrt{x_1^2 + y_1^2 + z_1^2})$$
$$-y_1 \ln(z_1 + \sqrt{x_1^2 + y_1^2 + z_1^2}) + z_1 \ln(y_2 + \sqrt{x_2^2 + y_1^2 + z_1^2})$$
$$+y_1 \ln(z_1 + \sqrt{x_2^2 + y_1^2 + z_1^2}) + z_1 \ln(y_2 + \sqrt{x_1^2 + y_2^2 + z_1^2})$$

$$+y_2\ln(z_1 + \sqrt{x_1^2 + y_2^2 + z_1^2})-$$
$$z_1\ln(y_2 + \sqrt{x_2^2 + y_2^2 + z_1^2})$$
$$-y_2\ln(z_1 + \sqrt{x_2^2 + y_2^2 + z_1^2})+$$
$$z_2\ln(y_1 + \sqrt{x_1^2 + y_1^2 + z_2^2})$$
$$+y_1\ln(z_2 + \sqrt{x_1^2 + y_1^2 + z_2^2})-$$
$$z_2\ln(y_1 + \sqrt{x_2^2 + y_1^2 + z_2^2})$$
$$-y_1\ln(z_2 + \sqrt{x_2^2 + y_1^2 + z_2^2})-$$
$$z_2\ln(y_2 + \sqrt{x_1^2 + y_2^2 + z_2^2})$$
$$-y_2\ln(z_2 + \sqrt{x_1^2 + y_2^2 + z_2^2})+$$
$$z_2\ln(y_2 + \sqrt{x_2^2 + y_2^2 + z_2^2})$$
$$+y_2\ln(z_2 + \sqrt{x_2^2 + y_2^2 + z_2^2})]$$

$$\Gamma_y = G\rho[y_1\arctan\frac{x_1z_1}{y_1\sqrt{x_1^2 + y_1^2 + z_1^2}}-$$
$$y_1\arctan\frac{x_2z_1}{y_1\sqrt{x_2^2 + y_1^2 + z_1^2}}-y_2\arctan\frac{x_1z_1}{y_2\sqrt{x_1^2 + y_2^2 + z_1^2}}$$
$$+y_2\arctan\frac{x_2z_1}{y_2\sqrt{x_2^2 + y_2^2 + z_1^2}}-y_1\arctan\frac{x_1z_2}{y_1\sqrt{x_1^2 + y_1^2 + z_2^2}}+$$
$$y_1\arctan\frac{x_2z_2}{y_1\sqrt{x_2^2 + y_1^2 + z_2^2}}+y_2\arctan\frac{x_1z_2}{y_2\sqrt{x_1^2 + y_2^2 + z_2^2}}$$
$$-y_2\arctan\frac{x_2z_2}{y_2\sqrt{x_2^2 + y_2^2 + z_2^2}}-z_1\ln(x_1 + \sqrt{x_1^2 + y_1^2 + z_1^2})$$
$$-x_1\ln(z_1 + \sqrt{x_1^2 + y_1^2 + z_1^2})+$$
$$z_1\ln(x_2 + \sqrt{x_2^2 + y_1^2 + z_1^2})$$
$$+x_2\ln(z_1 + \sqrt{x_2^2 + y_1^2 + z_1^2})+$$
$$z_1\ln(x_1 + \sqrt{x_1^2 + y_2^2 + z_1^2})$$
$$+x_1\ln(z_1 + \sqrt{x_1^2 + y_2^2 + z_1^2})-$$
$$z_1\ln(x_2 + \sqrt{x_2^2 + y_2^2 + z_1^2})$$
$$-x_2\ln(z_1 + \sqrt{x_2^2 + y_2^2 + z_1^2})+$$
$$z_2\ln(x_1 + \sqrt{x_1^2 + y_1^2 + z_2^2})$$
$$+x_1\ln(z_2 + \sqrt{x_1^2 + y_1^2 + z_2^2})-$$
$$z_2\ln(x_2 + \sqrt{x_2^2 + y_1^2 + z_2^2})$$
$$-x_2\ln(z_2 + \sqrt{x_2^2 + y_1^2 + z_2^2})-$$
$$z_2\ln(x_1 + \sqrt{x_1^2 + y_2^2 + z_2^2})$$
$$-x_1\ln(z_2 + \sqrt{x_1^2 + y_2^2 + z_2^2})+$$
$$z_2\ln(x_2 + \sqrt{x_2^2 + y_2^2 + z_2^2})$$
$$+x_2\ln(z_2 + \sqrt{x_2^2 + y_2^2 + z_2^2})]$$

$$
\begin{aligned}
\Gamma_z =& G\rho[z_1 \arctan\frac{x_1 z_1}{z_1\sqrt{x_1^2 + y_1^2 + z_1^2}} - \\
& z_1 \arctan\frac{x_2 y_1}{z_1\sqrt{x_2^2 + y_1^2 + z_1^2}} - z_1 \arctan\frac{x_1 y_2}{z_1\sqrt{x_1^2 + y_2^2 + z_1^2}} \\
& + z_1 \arctan\frac{x_2 y_2}{z_1\sqrt{x_2^2 + y_2^2 + z_1^2}} - z_2 \arctan\frac{x_1 y_1}{z_2\sqrt{x_1^2 + y_1^2 + z_2^2}} \\
& + z_2 \arctan\frac{x_2 y_1}{z_2\sqrt{x_2^2 + y_1^2 + z_2^2}} + z_2 \arctan\frac{x_1 y_2}{z_2\sqrt{x_1^2 + y_2^2 + z_2^2}} \\
& - z_2 \arctan\frac{x_2 z_2}{z_2\sqrt{x_2^2 + y_2^2 + z_2^2}} - y_1 \ln(x_1 + \sqrt{x_1^2 + y_1^2 + z_1^2}\,) \\
& - x_1 \ln(y_1 + \sqrt{x_1^2 + y_1^2 + z_1^2}\,) + \\
& y_1 \ln(x_2 + \sqrt{x_2^2 + y_1^2 + z_1^2}\,) \\
& + x_2 \ln(y_1 + \sqrt{x_2^2 + y_1^2 + z_1^2}\,) + \\
& y_2 \ln(x_1 + \sqrt{x_1^2 + y_2^2 + z_1^2}\,) \\
& + x_1 \ln(y_2 + \sqrt{x_1^2 + y_2^2 + z_1^2}\,) - \\
& y_2 \ln(x_2 + \sqrt{x_2^2 + y_2^2 + z_1^2}\,) \\
& - x_2 \ln(y_2 + \sqrt{x_2^2 + y_2^2 + z_1^2}\,) + \\
& y_2 \ln(x_1 + \sqrt{x_1^2 + y_1^2 + z_2^2}\,) \\
& + x_1 \ln(y_1 + \sqrt{x_1^2 + y_1^2 + z_2^2}\,) - \\
& y_1 \ln(x_2 + \sqrt{x_2^2 + y_1^2 + z_2^2}\,) \\
& - x_2 \ln(y_1 + \sqrt{x_2^2 + y_1^2 + z_2^2}\,) - \\
& y_2 \ln(x_1 + \sqrt{x_1^2 + y_2^2 + z_2^2}\,) \\
& - x_1 \ln(y_2 + \sqrt{x_1^2 + y_2^2 + z_2^2}\,) + \\
& y_2 \ln(x_2 + \sqrt{x_2^2 + y_2^2 + z_2^2}\,) \\
& + x_2 \ln(y_2 + \sqrt{x_2^2 + y_2^2 + z_2^2}\,)]
\end{aligned}
$$

1.10 Level ellipsoid of Somigliana-Pizzetti; best fitting ellipsoid to geoid

Millions of years ago when the earth was at liquid state, it formed as an ellipsoidal body at hydrostatic equilibrium. Later during the cooling period up to now, it has deviated from its initial hydrostatic equilibrium state. However, this deviation is still not more than some thousands meters. Furthermore, one of the especial equipotential surfaces of the earth, i.e., geoid, which fits to the surface of oceans in an optimum way, is still up a very high degree of approximation resembling an ellipsoid of revolution. Indeed, the deviation of geoid from an ellipsoid of revolution of the *Somigliana-Pizzetti* type is not more than 100m. Therefore, a reference ellipsoid of *Somigliana–Pizzetti* type can be considered as approximate geoid in first degree approximation. *Box 1-27* covers the definition of the *Somigliana-Pizzetti* ellipsoid, which was first proposed by *P. Pizzetti* (1894), and later by *C. Somigliana* (1930) as a *model level surface of the earth*. As an in-depth review of the reference ellipsoid of the type *Somigliana-Pizzetti*, recent research made by *E. Grafarend and A. Ardalan* (1999a, 1999b) can also be acknowledged.

Box 1-27: *Somigliana-Pizzetti* gravity field

Somigliana-Pizzetti gravity field is a model gravity field generated by an ellipsoidal with following properties

(i) Having the same mass M as that of the earth

(ii) Rotating with the same angular velocity ω as the earth

(iii) being a model equipotential surface /reference level surface/ with the geoid's potential w_0 as its gauge

Note: According to *Stokes theorem*, having defined the potential value on the known surface of the *reference ellipsoid* $\mathbb{E}^2_{a,b}$, the *gravity potential* out side $\mathbb{E}^2_{a,b}$ can be determine uniquely.

The *World Geodetic Datum 2000* (*WGD2000*) defined by *E. Grafarend* and *A. Ardalan* (1999a, 1999b) is an international reference ellipsoid generated according to *Somigliana Pizzetti* concept of a level ellipsoid. *WGD2000* is derived base on the current best estimates of the fundamental geodetic parameters $\{GM, J_0, \omega, W_0\}$ are listed in *Table* 1-1. *Table 1-2* offers the size and shape parameters $\{a, b\}$ of the WGD2000 in different permanent tide systems.

Table 1-1: Current best estimates of the fundamental geodetic parameters $\{GM, J_2, \omega, W_0\}$

Fundamental Parameters	GM km^3/s^2	J_2	ω rad/s	W_0 m^2/s^2
Zero Frequency	398600.4418^{III} ± 0.0008	$-4.841695485 \times 10^{-4\,IV}$ $\pm 4.66 \times 10^{-11}$	$7.292115 \times 10^{-5\,I}$ $\pm 10^{-12}$	62636855.80^{II} ± 0.5
Tide-Free	398600.4418^{III} ± 0.0008	$-4.8416537 \times 10^{-4\,IV}$ $\pm 3.561 \times 10^{-11}$	$7.292115 \times 10^{-5\,I}$ $\pm 10^{-12}$	62636855.80^{II} ± 0.5
Mean-Tide	398600.4418^{III} ± 0.0008	$-4.84183457 \times 10^{-4\,V}$ $\pm 3.561 \times 10^{-11}$	$7.292115 \times 10^{-5\,I}$ $\pm 10^{-12}$	62636855.80^{II} ± 0.5

I) Groten, 1997
II) Grafarend and Ardalan, 1997, and *Burša et al.*, 1997b
III) Ries et al., 1992 (in SI units)
IV) Tapley et al., 1996
V)Lemoine et al., 1996

Table 1-2: World Geodetic Datum 2000 (WGD2000) (*E. Grafarend* and *A. Ardalan* (1999a, 1999b)) as a *Somigliana-Pizzetti* type reference ellipsoid defined in *zero frequency*, *tide free*, and *mean-tide* permanent tide systems.

WGD2000 Parameters	a m	b m	ε m
Zero Frequency	6378136.602 ±0.053	6356751.860 ±0.052	521854.674 ±0.015
Tide-Free	6378136.572 ±0.053	6356751.920 ±0.052	521853.580 ±0.013
Mean-Tide	6378136.701 ±0.053	6356751.661 ±0.052	521858.317 ±0.013

1.11 The geoid potential value W_0

In *Section 1.10*, we defined the reference ellipsoid of Somigliana-Pizzetti type as an approximate figure of geoid. In other words, we look upon the reference ellipsoid of Somigliana-Pizzetti type as an equipotential surface of reference gravity field of the earth, which approximates the geoid in an optimum way. One of the most important parameters in the definition of a reference ellipsoid of *Somigliana-Pizzetti* type is the geoid's potential W_0. In fact, according to *E. Grafarend and A. Ardalan* (1999b), it is the leading parameter in definition of a reference ellipsoid of *Somigliana-Pizzetti* type. It is important to note that while the shape of geoid changes from one permanent tide system to another, its gravity potential, i.e. the W_0 value, remains constant (see *M. Burša*, 1995 for a proof). For our computations we will use following W_0 value, which has been derived by *E. Grafarend and A. Ardalan* (1997), and *M. Burša et al.* (1997b) and is used by *E. Grafarend and A. Ardalan* (1999) to define the WGD2000.

$$W_0 = (62636855.8 \pm 0.5)(m^2 / s^2) \tag{1.123}$$

The W_0 value is not constant value is varying in time, dominantly due to eustatic rise. *A. Ardalan and E. Grafarend* (1999) from the repeated GPS observations of the Baltic Sea Level Projects have derived a raise of 0.0086 $(m^2 / s^2) / year$ for the W_0 value.

1.12 The permanent tide effect

The tidal gravitational intensity and tidal gravitational potential of sun and moon and other planets can be split into two components: (i) the time varying component and (ii) the permanent or time invariant part. Geoid as an especial equipotential surface of the gravity potential field of the earth, by definition, is free from the effect of all masses which are outside the earth. The permanent tide component, like the time varying component, affects both the geometry and gravity space of the earth. However, since the permanent component of the tide is constant in course of time, is not observable, cannot be modelled empirically, and consequently, cannot be accurately estimated. Therefore, several concepts in dealing with the permanent part of the earth tide have been developed, which are as follows:

(i) mean permanent tide system
(ii) zero frequency permanent tide system
(iii) tide-free (or non- tidal) permanent tide system

Mean permanents tide system refers to a system where both the gravity and crust deformation caused by permanent tide is left intact (not corrected). In contrast, the *tide-free permanent-tide system* refers to the case where both the gravity and deformation of the permanent tide is removed. Somewhere between these two systems is the *zero frequency permanent-tide system*, in which the gravitational part of the permanent tide is removed while the deformation caused by the permanent tide is retained.

Let us now briefly review the history of permanent tide correction of the gravity data. Traditionally, gravity measurements were corrected for both the *periodical* and *permanent* parts of the tide. This means that the *tide-free system* was adopted. However, complete removal of the tide effect (including the permanent tide effect) demands a proper choice of *zero frequency Love number* k_{20}, which is not measurable and is just adopted base on some pure hypothetical assumptions. Besides, when removing the gravity effect of the permanent tide one must also correct the deformation caused by it. Once the deformation caused by permanent tide is corrected, one must also change the earth's *moments of inertia*, the *rotational velocity*, and the *centrifugal force*. Which makes the whole procedure quite complicated! Therefore, *Hankasalo* in (1964) suggested that the permanent part of the tide does not be removed from the gravity observation, i.e. using the *mean-tide system*. *Honkasalo's* suggestion was adopted in *International Gravity Standardisation Net 1971* (*IGSN71*). Since in the *mean-tide* permanent tide system the gravity data are affected by the masses, which are outside the earth, they do not fit into the Laplace differential equation, which is the field equation in most geoid computation methods. To avoid this problem *M. Heikkinen* in (1979) proposed that to revert to traditional correction of gravity data, i.e. tide-free system, this was also resolved by the IAG in 1979. However, this was still the matter of confusion as to what should be done for the indirect effects like deformation of the earth, changes in moment of inertia, and rotational velocity of the earth caused by complete removal of the permanent tide. As a results *M. Ekman* (1979, 1981) and *E. Groten* (1980, 1996a, 1996b) proposed a third permanent tide concept, which was later resolved by IAG in 1983, that to eliminate the attraction due to permanent tide but to leave its deformation intact. This was termed as *zero frequency tide system*.

Each of the above mentioned permanent tide systems has its own potential field, reference ellipsoid, and geoid (see *M. Ekman* (1989, 1995), *R. Rapp et al*. (1991) and *M. Burša* (1995a, 1995b)). It is important to note that while the shape of geoid changes from one tide system to another, its potential, W_0, remains constant (see *M. Burša*, 1995c). According to *E. Grafarend and A. Ardalan* (1999a, 1999b) the linear eccentricity ε of the reference ellipsoid WGD2000 varies by about $1\ m$ form tide-free to zero-frequency permanent tide system, i.e., the reference ellipsoid is $1\ m$ more oblate in zero-frequency tide system (see *Table 1-2*).

In terms of spherical geopotential field of the earth, the permanent tide is only affecting the J_{20} coefficient, i.e. the second zonal-geopotential coefficient. The transformation equations of J_{20}^* (fully normalised J_{20}) between different permanent tide systems according to *D. Smith* (1989) is as follows

$$\begin{aligned} &J_{20}^*(\text{mean tide}) - J_{20}^*(\text{zero frequency tide}) = \\ &-\frac{3.11080}{\sqrt{5}} \times 10^{-8} \end{aligned} \tag{1.124}$$

$$\begin{aligned} &J_{20}^*(\text{zero frequency tide}) - J_{20}^*(\text{tide-free}) \\ &= k_{20} \times (-\frac{3.11080}{\sqrt{5}} \times 10^{-8}) \end{aligned} \tag{1.125}$$

$$\begin{aligned} &J_{20}^*(\text{mean tide}) - J_{20}^*(\text{tide-free}) \\ &= -\frac{3.11080}{\sqrt{5}} \times 10^{-8} + k_{20} \times (-\frac{3.11080}{\sqrt{5}} \times 10^{-8}) \end{aligned} \tag{1.126}$$

subject to

$$J_{20}^* = J_{20} / \sqrt{5}$$

where k_0 is the zero frequency love number. In the case of EGM96, $k_{20} = 0.3$ is adopted.

1.13 Downward continuation problem

We mentioned that our solution technique to solve the fixed-free two-boundary-value problem is through the application of Abel-Poisson integral and its gradient to the *incremental* quantities which are harmonic, on the surface of the earth down to the surface of the reference ellipsoid. Now let us have a brief review of integral equations and their classifications. In general, an equation in which the unknown function is under the integral sign is called "*integral equation*". If the unknown function is only under the integral sign, then the equation is said to be of the "*first kind*". If the unknown function is both inside and outside the integral sign, the integral equation is of the "*second kind*". If the limits are fixed then the integral equation is called "*Fredholm integral equation*". Therefore, a *Fredholm integral equation of the first kind* is like

$$\int_a^b k(s,t)x(t)dt = g(s). \tag{1.127}$$

When the upper limit of the integral is also a variable, then we have a *Volterra integral equation*. The *Volterra integral equation of the first kind* can be written as

$$\int_a^s k(s,t)x(t)dt = g(s) \tag{1.128}$$

An especial type of Volterra integral equation with the kernel $k(s,t) = (s - t)^{\alpha-1}$ is known as *Abel integral equation* (*N. Abel*, 1823). Among the references on integral equations *C. Corduneanu* (1991), *J. Kondo* (1992), *W. Lovitt* (1950), *S. Mikhlin* (1961,1964), *A. Pipkin* (1991), *D. Porter and D. Stirling* (1990), *W. Press et al* (1992), *F. Tricomi* (1957), *E. Whittaker and G. Robinson* (1967), and *C. Baker* (1977) are outstanding.

Now let us return to our integral equation and see to which category of integral equations it fits. Clearly, it is of the form of *Fredholm integral equations of the first kind*. Besides it is a linear equation, therefore, more precisely it is of a *linear Fredholm integral equation of the first kind*. The kernel of *Abel-Poisson integral* is square integrable, and is also symmetric, i.e., $k(s,t) = k(t,s)$ (*G. Arfken*, 1985). A comparison of the *Able-Poisson integral* with the general form of *Fredholm integral equation of the first kind* (1.127), reveals that in our case, the known function $g(s)$ is *incremental* gravitational intensity and *incremental* gravitational potential at the surface of the earth. While the unknown function $x(t)$ is the *incremental* gravitational potential at the surface of the reference ellipsoid. Equation (1.127) in short hand notations may be written as

$$y = Ax \tag{1.129}$$

Where, in the language of functional analysis, A can be called a compact linear operator from *Hilbert space* H_1 into Hilbert space H_2. It is important to note that though (1.129) theoretically has a unique solution, however, in practice due to observation errors, discretization of the problem, and observations (equations) than unknowns, does not poses a unique solution. Consequently, (1.129) can be reformulated as

$$y + i = Ax \tag{1.130}$$

where i represents the inconsistencies of the observations y. To obtain an optimum solution for (1.130) one may resort to minimum norm solution $\hat{x}$ through

$$\hat{x} = (A^*A)^{-1}A^*y \tag{1.131}$$

where A^* is the adjoint of A.

This minimum norm solution if exists will be unique and have the property of being orthogonal to the null-space of A. However, it is well known that an equation of the type (1.129) or (1.130) is ill-posed (see for example *C. Baker*, 1977, *C. Baker and G. Miller*, 1982), which implies that minimum norm solution of (1.130) does not depend continuously on the left hand side of (1.130). *D. Phillips* in (1962) and later *A. Tikhonov* in (1963) proposed a regularisation method to solve the ill posed problems like (1.130), which is later known as *Phillips-Tikhonov regularisation method*. The *Phillips-Tikhonov regularisation* is based on minimisation of following functional for x^α.

$$F_\alpha(x^\alpha) = \|Ax^\alpha - y\|^2 + \alpha\|x^\alpha\|^2 \tag{1.132}$$

where α is a positive parameter and is called *regularisation parameter*. The minimum norm solution of (1.132) over a finite dimensional subspace V_m of H_1 is given by (see *F. Natterer* (1977), and *J. Marti* (1978, 1980) for example)

$$x_m^\alpha = (A^*A + \alpha I)^{-1}A^*y \tag{1.133}$$

Note that, x_m^α satisfies the following orthogonality condition in V_m.

$$\langle Ax_m^\alpha - y \mid A\xi\rangle + \alpha\langle x_m^\alpha \mid \xi\rangle = 0 \tag{1.134}$$

for all $\xi \in V_m$.

It is well known that the stability of the solution x_m^α depends on the size of the regularisation parameter α. That is, the bigger the regularisation parameter α the less the variance for the solution x_m^α. However, by increasing the regularisation parameter α we will increase the bias of the solution. Indeed, the optimum solution is the one, which compromises between variance and bias of the solution. Finding the optimum regularisation parameter α is a tedious process and requires lots of repetition of the solution. *A. Frommer and P. Maass* (1999) have proposed a fast method, which accelerates the process of finding a proper value for α by a factor of 3.

1.13.1 Discretization of the Abel-Poisson integral

In order to solve the *Able-Poisson integral* numerically it must be decretized. The standard method for discretizing an integral equation is based on interchange of the integration by summation. Following boxes, summarise our discretization scheme.

The important issue to mention here is that in our downward continuation scheme, we derive from both incremental quantities of the type gravitational intensity and gravitational potential at the surface of the earth the incremental gravitational potential at the surface of the reference ellipsoid. This is what which makes our approach different from usual downward continuation of gravity anomalies at the surface of the earth into gravity anomaly at the surface of the reference sphere (see for example *H. Nahavandchi* 1998). As a pioneer contribution to the discrete solution of a boundary-value problem *A. Bjerhammar* (1974) can be mentioned.

Box 1-28: Discretization of the ellipsoidal Abel-Poisson integral of *incremental* gravitational potential δW .

(i) Continues form of the integral equation

$$\delta W(\lambda,\phi,\eta) = \int\limits_{\mathbb{E}^2_{a,b}} dS'\left(\frac{w(\phi')}{S}\sum_{n=0}^{\infty}\sum_{m=-n}^{n}\frac{Q_{n|m|}(i\sinh\eta)}{Q_{n|m|}(i\sinh\eta_0)}\right) \times e_{nm}(\lambda',\phi')e_{nm}(\lambda,\phi)\delta W(\lambda',\phi') \tag{1.135}$$

$$= \frac{1}{S}\int\limits_{\mathbb{E}^2_{a,b}} dS'w(\phi')K(\lambda,\phi,\eta;\lambda',\phi',\eta_0)\delta W(\lambda',\phi')$$

(ii) Discretized form of the integral equation

$$\delta W(\mathbf{x}_p) = \frac{1}{S}\sum_{i=1}^{i\max}\sum_{j=1}^{j\max} a.\sqrt{b^2+\varepsilon^2\sin^2\bar{\phi}_{ij}} \times\cos\bar{\phi}_{ij}\Delta\lambda\Delta\phi w(\bar{\phi})K(\lambda,\phi,\eta;\bar{\lambda},\bar{\phi},\eta_0)\delta\bar{W}(\mathbf{X}_{P_{ij}}) \tag{1.136}$$

subject to

$$w(\bar{\phi}) := \frac{a}{\sqrt{b^2+\varepsilon^2\sin^2\bar{\phi}}}\left(\frac{1}{2}+\frac{1}{4}\frac{b^2}{a\varepsilon}\cdot\ln\frac{a+\varepsilon}{a-\varepsilon}\right) \tag{1.137}$$

$$S = \text{area}\ (\mathrm{E}^2_{a,b}) = 4\pi a\cdot\left\{\frac{1}{2}+\frac{1}{4}\frac{b^2}{a\varepsilon}\ln\frac{a+\varepsilon}{a-\varepsilon}\right\} \tag{1.138}$$

Box 1-29: Discretization of the ellipsoidal Abel-Poisson integral of *incremental* gravitational intensity $\delta\Gamma$.

(i) Continues form of the integral equation

$$\delta\Gamma(\mathbf{x}) = \gamma(\mathbf{x}) - \Gamma(\mathbf{x}) = \langle \mathbf{e}_\Gamma \,|\, \boldsymbol{\delta\Gamma}\rangle$$

$$= \left(\frac{1}{\sqrt{g_{11}}}\frac{\Gamma_\lambda}{\|\boldsymbol{\Gamma}\|}\frac{1}{S}\int\limits_{\mathbb{E}^2_{a,b}} dS'w(\phi')\frac{\partial K(\lambda,\phi,\eta;\lambda',\phi',\eta_0)}{\partial\lambda}\right.$$

$$+\frac{1}{\sqrt{g_{22}}}\frac{\Gamma_\phi}{\|\boldsymbol{\Gamma}\|}\frac{1}{S}\int\limits_{\mathbb{E}^2_{a,b}} dS'w(\phi')\frac{\partial K(\lambda,\phi,\eta;\lambda',\phi',\eta_0)}{\partial\phi}$$

$$+\frac{1}{\sqrt{g_{33}}}\frac{\Gamma_\eta}{\|\mathbf{\Gamma}\|}\frac{1}{S}\int_{\mathbb{E}^2_{a,b}} dS'w(\phi')\frac{\partial K(\lambda,\phi,\eta;\lambda',\phi',\eta_0)}{\partial\eta}\Bigg)$$
$$\times\delta W(\lambda',\phi') \tag{1.139}$$

(ii) Discretized form of the integral equation

$$\begin{aligned}\delta\Gamma(\mathbf{x}) &= \gamma(\mathbf{x})-\Gamma(\mathbf{x}) = \langle \mathbf{e}_\Gamma | \boldsymbol{\delta\Gamma}\rangle\\
&= \Bigg(\frac{1}{\sqrt{g_{11}}}\frac{\Gamma_\lambda}{\|\mathbf{\Gamma}\|}\frac{1}{S}\sum_i^{i\max}\sum_j^{j\max}(a.\sqrt{b^2+\varepsilon^2\sin^2\overline{\phi}_{ij}}\cos\overline{\phi}_{ij}\\
&\quad\times\Delta\lambda\Delta\phi w(\overline{\phi})\frac{\partial K(\lambda,\phi,\eta;\overline{\lambda},\overline{\phi},\eta_0)}{\partial\lambda})\\
&\quad+\frac{1}{\sqrt{g_{22}}}\frac{\Gamma_\phi}{\|\mathbf{\Gamma}\|}\frac{1}{S}\sum_i^{i\max}\sum_j^{j\max}(a.\sqrt{b^2+\varepsilon^2\sin^2\overline{\phi}_{ij}}\cos\overline{\phi}_{ij}\\
&\quad\times\Delta\lambda\Delta\phi w(\overline{\phi})\frac{\partial K(\lambda,\phi,\eta;\overline{\lambda},\overline{\phi},\eta_0)}{\partial\phi})\\
&\quad+\frac{1}{\sqrt{g_{33}}}\frac{\Gamma_\eta}{\|\mathbf{\Gamma}\|}\frac{1}{S}\sum_i^{i\max}\sum_j^{j\max}(a.\sqrt{b^2+\varepsilon^2\sin^2\overline{\phi}_{ij}}\cos\overline{\phi}_{ij}\\
&\quad\times\Delta\lambda\Delta\phi w(\overline{\phi})\frac{\partial K(\lambda,\phi,\eta;\overline{\lambda},\overline{\phi},\eta_0)}{\partial\eta})\Bigg)\delta\overline{W}(\mathbf{X}_{P_{ij}})\end{aligned} \tag{1.140}$$

subject to

$$w(\overline{\phi}) := \frac{a}{\sqrt{b^2+\varepsilon^2\sin^2\overline{\phi}}}\left(\frac{1}{2}+\frac{1}{4}\frac{b^2}{a\varepsilon}\cdot\ln\frac{a+\varepsilon}{a-\varepsilon}\right) \tag{1.141}$$

$$S = \text{area }(\mathrm{E}^2_{a,b}) = 4\pi a\cdot\left\{\frac{1}{2}+\frac{1}{4}\frac{b^2}{a\varepsilon}\ln\frac{a+\varepsilon}{a-\varepsilon}\right\} \tag{1.142}$$

2 Fixed-free two-boundary value problem—case study high-resolution geoid of Baden-Württemberg

In the previous chapter the theoretical foundation of a high-resolution geoid determination methodology based on fixed-free two-boundary value problem is established. Here we are going to test the derived methodology by calculating a high-resolution local geoid for the State Baden-Württemberg /Germany/ and comparing it with *European Gravimetric Quasi Geoid* (EGG97). Let us start with by introducing the input data.

2.1 Input data

To compute the high-resolution geoid of Baden-Württemberg, based on fixed-free two-boundary value problem, different type of data are collected and applied. These data are as follows:

- *Modulus of gravity intensity* and *geopotential numbers* at 1488 stations along the first order levelling network of the State Baden-Württemberg /Germany.

- $1km \times 1km$ Digital Terrain Model (DTM) of Baden-Württemberg.

- *Ellipsoidal* harmonic coefficients of external gravitational field of the earth up to degree/order 360/360.

- 157 GPS stations of *BWREF*.

There are currently over 14000 stations in Baden-Württemberg, along the gravimetric /precise/ levelling lines of first and second order, which are equipped with geopotential numbers. Since these station are too dense along the levelling lines we selected only 1488 stations along the *first order* levelling for are calculations. *Table 2-1* represents the first 10 records of these data set, and *Figure 2-1* shows the coverage of the data. As shown in *Table 2-1* the records are consist of *modulus of gravity intensity*, *geopotential number*, *Gauss-Krüger* map-projection coordinates (x, y), and the *normal heights*.

The GPS stations of *BWREF* are the *Baden-Württemberg* part of the coverage GPS network of the Germany (*DREF*). The 157 GPS coordinates of *BWREF*, which are provided to us via the kind grace of the State Geodesy Department of Baden-Württemberg, are plotted in *Figure 2-2*. Unfortunately, non-of these GPS stations are identical with the first order levelling benchmarks!

However, in our methodology, observations of the type gravity intensity and gravity potential must be reduced to the surface of the reference ellipsoid, and therefore, one need to access the GPS coordinates, i.e. *Gauss ellipsoidal coordinates* $\{l,b,h\}$, of the stations. To rescue the computations from such a data deficiency, not having GPS positioned gravity intensity and gravity potential stations, following strategy was applied.

(i) The *Gauss-Krüger* map-projection coordinates (x,y) of the gravity stations are readily transformed into Gauss ellipsoidal longitude and latitude $\{l,b\}$ of the corresponding reference ellipsoid (*Bessel ellipsoid* in this case).

(ii) By using the *global geoid computations* machinery, presented in *Chapter 3* the global geoidal undulation of the gravity stations is computed and used to convert the normal height of the stations into ellipsoidal height h.

Why do we accept such an approximation of using a *global geoidal undulation* and then apply it as the *quasi geoid height* to convert the *normal heights* into *ellipsoidal heights*? The answer lies in the fact that we estimated the accuracy of the available gravity data as 0.1 mGal. Considering the vertical variations of the gravity intensity of the earth, 10-cm accuracy is enough to express the vertical location of the gravity stations. As will be seen in chapter 3 our global geoid computation method can provide us with geoidal undulations of up to decimetre accuracy level. Besides, we know that the difference between quasi-geoid and geoid is not more than a few centimetres.

In this way, we succeeded to device a procedure, which solves the problem of lacking GPS coordinate of previously measured gravity stations.

For terrain reduction, one needs a DTM. *Figure 2-3* shows the topographic map of Baden-Württemberg generated by a 1×1 km DTM file that we used for of the terrain reduction.

Table 2-1: First ten records of the data file of 1488 benchmarks along the first order levelling lines of the state Baden-Württemberg, which are equipped with geopotential numbers and modulus of gravity intensity.

Station Number	Geopotential Number (kGal×m)	x (*Gauss Krüger*) (m)	y (*Gauss Krüger*) (m)	Modulus of Gravity Intensity(mGal)	Normal Height (m)
62230002	165.3371	3544533	5507536	981011.845	168.5363
62230009	163.6546	3539632	5507435	981010.520	166.8212
62230010	152.5039	3539866	5507993	981013.355	155.4544
62230029	137.9613	3537355	5513725	981017.475	140.6295
62230035	157.5725	3542163	5507084	981012.659	160.6213
62230051	150.9682	3538580	5509190	981014.076	153.8888
62230054	145.3050	3537951	5510651	981015.913	148.1157
62230058	155.3277	3537873	5512021	981014.554	158.3323
62230060	145.8274	3536954	5512452	981015.242	148.6480
62230064	158.9888	3539266	5508866	981012.456	162.0648

Having introduced the input data, let us start the computations of the high-resolution geoid of Baden-Württemberg by remove step, which will lead us to harmonic *incremental* gravitational intensity $\delta\Gamma(\mathbf{x})$ and incremental gravitational potential $\delta W(\mathbf{x})$ at the surface of the earth, the outer boundary. We will perform the remove process in two steps. In remove-step 1, we remove the effect of global gravitational field $\{\mathbf{\Gamma}_g, W_g\}$ and centrifugal field $\{\mathbf{\Gamma}_c, W_c\}$. Remove-step 2 is devoted to removal of the gravitational field of the local topographical masses $\{\mathbf{\Gamma}_t, W_t\}$, the so-called terrain reduction. The effect of global gravitational field $\{\mathbf{\Gamma}_g, W_g\}$ will be formulated via ellipsoidal harmonic expansion of the external gravitational field of the earth up to degree/order 360/360. Such an expansion requires ellipsoidal harmonic coefficients, which are derived from exact transformation of the spherical harmonic coefficients into ellipsoidal harmonic coefficients. In the next section, we will ponder on this transformation.

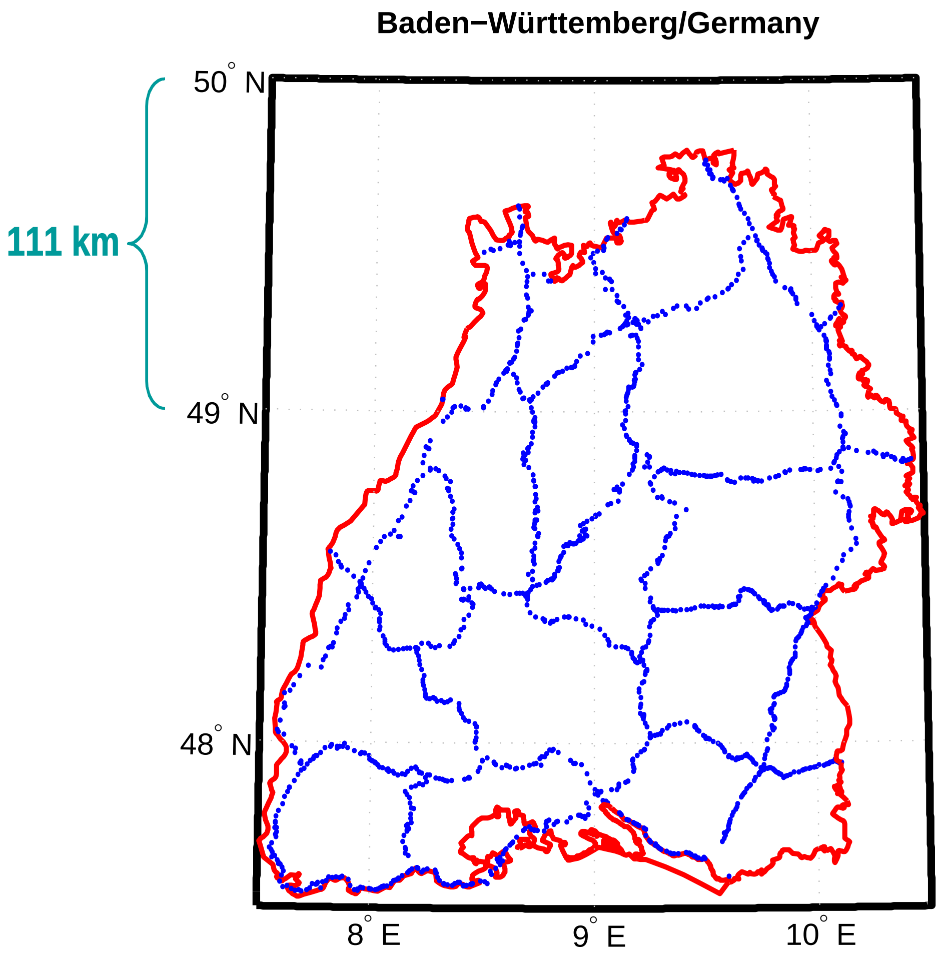

Figure 2-1: Coverage-map of 1488 gravity intensity and gravity potential stations along the first order levelling lines of Baden-Württemberg.

Map Projection Information:
Equidistant Conic Projection
Standard Parallels: 48° N and 49° N
Reference ellipsoid: WGD2000

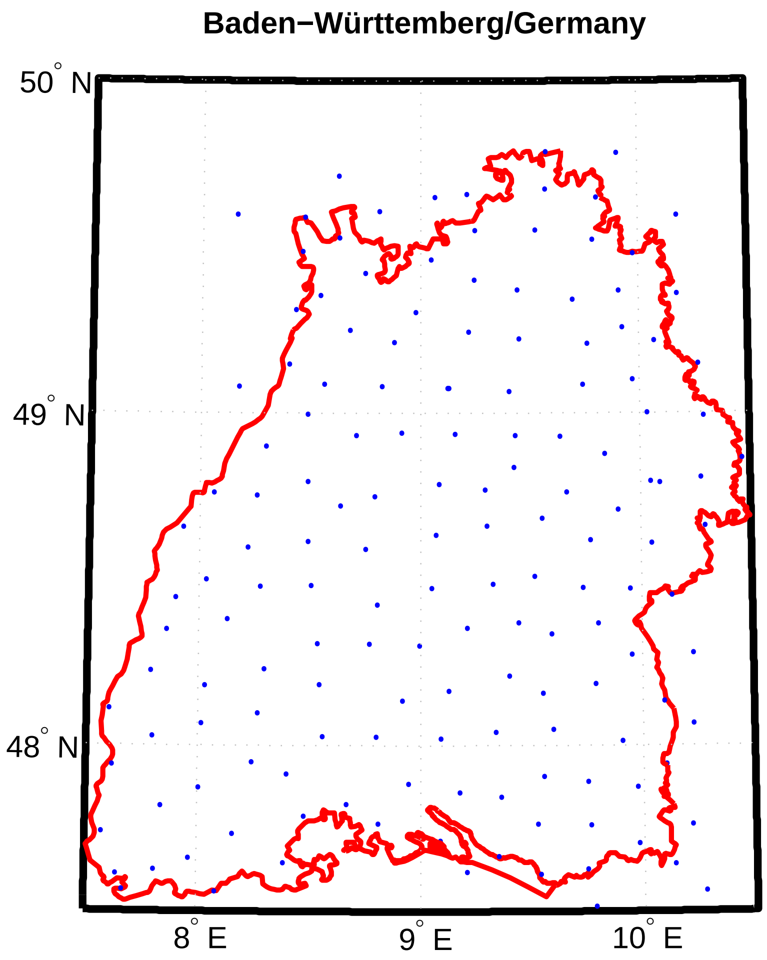

Figure 2-2: Distribution of the *BWREF* GPS stations of Baden-Württemberg. In total 157 GPS station.

<u>Map Projection Information:</u>
Equidistant Conic Projection
Standard Parallels: 48° N and 49° N
Reference ellipsoid: WGD2000

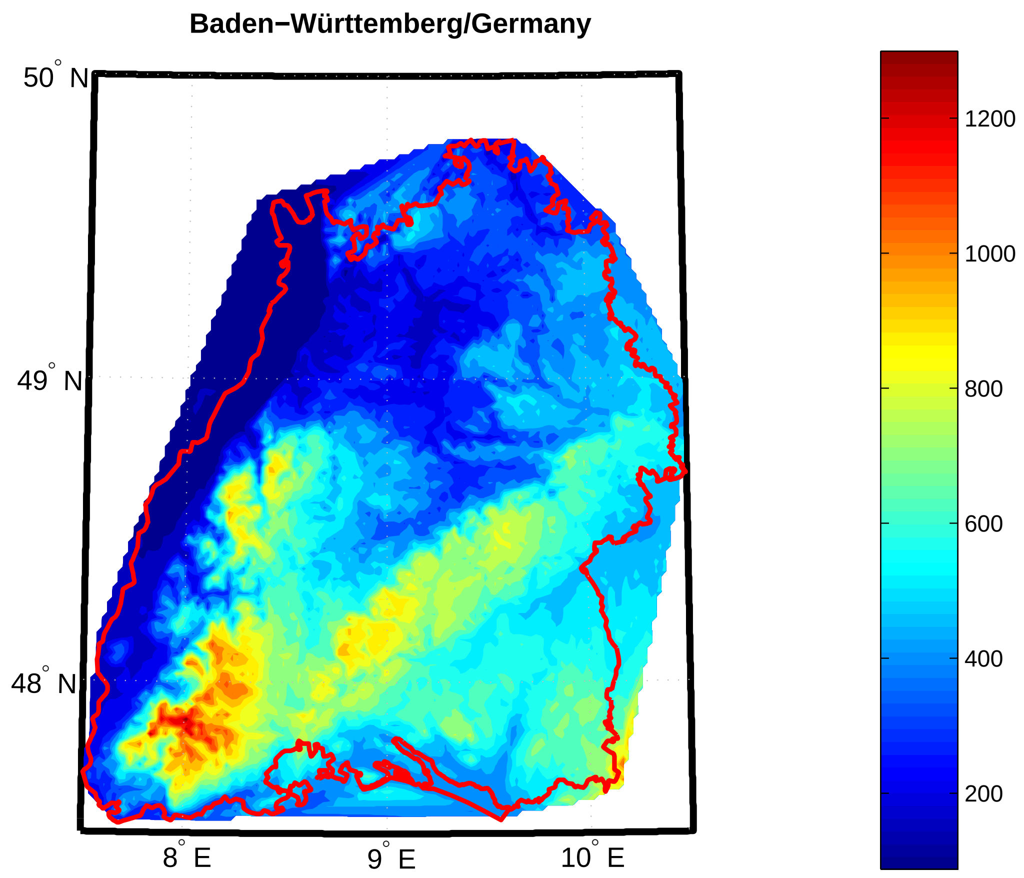

Figure 2-3: Topographic map of Baden-Württemberg, based on $1\text{km} \times 1\text{km}$ DTM file. Maximum elevation is 1426.9 m. and minimum elevation 87 m.

<u>*Map Projection Information:*</u>
Equidistant Conic Projection
Standard Parallels: $48^\circ N$ *and* $49^\circ N$
Reference ellipsoid: WGD2000

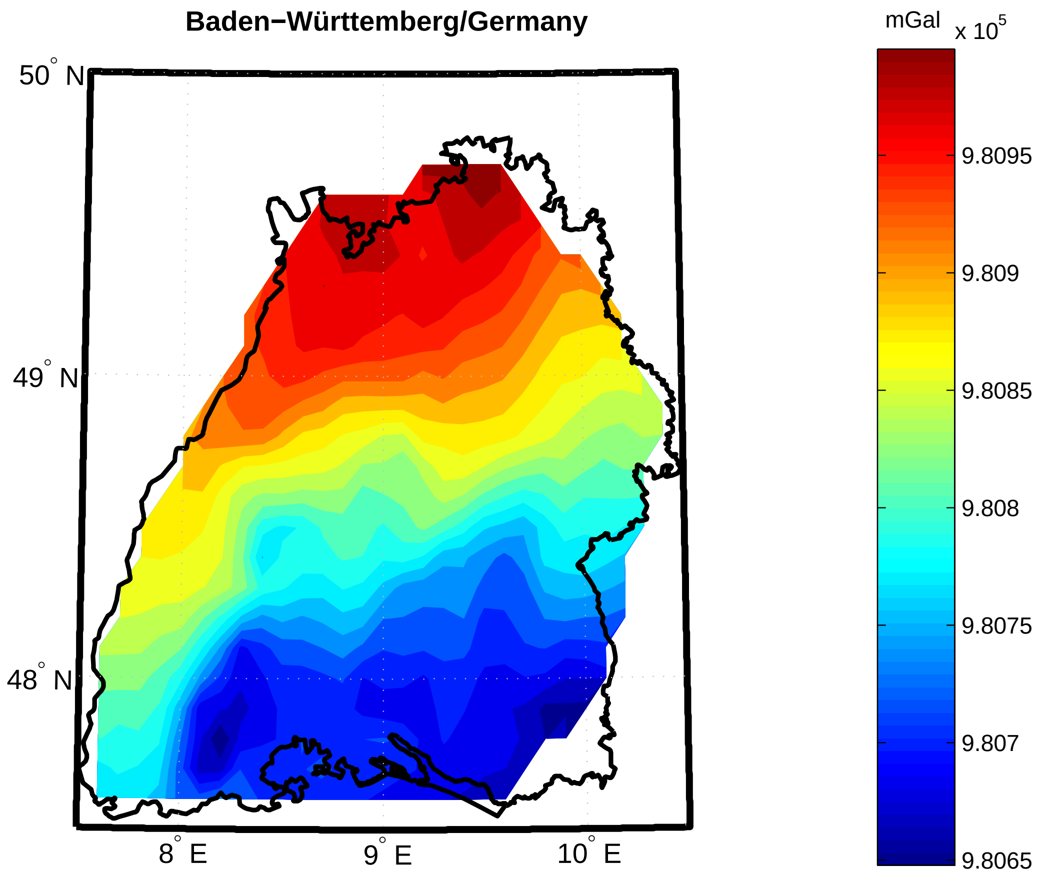

Figure 2-4: Variation of the *modulus of gravity intensity* in Baden-Württemberg. Modulus of gravity intensity varies from 980625.102 $mGal$ to 981017.587 $mGal$, with standard deviation of 100.221 $mGal$

<u>Map Projection Information:</u>
Equidistant Conic Projection
Standard Parallels: $48^{\circ}N$ *and* $49^{\circ}N$
Reference ellipsoid: WGD2000

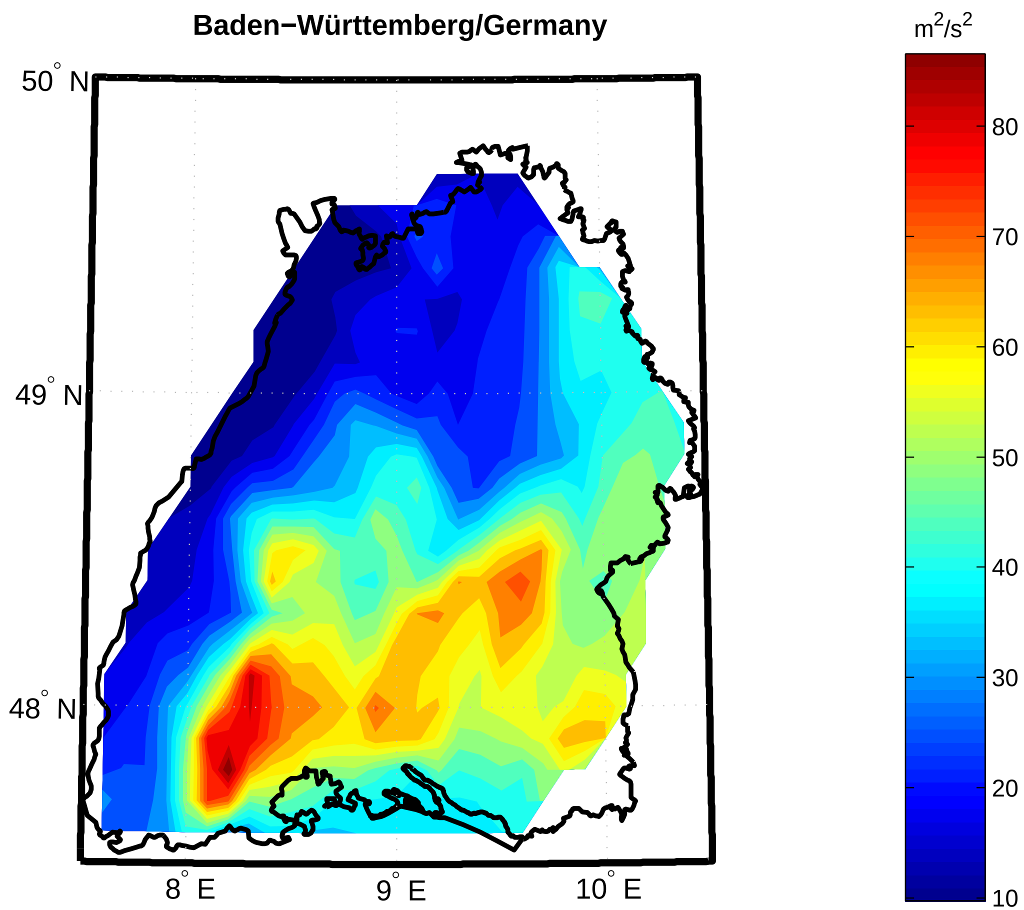

Figure 2-5: Variation of geopotential numbers in Baden-Württemberg. Geopotential numbers vary between $9.3948 m^2/s^2$ and $103.6360 m^2/s^2$, with standard deviation of $20.0744 m^2/s^2$.

<u>Map Projection Information:</u>
Equidistant Conic Projection
Standard Parallels: $48^\circ N$ and $49^\circ N$
Reference ellipsoid: WGD2000

2.2 Transformation of spherical harmonic coefficients into ellipsoidal harmonic coefficients

Nowadays it is a common practice to represent the "*Standard Gravity Earth Models*" in terms of spherical harmonics. Fortunately, precise transformation relations between spherical and ellipsoidal harmonic coefficients are available and therefore one can transfer the spherical harmonic coefficients into ellipsoidal ones without any loss of accuracy. *Box 2-1* offers a summary of the transformation formulae of spherical harmonic coefficients into ellipsoidal harmonic coefficients according to *C. Jekeli* (1981, 1988). In conjunction with the ellipsoidal harmonics, contributions by *D. Gleason* (1988, 1989), *G. Sona* (1996) and *J. Yu and H. Cao* (1996) should also be acknowledged.

Box 2-1: Transformation of spherical harmonic coefficients into ellipsoidal harmonic coefficients

Spherical harmonic coefficients, $u_{n,m}(sphere)$, can be uniquely transformed into ellipsoidal harmonic coefficients, $u_{n,m}(ellipsoid)$ via

$$u_{n,m}(ellipsoid) = Q^{*}_{n,|m|}(\sinh\eta_0)\sum_{l=0}^{(n-m)/2}\lambda_{n,|m|,l}\,u_{n-2|m|,|m|}(sphere) \quad (2.1)$$

$$\lambda_{n,m,l} = \frac{(2n-2l)!\,n!}{(2n)!\,l!\,(n-1)!}\left[\frac{(2n-4l+1)(n-m)(n+m)!}{(2n+1)(n-2l+m)!(n-2l-m)!}\right]^{1/2}\left(\frac{\varepsilon}{a}\right)^{2l} \quad (2.2)$$

$$\forall n \in [0,\infty) \text{ and } m \in [-n,+n] \quad (2.3)$$

By expanding the factorials in (2.2), one can reach to the following recursive formula, which is numerically stable especially for high degree/orders.

$$
\begin{aligned}
&\lambda_{n,m,k} = \\
&= [(2n-4l+1)(n-2l-m+1)(n-2l-m+2) \\
&\times(n-2l+m+1)(n-2l+m+2)]^{1/2} \\
&/[2k(2n-2l+1)(2n-4l+5)^{1/2}]\times\left(\frac{\varepsilon}{a}\right)^{2l}\lambda_{n,m,l-1} \\
&\forall\, l \in [1,(n-m)/2],\ n \in [0,\infty) \text{ and } m \in [-n,+n]
\end{aligned}
\tag{2.4}
$$

with the start value

$$
\lambda_{n,m,0} = 1 \quad \forall\, n, m \tag{2.5}
$$

$Q^*_{n,|m|}(\sinh\eta_0)$ are *associated Legendre functions of the second kind*, see equation (C.20) for their corresponding recursive relations.

As one can read from (2.1)-(2.5) each of the ellipsoidal harmonic coefficients $u_{n,m}(ellipsoid)$ is equal to the spherical harmonic coefficients of the same degree and order $u_{n,m}(sphere)$ plus a linear combination of spherical harmonic coefficients of the lower degree but the same order. There are three parameters involved in (2.1), namely linear eccentricity $\varepsilon = \sqrt{a^2 - b^2}$, and the size parameters η_0, and a. In fact, two of these parameters, say $\{\eta_0, \varepsilon\}$, are enough to determine the shape and size of a reference ellipsoid $\tilde{\mathbb{E}}^2_{\varepsilon\cosh\eta_0,\varepsilon\sinh\eta_0}$ uniquely. The question now arises as to which reference ellipsoid these parameters are related. The size parameter a in (2.2) can be identified from the identity $a \equiv R$, where R is the scale factor normally given with the spherical harmonic coefficients. In fact, R is the reference sphere $\mathbb{S}^2_{r=R}$ out of which the spherical harmonic expansion is uniformly convergent. That is, it defines the validity space of spherical harmonic expansion of external gravitational field of the earth. The sphere $\mathbb{S}^2_{r=R}$ in ellipsoidal harmonic expansion of external gravitational field of the earth is replaced by the reference ellipsoid $\tilde{\mathbb{E}}^2_{\varepsilon\cosh\eta_0,\varepsilon\sinh\eta_0}$. Similar to $\mathbb{S}^2_{r=R}$, $\tilde{\mathbb{E}}^2_{\varepsilon\cosh\eta_0,\varepsilon\sinh\eta_0}$ defines the validity space of the ellipsoidal harmonic expansion. While $\varepsilon\cosh\eta_0 = a$ is determined via the identity $a \equiv R$, the selection of $\varepsilon\sinh\eta_0 = b$ should be determined according to second zonal spherical harmonic J_{20}. Especially when one is interested in a Somigliana-Pizzetti type reference ellipsoid as the validity space of ellipsoidal harmonic expansion. As one knows the reference ellipsoid of *Somigliana-Pizzetti* type is uniquely determined via four fundamental geodetic parameters J_{20}, Ω, W_0, and GM (see *Grafarend and Ardalan*, 1999a, 1999b).

In our case, the ellipsoidal harmonic coefficients are supplied from the transformation of the spherical harmonic coefficients of *EGM96* (*F. Lemoine et al.*, 1996 and 1998). *Table 2-2* is a collection of some spherical harmonic coefficients of *EGM96*. The harmonic coefficients of *EGM96* are compatible with the following model.

$$U(l,b_s,r) = \frac{gm}{r}(1 + \sum_{n=2}^{360}(\frac{R}{r})^n \sum_{m=-n}^{n} u_{nm}e_{nm}(l,b_s)) \tag{2.6}$$

$e_{nm}(l,b_s)$ are surface spherical harmonics

$$e_{nm}(l,b_s) = P^*_{n|m|}(\sin b_s)\begin{bmatrix}\cos ml & \forall m \geq 0 \\ \sin|m|l & \forall m < 0\end{bmatrix} \tag{2.7}$$

In (2.6) $\{l,b_s,r\}$ are spherical coordinates of the computational point, R = 6 378 136.3 m is the scale factor which defines the radius of the reference sphere $\mathbb{S}^2_{r=R}$ out of which the series expansion of (2.6) is uniformly convergent. The product of *Newton* gravitational constant and the mass of the earth in the *EGM96* (*F. Lemoine et al.*, 1998) model is *gm*=3 986 004.415E+8 m^3/s^2. The spherical harmonic coefficients of *EGM96* are in tide free system. However, they can be transferred into *mean-tide* or *zero-frequency* permanent tide systems via the formulae given in *Section 1.12*.

Table 2-2: Some spherical harmonic coefficients of the *EGM96* global geopotential model.

n	m	$u_{n,m}$	$u_{n,-m}$	$\sigma_{u_{n,m}}$	$\sigma_{u_{n,-m}}$
2	0	0.484165371E–03	0.000000000E+00	0.35610E–10	0.00000E+00
2	1	–0.18698763E–09	0.119528012E–08	0.10000E–29	0.10000E–29
2	2	0.243914352E–05	–0.14001668E–05	0.53739E–10	0.54353E–10
3	0	0.957254173E–06	0.000000000E+00	0.18094E–10	0.00000E+00
3	1	0.202998882E–05	0.248513158E–06	0.13965E–09	0.13645E–09
3	2	0.904627768E–06	–0.61902594E–06	0.10962E–09	0.11182E–09
3	3	0.721072657E–06	0.141435626E–05	0.95156E–10	0.93285E–10
4	0	0.539873863E–06	0.000000000E+00	0.10423E–09	0.00000E+00
4	1	–0.53632161E–06	–0.47344026E–06	0.85674E–10	0.82408E–10
4	2	0.350694105E–06	0.662671572E–06	0.16000E–09	0.16390E–09

4	3	0.990771803E–06	–0.20092836E–06	0.84657E–10	0.82662E–10
4	4	–0.18856080E–06	0.308853169E–06	0.87315E–10	0.87852E–10
5	0	0.685323475E–07	0.000000000E+00	0.54383E–10	0.00000E+00
5	1	–0.62101212E–07	–0.94422612E–07	0.27996E–09	0.28082E–09
5	2	0.652438297E–06	–0.32334961E–06	0.23747E–09	0.24356E–09
5	3	–0.45195540E–06	–0.21484719E–06	0.17111E–09	0.16810E–09
5	4	–0.29530164E–06	0.496658876E–07	0.11981E–09	0.11849E–09
5	5	0.174971983E–06	–0.66938427E–06	0.11642E–09	0.11590E–09
6	6	0.967616121E–08	–0.23719200E–06	0.11332E–09	0.11518E–09
7	7	0.109185148E–08	0.244415707E–07	0.13599E–09	0.13564E–09
8	8	–0.12409249E–06	0.120533165E–06	0.15695E–09	0.15769E–09
9	9	–0.47747538E–07	0.966412847E–07	0.18551E–09	0.18432E–09
10	10	0.100538634E–06	–0.24014844E–07	0.15964E–09	0.15956E–09
20	20	0.401448327E–08	–0.12045064E–07	0.36744E–09	0.36712E–09
36	36	0.460146465E–08	–0.59424533E–08	0.44653E–09	0.44731E–09
60	60	0.423068069E–08	0.39298378E–09	0.42181E–09	0.43090E–09
180	180	–0.40657270E–09	–0.58772611E–09	0.18849E–09	0.18849E–09
240	240	–0.23078058E–09	–0.46085798E–10	0.12839E–09	0.12835E–09
300	300	–0.50233688E–10	–0.10127553E–09	0.89613E–10	0.89644E–10
360	360	–0.44751638E–24	–0.83022494E–10	0.50033E–10	0.50033E–10

Some of the computed ellipsoidal harmonic coefficients are represented in *Table 2-3*. These coefficients are compatible with the following series expansion, which is convergent outside the reference ellipsoid $\tilde{\mathbb{E}}^2_{\varepsilon\cosh\eta_0,\varepsilon\sinh\eta_0}$. $\varepsilon\cosh\eta_0 = a$ = 6 378 136.3 m is coming from identity $a = \mathbb{S}^2_{r=R}$, and $\varepsilon\sinh\eta_0 = b$=6 356 751.647m is the linear eccentricity ε = 521 853.580 (m) of *WGD 2000* in *tide free system* (*E. Grafarend and A. Ardalan* (1999b)) which has been computed based on four fundamental geodetic parameters including the J_{20} coefficient of EGM96.

$$U(\lambda,\phi,\eta) = \frac{gm}{a}\sum_{n=0}^{360}\sum_{m=-n}^{+n} u_{nm}\,\frac{Q^*_{n,|m|}(\sinh\eta)}{Q^*_{n,|m|}(\sinh\eta_0)}e_{nm}(\lambda,\phi) \tag{2.8}$$

where gm=3 986 004.415E+8 m^3/s^2. $Q^*_{n,|m|}(\sinh\eta)$ are the numerically stabilised *associated Legendre functions of the second kind* (see (C.20)).

Table 2-3: Ellipsoidal harmonic coefficients; valid for the outer space of the reference ellipsoid $\tilde{\mathbb{E}}^2_{\varepsilon\cosh\eta_0,\varepsilon\sinh\eta_0}$ (η_0 = 3.194 713 538 106 130; ε = 521 853.580 (m) in tide free system (*E. Grafarend and A. Ardalan*, 1999b)

n	m	$u_{n,m}$	$u_{n,-m}$
0	0	1.00111910296E+000	0.00000000000E+000
1	0	0.00000000000E+000	0.00000000000E+000
1	1	0.00000000000E+000	0.00000000000E+000
2	0	5.15993819297E–004	0.00000000000E+000
2	1	–1.87706137878E–010	1.19987299652E–009
2	2	2.44499801919E–006	–1.40352755310E–006
3	0	9.62981735654E–007	0.00000000000E+000
3	1	2.04137403489E–006	2.49906947306E–007
3	2	9.08684801995E–007	–6.21802123549E–007
3	3	7.22957621328E–007	1.41805355446E–006
4	0	–2.52341695041E–007	0.00000000000E+000
4	1	–5.40263430110E–007	–4.76914568602E–007
4	2	3.59725179139E–007	6.63040468604E–007
4	3	9.95620481704E–007	–2.01911680303E–007
4	4	–1.89079400983E–007	3.09702607341E–007
5	0	7.49051604596E–008	0.00000000000E+000
5	1	–5.11340335153E–008	–9.38679285003E–008
5	2	6.62145933033E–007	–3.28971299283E–007
5	3	–4.52836882666E–007	–2.11878169088E–007
5	4	–2.96830497182E–007	4.99230202378E–008
5	5	1.75469711771E–007	–6.71288421225E–007
6	6	9.70435570236E–009	–2.37883139282E–007
7	7	1.09509071286E–009	2.45140824272E–008
8	8	–1.24465828265E–007	1.20895792530E–007
9	9	–4.78928038200E–008	9.69353023612E–008
10	10	1.00847319743E–007	–2.40885781042E–008
20	20	4.02735731045E–009	–1.20836917488E–008
36	36	4.61652960655E–009	–5.96190863784E–009
60	60	4.24468051530E–009	3.94284209853E–010
120	120	–4.58322787954E–010	–1.59665934569E–009
180	180	–4.07932875977E–010	–5.89692332581E–010
240	240	–2.31553724510E–010	–4.62401899146E–011
300	300	–5.04021159193E–011	–1.01615094489E–010
360	360	–4.49017687390E–025	–8.33010128012E–011

2.3 Remove steps

2.3.1 Remove-step 1: Removal of the global gravitational field and centrifugal field

Let us now get started with the removal of the modelled gravitational field, via the ellipsoidal harmonics expansion of the external gravitational field of the earth up to degree/order 360/360 in mean-tide permanent tide system (see *Section 1.12*, *page 64* for the definition of different permanent tide systems). We will also include the effect of the atmospheric masses in the expansion by adopting a proper gravitational constant GM, which includes the mass of the earth's atmosphere (*J. C. Ries*, 1992, and *E. Groten*, 1997). Such a reference field represents the effect of global and regional masses up to the features of 50-60 km wavelength (*F.G. Lemoine* et al. 1996).

In *Table 2-4* we have a collection of the ellipsoidal coordinates of a few first stations along the first order levelling lines of Baden-Württemberg. Ellipsoidal heights in *Table 2-4* are computed from global geoidal heights as we explained before. Transformation of the *Gauss ellipsoidal coordinates* in to *Jacobi ellipsoidal coordinates*, application of the harmonic expansion up to degree/order 360/360, and finally addetively combination of the gravitation of centrifugal field have led to the gravity intensity and *gravity potential* values represented in *Table 2-5* for few first stations. The components of gravity intensity vector $\{\Gamma_\lambda, \Gamma_\phi, \Gamma_\eta\}$ in *Table 2-5* are with respect to Jacobi ellipsoidal base vectors $\{\mathbf{e}_\lambda, \mathbf{e}_\phi, \mathbf{e}_\eta\}$.

Table 2-4: Gauss ellipsoidal coordinates $\{l,b\}$ and computed ellipsoidal height h of the stations along the first order levelling lines of Baden-Württemberg. Ellipsoidal heights are computed by adding the geoidal undulations obtained from global geoid computations to the normal height of the stations.

Point #	l	b	h
62230002	9.617432869327196	49.70393405021537	216.2858
62230009	9.549475653403452	49.70336818565175	214.5746
62230010	9.552776702951630	49.70837001544190	203.2078
62230029	9.518509890067718	49.76007033876102	188.3084
62230035	9.584526828221160	49.70004039950568	208.3931
62230051	9.535064264303526	49.71921659854684	201.6186
62230054	9.526483136723766	49.73239317921308	195.8455

62230058	9.525534139567768	49.74471645302996	206.0335
62230060	9.512823290742048	49.74864893644236	196.3530
62230064	9.544545338173982	49.71625901365535	209.8245

Table 2-5: *Gravity potential* $W(\lambda,\phi,u)$ and gravity intensity $\mathbf{\Gamma}(\lambda,\phi,\eta) = \Gamma_\lambda(\lambda,\phi,\eta)\mathbf{e}_\lambda + \Gamma_\phi(\lambda,\phi,\eta)\mathbf{e}_\phi + \Gamma_\eta(\lambda,\phi,\eta)\mathbf{e}_\eta$, i.e. gravitational potential and gravitational intensity of ellipsoidal harmonic expasion up to degree/order 360/360) plus the centrifugal potetnial.

Point #	$\Gamma_\lambda(\lambda,\phi,\eta)$	$\Gamma_\phi(\lambda,\phi,\eta)$	$\Gamma_\eta(\lambda,\phi,\eta)$	$W(\lambda,\phi,\eta)$
62230002	−1.6555811	−3.3619748E+003	−9.8103153E+005	62635215.695
62230009	1.17430700	−3.3628428E+003	−9.8103115E+005	62635232.500
62230010	0.97152330	−3.3625811E+003	−9.8103513E+005	62635343.989
62230029	1.60192981	−3.3604347E+003	−9.8104346E+005	62635489.868
62230035	−0.2185657	−3.3625705E+003	−9.8103330E+005	62635293.172
62230051	1.53373573	−3.3622664E+003	−9.8103622E+005	62635359.509
62230054	1.68881819	−3.3617205E+003	−9.8103895E+005	62635416.071
62230058	1.54428288	−3.3611176E+003	−9.8103682E+005	62635316.061
62230060	1.99370219	−3.3610418E+003	−9.8103991E+005	62635410.995
62230064	1.19159537	−3.3622976E+003	−9.8103360E+005	62635279.030

Removal of the calculated gravity and centrifugal intensity fields $\{\mathbf{\Gamma}_g(\mathbf{x}), \mathbf{\Gamma}_c(\mathbf{x})\}$, and gravity and centrifugal potential fields $\{W_g(\mathbf{x}), W_c(\mathbf{x})\}$ form the observed gravity intensity $\gamma(\mathbf{x})$ and geopotential number $c(\mathbf{x})$ generates the *incremental* pseudo observations of the remove step 1 as follows.

$$\delta\Gamma_1 = \gamma(\mathbf{x}) - \|\mathbf{\Gamma}_g(\mathbf{x}) + \mathbf{\Gamma}_c(\mathbf{x})\| \tag{2.9}$$

$$\delta W_1(\mathbf{x}) = w_0 - c(\mathbf{x}) - (W_g(\mathbf{x}) + W_c(\mathbf{x})) \tag{2.10}$$

Figure 2-6 shows the variation of the *incremental* gravity intensity $\delta\Gamma_1 = \gamma(\mathbf{x}) - \|\mathbf{\Gamma}_g(\mathbf{x}) + \mathbf{\Gamma}_c(\mathbf{x})\|$ while *Figure 2-7* presents the variation of *incremental gravity potential* $\delta W_1(\mathbf{x}) = w_0 - c(\mathbf{x}) - (W_g(\mathbf{x}) + W_c(\mathbf{x}))$ within the state Baden-Württemberg. A comparison between these two figures and topographical map of the state Baden-Württemberg shows a high correlation between topography and the *incremental* quantities of the type $\delta\Gamma_1(\mathbf{x})$, and $\delta W_1(\mathbf{x})$.

Note that the *incremental* quantities $\delta\Gamma_1(\mathbf{x})$ and $\delta W_1(\mathbf{x})$ due to the remaining effect of topographical masses are not harmonic in space between the surface of the earth and the reference ellipsoid. Therefore, we have to proceed to the remove-step 2 to remove the effect of the topographical masses between the surface of the earth and the reference ellipsoid.

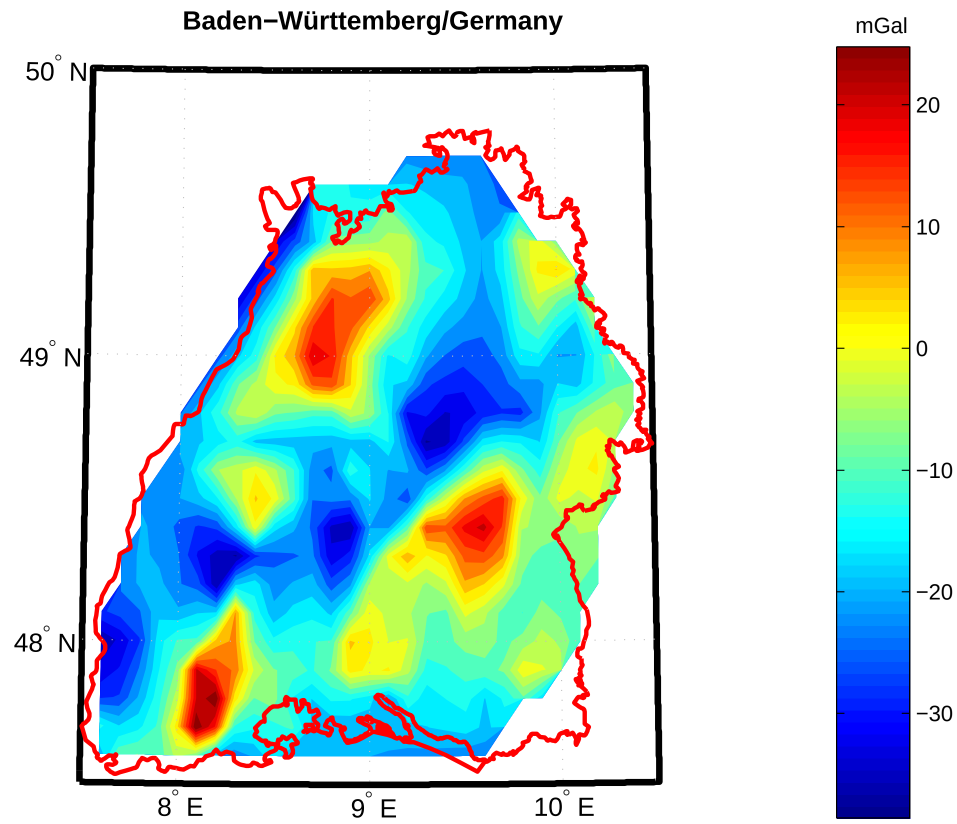

Figure 2-6: *Incremental* gravitational intensity $\delta\Gamma_1 = \gamma(\mathbf{x}) - \|\mathbf{\Gamma}_g(\mathbf{x}) + \mathbf{\Gamma}_c(\mathbf{x})\|$.

minimum: $-40.7307 mGal$

maximum: $44.8557 mGal$

standard deviation: $14.9594 mGal$.

Map Projection Information:

Equidistant Conic Projection

Standard Parallels: $48^\circ N$ *and* $49^\circ N$

Reference ellipsoid: WGD2000

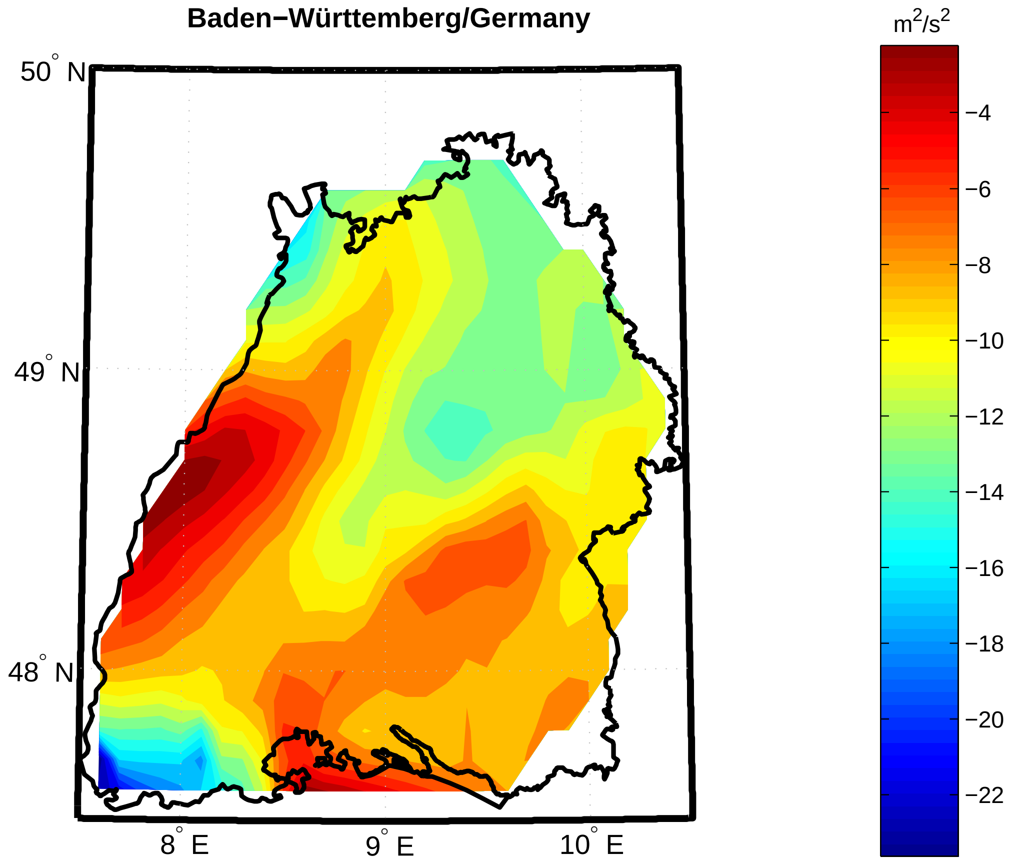

Figure 2-7: *Incremental gravitational potential* $\delta W_1(\mathbf{x}) = w_0 - c(\mathbf{x}) - (W_g(\mathbf{x}) + W_c(\mathbf{x}))$.

minimum: $-24.1242\ m^2/s^2$

maximum: $-0.4859\ m^2/s^2$

standard deviation: $3.5054 m^2/s^2$.

<u>Map Projection Information:</u>

Equidistant Conic Projection

Standard Parallels: $48^\circ N$ *and* $49^\circ N$

Reference ellipsoid: WGD2000

2.3.2 Remove-step 2: Terrain reduction

In this section, we are going to remove the effect of the near zone masses, i.e. those features, with the wavelength signature smaller than 50 km. These features are specifically the terrain masses between the evaluation point and the reference ellipsoid in a radius of 50 km. Since after removal of the global field of ellipsoidal expansion of degree/order 360/360 we are left with the terrain reduction in a very small area of 50km around the computational point, *Newton integral* over the local topographical masses in planar approximation can be used. Our computations will be based on the $1km \times 1km$ DTM of Baden-Württemberg. In *Table 2-6* we have presented the computed components of gravitational intensity vector and gravitational potential of the topographical masses above the reference ellipsoid for first few points of the data file. As it is shown in *Figure 2-8*, the gravitational potential of topographical masses varies from 7.9147 m^2/s^2 to 43.8092 m^2/s^2. While the variation of modulus of gravitational intensity of topographical masses is in the range of 12.8281 $mGal$ to 116.1205 $mGal$ (see *Figure 2-9*).

Table 2-6: Components of gravitational intensity $\mathbf{\Gamma}_t(\lambda,\phi,\eta) = \Gamma^t_\lambda(\lambda,\phi,\eta)\mathbf{e}_\lambda + \Gamma^t_\phi(\lambda,\phi,\eta)\mathbf{e}_\phi + \Gamma^t_\eta(\lambda,\phi,\eta)\mathbf{e}_\eta$, and gravitational potential $W_t(\lambda,\phi,u)$ of topographical masses above the reference ellipsoid in a radius of 50 km around the calculation point on the surface of the earth.

Point Number	$\Gamma^t_\lambda(\lambda,\phi,\eta)$	$\Gamma^t_\phi(\lambda,\phi,\eta)$	$\Gamma^t_\eta(\lambda,\phi,\eta)$	$W_t(\lambda,\phi,\eta)$
62230002	-5.92824087480	17.261785707447	17.072932032384	14.689611148642
62230009	-17.2446915753	19.189213142762	11.114474898814	15.346037198767
62230010	-13.7808568003	14.536577761860	9.1167297407813	15.048740751344
62230029	-17.3493376865	18.277618517675	3.5142792402904	13.419714623244
62230035	-11.7474735835	16.640619156541	7.5337639810504	15.155360544636
62230051	-15.6656953272	16.403883180832	11.239167196206	14.837037432880
62230054	-16.8080770601	21.704855889545	15.497083059203	14.328597688369
62230058	-16.5332867443	12.787059877719	9.1071905887855	13.984919022785
62230060	-16.0153271264	17.309657708463	4.5533377594874	14.079678751739
62230064	-15.6648372568	16.406435815567	11.236636966120	14.837037432880

Removal of the gravitational intensity $\mathbf{\Gamma}_t(\mathbf{x})$ and potential $W_t(\mathbf{x})$ of the local topographical masses in a radius of $50km$ around the calculation points, as well as, gravitational and centrifugal intensity $\{\mathbf{\Gamma}_g(\mathbf{x}), \mathbf{\Gamma}_c(\mathbf{x})\}$, and gravitational and centrifugal potential $\{W_g(\mathbf{x}), W_c(\mathbf{x})\}$ form the observed *modulus of gravity intensity* $\gamma(\mathbf{x})$ and geopotential number $c(\mathbf{x})$ generates the *incremental* pseudo observations ($\delta\Gamma_2(\mathbf{x})$, and $\delta W_2(\mathbf{x})$) of the remove-step 2.

$$\delta\Gamma_2(\mathbf{x}) = \gamma(\mathbf{x}) - \|\mathbf{\Gamma}_g(\mathbf{x}) + \mathbf{\Gamma}_c(\mathbf{x}) + \mathbf{\Gamma}_t(\mathbf{x})\| \tag{2.11}$$

$$\delta W_2(\mathbf{x}) = w_0 - c(\mathbf{x}) - (W_g(\mathbf{x}) + W_c(\mathbf{x}) + W_t(\mathbf{x})) \tag{2.12}$$

A comparison of *Figure 2-9* and *Figure 2-10* with *Figure 2-7* and *Figure 2-8* reveals the fact that in the process of generating the harmonic *incremental* gravitational potential in remove-step 2 we have made the *incremental* fields of gravitational potential and gravitational intensity a bit rougher. Why do we have such a result? The answer is that the global potential and intensity fields computed from the ellipsoidal harmonic expansion are based on actually observed gravity field information, embedded in the coefficients. Therefore, it naturally fits better to the real gravitational potential and gravitational intensity field, than the gravitational intensity and potential computed by Newton integral over the terrain masses in planar approximation and constant mass density ($\rho = 2.67\ g/cm^3$). It is important to note that by removing the global intensity and potential field of ellipsoidal harmonic expansion of degree/order 360/360 we do not need to consider any isostasy effect, because it is implanted in *ellipsoidal harmonic expansion of degree/order 360/360!*

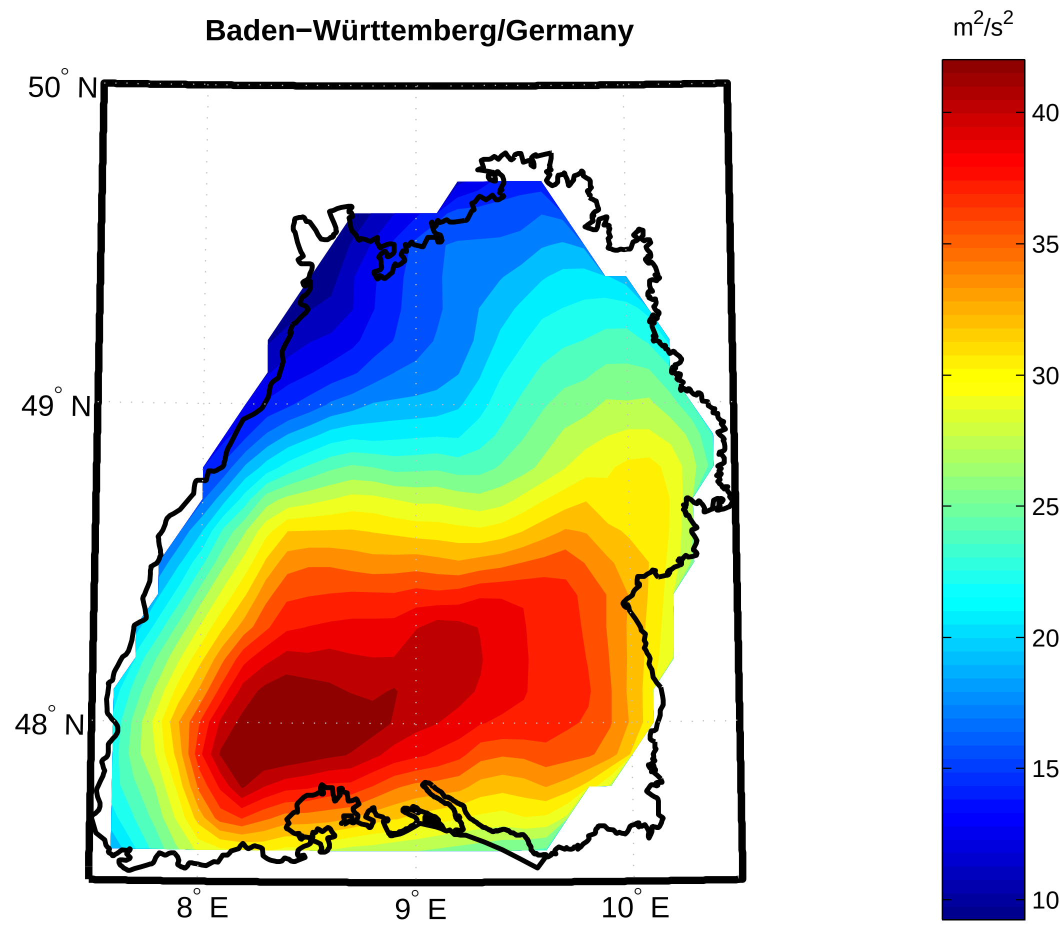

Figure 2-8: Gravitational potential of topographical masses above reference ellipsoid in an area of $50km$ $50km$ around the calculation points. Computations are based on $1km \times 1km$ DTM model and planar approximation. The gravitational potential of topographical masses varies between $7.9147\ m^2/s^2$ to $43.8092\ m^2/s^2$.

Map Projection Information:
Equidistant Conic Projection
Standard Parallels: $48^\circ N$ and $49^\circ N$
Reference ellipsoid: WGD2000

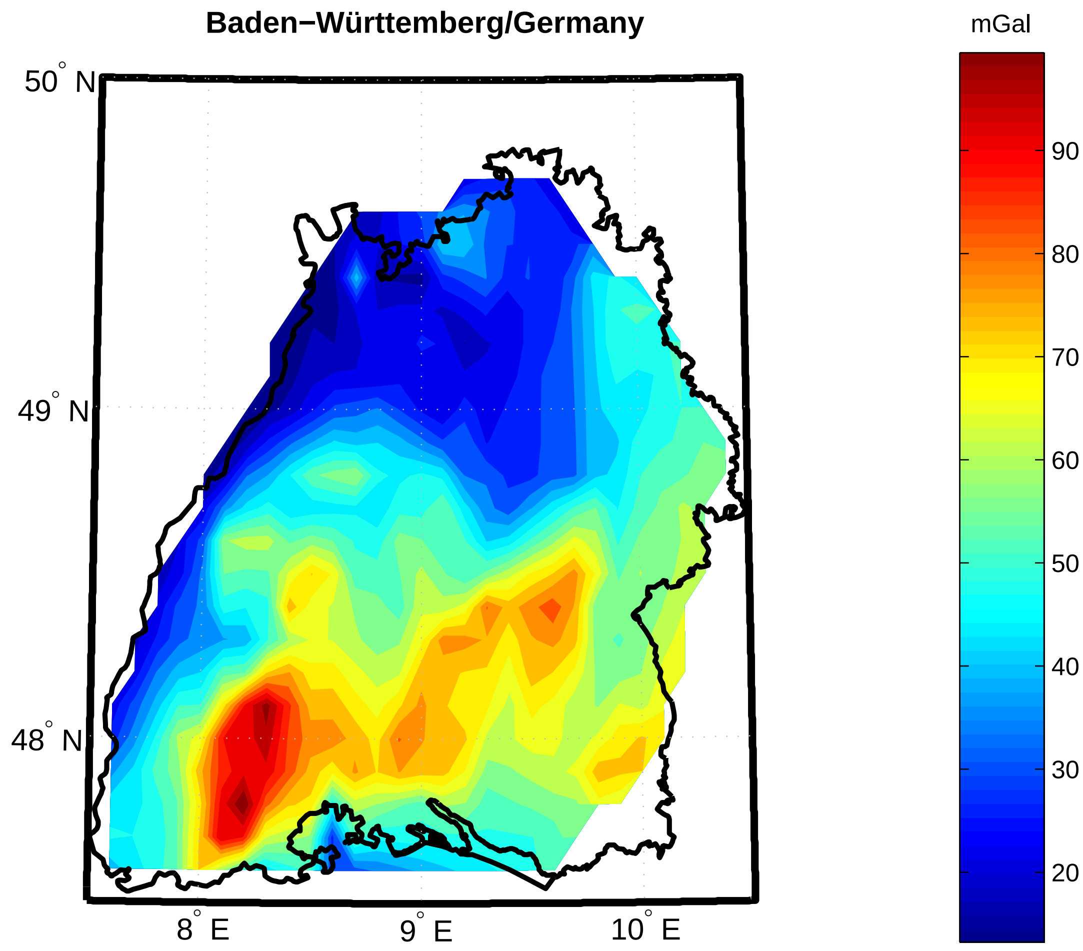

Figure 2-9: Modulus of gravitational intensity of topographical masses in a radius of $50km$ around computation point above the reference ellipsoid. Calculations are based on a $1km \times 1km$ local DTM model and planar approximation. The norm of gravitational intensity of topographical masses varies from 12.8281 $mGal$ to 116.1205 $mGal$.

<u>Map Projection Information:</u>
Equidistant Conic Projection
Standard Parallels: $48^\circ N$ *and* $49^\circ N$
Reference ellipsoid: WGD2000

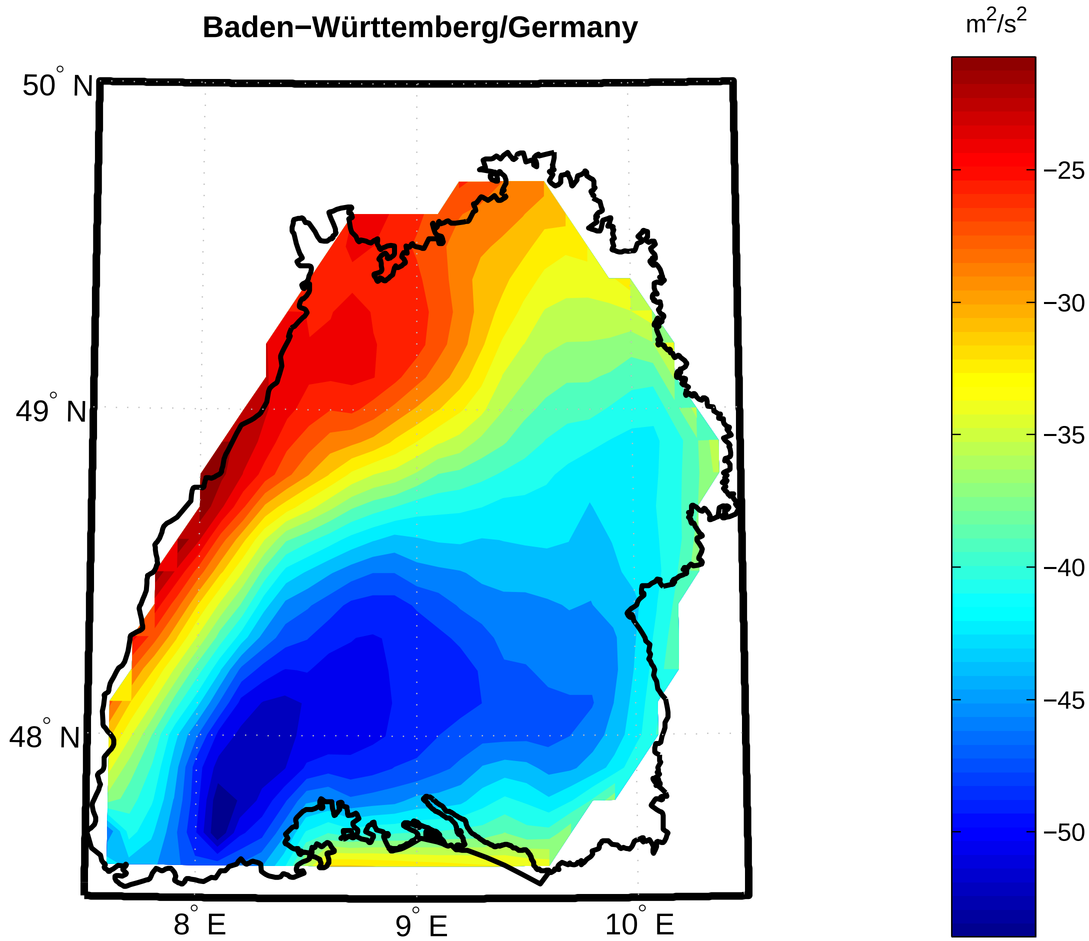

Figure 2-10: *Incremental* potential after remove-step 2. The *incremental* potential varies in the interval $[-59.1281 m^2/s^2, -16.9759\ m^2/s^2]$ with standard deviation of $8.3188 m^2/s^2$.

<u>Map Projection Information:</u>
Equidistant Conic Projection
Standard Parallels: 48°N and 49°N
Reference ellipsoid: WGD2000

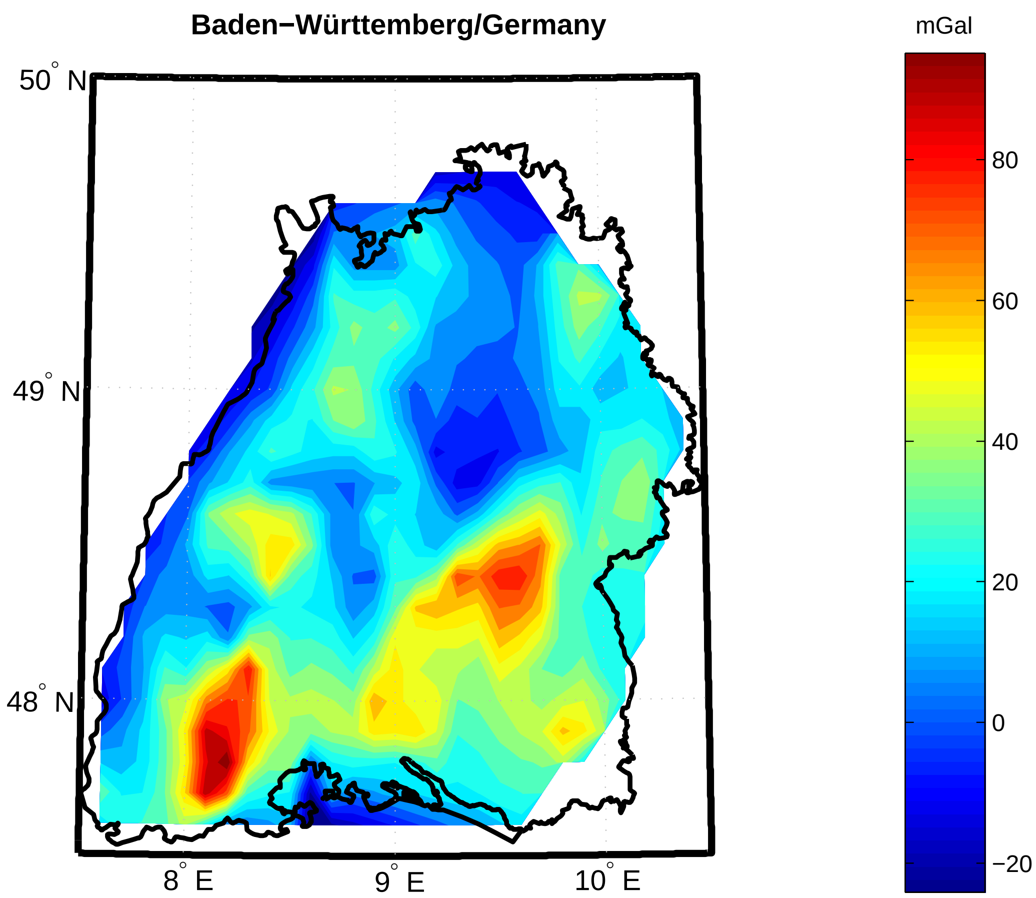

Figure 2-11: Modulus of *incremental* gravity intensity after remove-step 2. The modulus of *incremental* gravity intensity varies in the interval $[-32.8583 mGal, 127.5585\ mGal]$ with standard deviation of 25.5092 $mGal$.

<u>Map Projection Information:</u>
Equidistant Conic Projection
Standard Parallels: $48^\circ N$ *and* $49^\circ N$
Reference ellipsoid: WGD2000

2.4 Downward continuation step

Here we will present the detailed results of downward continuation of the harmonic pseudo-observables derived from the remove-step 2. Our downward continuation machinery is *Abel-Poisson integral* in discrete form as derived in *Section 1.13.1* (*page 68*). It is a well-know fact that integral equations of the first kind are very sensitive to errors of observations. That is, for example, in *Abel-Poisson integral,* written in compact form as

$$\int_a^b k(s,t)x(t)dt = g(s) \tag{2.13}$$

any small error in the observations $g(s)$ will be magnified and transferred into unknowns $x(t)$. To reduce the effect of errors on the pseudo observables one can replace the original observables by some mean values. Following that idea we overlaid a $6' \times 6'$ gird over the data points, averaged the *incremental* observables within each cell of the grid, and attributed the mean value to the centeroid of the averaged points within the cells. *Figure 2-12* shows the adopted grid for averaging while *Figure 2-13* displays the averaged data points.

Let us now have a glance at the variations of the *incremental* quantities $\delta\Gamma_2$ and δW_2 after averaging in *Figure 2-14* and *Figure 2-15*. The figures show that the averaging process does not change overall picture of the variations of the disturbing quantities but behaves like a low-pass filter.

For the numerical integration of *Abel-Poisson integral* over the reference ellipsoid $\mathbb{E}^2_{a,b}$ we select a $12' \times 12'$ grid over the geographical region $7.5^\circ \le \lambda \le 10.5^\circ$ and $57.5^\circ \le \phi \le 50^\circ$, which results in $15 \times 13 = 198$ unknowns of the type mean *incremental* gravitational potential on the surface of reference ellipsoid $\mathbb{E}^2_{a,b}$ against 228 observations of the type $\delta\Gamma_2$ and 228 observations of the type δW_2. That is we have an over-determined case of 456 equations to determine 198 unknowns. Since we are going to use two different types of observables simultaneously we have to think of the relative weight between the two types of observations amongst the other numerical problems of solving an insatiable integral equation of the first kind. Therefore, it is reasonable to solve the problem first for each type of observables separately, and then derive the combined solution. Let us first start with the observables of the type *incremental* gravitational potential δW_2.

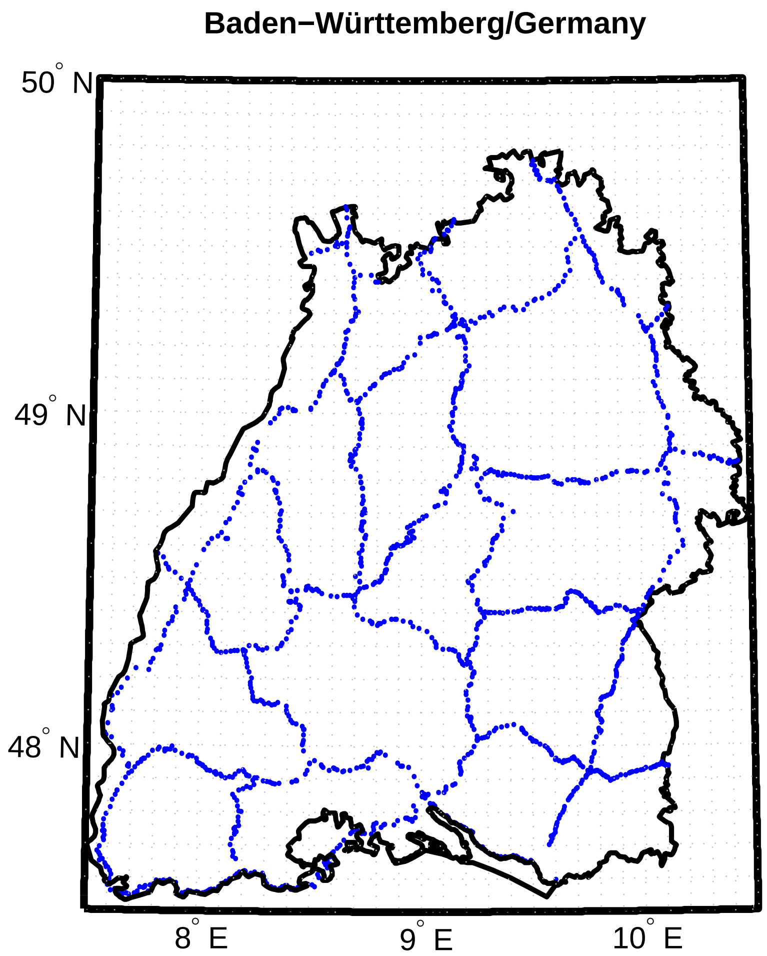

Figure 2-12: The overlaid $6' \times 6'$ grid over the data points.

Map Projection Information:
Equidistant Conic Projection
Standard Parallels: $48^\circ N$ *and* $49^\circ N$
Reference ellipsoid: WGD2000

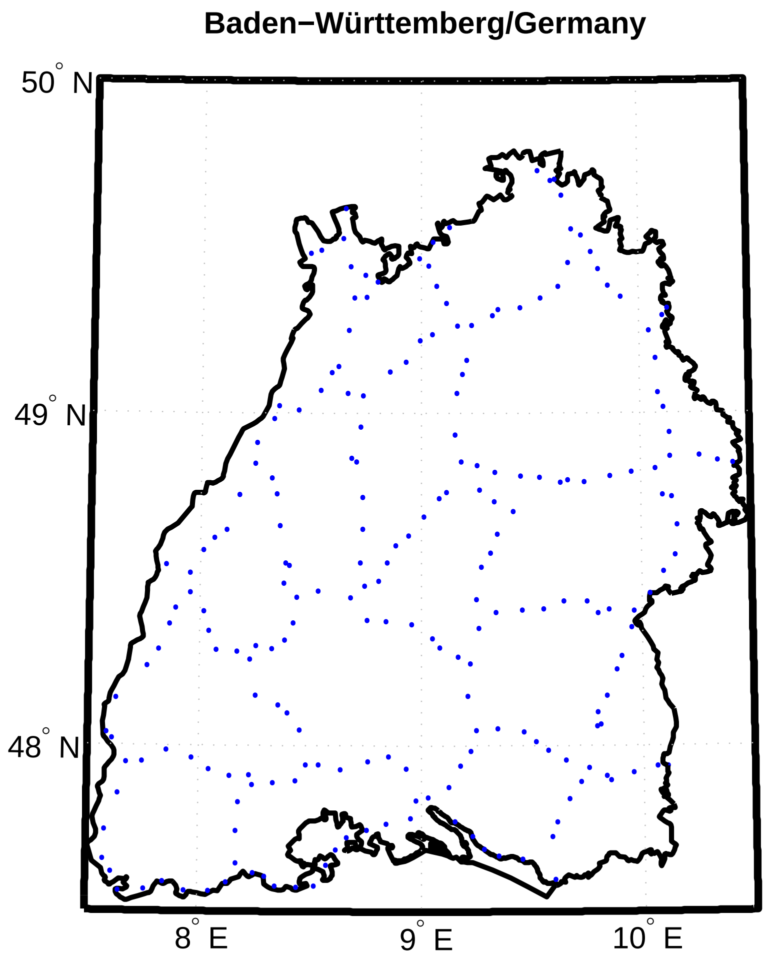

Figure 2-13: 228 averaged data points in $6' \times 6'$ grid.

Map Projection Information:
Equidistant Conic Projection
Standard Parallels: $48^{\circ}N$ *and* $49^{\circ}N$
Reference ellipsoid: WGD2000

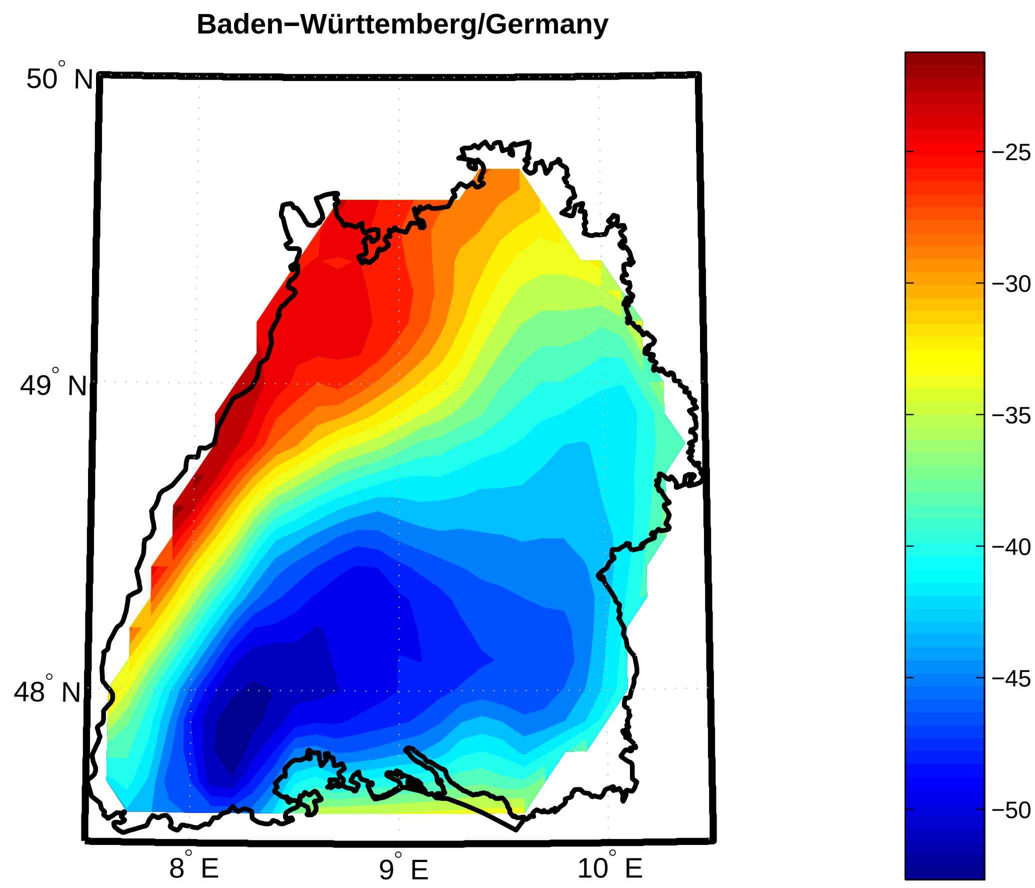

Figure 2-14: Averaged *incremental* gravitational potential δW_2. Variations are in the interval $[-53.2306 m^2/s^2, -19.2751 m^2/s^2]$ with standard deviation of $8.6191 m^2/s^2$.

<u>*Map Projection Information:*</u>
Equidistant Conic Projection
Standard Parallels: $48^\circ N$ *and* $49^\circ N$
Reference ellipsoid: WGD2000

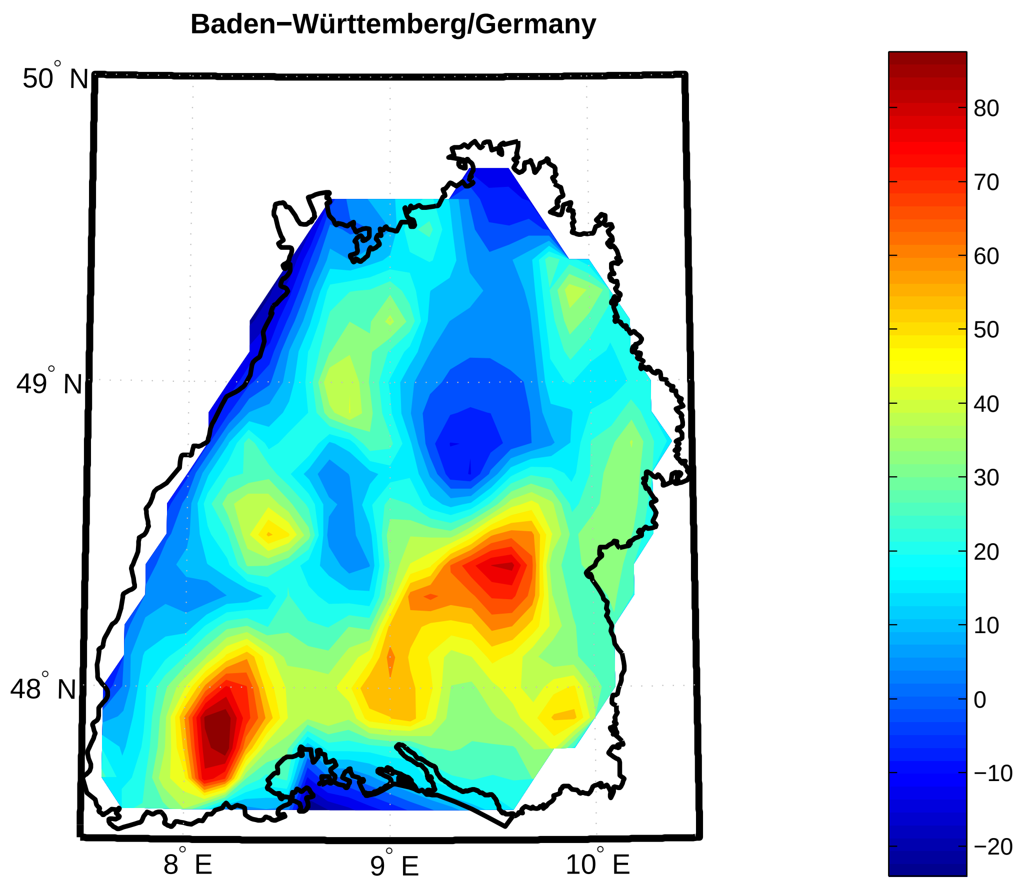

Figure 2-15: Averaged modulus of *incremental* gravitational intensity $\delta\Gamma_2$. Variations are in the interval $[-31.3276 mGal, 107.8387 mGal]$ with standard deviation of $24.147469 mGal$.

<u>Map Projection Information:</u>
Equidistant Conic Projection
Standard Parallels: $48^\circ N$ *and* $49^\circ N$
Reference ellipsoid: WGD2000

2.4.1 Case 1: Solution for the disturbing Gravitational potential $\delta \mathbf{W}_2$

The following discretized integral-equation (c.f. *Section 1.13.1*) provides us with observation equations for determination of unknown *incremental* gravitational potential δW_2 .

$$\begin{aligned} \delta W(\mathbf{x}_P) &= \frac{1}{S}\sum_{i=1}^{i_{\max}}\sum_{j=1}^{j_{\max}} a.\sqrt{b^2 + \varepsilon^2 \sin^2 \overline{\phi}_{ij}} \\ &\times \cos \overline{\phi}_{ij} \Delta\lambda\Delta\phi w(\overline{\phi}) K(\lambda,\phi,\eta;\overline{\lambda},\overline{\phi},\eta_0)\delta\overline{W}(\mathbf{X}_{P_{ij}}) \end{aligned} \tag{2.14}$$

where

$$w(\overline{\phi}) := \frac{a}{\sqrt{b^2 + \varepsilon^2 \sin^2 \overline{\phi}}}\left(\frac{1}{2} + \frac{1}{4}\frac{b^2}{a\varepsilon}\cdot \ln\frac{a+\varepsilon}{a-\varepsilon}\right) \tag{2.15}$$

$$S = \text{area }(\mathrm{E}^2_{a,b}) = 4\pi a \cdot \left\{\frac{1}{2} + \frac{1}{4}\frac{b^2}{a\varepsilon}\ln\frac{a+\varepsilon}{a-\varepsilon}\right\}, \tag{2.16}$$

and $K(\lambda,\phi,\eta;\overline{\lambda},\overline{\phi},\eta_0)$ stands for ellipsoidal *Abel-Poisson kernel* (c.f. *Box 1-9*, *page 27*). Equation (2.14) is a linear equation and can be written in matrix notations as

$$\mathbf{y} + \mathbf{i} = \mathbf{A}\mathbf{x} \tag{2.17}$$

where $\mathbf{y} = \delta\mathbf{W}_2(\mathbf{x}_P)$ is the vector of pseudo-observations and $\mathbf{x} = \delta\mathbf{W}_2(\mathbf{X}_P)$ is the vector of unknowns and $\mathbf{i}$ is the vector of inconsistencies. In this case $\mathbf{A}$ is a 228×195 matrix.

First, the rank of the matrix $\mathbf{A}^T\mathbf{A}$ is computed and it turned out to be 195, which guaranties the existence and *uniqueness* of the discretized problem! However, the condition number of $\mathbf{A}^T\mathbf{A}$, i.e. the ratio of the largest singular value of $\mathbf{A}^T\mathbf{A}$ to the smallest one, is 6.6×10^{25}, which indicates an ill conditioned problem. Therefore, the weighted least-square solution of (2.17) with weight function $\mathbf{P}$

$$\hat{\mathbf{x}} = (\mathbf{A}^T\mathbf{P}\mathbf{A})^{-1}\mathbf{A}^T\mathbf{P}\mathbf{y} \tag{2.18}$$

which minimises the functional

$$F(\mathbf{x}) = \|\mathbf{A}\mathbf{x} - \mathbf{y}\|^2 \tag{2.19}$$

would not produce any reliable result and one has to resort to one of the regularisation methods. We select the *Phillips-Tikhonov regularisation* method, which has proven itself as the most efficient one. *Phillips-Tikhonov regularisation* is based on reformulation of (2.19) as follows: Instead of searching for $\hat{\mathbf{x}}$, which minimises (2.19), looking for $\hat{\mathbf{x}}^{\alpha}$ which minimises the functional

$$F_{\alpha}(\mathbf{x}^{\alpha}) = \|\mathbf{A}\mathbf{x}^{\alpha} - \mathbf{y}\|^2 + \alpha\|\mathbf{x}^{\alpha}\|^2 \tag{2.20}$$

where α is a positive parameter, called *regularisation parameter*. The minimum norm solution of (2.20) is

$$\hat{\mathbf{x}}^{\alpha} = (\mathbf{A}^T\mathbf{P}\mathbf{A} + \alpha\mathbf{I})^{-1}\mathbf{A}^T\mathbf{P}\mathbf{y}. \tag{2.21}$$

For the observables be of the same kind and the same accuracy, the weight matrix can be considered as unit matrix, i.e. $\mathbf{P} = \mathbf{I}$. Therefore, (2.21) can be written as

$$\hat{\mathbf{x}}^{\alpha} = (\mathbf{A}^T\mathbf{A} + \alpha\mathbf{I})^{-1}\mathbf{A}^T\mathbf{y} \tag{2.22}$$

We already mentioned that the condition number of $\mathbf{A}^T\mathbf{A}$ is 6.6×10^{25}, which indeed is a very large condition number! However, for example $\alpha = 1$, reduces the condition number of $(\mathbf{A}^T\mathbf{A} + \alpha\mathbf{I})$ to 20.5, which guaranties a stable solution. Of course, in expense of the bias is introduced by α. Let us see how much bias is introduced by condition number $\alpha = 1$ by looking into the vector of estimated inconsistencies $\hat{\mathbf{i}}$

$$\hat{\mathbf{i}} = \mathbf{A}\hat{\mathbf{x}} - \mathbf{y}. \tag{2.23}$$

The maximum value of estimated inconsistencies for $\alpha = 1$ is 31.3248 m^2/s^2 ($\max(\hat{\mathbf{i}}) = 31.3248\ m^2/s^2$). *Figure 2-17* shows the plot of the maximum estimated inconsistencies per different regularisation parameters. Now the question arises as to what regularisation parameter should be adopted. In other words, is there any optimum regularisation parameter α which can compromise between stability of the solution and bias? The answer is yes, and such a regularisation can be obtained by studying the variation of the mean square error of $\hat{x}^{\alpha}$ ($MSE\{\hat{x}^{\alpha}\}$) versus the regularisation parameter α. The following formula borrowed from *E. Grafarend and B. Schaffrin* (1993, page 124) provides us with an estimation of MSE matrix of the downward continued incremental gravitational potential $\hat{\mathbf{x}}^{\alpha}$.

$$MSE\{\hat{\mathbf{x}}^{\alpha}\} = \sigma_0^2(\mathbf{A}^T\mathbf{A} + \alpha\mathbf{I})^{-1}\mathbf{A}^T A(\mathbf{A}^T\mathbf{A} + \alpha\mathbf{I})^{-1} + \boldsymbol{\beta}\boldsymbol{\beta}^{\mathbf{T}} \tag{2.24}$$

where

$$\boldsymbol{\beta} = -(\alpha\mathbf{I} + \mathbf{A}^T\mathbf{A})^{-1}(\alpha E\{\mathbf{x}\}). \tag{2.25}$$

Indeed the expected value of the unknown parameter $E\{\mathbf{x}\}$ appearing in (2.25) is unknown. However since $MSE\{\hat{\mathbf{x}}^{\alpha}\}$ is not sensitive to $E\{\mathbf{x}\}$, in practice instead of $E\{\mathbf{x}\}$ one can use any estimated value of $\hat{\mathbf{x}}^{\alpha}$ derived from a very small regularisation parameter α. Figure 2-16 shows the variations of the trace of $MSE\{\hat{\mathbf{x}}^{\alpha}\}$ against the regularisation parameter α. We have also a plot of estimated inconsistencies $\hat{\mathbf{i}}$ versus condition number α in Figure 2-17 and the condition number of $\mathbf{A}^T\mathbf{A} + \alpha\mathbf{I}$ versus the regularisation parameter α in Figure 2-18. Based on Figure 2-16, variations of the trace of $MSE\{\hat{\mathbf{x}}^{\alpha}\}$ against the regularisation parameter α, one can conclude that the optimum regularisation parameter in this case is $\alpha = 0.7$.

The regularised downward continued incremental gravitational potential $\delta W_2(\mathbf{X}_P)$, based on the optimum regularisation parameter $\alpha = 0.7$, is shown in Figure 2-19. In Figure 2-20, we have a plot of square root of the diagonal elements of $MSE\{\hat{\mathbf{x}}^{\alpha}\}$ based on optimum regularisation parameter $\alpha = 0.7$. As it can be observed in Figure 2-20 the standard error of the downward continued incremental gravitational potentials is quite small, except in some spots/cells. Whoever, even within those spots the accuracy is enough as compared with the accuracy of the observations.

The difference between the incremental gravitational potential at the reference ellipsoid (from downward continuation based on the optimum regularisation parameter $\alpha = 0.7$.) and at the surface of the Earth is shown in *Figure 2-21*. The black spots are areas without surface data.

Having settled with regularisation let us start with restore process.

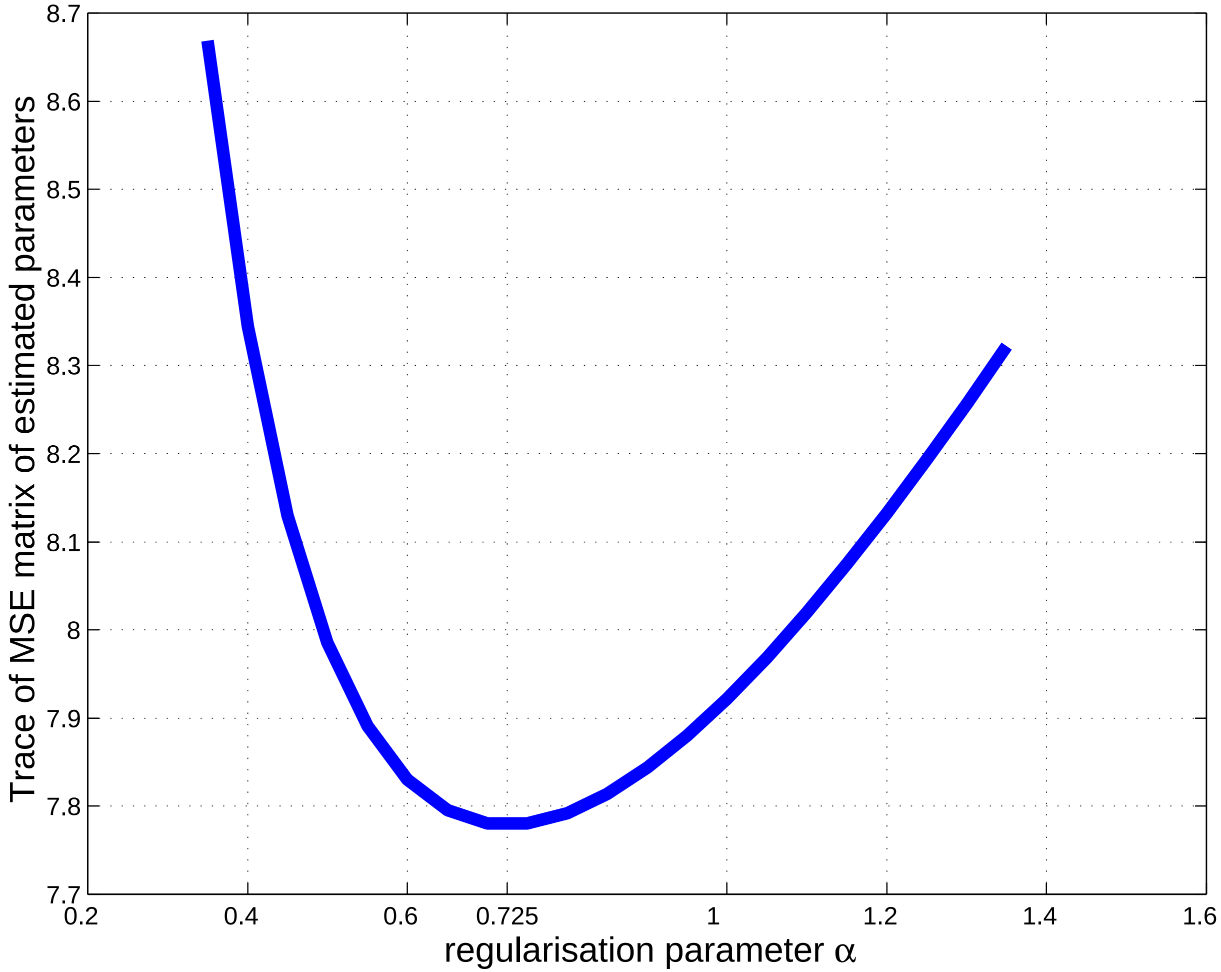

Figure 2-16: Trace of Mean Square Error matrix $\mathrm{MSE}\{\hat{\mathbf{x}}^{\alpha}\}$ of estimated parameters versus the regularisation parameter α. As one can see the optimum regularisation parameter is 0.725 ± 0.02.

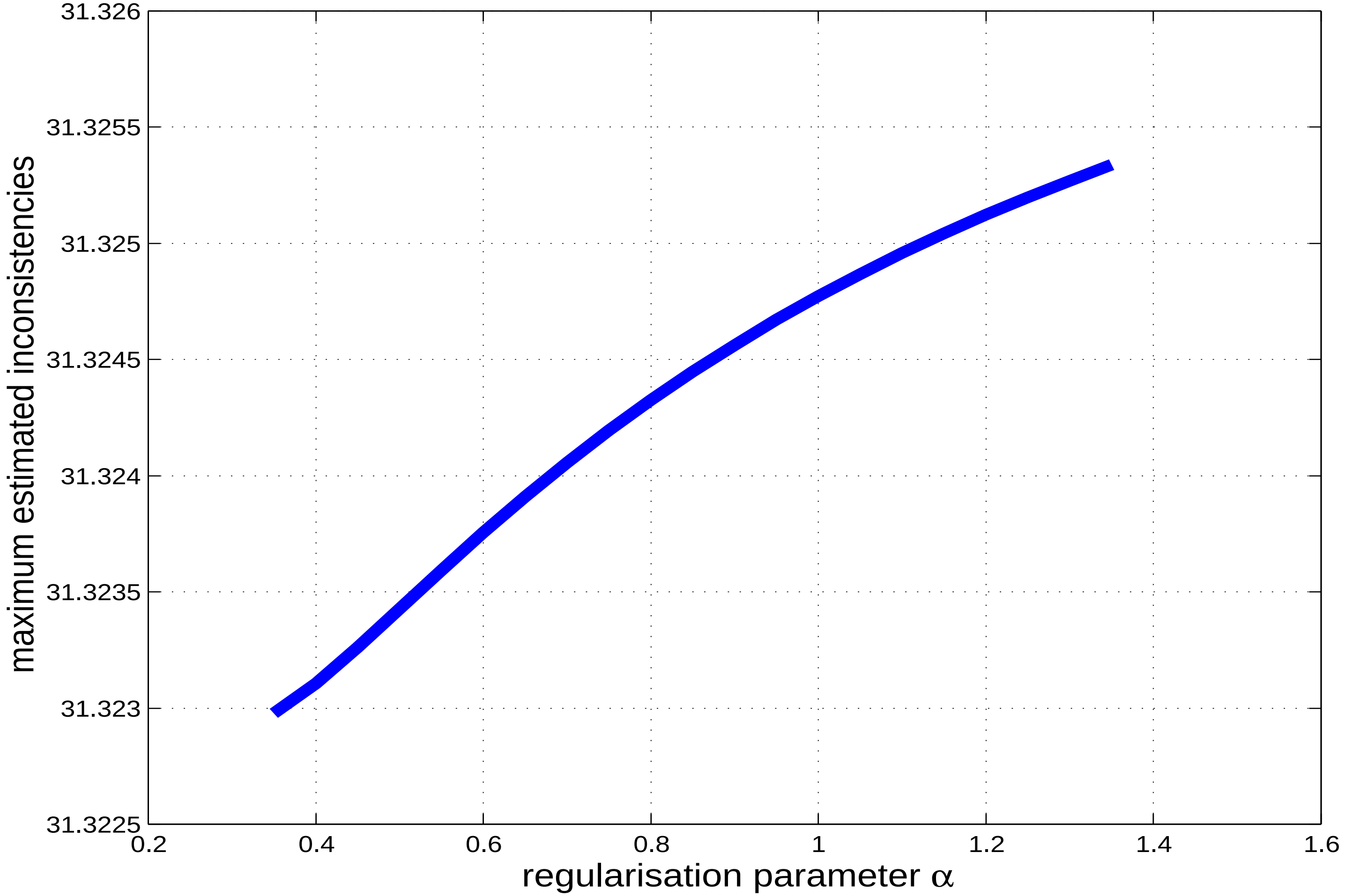

Figure 2-17: Maximum estimated inconsistencies versus regularisation parameter.

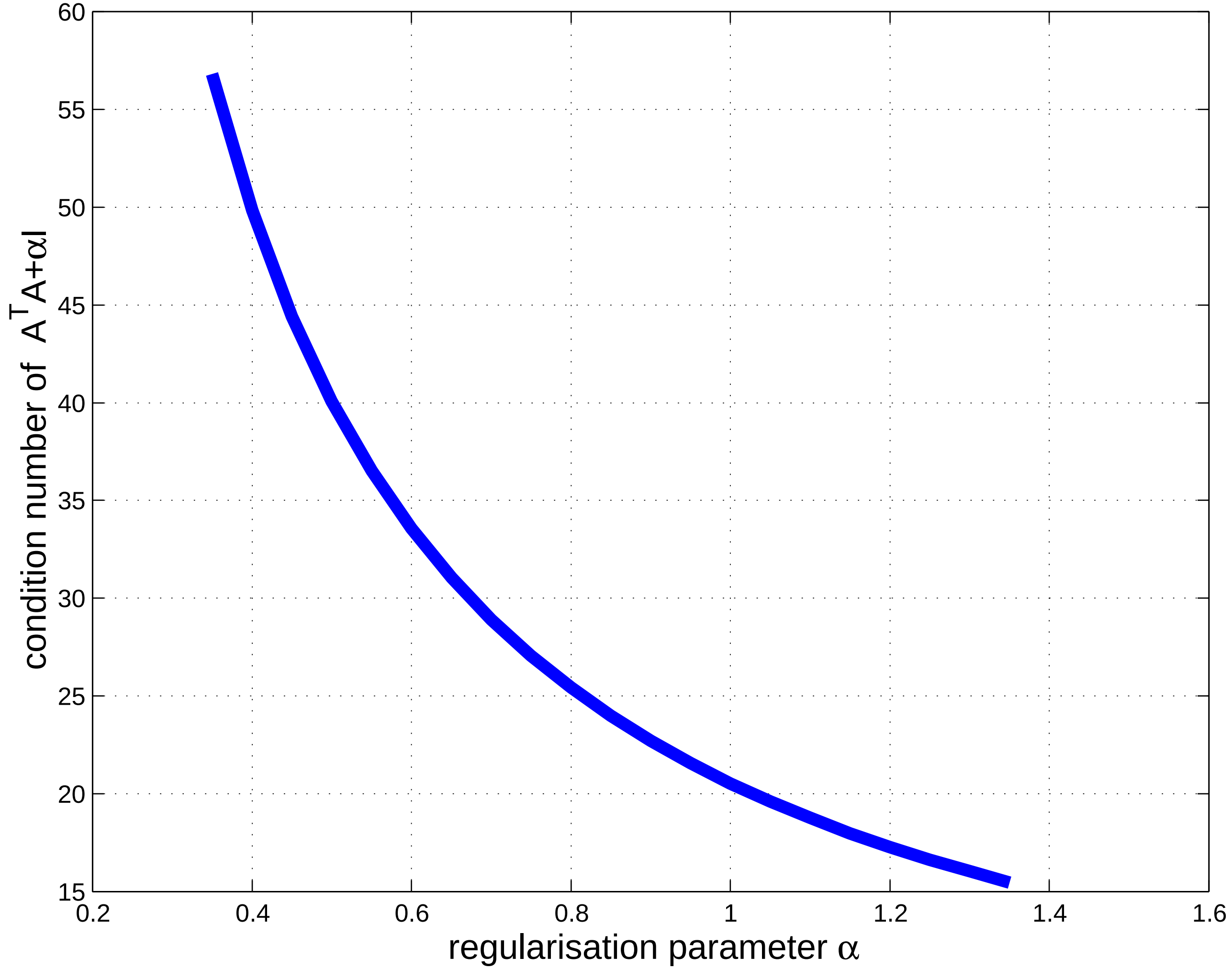

Figure 2-18: Condition number of $\mathbf{A}^T\mathbf{A} + \alpha\mathbf{I}$ versus the regularisation parameter α

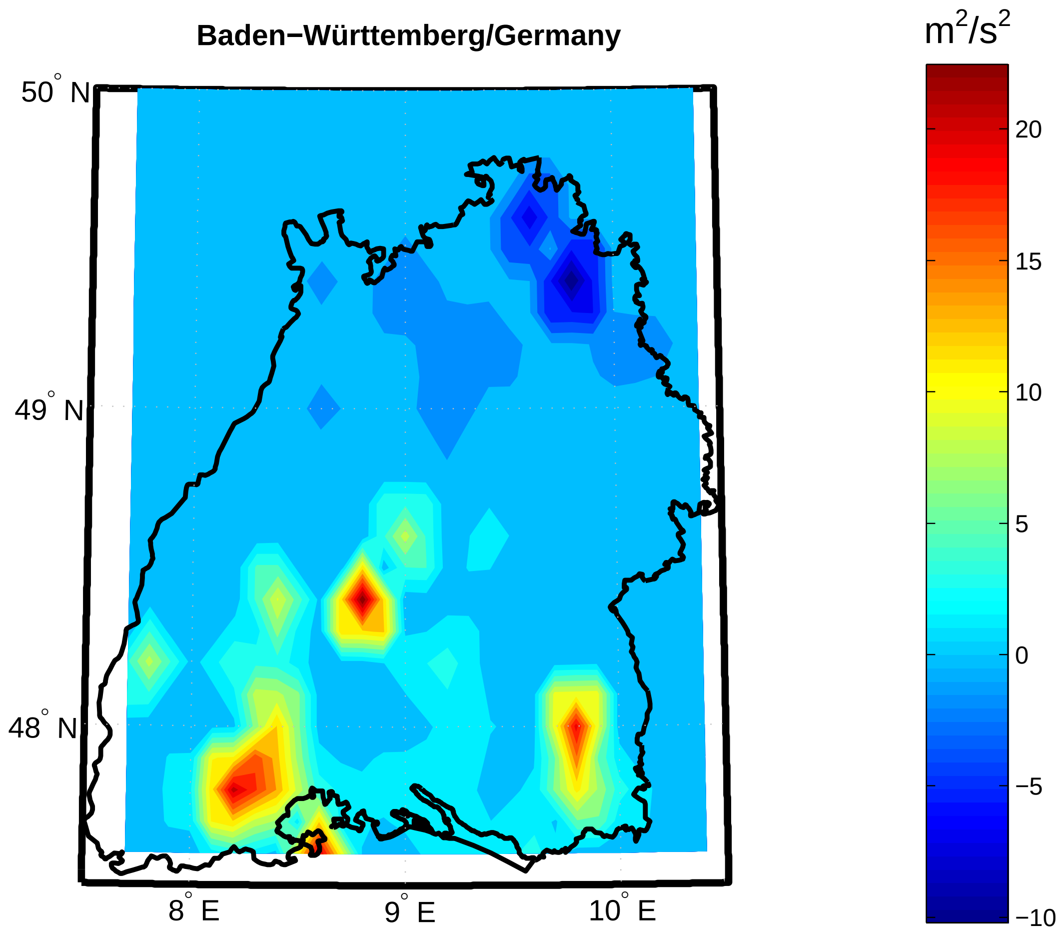

Figure 2-19: Downward continued *incremental* gravitational potential $\delta\hat{W}_2(\mathbf{X}_P)$ based on the optimum regularisation parameter $\alpha = 0.7$.

Map Projection Information:
Equidistant Conic Projection
Standard Parallels: $48^\circ N$ and $49^\circ N$
Reference ellipsoid: WGD2000

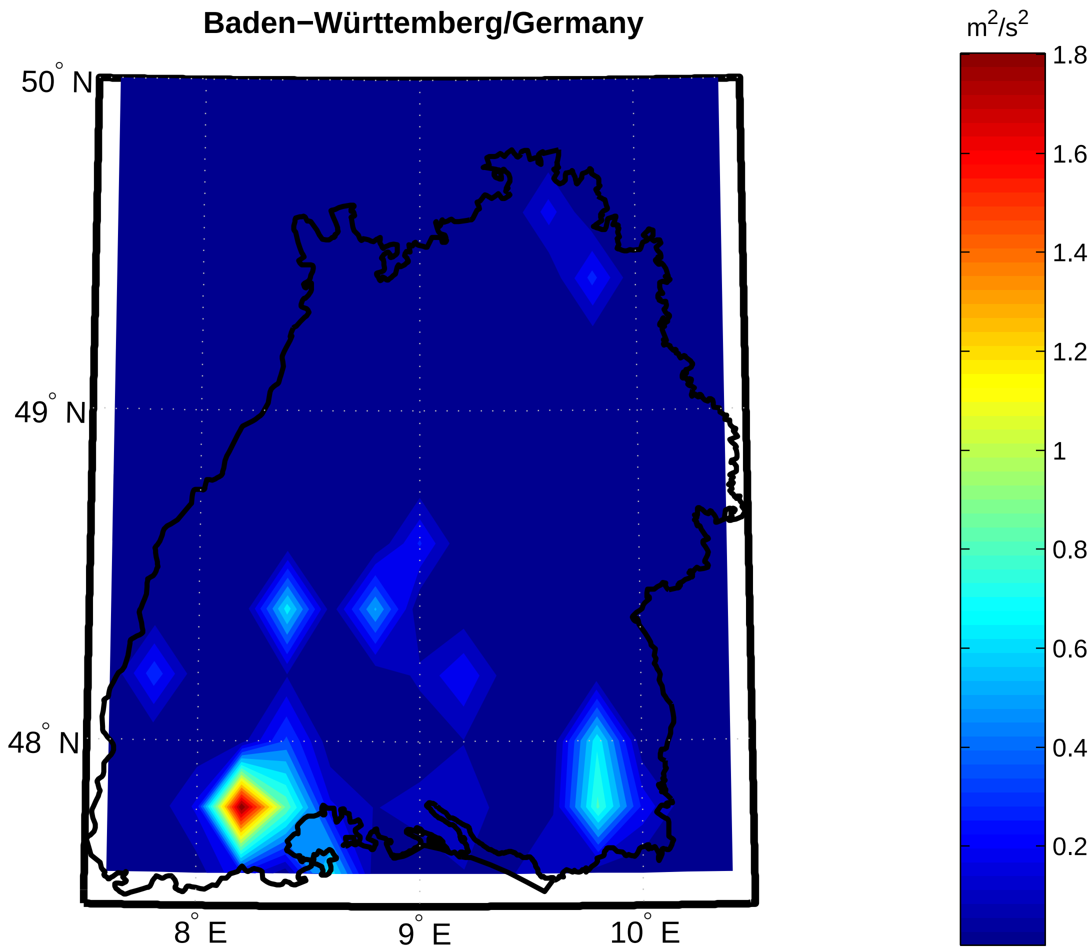

Figure 2-20: Standard deviation of downward continued incremental gravitational potential based on the optimum regularisation parameter $\alpha = 0.7$.

Map Projection Information:
Equidistant Conic Projection
Standard Parallels: □ *and* $49^\circ N$
Reference ellipsoid: WGD2000

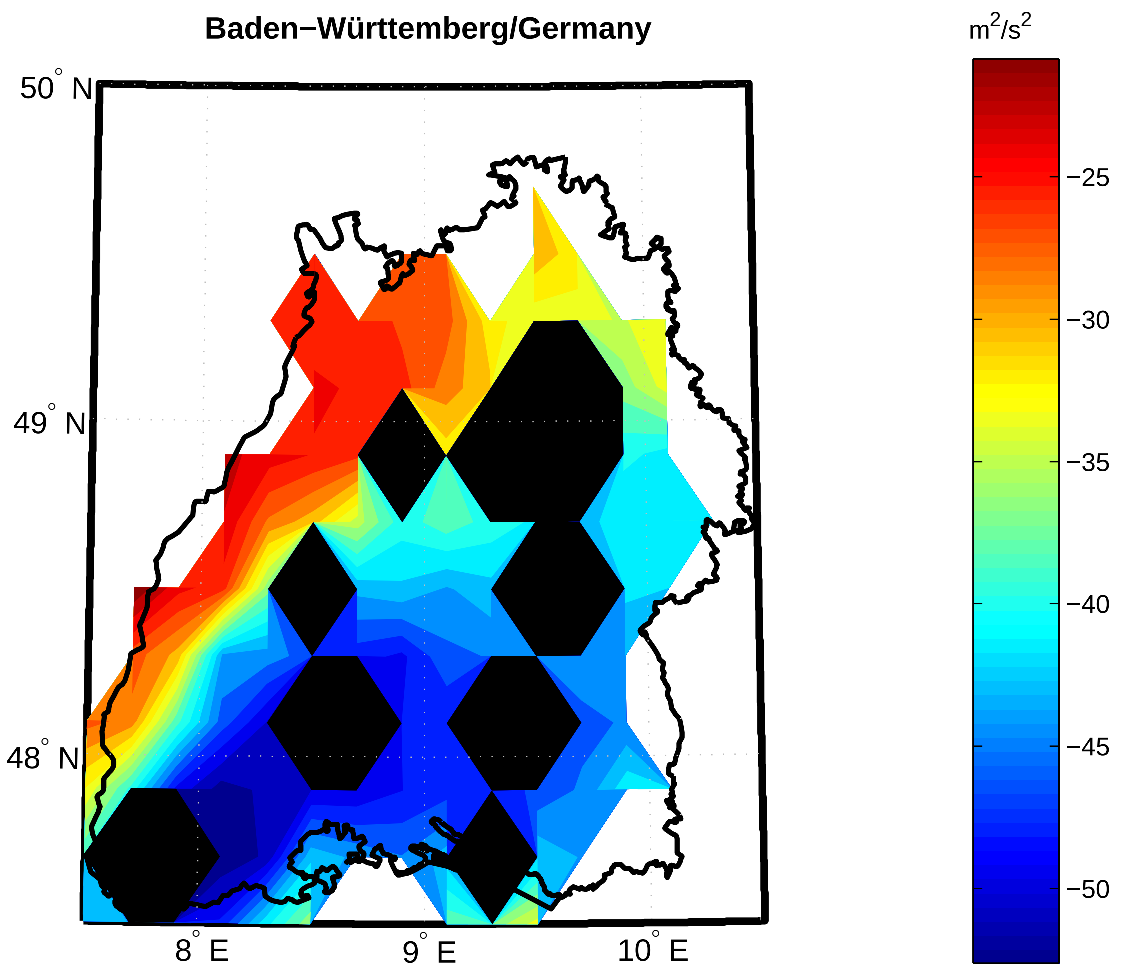

Figure 2-21: Difference between the incremental gravitational potential on the ellipsoid (from downward continuation based on the optimum regularisation parameter $\alpha = 0.7$.) and on the surface of the Earth. The black spots are areas without surface data.

<u>*Map Projection Information:*</u>
Equidistant Conic Projection
Standard Parallels: $48^\circ N$ *and* $49^\circ N$
Reference ellipsoid: WGD2000

2.4.2 Restore-step 1: Restoration of the gravitational potential of topographical masses

Having transformed the pseudo-observations of type *incremental* gravitational potential form the surface of the earth into the surface of reference ellipsoid $\mathbb{E}^2_{a,b}$, we can now restore those removed potentials of global ellipsoidal harmonic model and of topographical masses both for the computational points at the surface of the reference ellipsoid. In this section, we restore the effects of removed topographical masses, and leave the restoration of the global ellipsoidal harmonic field to the next section.

At the surface of the ellipsoid, the computational points are under the topographical masses, therefore, the topographical potential acts in the opposite direction to the potential of the bulk masses of the earth. That is, the potential of topographical masses $U^t(\bar{\mathbf{X}}_P)$ must be subtracted form the downward continued *incremental* gravitational potential $\delta\hat{W}_2(\mathbf{X}_P)$.

$$\delta\hat{W}_1(\mathbf{X}_P) = \delta\hat{W}_2(\mathbf{X}_P) - U^t(\bar{\mathbf{X}}_P) \tag{2.26}$$

In (2.26) $U^t(\bar{\mathbf{X}}_P)$ is the terrain potential computed for the centre of computational cell $\bar{\mathbf{X}}_P$ on the surface of the reference ellipsoid. See *Figure 2-22* for a contour map plot of the gravitational potential of the topographical masses for the case where computation point is on the surface of the reference ellipsoid. Here again the planar approximation and constant mass density ($\rho = 2.67\ g/cm^3$) is adopted, and the integral over terrain masses is extended to a radius of 50km around the computational point.

Figure 2-23 shows the contour map of *incremental* gravitational potential $\delta\hat{W}_1(\bar{\mathbf{X}}_P)$ at the surface of reference ellipsoid after restoration of the gravitational potential of terrain masses.

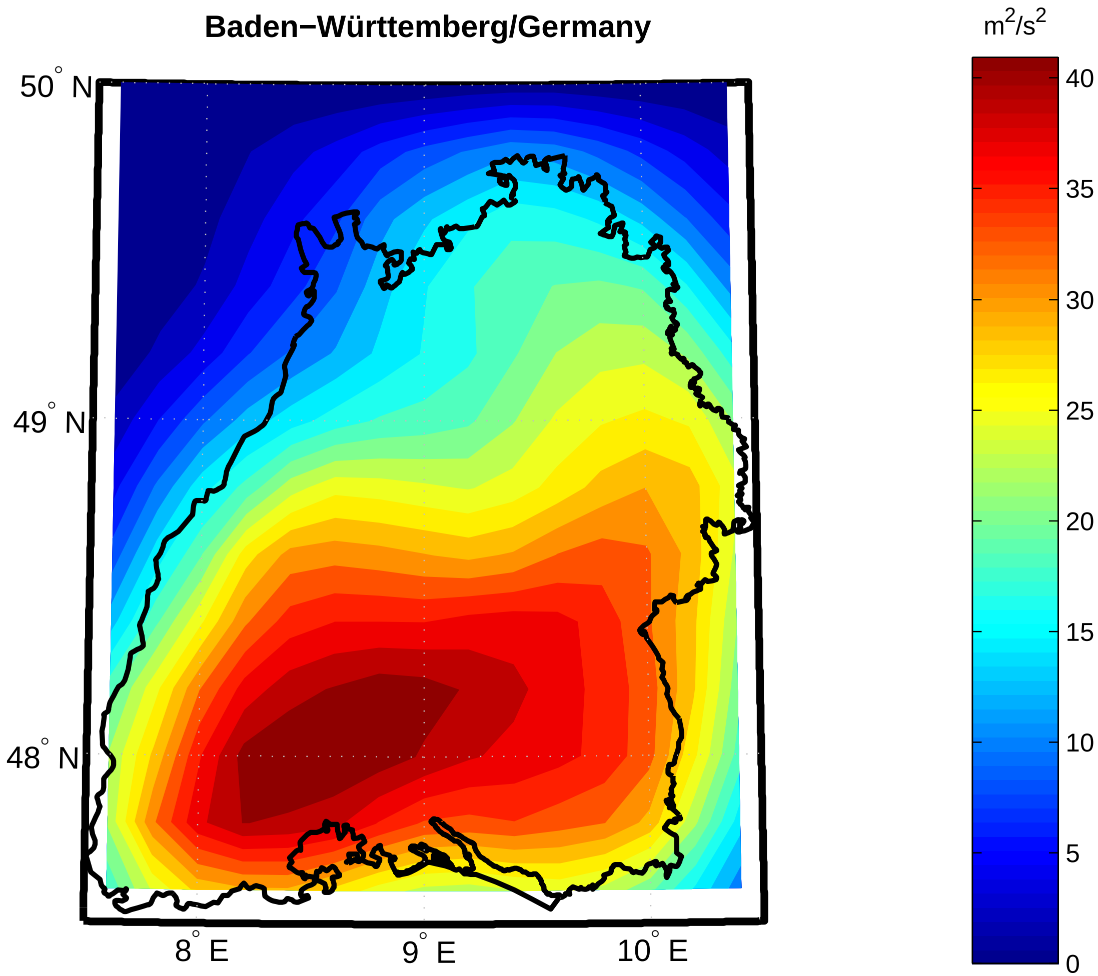

Figure 2-22: Gravitational potential of the terrain masses in a radius of 50km around the computational point, where the computational point is on the surface of reference ellipsoid. The computations are based on $1km \times 1km$ DTM model, planar approximation, and constant density ($\rho = 2.67\ g/cm^3$).

Map Projection Information:
Equidistant Conic Projection
Standard Parallels: $48^\circ N$ *and* $49^\circ N$
Reference ellipsoid: WGD2000

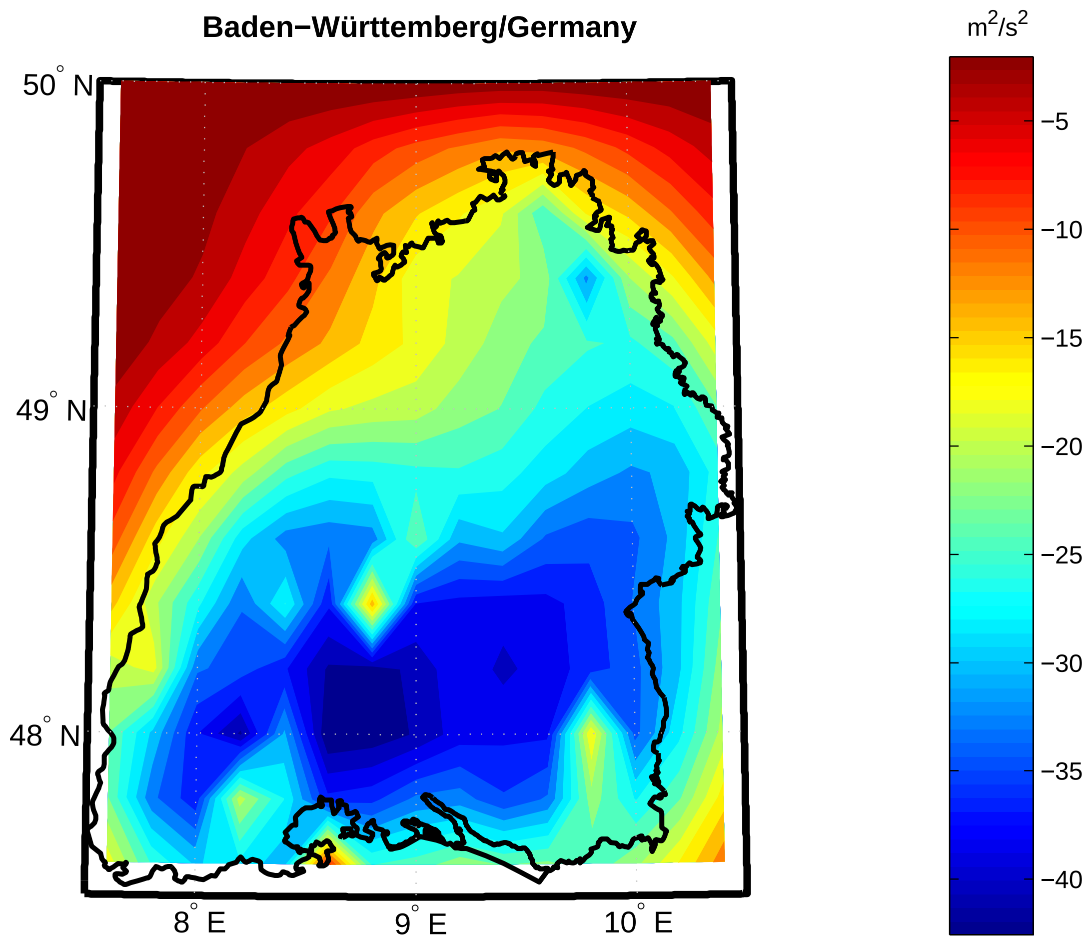

Figure 2-23: *Incremental* gravitational potential $\delta\hat{W}_1(\overline{\mathbf{X}}_P)$ at the surface of reference ellipsoid after restoration of the gravitational potential of topographical masses.

Map Projection Information:
Equidistant Conic Projection
Standard Parallels: $48^\circ N$ *and* $49^\circ N$
Reference ellipsoid: WGD2000

2.4.3 Restore-step 2: Restoration of global gravitational potential model and centrifugal potential

After restoration of the removed topographical masses, let us restore the gravitational potential of the global ellipsoidal harmonic model $U^g(\bar{\mathbf{X}}_P)$ and centrifugal potential $V^c(\bar{\mathbf{X}}_P)$. Using ellipsoidal harmonic coefficients and ellipsoidal harmonic expansion up to degree/order 360/360, we compute the gravitational potential at the centre of the cells on the surface of reference ellipsoid (see *Figure 2-24*). Centrifugal potential at the centre of the cells $V^c(\bar{\mathbf{X}}_P)$ is also computed. *Figure 2-25* presents the contour map of the centrifugal potential.

Finally, after all restoration we have the gravitational potential $W(\bar{\mathbf{X}}_P)$ at the surface of reference ellipsoid (see *Figure 2-26*).

$$W(\bar{\mathbf{X}}_P) = \delta\hat{W}_2(\bar{\mathbf{X}}_P) - U^t(\bar{\mathbf{X}}_P) + U^g(\bar{\mathbf{X}}_P) + V^c(\bar{\mathbf{X}}_P) \tag{2.27}$$

Now we are ready to apply the Bruns formula to the downward continued gravity potential to derive the geoidal undulations.

2.4.4 Application of ellipsoidal Bruns formula

Having computed the gravity potential at the surface of reference ellipsoid now we can compute the potential geoid, i.e. the geoid based on geopotential numbers. To keep the promise of performing all the computations at the ellipsoidal approximation level, we use the following non-linear ellipsoidal *Bruns formula* (see *Section 1.7*) to convert the potential values $W(\bar{\mathbf{X}})$ into geoidal heights $h(\bar{\mathbf{X}})$.

$$\left\{\begin{aligned} h(\bar{\mathbf{X}}) = {} & \delta W(\bar{\mathbf{X}}) \frac{\varepsilon^2 \cosh\eta\,(\cosh^2\eta - \cos^2\phi)^{1/2}}{gm} \\ & - \left(\delta W(\bar{\mathbf{X}})\right)^2 \left(\frac{\varepsilon^2 \cosh\eta\,(\cosh^2\eta - \cos^2\phi)^{1/2}}{gm}\right)^3 \\ & \times\left(\frac{1}{2} gm \frac{\sinh\eta\left(2\cosh^2\eta - \cos^2\phi\right)}{\varepsilon^3 \cosh^2\eta\,(\cosh^2\eta - \cos^2\phi)^2}\right) + \mathcal{O}(e^2) \end{aligned}\right. \tag{2.28}$$

where

$$\delta W(\bar{\mathbf{X}}) = w_0 - W(\bar{\mathbf{X}}_P). \tag{2.29}$$

Figure 2-27 presents the contour map of the potential geoid of Baden-Württemberg.. For comparison with *European gravimetric quasi-geoid 1997* (*EGG97, H. Denker and W. Torge*, 1998) we refer to *Figure 2-28*.

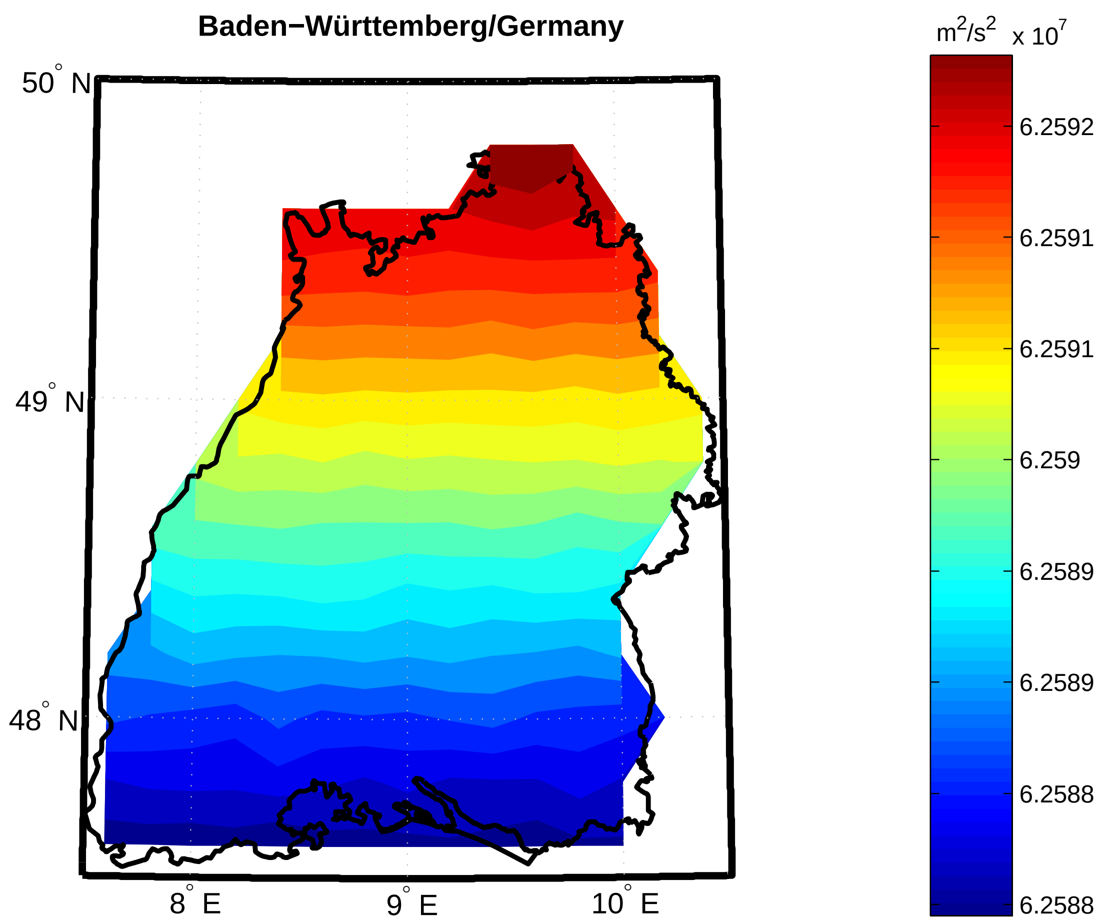

Figure 2-24: Gravitational potential of ellipsoidal harmonic model of degree/order 360/360 computed for the centre of the cells at the surface of reference ellipsoid $\mathbb{E}^2_{a,b}$.

<u>Map Projection Information:</u>
Equidistant Conic Projection
Standard Parallels: $48^\circ N$ *and* $49^\circ N$
Reference ellipsoid: WGD2000

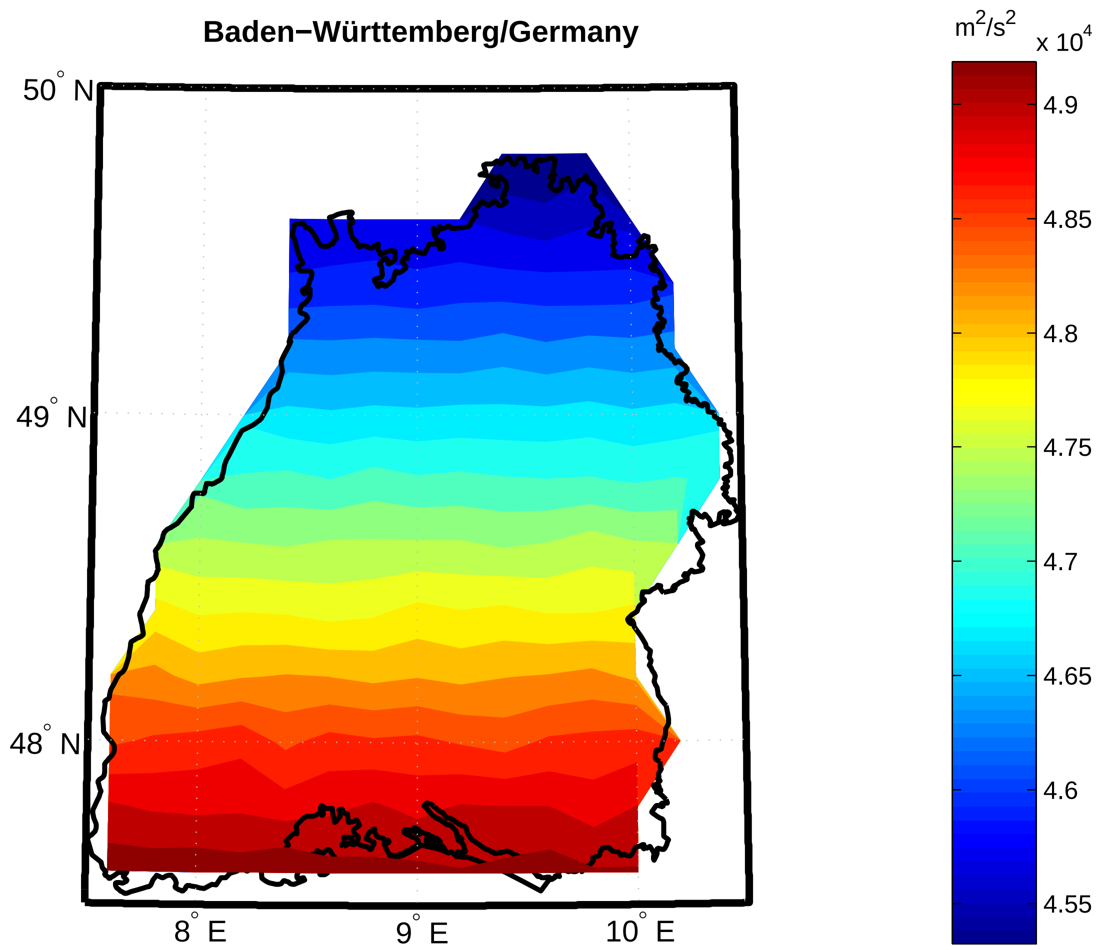

Figure 2-25: Centrifugal potential computed for the centre of the cells at surface of reference ellipsoid $\mathbb{E}^2_{a,b}$.

<u>Map Projection Information:</u>
Equidistant Conic Projection
Standard Parallels: 48° N and 49° N
Reference ellipsoid: WGD2000

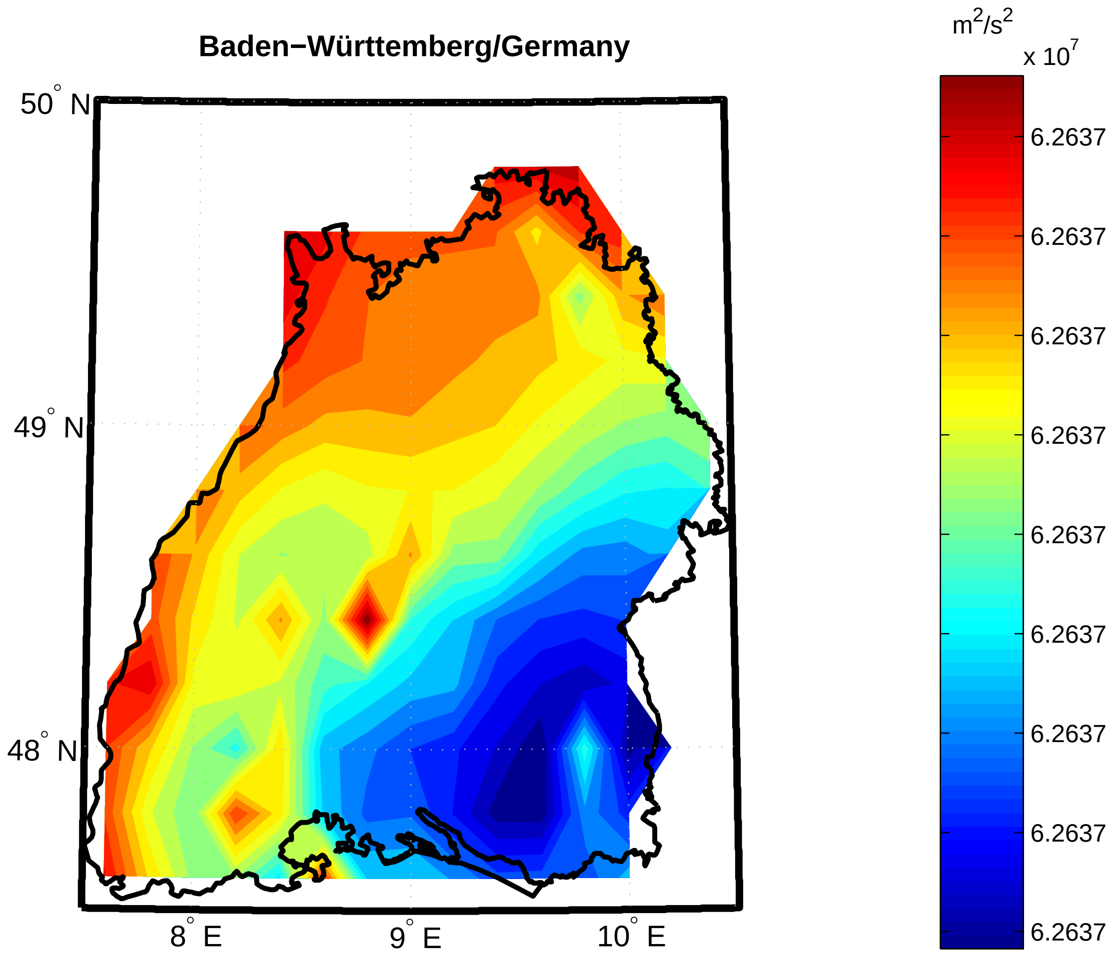

Figure 2-26: Gravity potential at the surface of reference ellipsoid derived from downward continuation of potential data after all restorations.

<u>Map Projection Information:</u>
Equidistant Conic Projection
Standard Parallels: 48° N and 49° N
Reference ellipsoid: WGD2000

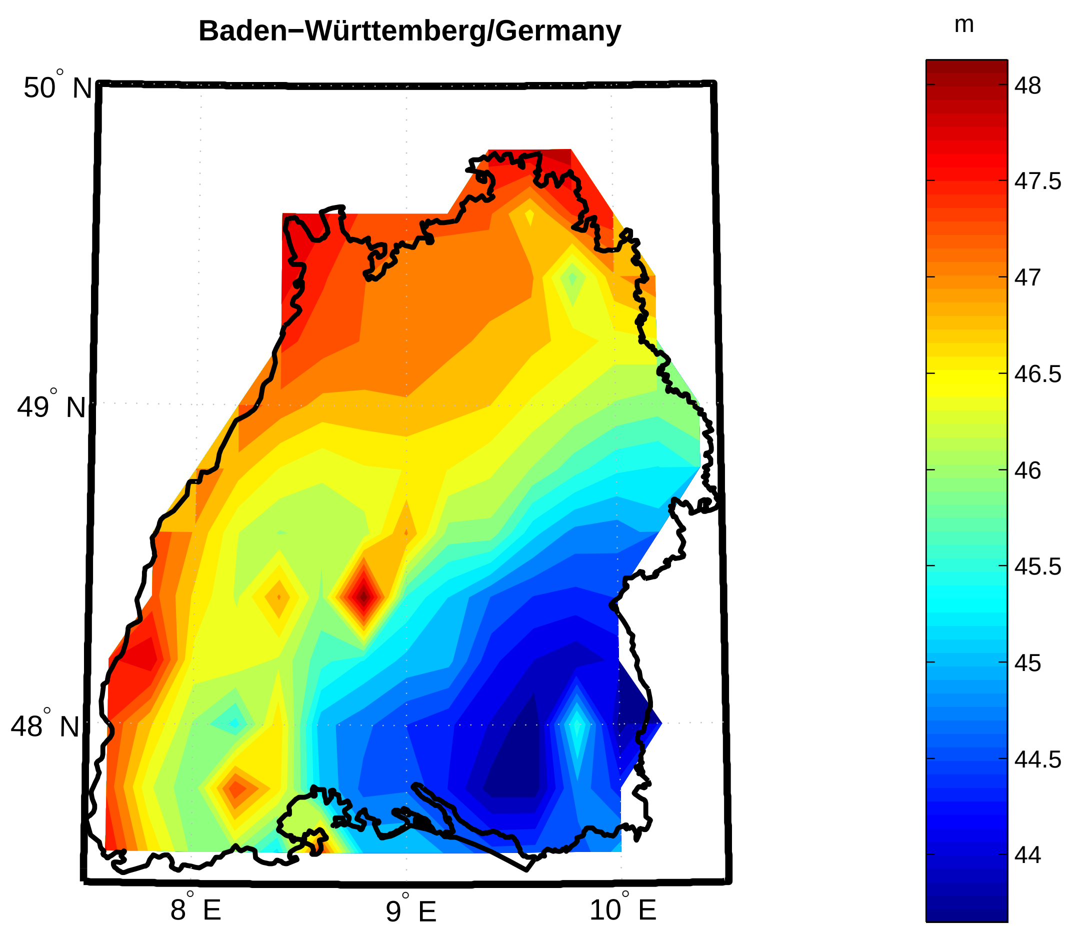

Figure 2-27: Potential geoid of the State Baden-Württemberg with respect to WGD2000 in tide free system.

Map Projection Information:
Equidistant Conic Projection
Standard Parallels: $48^\circ N$ *and* $49^\circ N$
Reference ellipsoid: WGD2000

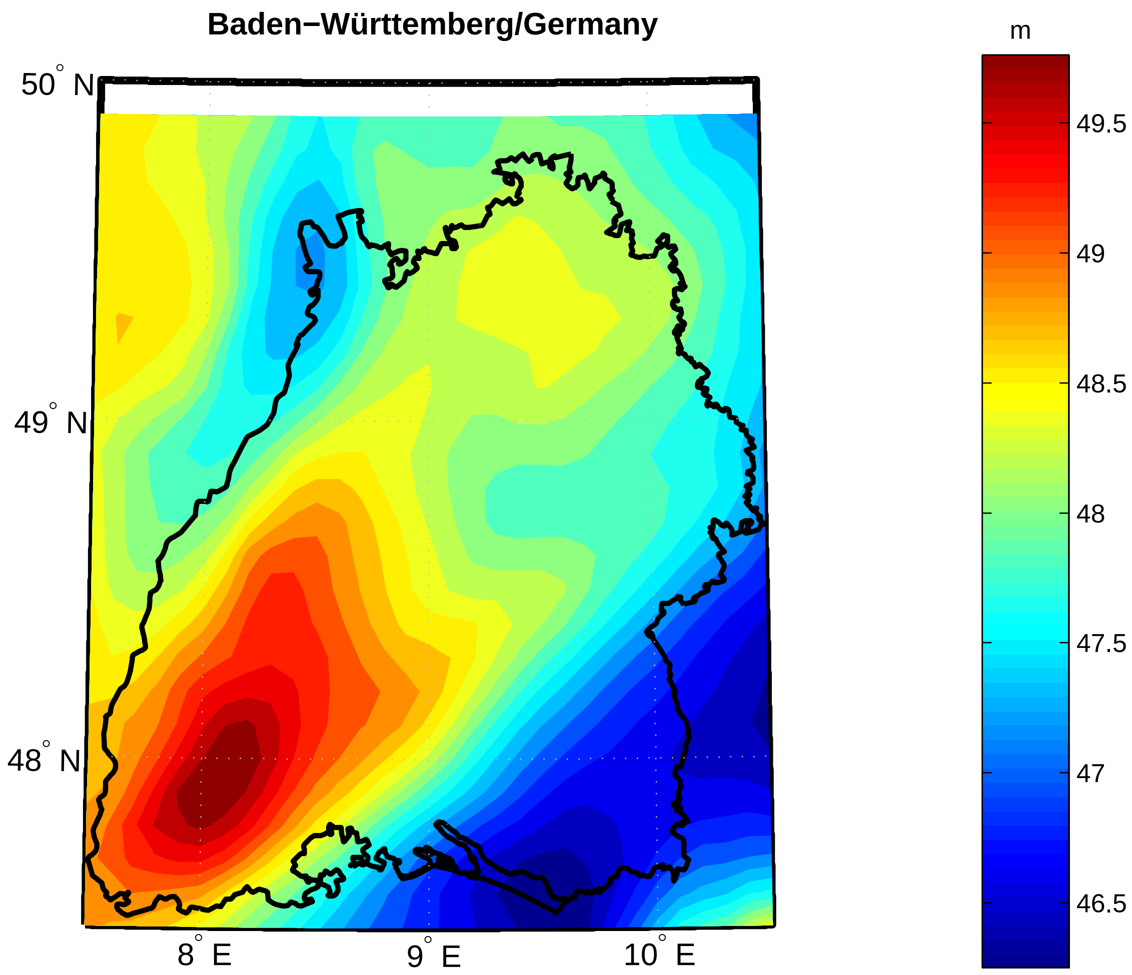

Figure 2-28: Baden-Württemberg part of European quasi-gravimetric geoid 1997 (EGG97) with respect to GRS80.

<u>Map Projection Information:</u>
Equidistant Conic Projection
Standard Parallels: 48° N and 49° N
Reference ellipsoid: WGD2000

2.4.5 Case 2: Solution for the modulus of incremental gravitation intensity $\delta\Gamma_2$

The following discretized integral equation (c.f. *Section 1.13.1 page 68*) provides us with observation equations for the observables of the type modulus of *incremental* gravitational intensity $\delta\Gamma_2$.

$$\begin{aligned}
\delta\Gamma(\mathbf{x}) &= \gamma(\mathbf{x}) - \Gamma(\mathbf{x}) = \langle \mathbf{e}_\Gamma | \boldsymbol{\delta\Gamma} \rangle \\
&= \Bigg(\frac{1}{\sqrt{g_{11}}} \frac{\Gamma_\lambda}{\|\boldsymbol{\Gamma}\|} \frac{1}{S} \sum_i^{i\max} \sum_j^{j\max} a.\sqrt{b^2 + \varepsilon^2 \sin^2 \bar{\phi}_{ij}} \\
&\quad \times \cos \bar{\phi}_{ij} \Delta\lambda \Delta\phi w(\bar{\phi}) \frac{\partial K(\lambda, \phi, \eta; \bar{\lambda}, \bar{\phi}, \eta_0)}{\partial \lambda} \\
&\quad + \frac{1}{\sqrt{g_{22}}} \frac{\Gamma_\phi}{\|\boldsymbol{\Gamma}\|} \frac{1}{S} \sum_i^{i\max} \sum_j^{j\max} a.\sqrt{b^2 + \varepsilon^2 \sin^2 \bar{\phi}_{ij}} \\
&\quad \times \cos \bar{\phi}_{ij} \Delta\lambda \Delta\phi w(\bar{\phi}) \frac{\partial K(\lambda, \phi, \eta; \bar{\lambda}, \bar{\phi}, \eta_0)}{\partial \phi} \\
&\quad + \frac{1}{\sqrt{g_{33}}} \frac{\Gamma_\eta}{\|\boldsymbol{\Gamma}\|} \frac{1}{S} \sum_i^{i\max} \sum_j^{j\max} a.\sqrt{b^2 + \varepsilon^2 \sin^2 \bar{\phi}_{ij}} \\
&\quad \times \cos \bar{\phi}_{ij} \Delta\lambda \Delta\phi w(\bar{\phi}) \frac{\partial K(\lambda, \phi, \eta; \bar{\lambda}, \bar{\phi}, \eta_0)}{\partial \eta} \Bigg) \delta\bar{W}(\mathbf{X}_{P_{ij}})
\end{aligned} \tag{2.30}$$

where the weight function

$$w(\bar{\phi}) := \frac{a}{\sqrt{b^2 + \varepsilon^2 \sin^2 \bar{\phi}}} \left(\frac{1}{2} + \frac{1}{4} \frac{b^2}{a\varepsilon} \cdot \ln \frac{a + \varepsilon}{a - \varepsilon} \right), \tag{2.31}$$

and the area element

$$S = \text{area } (\mathrm{E}^2_{a,b}) = 4\pi a \cdot \left\{ \frac{1}{2} + \frac{1}{4} \frac{b^2}{a\varepsilon} \ln \frac{a + \varepsilon}{a - \varepsilon} \right\}. \tag{2.32}$$

The derivatives of ellipsoidal Abel-Poisson kernel are those defined in *Box 1-11* (*page 28*) and *Box 1-13* (36). In (2.30) The vector $\boldsymbol{\Gamma}$ is the sum of all removed intensity vectors, i.e. gravitational intensity $\boldsymbol{\Gamma}_g(\mathbf{x})$ of ellipsoidal harmonic expansion of degree/order 360/360, centrifugal intensity $\boldsymbol{\Gamma}_c(\mathbf{x})$, and gravitational intensity $\boldsymbol{\Gamma}_c(\mathbf{x})$ of topographical/terrain masses.

$$\boldsymbol{\Gamma} = \Gamma_\lambda \mathbf{e}_\lambda + \Gamma_\phi \mathbf{e}_\phi + \Gamma_\eta \mathbf{e}_\eta = \boldsymbol{\Gamma}_g(\mathbf{x}) + \boldsymbol{\Gamma}_c(\mathbf{x}) + \boldsymbol{\Gamma}_t(\mathbf{x}) \tag{2.33}$$

Equations (2.30) are linear equations and can be written in matrix notations as

$$\mathbf{y} + \mathbf{i} = \mathbf{A}\,\mathbf{x} \tag{2.34}$$

where $\mathbf{y} = \delta\boldsymbol{\Gamma}_2(\mathbf{x}_P)$ is the vector of observations, $\mathbf{i}$ vector of inconsistencies, and $\mathbf{x} = \delta\mathbf{W}_2(\mathbf{X}_P)$ is the vector of unknowns. The coefficient matrix $\mathbf{A}$ is a 228×195 matrix (see *Section 2.4.1*, *page 99*). The numerical rank of $\mathbf{A}$, i.e. the number of non-zero singular values of $\mathbf{A}$, is found out to be 195, which implies that the discrete solution does exist and is unique! However, the condition number of $\mathbf{A}^T\mathbf{A}$, i.e. the ratio of the largest singular value to the smallest one, is 8.4×10^{25}, which shows that the problem is ill conditioned. Therefore, the least square solution based on the minimisation of the functional

$$F(\mathbf{x}) = \|\mathbf{A}\mathbf{x} - \mathbf{y}\|^2 \tag{2.35}$$

Does not lead to a stable solution! The regularised solution can be obtained by, for example, Phillips-Tikhonov regularisation, which is based on reformulation of (2.35) as

$$F_\alpha(\mathbf{x}^\alpha) = \|\mathbf{A}\mathbf{x}^\alpha - \mathbf{y}\|^2 + \alpha\|\mathbf{x}^\alpha\|^2 \tag{2.36}$$

where α is the positive regularisation parameter. The minimum norm solution of (2.36) $\hat{\mathbf{x}}^\alpha$ is

$$\hat{\mathbf{x}}^\alpha = (\mathbf{A}^T\mathbf{P}\mathbf{A} + \alpha\mathbf{I})^{-1}\mathbf{A}^T\mathbf{P}\mathbf{y} \tag{2.37}$$

For the equally accurate observables, the weight matrix can be considered unit matrix, i.e. $\mathbf{P} = \mathbf{I}$, and (2.37) can be written as

$$\hat{\mathbf{x}}^\alpha = (\mathbf{A}^T\mathbf{A} + \alpha\mathbf{I})^{-1}\mathbf{A}^T\mathbf{y} \tag{2.38}$$

Considering $\alpha = 1$ as the regularisation parameter, condition number of $(\mathbf{A}^T\mathbf{A} + \alpha\mathbf{I})$ amounts to 1.0, which suggests a stable solution. However, this regular solution is at the price of introducing some biases. Let us see how much bias is introduced by such a regularisation parameter $\alpha = 1$. Estimated inconsistencies $\hat{\mathbf{i}}$

$$\hat{\mathbf{i}} = \mathbf{A}\hat{\mathbf{x}} - \mathbf{y} \tag{2.39}$$

can give us an estimate of the bias mixed with observation errors. For the case $\alpha = 1$, $\mathrm{cond}(\mathbf{A}^T\mathbf{A} + \alpha\mathbf{I}) = 1.0$ was derived. In Figure 2-9 we have a plot of the variations of maximum absolute value of the bias per different regularisation parameters in the interval $[1 \times 10^{-6}, 1.2 \times 10^{-4}]$. *Figure 2-30* shows the variations of condition number of $(\mathbf{A}^T\mathbf{A} + \alpha\mathbf{I})$ versus the regularisation parameter α. To get an estimate of the inconsistencies before applying the regularisation, in *Figure 2-32* we present a contour map of the estimated inconsistencies of the observations based on regularisation parameter $\alpha = 4.9 \times 10^{-28}$, which is practically zero. However, since this regularisation parameter is almost zero, the matrix $(\mathbf{A}^T\mathbf{A} + \alpha\mathbf{I})$ has a very poor condition number, which will result in very large mean square error (MSE) for the estimated parameters $\hat{\mathbf{x}} = \delta\hat{\mathbf{W}}_2(\mathbf{X}_P)$. This can be observed very well in *Figure 2-29* where shown the plot of the trace of MSE$\{\hat{\mathbf{x}}^{\alpha}\}$ versus the regularisation parameters. The result of downward continuation, $\hat{\mathbf{x}} = \delta\hat{\mathbf{W}}_2(\mathbf{X}_P)$, based on regularisation parameter $\alpha = 4.9 \times 10^{-28}$, is depicted in *Figure 2-33*. As the figure shows, we have only some edge effects, and no signal. Let us see what will happen if we remove the edge effect. *Figure 2-34* shows the results after deleting the data outside the Baden-Württemberg. Still there is no evidence of any signal. A study of the *Figure 2-29* can direct us towards the optimum regularisation parameter. As *Figure 2-29* shows the optimum regularity parameter is $\alpha = 0.001$. *Figure 2-35* shows the downward continued *incremental* gravitational potential $\hat{\mathbf{x}} = \delta\hat{\mathbf{W}}_2(\mathbf{X}_P)$, while *Figure 2-36* depicts the estimated bias $\hat{\mathbf{i}} = \mathbf{A}\hat{\mathbf{x}} - \mathbf{y}$ based on regularity parameter $\alpha = 0.001$. Now the downward continuation is quite stable, however we have some biases, which is the price we paid for a stable solution! However this bias in most areas is still bellow the accuracy of the observations!

Using the error propagation formula (2.24), we can estimate the Mean *Square Error* matrix of the downward continued incremental gravitational potential $\hat{\mathbf{x}}^{\alpha}$. *Figure 2-20* provides us with a plot of square root of the diagonal elements of $MSE(\hat{\mathbf{x}}^{\alpha})$. As it is inferred from *Figure 2-20* the standard error of the downward continued incremental gravitational potentials are quite small, except in some small spots where we have lower accuracy. Whoever, even within those spots the accuracy is enough as compared with the accuracy of the observations.

One may be interested to know how the regularised downward continued incremental gravitational intensity differs from the downward continued incremental gravity potential. *Figure 2-38* shows the difference of incremental gravitational potential (from downward continued *incremental gravitational potential data*) and incremental gravitational potential (from downward continued *incremental gravitational intensity data*).

Now that we settled the regularisation problem let us, proceed into restore process.

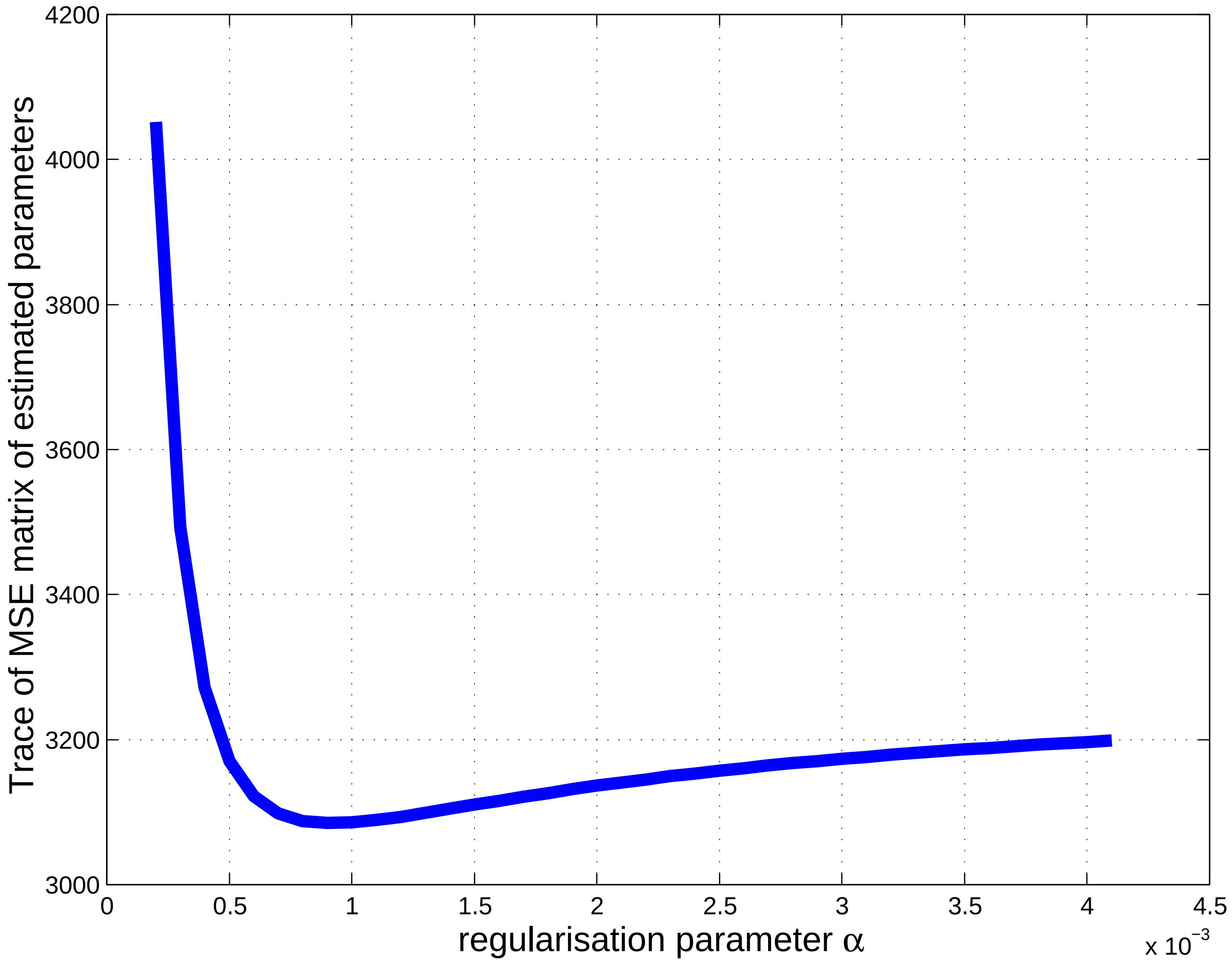

Figure 2-29: Trace of MSE{ $\hat{\mathbf{x}}^{\alpha}$ } matrix of estimated parameters versus the regularisation parameter α. For downward continuation of incremental gravitational intensity. As one can see the optimum regularisation parameter is 0.001.

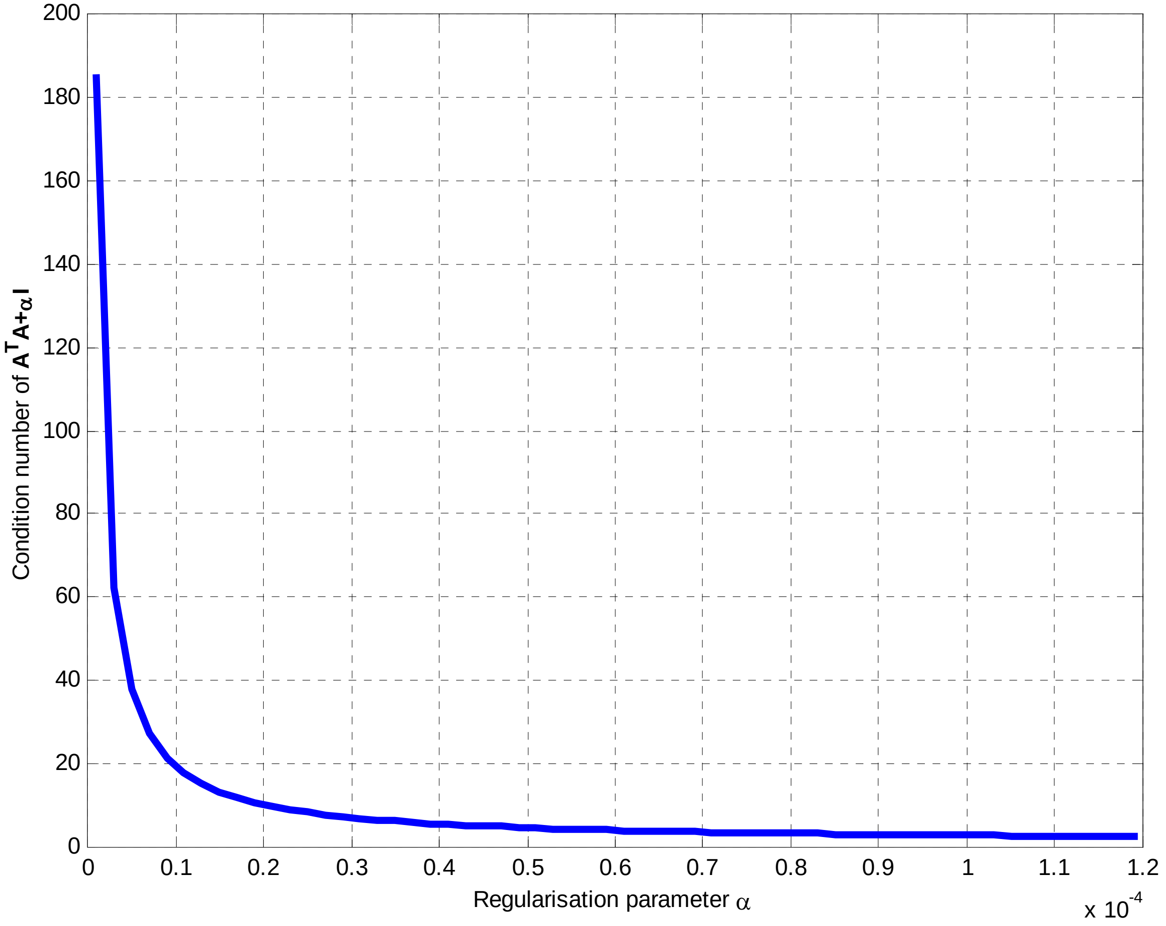

Figure 2-30: Variation of the condition number of $\mathbf{A}^T\mathbf{A} + \alpha\mathbf{I}$ versus the regularisation parameter α .

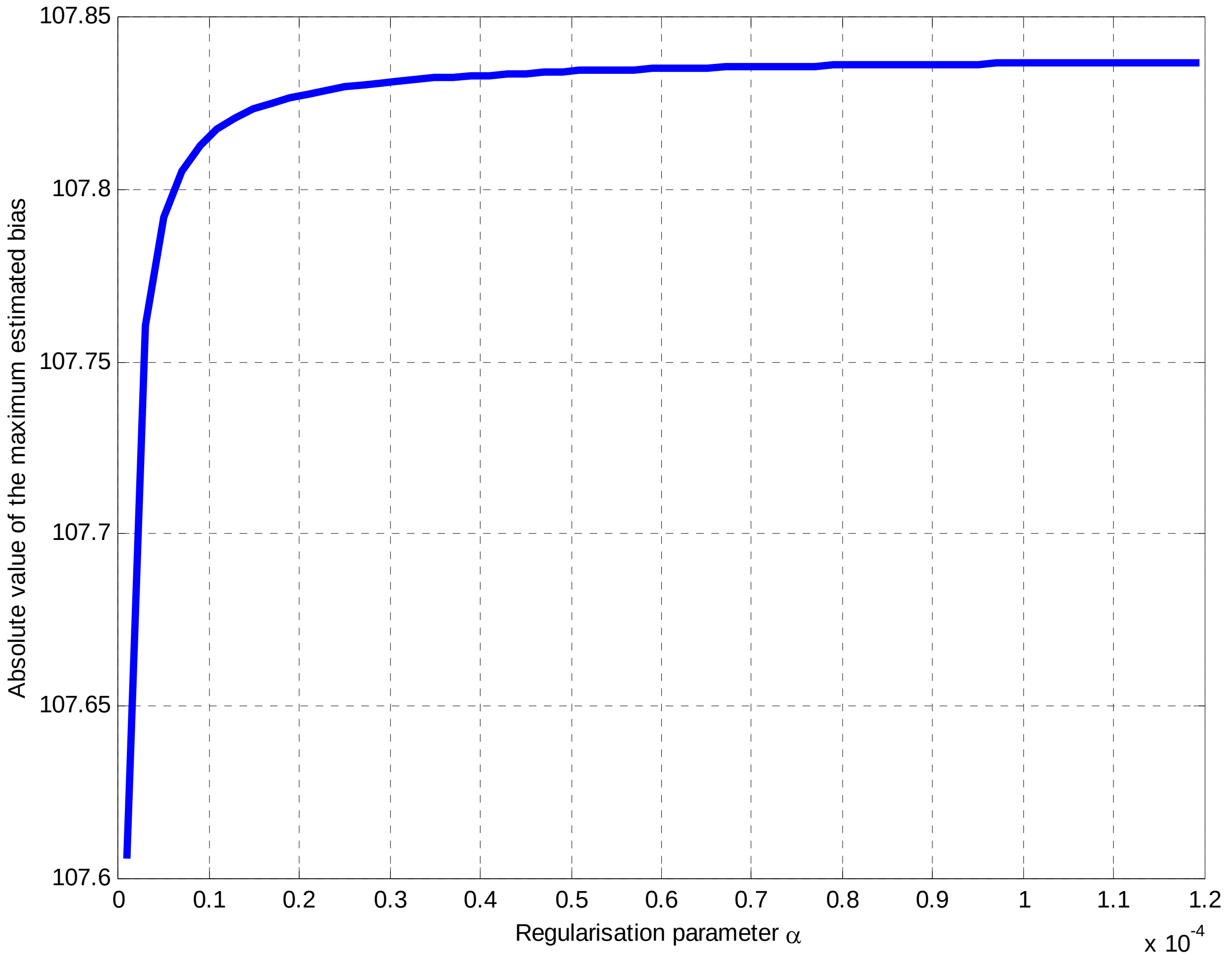

Figure 2-31: Maximum absolute value of the bias (in mGal) vs. the regularisation parameter.

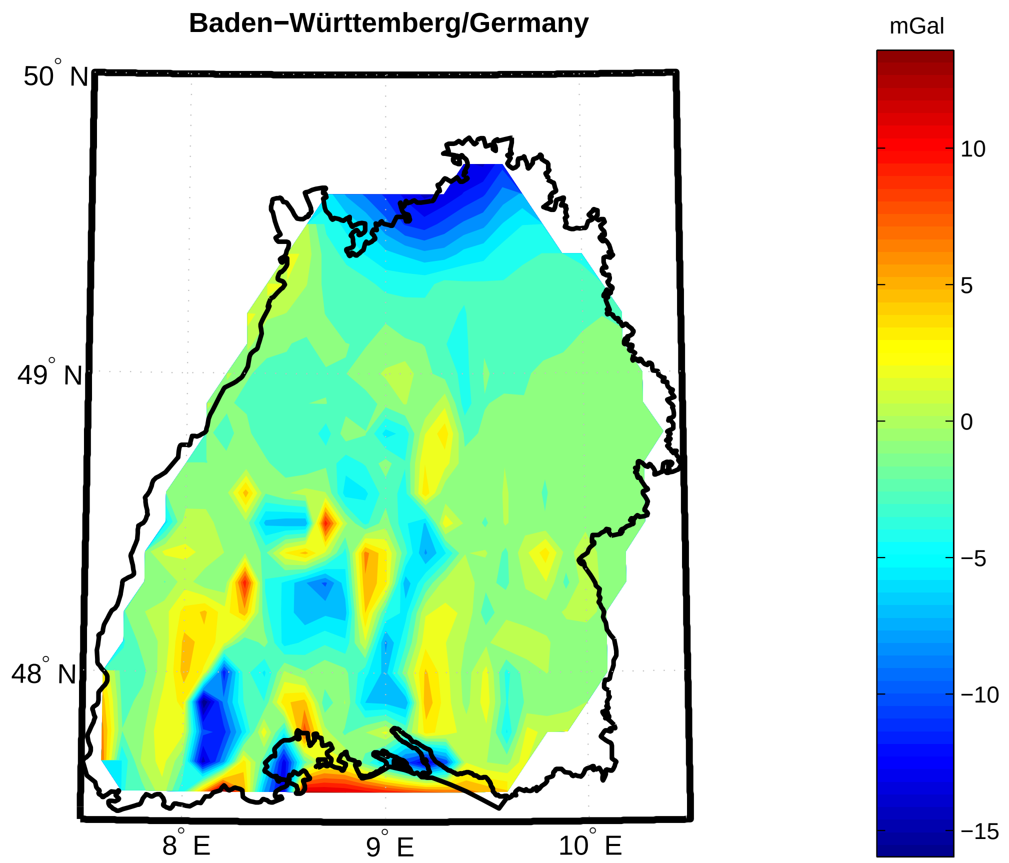

Figure 2-32: Map of the estimated bias of observations after application of the regularisation parameter $\alpha = 4.9 \times 10^{-28}$. Very little bias is introduced by the regularisation parameter.

<u>Map Projection Information:</u>
Equidistant Conic Projection
Standard Parallels: 48°N and 49°N
Reference ellipsoid: WGD2000

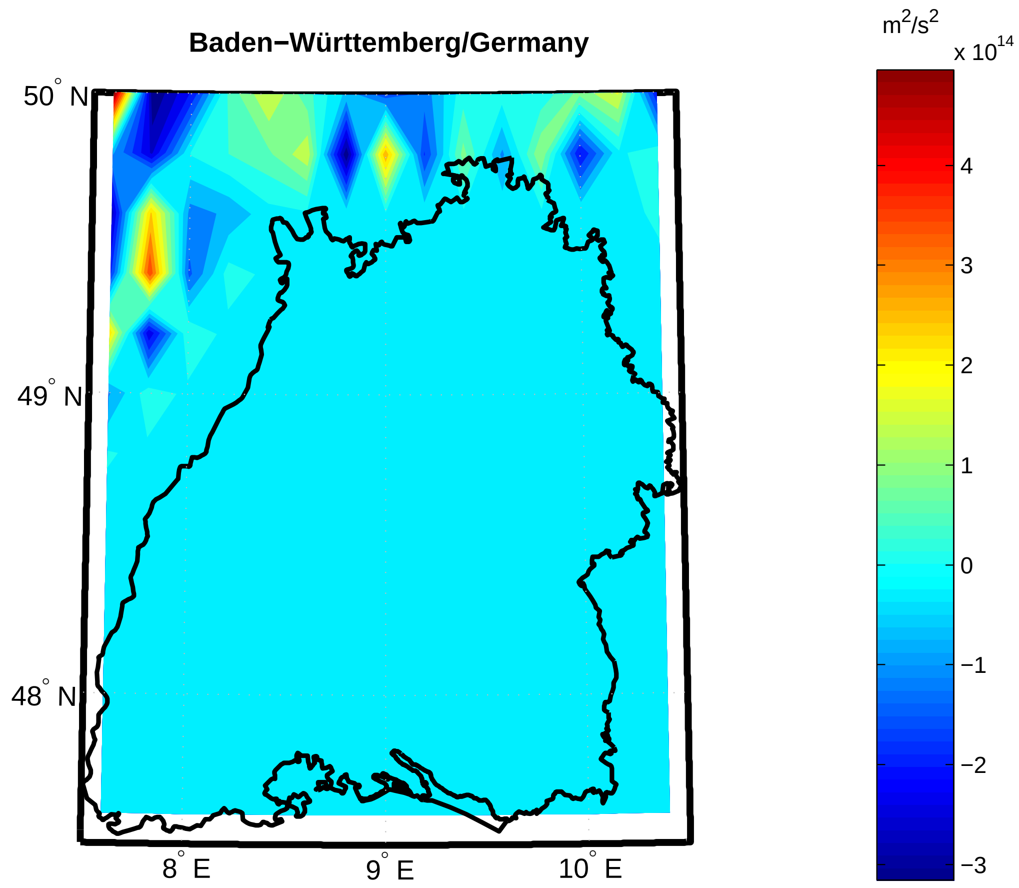

Figure 2-33: Downward continued *incremental* gravitational potential $\hat{\mathbf{x}} = \delta\hat{\mathbf{W}}_2(\mathbf{X}_P)$ based on regularisation parameter 4.9×10^{-28}. Due to instability of the downward continuation we cannot see any signal.

Map Projection Information:
Equidistant Conic Projection
Standard Parallels: $48^\circ N$ *and* $49^\circ N$
Reference ellipsoid: WGD2000

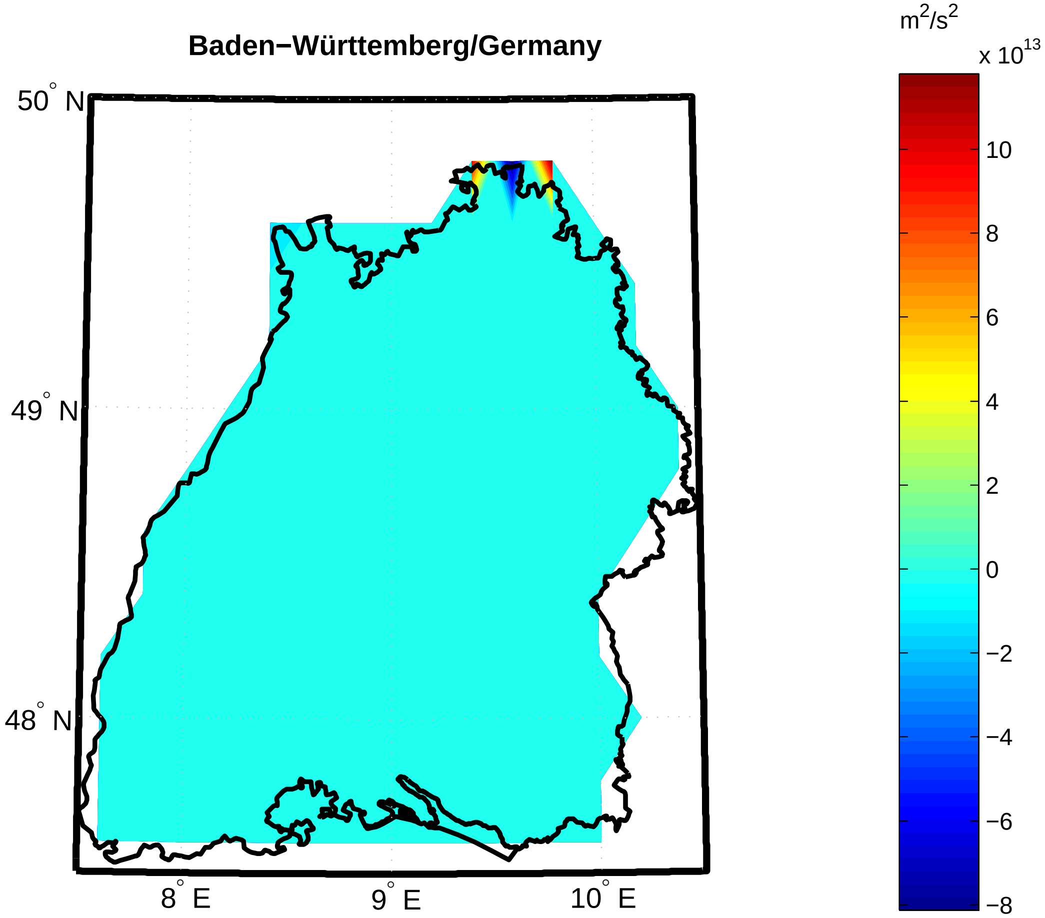

Figure 2-34: Downward continued *incremental* gravitational potential $\hat{\mathbf{x}} = \delta\hat{\mathbf{W}}_2(\mathbf{X}_P)$ based on regularisation parameter 4.9×10^{-28}, after removing the data outside the region. Still there is no signal visible.

Map Projection Information:
Equidistant Conic Projection
Standard Parallels: $48^\circ N$ *and* $49^\circ N$
Reference ellipsoid: WGD2000

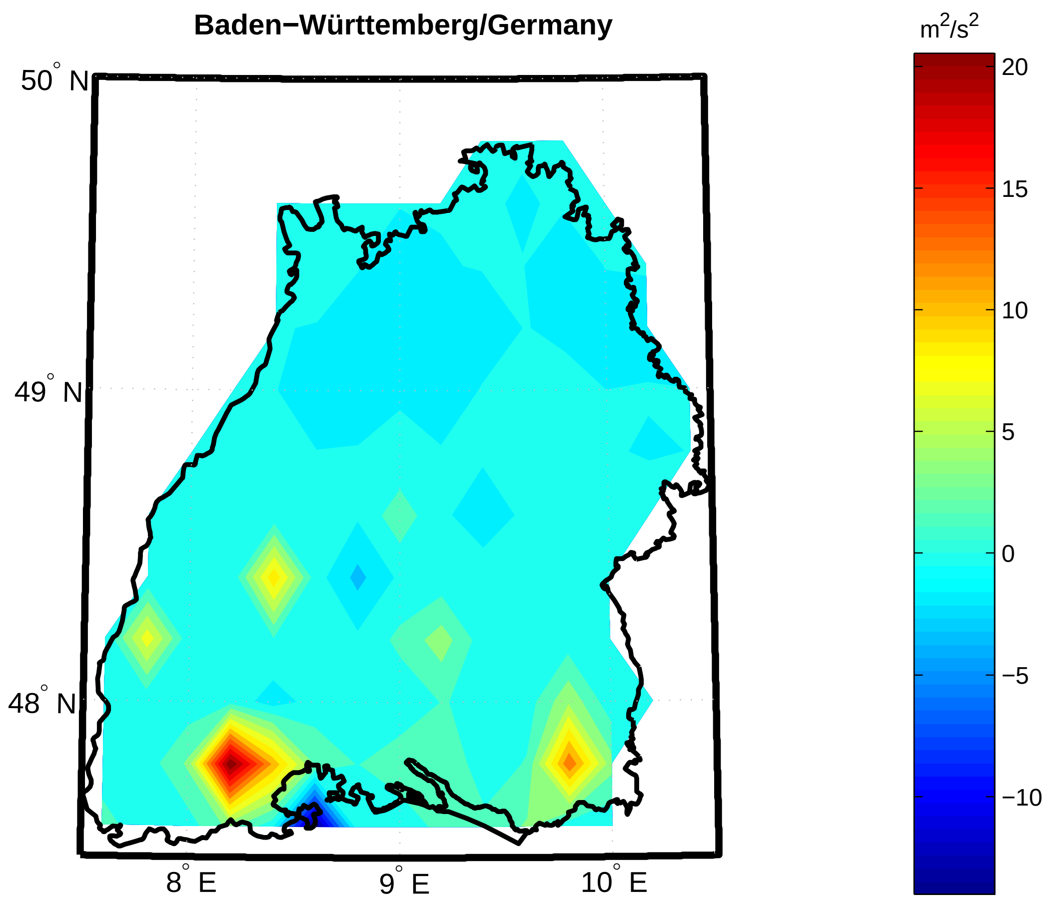

Figure 2-35: Stabilised downward continued *incremental* gravitational potential $\hat{\mathbf{x}} = \delta\hat{\mathbf{W}}_2(\mathbf{X}_P)$ based on the regularisation parameter $\alpha = 0.001$, after removal of the edge effects.

Map Projection Information:
Equidistant Conic Projection
Standard Parallels: $48^\circ N$ *and* $49^\circ N$
Reference ellipsoid: WGD2000

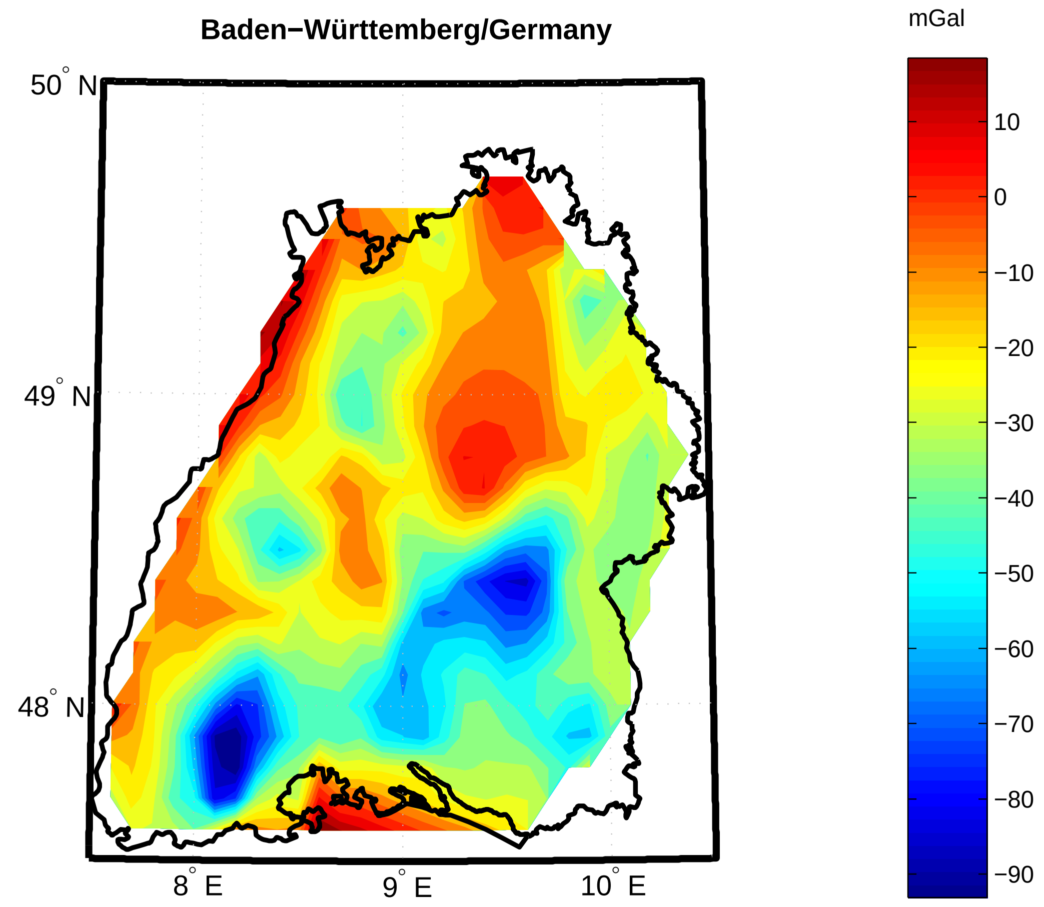

Figure 2-36: Map of the estimated bias based on regularisation parameter $\alpha = 0.001$. Note the biases at the mountainous areas.

Map Projection Information:
Equidistant Conic Projection
Standard Parallels: 48° N and 49° N
Reference ellipsoid: WGD2000

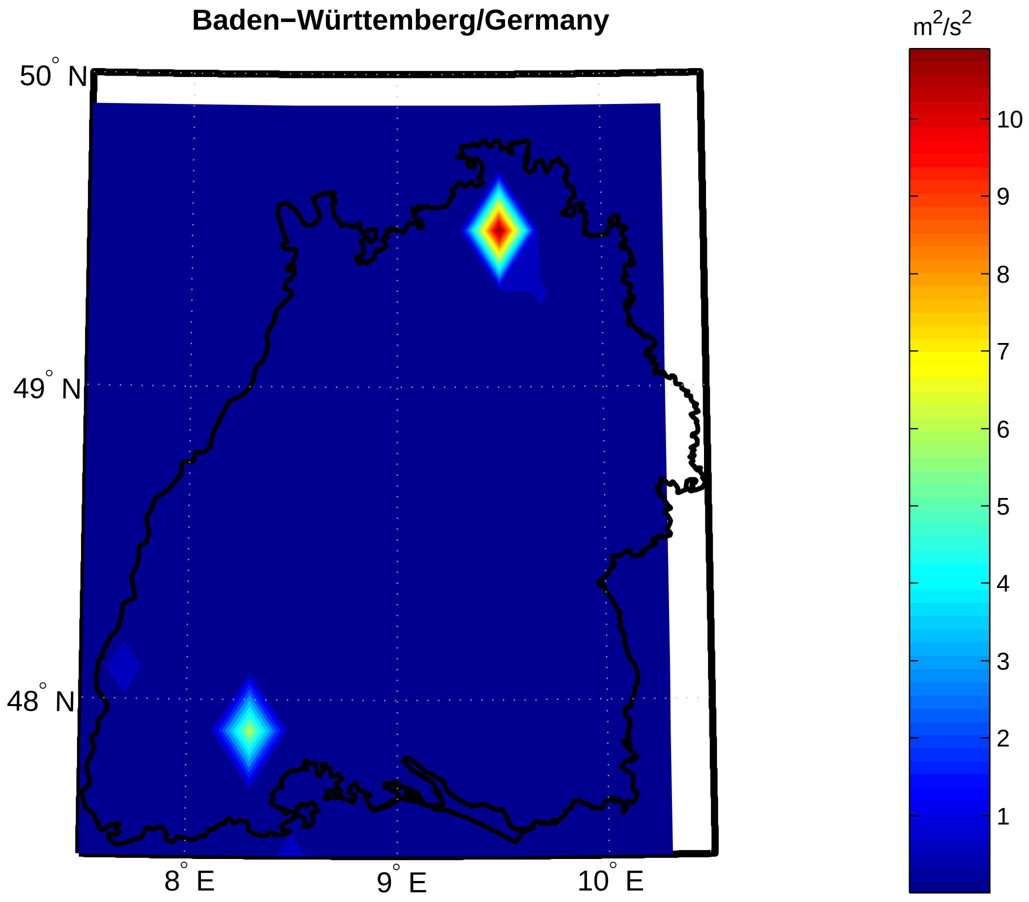

Figure 2-37: STD of downward continued incremental gravitational potential based on the optimum regularisation parameter $\alpha = 0.7$.

Average: 0.0046.

<u>Map Projection Information:</u>
Equidistant Conic Projection
Standard Parallels: 48°N and 49°N
Reference ellipsoid: WGD2000

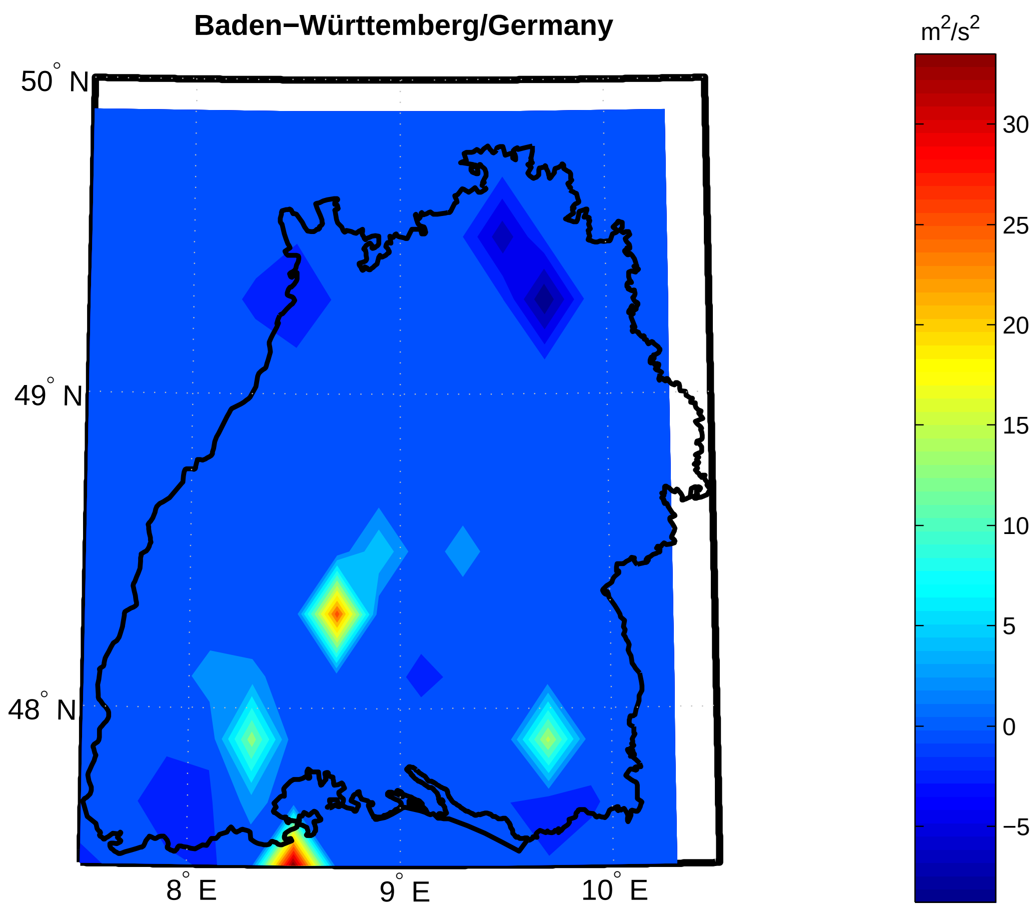

Figure 2-38: The difference of incremental gravitational potential (from downward continued *incremental gravitational potential data*) and incremental gravitational potential (from downward continued *incremental gravitational intensity data*).

Map Projection Information:
Equidistant Conic Projection
Standard Parallels: 48° N and 49° N
Reference ellipsoid: WGD2000

2.4.6 Restore-step 1: Restoration of the gravitational intensity of topographical masses

After transformation of the input *incremental* data form the surface of the earth, onto the reference ellipsoid $\mathbb{E}^2_{a,b}$ we can return the *actual* physical situation of the gravity space back to its initial state. That is now we can restore the effect of removed topographical masses and the global ellipsoidal harmonic model. This section is devoted to restoration of removed topographical masses, while the restoration of the global ellipsoidal harmonic model is left to the next section.

Since now the topographical masses are on top of the computational points the effect of gravitational potential $U^t(\overline{\mathbf{X}}_P)$ must be subtracted form the downward continued *incremental* gravitational potential $\delta\hat{W}_2(\mathbf{X}_P)$.

$$\delta\hat{W}_1(\mathbf{X}_P) = \delta\hat{W}_2(\mathbf{X}_P) - U^t(\overline{\mathbf{X}}_P) \tag{2.40}$$

$U^t(\overline{\mathbf{X}}_P)$ is the terrain potential, computed for the centre of computational cell $\overline{\mathbf{X}}_P$ on the surface of the reference ellipsoid. *Figure 2-22* shows the calculated gravitational potential of the topographical masses for the case that the computation point is on the surface of reference ellipsoid.

Figure 2-29 shows the contour map of *incremental* gravitational potential $\delta\hat{W}_1(\overline{\mathbf{X}}_P)$ at the surface of reference ellipsoid after restoration of the gravitational potential of terrain masses.

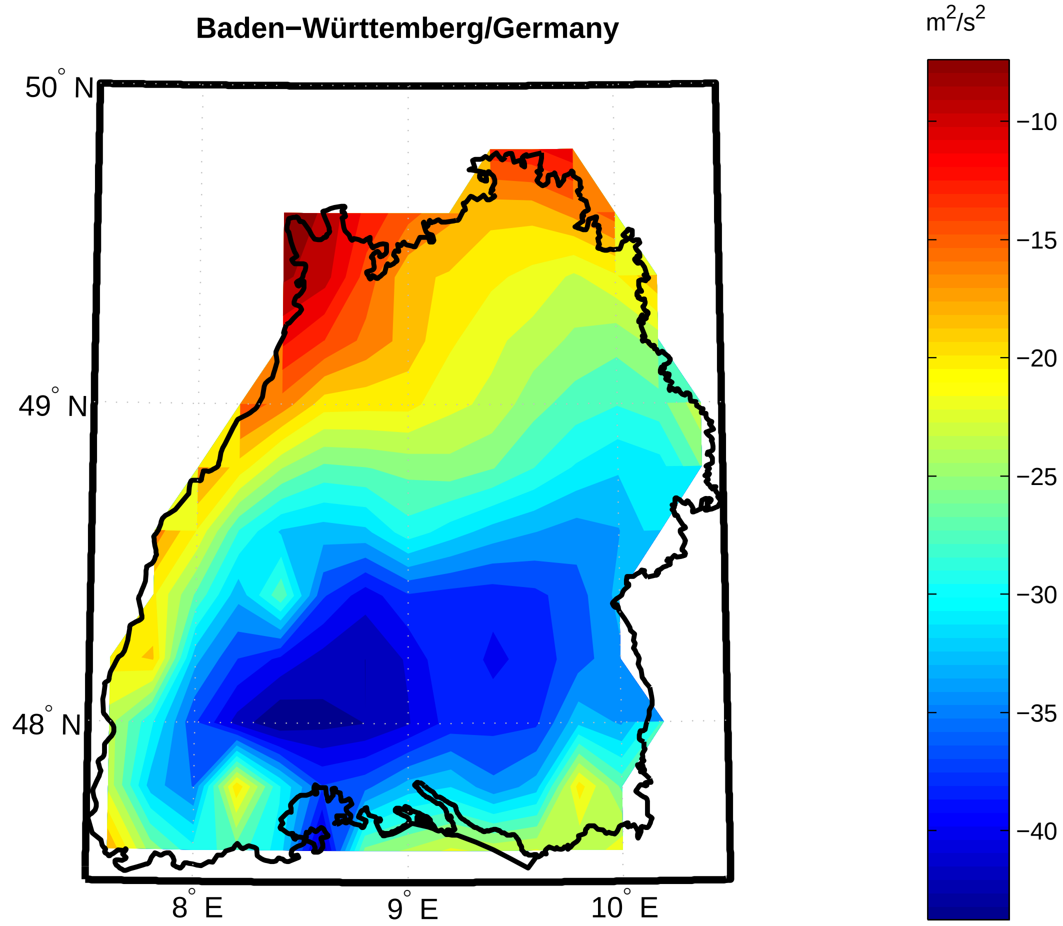

Figure 2-39: *Incremental* gravitational potential $\delta\hat{W}_1(\overline{\mathbf{X}}_P)$ at the surface of reference ellipsoid after restoration of the gravitational potential of terrain masses.

<u>Map Projection Information:</u>
Equidistant Conic Projection
Standard Parallels: 48° N and 49° N
Reference ellipsoid: WGD2000

2.4.7 Restore-step 2: Restoration of global gravitational potential model and centrifugal potential

After restoration of the effect of removed terrain masses, let us new restore the two last potentials, i.e. gravitational potential of the global ellipsoidal harmonic model $U^g(\bar{\mathbf{X}}_P)$ and centrifugal potential. Using the ellipsoidal harmonic expansion of degree/order 360/360, we calculate the gravitational potential of the centre of computation cells on the surface of reference ellipsoid (see *Figure 2-24*). Mean centrifugal potentials are also calculated for individual calculation cells $V^c(\bar{\mathbf{X}}_P)$. The map of computed centrifugal potential for the points on the surface of reference ellipsoid is shown in *Figure 2-25*. Finally, let us see the plot of the *gravity potential* $\hat{W}(\bar{\mathbf{X}}_P)$ at the surface of reference ellipsoid derived after all restorations in *Figure 2-40*.

$$\hat{W}(\bar{\mathbf{X}}_P) = \delta\hat{W}_2(\bar{\mathbf{X}}_P) - U^t(\bar{\mathbf{X}}_P) + U^g(\bar{\mathbf{X}}_P) + V^c(\bar{\mathbf{X}}_P) \tag{2.41}$$

Having calculated the gravity potential at the surface of reference ellipsoid now we are able to use the *Bruns formula* to obtain the geoid for the *Case 2* "*gravity geoid*".

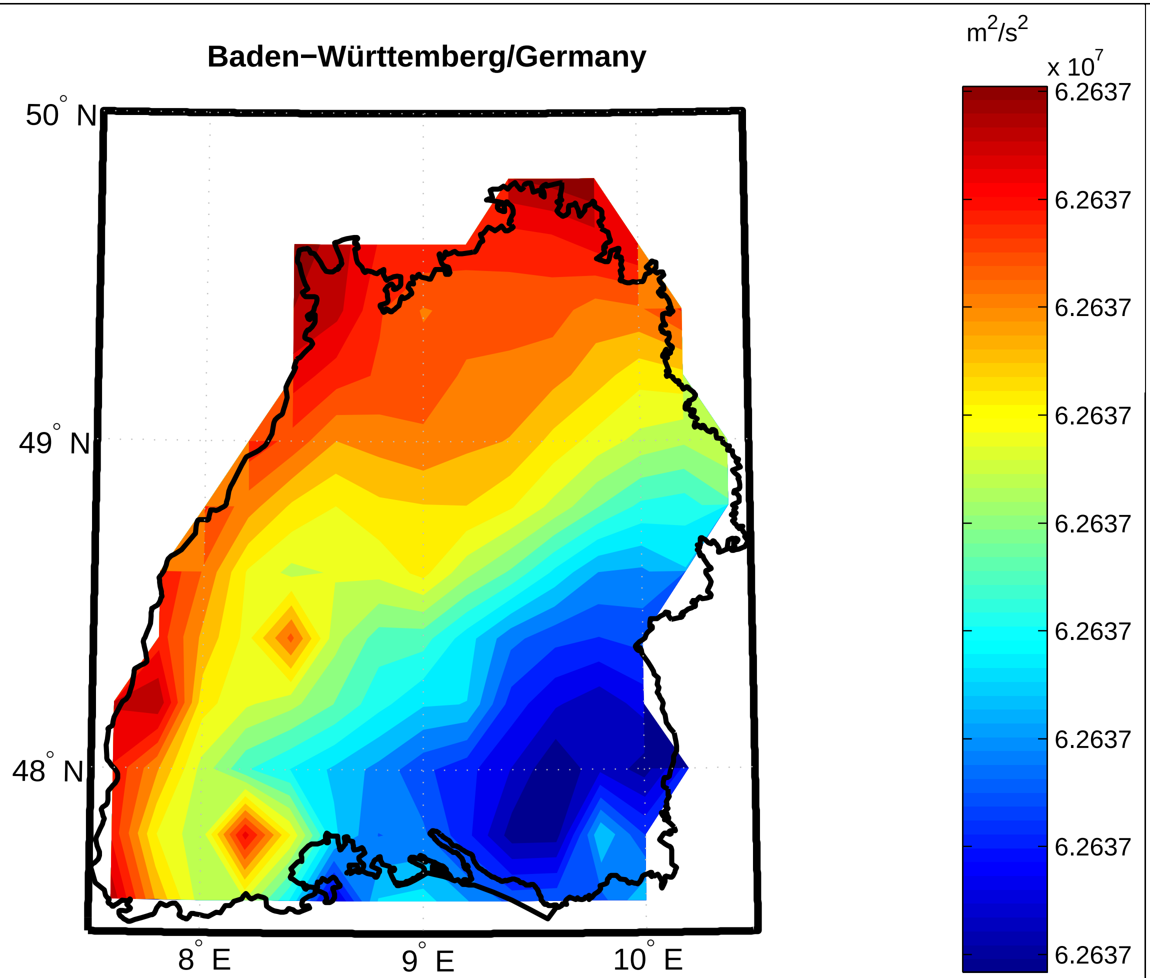

Figure 2-40: Gravity potential $\hat{W}(\bar{\mathbf{X}}_P)$ at the surface of reference ellipsoid derived from downward continued gravity intensity data after all restorations.

Map Projection Information:
Equidistant Conic Projection
Standard Parallels: 48° N and 49° N
Reference ellipsoid: WGD2000

2.4.8 Application of ellipsoidal Bruns formula

Having computed the gravity potential at the surface of reference ellipsoid, now we are at the position to compute the "*gravity-geoid*", i.e. the geoid based on the observables of the type *modulus of gravity intensity*. To keep the ellipsoidal approximation that we have maintained so far we use the following non-linear ellipsoidal *Bruns formula* which was derived in *Section 1.7* (*page 40*).

$$\begin{cases} h = \delta W(\mathbf{X}) \dfrac{\varepsilon^2 \cosh\eta (\cosh^2\eta - \cos^2\phi)^{1/2}}{gm} \\ \quad -(\delta W(\mathbf{X}))^2 (\dfrac{\varepsilon^2 \cosh\eta (\cosh^2\eta - \cos^2\phi)^{1/2}}{gm})^3 \\ \quad \times(\dfrac{1}{2} gm \dfrac{\sinh\eta \left(2\cosh^2\eta - \cos^2\phi\right)}{\varepsilon^3 \cosh^2\eta (\cosh^2\eta - \cos^2\phi)^2}) + \mathcal{O}(e^2) \end{cases} \tag{2.42}$$

where

$$\delta W(\mathbf{X}) = w_0 - \delta \bar{W}(\mathbf{X}_P) \tag{2.43}$$

Figure 2-41 presents the contour map of the gravity geoid of Baden-Württemberg. For comparison with *European gravimetric quasi-geoid 1997* (*EGG97 H. Denker and W. Torge*, 1998) we refer to *Figure 2-28*.

Let us also compare the gravity-geoid with the potential-geoid that we derive before. *Figure 2-42* shows the difference between potential-geoid and gravity-geoid. As one can see the two geoid solutions are differing by (0.058±0.029)m, which shows a high level of consistency between the two solutions.

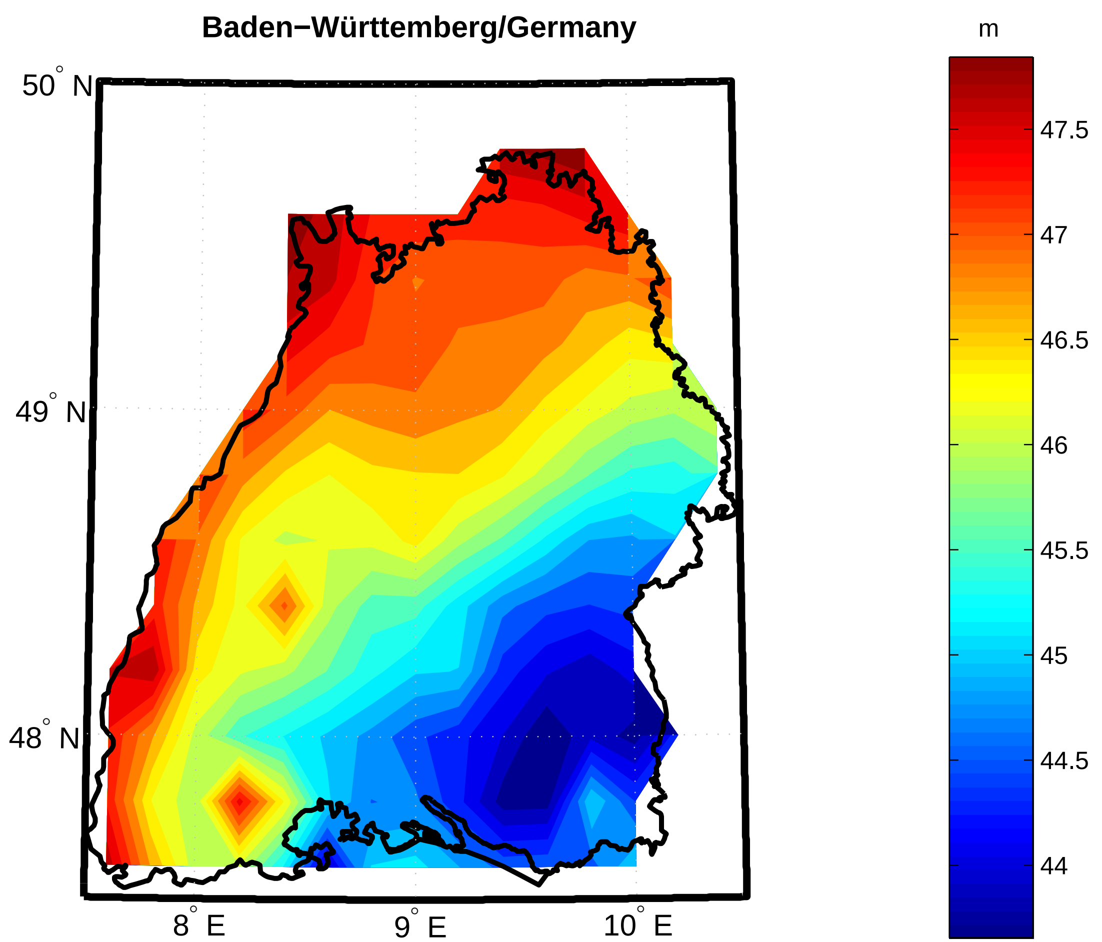

Figure 2-41: Gravity geoid of the state Baden-Württemberg with respect to WGD2000 in tide free, permanent tide system.

Map Projection Information:
Equidistant Conic Projection
Standard Parallels: 48° N and 49° N
Reference ellipsoid: WGD2000

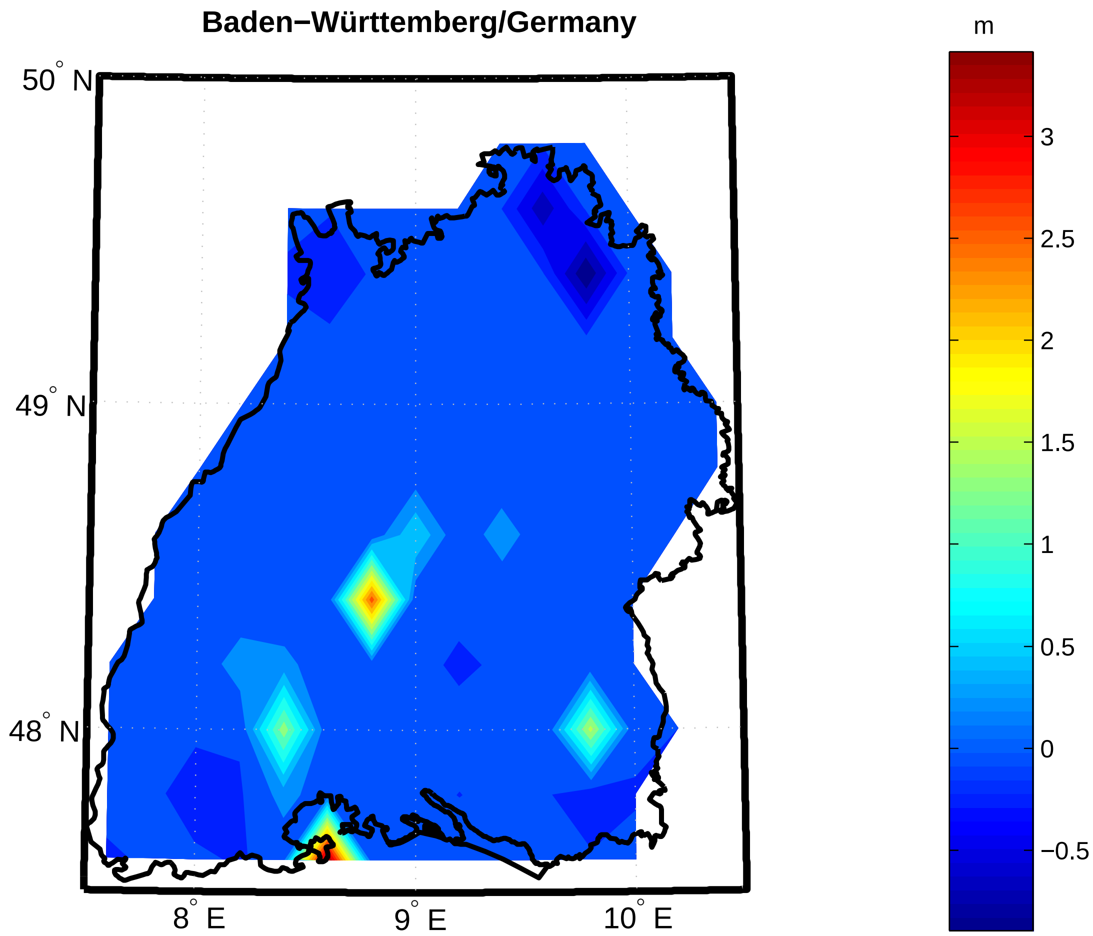

Figure 2-42: potential-geoid minus Gravity-geoid.

mean = (0.058±0.029)m,

max = 3.628m,

min = -0.893m.

Map Projection Information:
Equidistant Conic Projection
Standard Parallels: 48° N and 49° N
Reference ellipsoid: WGD2000

2.4.9 Case 3: Combined solution

Final now we can introduce the high-resolution geoid of Baden-Württemberg, in the World Geodetic Datum 2000 (tide free); based upon collocation of linearized observational functionals of the type GPS, *gravity potential* and gravity intensity. This can be obtained via a combined solution based on the already obtained optimum regularisation parameters $\{\alpha_1, \alpha_2\}$ as follows.

$$\hat{\mathbf{x}}^{\alpha} = \left(\begin{bmatrix} \mathbf{A}_1 \\ \mathbf{A}_2 \end{bmatrix}^T \begin{bmatrix} \mathbf{A}_1 \\ \mathbf{A}_2 \end{bmatrix} + \begin{bmatrix} \alpha_1 \mathbf{I} \\ \alpha_2 \mathbf{I} \end{bmatrix} \right)^{-1} \begin{bmatrix} \mathbf{A}_1 \\ \mathbf{A}_2 \end{bmatrix}^T \begin{bmatrix} \mathbf{y}_1 \\ \mathbf{y}_2 \end{bmatrix} \tag{2.44}$$

where $\mathbf{A}_1$ and $\mathbf{A}_2$ are those coefficient matrices used in case 1 and case 2 respectively. *Figure 2-43* shows the final geoid obtained from the combined solution.

2.5 Conclusions

We have illustrated the first attempt to solve for a high-resolution local geoid, using combined observations of the type *modulus of gravity intensity* and *geopotential numbers*. We demonstrated how GPS observations could be efficiently combined with gravity type information in a boundary value problem for geoid determination. A boundary-value problem which, can incorporate all available pieces of information in a precise way towards computation of a high-resolution local geoid. The highlights of our approach are as follows:

(1) Application of high degree/order global geopotential model, which provides us with the global gravity and isostasy information.

(2) Using observables of the type gravity intensity (from gravimetric observation), and gravity potential (form precise levelling) in a combined model for geoid determination.

(3) Remaining at the *level of ellipsoidal approximation* throughout the computations.

(4) Presenting a method, which works based on local gravity information.

(5) Converting surface observations of the type gravity intensity and gravity potential (through remove, downward continuation, and restore) to the gravity potential on the surface of the reference equipotential surface.

(6) Using non-linear ellipsoidal Bruns formula to convert the incremental gravity potential on the surface of reference ellipsoid to the geoidal undulations.

(7) Formulating the whole computations with respect to the reference ellipsoid.

Our results in spite of some shortcomings in the data (e.g. unavailability of GPS observation, and poor geometrical coverage of the gravity data) are quite promising.

In summary, we have tested a boundary value problem, which can address the future trend of geoid determination!

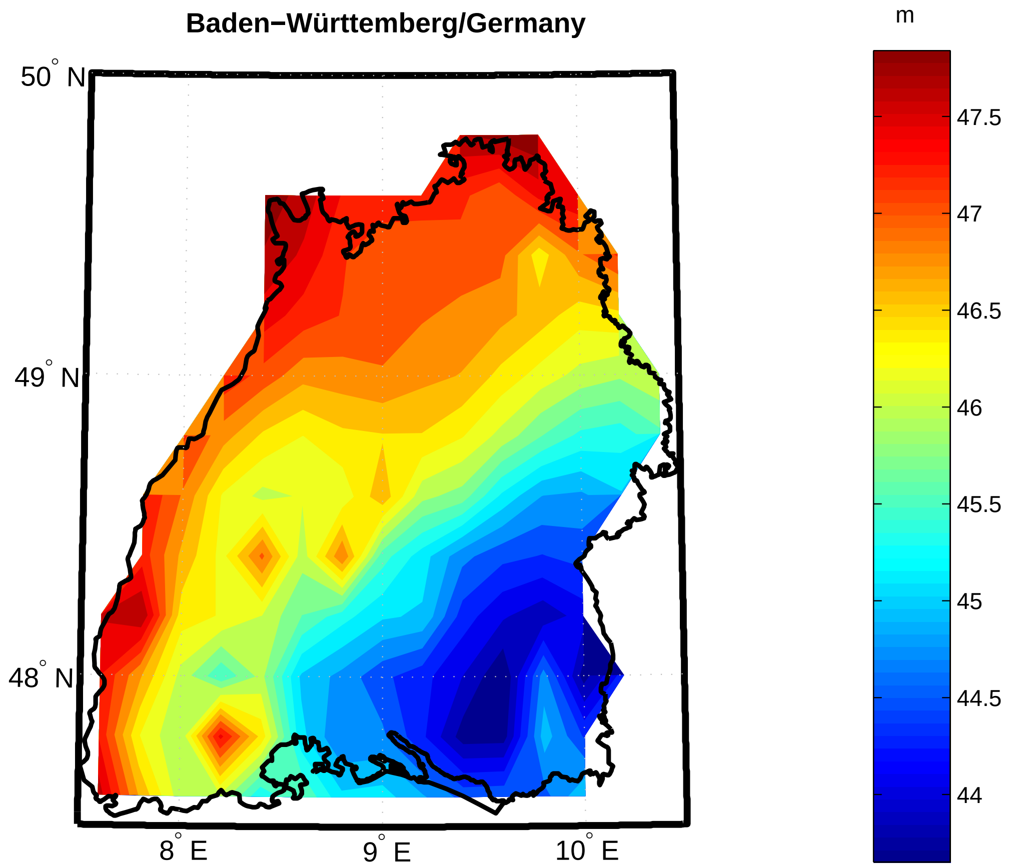

Figure 2-43: High-resolution geoid of Baden-Württemberg, in The World Geodetic Datum 2000 (tide free); based upon collocation of linearized observational functionals of the type GPS, *gravity potential* and gravity intensity.

__Map Projection Information:__
Equidistant Conic Projection
Standard Parallels: $48^\circ N$ *and* $49^\circ N$
Reference ellipsoid: WGD2000

3 Global geoid computation as a solution of the implicit function theorem

In this chapter, we are going to present the problem of *Global Geoid Computation* as a realisation of *implicit function theorem*. Based on the *implicit function theorem* we construct a geoid determination procedure, which describes the problem of geoid computation *at-large*! The *global geoid* computation will then be presented as an example of the application of *implicit function theorem* to geoid computations.

The aforementioned global geoid will be achieved by ellipsoidal harmonic expansion of external gravitational field of the earth up to degree/order 360/360, and nonlinear ellipsoidal Bruns formula, which presents the features with 50-60 km wavelength signature. Such a resolution covers all global details of geoid. As will be shown if we are interested in using a global geopotential model to present the geoidal heights with respect to an ellipsoid of revolution, say international reference ellipsoid of WGD2000, then the only rigorous way is through the application of *ellipsoidal harmonic expansion* and *ellipsoidal Bruns formula*.

Let us now start the problem of global geoid determination by introducing the implicit function theorem.

3.1 Implicit function theorem

Let $w(\lambda, \phi, u)$ be the presentation of the scalar gravity- potential field of the earth in terms of Jacobi ellipsoidal coordinates $\{\lambda, \phi, u\}$ {Jacobi ellipsoidal longitude, Jacobi ellipsoidal latitude, and Jacobi ellipsoidal height}. See *Appendix A.1.3*, for the definition of Jacobi ellipsoidal coordinates $\{\lambda, \phi, u\}$. $w(\lambda, \phi, u) = w_0$ presents an especial equipotential surface of the earth, which according to *Gauss-Listing* school, is called *geoid*. w_0 is the gravity potential of geoid. Furthermore, let us assume that $[x, y, z]^T$ according to the following definition is the shape function of geoid.

$$\begin{bmatrix} x \\ y \\ z \end{bmatrix} = \begin{bmatrix} \sqrt{u^2 + \varepsilon^2} & 0 & 0 \\ 0 & \sqrt{u^2 + \varepsilon^2} & 0 \\ 0 & 0 & u \end{bmatrix} \begin{bmatrix} \cos\phi\cos\lambda \\ \cos\phi\sin\lambda \\ \sin\phi \end{bmatrix} \tag{3.1}$$

However, as was mentioned in *Introduction* we are normally interested in presentation of geoid with respect to a reference equipotential surface of ellipsoidal type, for example the reference ellipsoid $\mathbb{E}^2_{a,b}$ of WGD2000. Such a presentation can be achieved in terms of incremental shape function $\delta u = u - b$. Where b is the semi-minor axis of the reference ellipsoid /reference equipotential surface/ $\mathbb{E}^2_{a,b}$. Accordingly, (3.1) can be written as

$$\begin{bmatrix} x \\ y \\ z \end{bmatrix} = \begin{bmatrix} \sqrt{(b + \delta u)^2 + \varepsilon^2} & 0 & 0 \\ 0 & \sqrt{(b + \delta u)^2 + \varepsilon^2} & 0 \\ 0 & 0 & b + \delta u \end{bmatrix} \begin{bmatrix} \cos\phi\cos\lambda \\ \cos\phi\sin\lambda \\ \sin\phi \end{bmatrix} \tag{3.2}$$

By means of *B. Taylor* series expansion of the type $\sqrt{1 + x} = 1 + \frac{1}{2}x - \frac{1}{8}x^2 + \frac{1}{16}x^3 - \frac{5}{128}x^4 + \cdots$ for $x \ll 1$, from (3.2) one can reach to (3.4) through following steps.

$$\begin{bmatrix} x \\ y \\ z \end{bmatrix} =$$

$$\begin{bmatrix} (b + \varepsilon^2)\sqrt{1 + \dfrac{\delta u^2 + 2b\,\delta u + \varepsilon^2}{(b + \varepsilon)^2}} & 0 & 0 \\ 0 & (b + \varepsilon^2)\sqrt{1 + \dfrac{\delta u^2 + 2b\,\delta u + \varepsilon^2}{(b + \varepsilon)^2}} & 0 \\ 0 & 0 & b + \delta u \end{bmatrix}$$

$$\times \begin{bmatrix} \cos\phi\cos\lambda \\ \cos\phi\sin\lambda \\ \sin\phi \end{bmatrix}$$

$$\doteq \begin{bmatrix} (b+\varepsilon^2)\left(1+\frac{1}{2}\frac{\delta u^2+2b\,\delta u+\varepsilon^2}{(b+\varepsilon)^2}\right) & 0 & 0 \\ 0 & (b+\varepsilon^2)\left(1+\frac{1}{2}\frac{\delta u^2+2b\,\delta u+\varepsilon^2}{(b+\varepsilon)^2}\right) & 0 \\ 0 & 0 & b+\delta u \end{bmatrix}$$

$$\times \begin{bmatrix} \cos\phi\cos\lambda \\ \cos\phi\sin\lambda \\ \sin\phi \end{bmatrix}$$

$$= \begin{bmatrix} (b+\varepsilon^2) & 0 & 0 \\ 0 & (b+\varepsilon^2) & 0 \\ 0 & 0 & b \end{bmatrix} \begin{bmatrix} \cos\phi\cos\lambda \\ \cos\phi\sin\lambda \\ \sin\phi \end{bmatrix} \tag{3.3}$$

$$+ \begin{bmatrix} \left(\frac{1}{2}\frac{\delta u^2+2b\,\delta u+\varepsilon^2}{(b+\varepsilon)}\right) & 0 & 0 \\ 0 & \frac{1}{2}\frac{\delta u^2+2b\,\delta u+\varepsilon^2}{(b+\varepsilon)} & 0 \\ 0 & 0 & \delta u \end{bmatrix} \begin{bmatrix} \cos\phi\cos\lambda \\ \cos\phi\sin\lambda \\ \sin\phi \end{bmatrix}$$

$$= \mathbf{X} + \delta\mathbf{X} \tag{3.4}$$

Where

$$\mathbf{X} = \begin{bmatrix} (b+\varepsilon^2) & 0 & 0 \\ 0 & (b+\varepsilon^2) & 0 \\ 0 & 0 & b \end{bmatrix} \begin{bmatrix} \cos\phi\cos\lambda \\ \cos\phi\sin\lambda \\ \sin\phi \end{bmatrix} \tag{3.5}$$

presents the transformation equation of the reference ellipsoid, $u = b$, form the Jacobi ellipsoidal coordinates $\{\lambda, \phi, u\}$ into Cartesian coordinates $\{x, y, z\}$, and

$$\delta\mathbf{X} = \begin{bmatrix} \left(\frac{1}{2}\frac{\delta u^2 + 2b\,\delta u + \varepsilon^2}{(b+\varepsilon)}\right) & 0 & 0 \\ 0 & \frac{1}{2}\frac{\delta u^2 + 2b\,\delta u + \varepsilon^2}{(b+\varepsilon)} & 0 \\ 0 & 0 & \delta u \end{bmatrix} \begin{bmatrix} \cos\phi\cos\lambda \\ \cos\phi\sin\lambda \\ \sin\phi \end{bmatrix} \tag{3.6}$$

is the transformation equation of the incremental shape function δu (with respect to the reference ellipsoid $\mathbb{E}^2_{a,b}$) form the Jacobi ellipsoidal coordinates $\{\lambda, \phi, u\}$ into Cartesian coordinates $\{x,y,z\}$.

Due to the separation between the reference equipotential surface $\mathbb{E}^2_{a,b}$ and the geoid δu, the actual potential $w(\lambda,\phi,b)$ on the surface of the reference equipotential surface differs from the reference potential $U_0 = w_0$ by the incremental potential δW.

$$\begin{aligned} \delta W &= w(\lambda,\phi,b) - U_0 \\ &= w(\lambda,\phi,b) - w_0 \end{aligned} \tag{3.7}$$

Since δW caused by the separation δu of geoid and the reference equipotential surface, it can be written as a function of δu as follows.

$$\delta W = \delta W(\lambda, \phi, \delta u) \tag{3.8}$$

or

$$f(\lambda, \phi, \delta u, \delta W) = \delta w(\lambda, \phi, \delta u) - \delta W = 0 \tag{3.9}$$

Introducing the new variables

$$\begin{aligned} x_1 &:= \lambda \\ x_2 &:= \phi \\ x_3 &:= \delta u \\ x_4 &:= \delta w \end{aligned} \tag{3.10}$$

(3.9) can be written as

$$f(x_1,x_2,x_4;x_3) = 0 \tag{3.11}$$

According to the *implicit function theorem* (introduced in *Table 3-1* after *E. Grafarend and B. Schaffrin* (1993)) the function (3.8) can be inverted to an explicit form in $x_3 = \delta u$

$$x_3 = g(x_1,x_2,x_4) \tag{3.12}$$

if and only if the rank of the *Jacobian matrix* $\mathbf{J} = \left[\dfrac{\partial f(x_1,x_2,x_4;x_3)}{\partial x_3}\right]$ be equal to 1 ($r = 1$ see *Table 3-1*), or equivalently the determinant of the Jacobian matrix $\mathbf{J}$ be non-zero.

$$\det(\mathbf{J}) = \det(\left[\frac{\partial f(x_1,x_2,x_3)}{\partial x_3}\right]) \neq 0. \tag{3.13}$$

The implicit function theorem offers the condition, which must be fulfilled to get the explicit form $x_3 = g(x_1,x_2,x_4)$, but does not say anything on the way that such a solution can be obtained. However, if we can succeed to determine the function $x_3 = g(x_1,x_2,x_4)$, we have the incremental shape function of geoid $\delta u = x_3$ as a function of incremental gravity potential on the surface of the reference ellipsoid $\delta W = x_4$ and surface Jacobi ellipsoidal coordinates $\{\lambda,\phi\} = \{x_1,x_2\}$. *Example 3-1* presents the application of the implicit function theorem to determination of the shape function equipotential surface $U(r) = c$ of the gravitational field $U(r)$ of a massive sphere $\mathbb{S}^2_R$ (see *Figure 3-1*).

Considering the explicit function (3.12) is available (3.4) can be written as follows.

$$\begin{bmatrix} x \\ y \\ z \end{bmatrix} = \begin{bmatrix} (b+\varepsilon^2) & 0 & 0 \\ 0 & (b+\varepsilon^2) & 0 \\ 0 & 0 & b \end{bmatrix} \begin{bmatrix} \cos\phi\cos\lambda \\ \cos\phi\sin\lambda \\ \sin\phi \end{bmatrix}$$

$$+\begin{bmatrix} \left(\dfrac{1}{2}\dfrac{g(\lambda,\phi,\delta W)^2+2bg(\lambda,\phi,\delta W)+\varepsilon^2}{(b+\varepsilon)}\right) & 0 & 0 \\ 0 & \dfrac{1}{2}\dfrac{g(\lambda,\phi,\delta W)^2+2bg(\lambda,\phi,\delta W)+\varepsilon^2}{(b+\varepsilon)} & 0 \\ 0 & 0 & g(\lambda,\phi,\delta W) \end{bmatrix}$$

$$\times\begin{bmatrix} \cos\phi\cos\lambda \\ \cos\phi\sin\lambda \\ \sin\phi \end{bmatrix} \tag{3.14}$$

In the next section, we will determine the relation between the incremental potential δW and the incremental shape height δu, in its most general sense, called “generalised Bruns formula”.

Table 3-1: Implicit function theorem.

The vector function $\mathbf{F}(\mathbf{x})$ of vector variables $\mathbf{x} = [\mathbf{x}_1; \mathbf{x}_2] = [x_1, \ldots, x_{m-r}; x_{m-r+1}, \ldots, x_m]$ defined as

$$\mathbf{F}(\mathbf{x}_1, \mathbf{x}_2) = \begin{bmatrix} F_1(x_1, \ldots, x_{m-r}; x_{m-r+1}, \ldots, x_m) \\ F_2(x_1, \ldots, x_{m-r}; x_{m-r+1}, \ldots, x_m) \\ \vdots \\ F_r(x_1, \ldots, x_{m-r}; x_{m-r+1}, \ldots, x_m) \end{bmatrix} = 0 \tag{3.15}$$

can be converted into an explicit form in $\mathbf{x}_2$, i.e.

$$\mathbf{x}_2 = \mathbf{G}(\mathbf{x}_1) = \begin{bmatrix} G_1(x_1, \ldots, x_{m-r}) \\ G_2(x_1, \ldots, x_{m-r}) \\ \vdots \\ G_r(x_1, \ldots, x_{m-r}) \end{bmatrix} = \begin{bmatrix} x_{m-r+1}, \ldots, x_m \\ x_{m-r+1}, \ldots, x_m \\ \vdots \\ x_{m-r+1}, \ldots, x_m \end{bmatrix} \tag{3.16}$$

if and only if the rank of the Jacobian matrix $\mathbf{J} = \left[\dfrac{\partial \mathbf{F}(\mathbf{x}_1; \mathbf{x}_2)}{\partial \mathbf{x}_2} \right]$ be equal to r

$$\operatorname{rank}(\mathbf{J}) = \operatorname{rank}\left(\left[\frac{\partial \mathbf{F}(\mathbf{x}_1; \mathbf{x}_2)}{\partial \mathbf{x}_2} \right] \right) = r \tag{3.17}$$

or equivalently the determinant of $\mathbf{J}$ be non-zero.

$$\det(\mathbf{J}) = \det\left(\left[\frac{\partial \mathbf{F}(\mathbf{x}_1; \mathbf{x}_2)}{\partial \mathbf{x}_2} \right] \right) \neq 0 \tag{3.18}$$

Example 3-1: The shape function of the equipotential surfaces of a massive sphere.

Given the potential of a homogenous massive sphere $\mathbb{S}_R^2$ (see *Figure 3-1*), with following gravitational potential field

$$U(r) = \begin{cases} \dfrac{1}{2} \dfrac{gm}{R^3} [3R^2 - r^2] & \text{for inner space } r \leq R \\ \dfrac{gm}{r} & \text{for outer space } r > R \end{cases} \tag{3.19}$$

we want to determine the shape function of the equipotential surface $U(r) = c = const.$ for following two cases:

"Case a: For the inner space (Zone A)"

$$U(r) = \frac{1}{2} \frac{gm}{R^3} [3R^2 - r^2] = c \tag{3.20}$$

or in terms of new variables $x_1 := r$ and $x_2 := c$

$$f(x_2;x_1) = \frac{1}{2}\frac{gm}{R^3}[3R^2 - x_1] - x_2 = 0 \tag{3.21}$$

According to implicit function theorem $f(x_2;x_1)$ can be converted into an explicit form in x_1, i.e. $x_1 = g(x_2)$ if and only if the rank of the Jacobian matrix $\mathbf{J} = \left[\frac{\partial f(x_2;x_1)}{\partial x_1}\right]$ is equal to 1 ($r = 1$, see *Table 3-1*), or equivalently determinant of the Jacobian matrix $\mathbf{J}$ is non-zero.

$$\mathbf{J} = \left[\frac{\partial f(x_2;x_1)}{\partial x_1}\right] = -\frac{gm}{R^3}x_1 \tag{3.22}$$

Therefore,

$$\det(\mathbf{J}) = \det(\left[\frac{\partial f(x_2;x_1)}{\partial x_1}\right]) = -\frac{gm}{R^3}x_1. \tag{3.23}$$

$\det(\mathbf{J})$ is non-zero for $x_1 > 0$. Therefore, $f(x_2;x_1)$ can be converted into an explicit form in x_1 for all those values $x_1 > 0$, as follows

$$x_1 = \sqrt{3R^2 - \frac{2R^3}{gm}x_2} \tag{3.24}$$

In (3.24) since all quantities on the right-hand-side of the equation are constant the left-hand-side must also be a constant, $x_1 = r = const$. Therefore, the shape of the equipotential surface $U(r) = c$ is the sphere $\mathbb{S}^2_{\sqrt{3R^2 - \frac{2R^3}{gm}x_2}}$

"Case b: For the outer space, zone B"

$$U(r) = \frac{gm}{r} = c \tag{3.25}$$

By introducing new variables $x_1 := r$ and $x_2 = c$ (3.25) can be written as

$$f(x_2;x_1) = \frac{gm}{x_1} - x_2 = 0 \tag{3.26}$$

According to implicit function theorem $f(x_2;x_1)$ can be converted into an explicit form in x_1, i.e. $x_1 = g(x_2)$, if and only if the rank of the Jacobian matrix $\mathbf{J} = \left[\frac{\partial f(x_2;x_1)}{\partial x_1}\right]$ is equal to 1 ($r = 1$, see *Table 3-1*), or equivalently determinant of the Jacobian matrix $\mathbf{J}$ is non-zero.

$$\mathbf{J} = \left[\frac{\partial f(x_2;x_1)}{\partial x_1}\right] = -\frac{gm}{x_1{}^2}\left[\begin{matrix}\neq 0 & \text{for } x_1 < \infty \\ = 0 & \text{for } x_1 \to \infty\end{matrix}\right. \tag{3.27}$$

$$\Rightarrow \det(\mathbf{J}) = \det(\left[\frac{\partial f(x_2;x_1)}{\partial x_1}\right]) = -\frac{gm}{x_1{}^2}. \tag{3.28}$$

$\det(\mathbf{J})$ is zero for $x_1 \to \infty$. Therefore, $f(x_2;x_1)$ can be converted into an explicit form in x_1 for $x_1 < \infty$, as follows

$$x_1 = \frac{gm}{x_2} \tag{3.29}$$

since in (3.29) all quantities on the right-hand-side of the equation are constant the left-hand-side must also be a constant, $x_1 = r = const$. Therefore, the shape of the equipotential surface $U(r) = c$ is the sphere $\mathbb{S}^2_{\frac{gm}{x_2}}$.

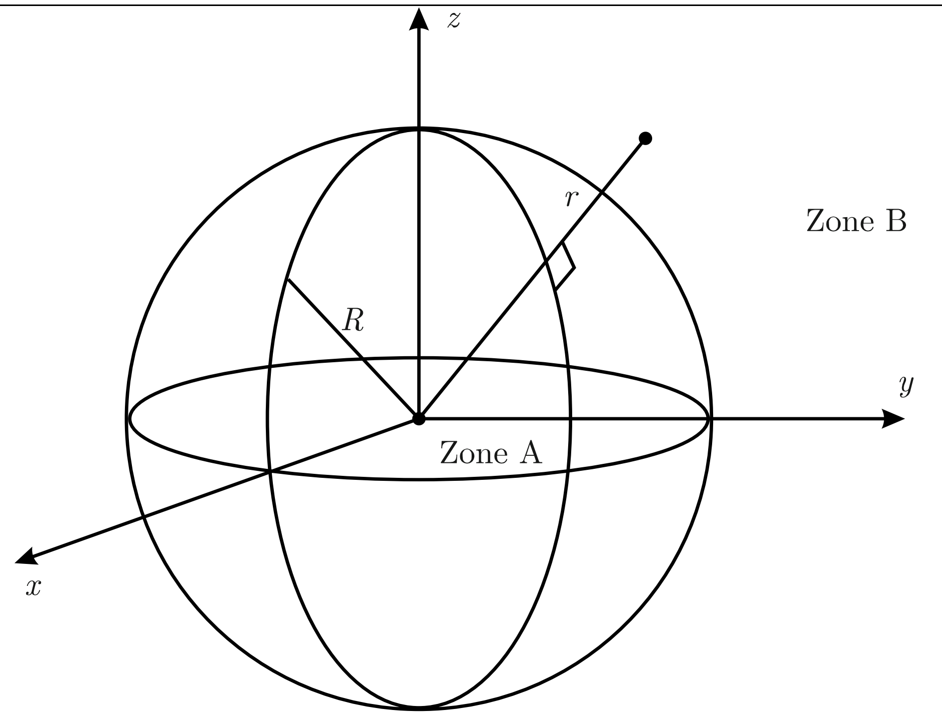

Figure 3-1: Homogeneous stationary massive sphere $\mathbb{S}^2_R$, inner zone A, and the outer zone B.

Example 3-2: Shape function of the equipotential surface of a rotational massive sphere, with constant mass density.

Given the external gravity potential of a homogenous massive sphere $\mathbb{S}^2_R$ (see *Figure 3-1*), as follows.

$$W(\phi, r) = \underbrace{\frac{gm}{r}}_{\substack{\text{Gravitational}\\ \text{field}}} + \underbrace{\frac{1}{2}\omega^2 r^2 \cos^2\phi}_{\substack{\text{Centrifugal}\\ \text{field}}} \quad \text{for } r > R \tag{3.30}$$

we want to determine the shape function of the equipotential surface $W(\phi, r) = c = const.$, i.e.

$$W(\phi,r)=\underbrace{\frac{gm}{r}}_{\substack{\text{Gravitational}\\ \text{field}}}+\underbrace{\frac{1}{2}\omega^2 r^2\cos^2\phi}_{\substack{\text{Centrifugal}\\ \text{field}}}=c \qquad \text{for } r>R \tag{3.31}$$

Introducing a new set of variables $\{x_1,x_2,x_3\}=\{\phi,r,c\}$, (3.31) can be written as follows

$$f(x_1,x_3;x_2)=\underbrace{\frac{gm}{x_2}}_{\substack{\text{Gravitational}\\ \text{field}}}+\underbrace{\frac{1}{2}\omega^2 x_2{}^2\cos^2 x_1}_{\substack{\text{Centrifugal}\\ \text{field}}}-x_3=0 \tag{3.32}$$

According to implicit function theorem (3.32) can be converted into an explicit form in x_2 provided that the rank of the Jacobian matrix $\mathbf{J}=\left[\frac{\partial f(x_1,x_3;x_2)}{\partial x_2}\right]$ is equal to 1 (r=1 see *Table 3-1*), or equivalently the determinate of the Jacobian matrix $\mathbf{J}$ is non zero. The Jacobian matrix $\mathbf{J}$

$$\mathbf{J}=\left[\frac{\partial f(x_1,x_3;x_2)}{\partial x_2}\right]=-\frac{gm}{x_2^2}+\omega^2 x_2\cos^2 x_1 \tag{3.33}$$

is zero for

$$x_2=\sqrt[3]{\frac{gm}{\omega^2\cos^2 x_1}}. \tag{3.34}$$

Therefore, for

$$x_2\neq\sqrt[3]{\frac{gm}{\omega^2\cos^2 x_1}} \tag{3.35}$$

(3.32) can be inverted into an explicit form in x_2 as follows.

$$(\frac{1}{2}\omega^2\cos^2 x_1)x_2{}^3-x_3x_2+gm=0 \tag{3.36}$$

or assuming $a=\frac{1}{2}\omega^2\cos^2 x_1$, $b=x_3$, $c=gm$, (3.36) can be written as

$$ax_2^3-bx_2+c=0 \tag{3.37}$$

which results in three solutions for x_2, two complex and one real. The real solution is given in equation (3.38) bellow.

$$\begin{aligned}x_2=&\frac{1}{6}\frac{\left[-108a^2c+12a^2\left(-12\frac{b^3}{a}+81c^2\right)^{1/2}\right]^{1/3}}{a}\\ &+2\frac{b}{\left[-108a^2c+12a^2\left(-12\frac{b^3}{a}+81c^2\right)^{1/2}\right]^{1/3}}\end{aligned} \tag{3.38}$$

3.2 Generalised Bruns formula

To derive a generalised form for the *Bruns Formula*, let us assume that geoid is to be determined with respect to a given reference equipotential surface $W = w_0$. That is, we are looking for the incremental height of geoid h, which is normal to the reference equipotential surface $W = w_0$.

Let us start with the following *B. Taylor* expansion of geoid's potential w_0, based on the expansion point $w(\mathbf{X})$. $w(\mathbf{X})$ is the actual potential at point $\mathbf{X}$ on the surface of the reference equipotential surface.

$$\begin{aligned} w_0 &= w(\mathbf{X}) + \frac{1}{1!}\nabla_N w(\mathbf{X})h \\ &+\frac{1}{2!}\nabla_N(\nabla_N w(\mathbf{X}))h^2 + \cdots =: W(\mathbf{X}) \end{aligned} \tag{3.39}$$

where ∇_N is the directional derivative along the normal direction to the surface of reference equipotential surface, i.e.

$$\nabla_N w(\mathbf{X}) = \langle \operatorname{grad} w(\mathbf{X}) \mid \mathbf{n} \rangle \tag{3.40}$$

$\mathbf{n}$ is the unit normal vector of the reference equipotential surface, h is the incremental height of geoid along the surface normal of the reference equipotential surface. (See *Appendix F*, *page 236* for the advantage of using the directional derivative operator). Upon transformation of $w(\mathbf{X})$ to the left-hand side of the equation (3.39) we have

$$\begin{aligned} -\delta W(\mathbf{X}) = W(\mathbf{X}) - w(\mathbf{X}) &= +\frac{1}{1!}\nabla_N w(\mathbf{X})h \\ &+\frac{1}{2!}\nabla_N(\nabla_N w(\mathbf{X}))h^2 + \cdots \\ &= \sum_{n=1}^{\infty} a_{1n} h^n . \end{aligned} \tag{3.41}$$

(3.41) is a homogeneous polynomial in terms of h, and according to *E. Grafarend et al.* (1996) can be inverted to

$$h = \sum_{n=1}^{\infty} b_{1n}(-\delta w)^n \tag{3.42}$$

provided that a_{10} is non-zero. a_{10} is the derivative of $w(\mathbf{X})$ with respect to the h, surface normal of the reference equipotential surface. Note that it is exactly the same condition imposed by implicit function theorem to bridge from the implicit form (3.11) to the explicit form (3.12)! Therefore, the inverse homogeneous polynomial (3.42) is indeed an explicit solution for h according to *implicit function theorem*! In physical sense, the required condition is fulfilled if the gradient of the actual gravity potential, i.e.

gravity vector, is not tangent to the surface of reference equipotential surface $W = w_0$.

Table 3-2 shows how the coefficients b_{1n} can be derived recursively from $b_{11} = 1/a_{11}$, and the other coefficients a_{1n} $\forall n = 1,\dots,\infty$.

Table 3-2: Recursive relations for determination of the coefficients b_{1n} of the inverse homogenous polynomial.

Given the *homogenous polynomial*

$$\Delta w = \sum_{n=1}^{\infty} a_{1n} h^n \tag{3.43}$$

the inverse homogenous polynomial

$$h = \sum_{n=1}^{\infty} b_{1n} \Delta w^n \tag{3.44}$$

can be derived from the following *recursive relations*

$$b_{1n} = (-\sum_{i=1}^{n-1} b_{1i} a_{1i}) a_{nn}^{-1} \qquad \forall n \geq 2 \tag{3.45}$$

subject to

$$a_{nm} = \sum_{i=1}^{n-(m-1)} a_{1i} \otimes a_{m-1n-i} \qquad \forall m \leq n \tag{3.46}$$

($\otimes$ is the Kronecker product)

$$a_{nn}^{-1} = (a_{11}^{n})^{-1} = (a_{11}^{-1})^n \tag{3.47}$$

with start values

$$b_{11} = a_{11}^{-1} \tag{3.48}$$

$$b_{12} = -a_{11}^{-3} a_{12} \tag{3.49}$$

subject to

$$a_{11} \neq 0$$

Note that (3.42) is without any approximation and is valid for any reference equipotential surface / reference level surface $W(\mathbf{X}) = w_0$. Therefore, let us call (3.42) the "*Generalised Bruns Formula*".

Table 3-3 provides us with a set of simple models, which can be used as the reference gravity field, in spherical and ellipsoidal approximation. These are the only reference fields, which produce reference equipotential surfaces of the type sphere or ellipsoid of revolution! However, if we want to be faithful to the resolution $N^\circ 7$ of IUGG, presented in The *Geodesist's Handbook* (*H. Moritz*, 2000), concerning the use of an equipotential ellipsoid as the international reference equipotential surface, the second or third model in *Table 3-3* should be adopted.

The Bruns formula (3.42) is so far exact and without any approximation. However, this formula is not in a practical form. Namely due to of the calculation of the coefficients b_{1n} in (3.42) which requires the actual gravity potential $w(\mathbf{X})$ as an analytical continuously differentiable function, so that directional derivative along the normal to the reference equipotential surface can be computed. To overcome this problem one can perform the directional derivative on an approximation form of the actual gravity potential. Though the choice of such an approximate formula is quite free, however computational ease would be achieved if one chooses the one, which produces the reference level surface identical to reference equipotential surface. In *Table 3-4*, we have a collection of two different reference fields and their corresponding Bruns formula, both up to the linear part. In the next chapter, we will present a more accurate version of ellipsoidal Bruns formula presented in *Table 3-4*, which includes the effect of second order term in $\delta W(\mathbf{X})$. As one can recognise, the first row of *Table 3-4* contains the traditional Bruns formula $\delta r = \frac{\delta w(R)}{GM / R^2} = \frac{T}{\gamma}$. Such a Bruns formula is only valid for presentation of the geoid with respect to a reference sphere $\mathbb{S}_R^2$, the level sphere $W = \frac{GM}{R} = w_0$. Unfortunately, in literature quite often by mistake the incremental heights derived from $\delta r = \frac{\delta w(R)}{GM / R^2}$ are considered as the geoidal height with respect to *reference ellipsoid*!

Here since we are interested in presenting the geoidal height with respect to *international ellipsoidal WGD2000* the second model in *Table 3-3* is selected, and we have gone up to the third order term, $\mathcal{O}(\delta w^3)$, in the inverse polynomial expansion (3.42).

Now that we derived the generalised Bruns formula, we can offer a general procedure for geoid determination.

Table 3-3: Different choices of reference gravity/gravitational field.

reference field $W(\mathbf{X})$	reference equipotential surface $\mathbf{X} = \mathbf{X}(w_0)$
$W(r) = \dfrac{GM}{r}$	sphere $\mathbb{S}^2_R$ $x^2 + y^2 + z^2 = (\dfrac{GM}{w_0})^2$
$W(\phi,u) = \dfrac{GM}{\varepsilon}\operatorname{arc\,cot}(\dfrac{u}{\varepsilon})$	ellipsoid of revolution $\mathbb{E}^2_{a,b}$ $\dfrac{x^2+y^2}{\varepsilon^2 + \varepsilon^2\cot^2(\frac{\varepsilon w_0}{GM})} + \dfrac{z^2}{\varepsilon^2\cot^2(\frac{\varepsilon w_0}{GM})}$
$W(\phi,u) = \dfrac{GM}{\varepsilon}\operatorname{arc\,cot}(\dfrac{u}{\varepsilon}) + \dfrac{1}{6}\Omega^2 a^2 \dfrac{(3\frac{u^2}{\varepsilon^2}+1)\operatorname{arc\,cot}(\frac{u}{\varepsilon}) - 3\frac{u}{\varepsilon}}{(3\frac{b^2}{\varepsilon^2}+1)\operatorname{arc\,cot}(\frac{b}{\varepsilon}) - 3\frac{b}{\varepsilon}}(3\sin^2\phi - 1) + \dfrac{1}{2}\Omega^2(u^2+\varepsilon^2)\cos^2\phi$	ellipsoid of revolution $\mathbb{E}^2_{a,b}$, e.g. WGD 2000 $\dfrac{x^2+y^2}{a^2_{WGD2000}} + \dfrac{z^2}{b^2_{WGD2000}}$

Table 3-4: Two different types of reference field and their respective Bruns formulas.

Reference field	Reference equipotential surface	Bruns formula (up to linear term)
$W(r) = \dfrac{GM}{r}$	sphere $\mathbb{S}^2_R$	$\delta r = \dfrac{\delta W(R)}{GM / R^2}$
$W(\phi,u) = \dfrac{GM}{\varepsilon}\operatorname{arc\,cot}(\dfrac{u}{\varepsilon})$	ellipsoid of revolution $\mathbb{E}^2_{a,b}$	$\delta u = \dfrac{\delta W(u=b)}{gm / (\sqrt{u^2+\varepsilon^2}\sqrt{u^2+\varepsilon^2-\varepsilon^2\cos^2\phi})}$

3.3 Ellipsoidal Bruns Transformation

In the previous chapter, we derived the most general form of the *Bruns transformation*. Here, we derive an especial *non-linear ellipsoidal* form of it in terms of *Jacobi ellipsoidal coordinates* $\{\lambda, \phi, u\}$. If we limit ourselves to the order of accuracy of first eccentricity squared $\mathcal{O}(e^2)$ ($e^2 = (a^2 - b^2)/a^2$) then the first term of ellipsoidal harmonic expansion, $U(\lambda, \phi, u) = gm/\varepsilon \operatorname{arccot}(\frac{u}{\varepsilon})$, can be used as the reference gravitational field. The order of accuracy of $\mathcal{O}(e^2)$ is enough for the geoid determination at centimetre accuracy level (see e.g. *Z. Martinec* 1998a, and *Z. Martinec and Grafarend* 1997a, 1997b). Such a reference field besides its simple form has the property of having ellipsoidal level surfaces (see *Box 1-20* for the proof). Since we want to present the geoidal undulations with respect to reference equipotential surface of WGD2000, such a model is a correct choice.

Box 1-17 presents the definition of the gradient of the scalar function $U(\lambda, \phi, u)$ as the covariant derivative $D_\mu U$ of the function $U(\lambda, \phi, u)$ with respect to contravariant base vectors $\boldsymbol{\mu}^\mu$. The contravariant base vectors are replaced by $g^{\mu\nu}\boldsymbol{\mu}_\nu$, the transformation relation between the covariant base vectors and contravariant ones. The non-normalised covariant base vectors $\boldsymbol{\mu}_\nu$ are further written in terms of normalised base vectors $\mathbf{e}_\nu$ multiplied by the norm of $\boldsymbol{\mu}_\nu$ ($\boldsymbol{\mu}_\nu = \sqrt{g_{\nu\nu}}\mathbf{e}_\nu$). Finally the orthogonality of the *Jacobi ellipsoidal* base vectors has led to special representations of (1.63) and (1.64). *Box 1-18* provides us with the directional derivative along the surface-normals of reference ellipsoid $\mathbb{E}^2_{a,b}$, while *Box 1-19* presents the application of the directional derivatives to the reference gravitational potential field $U(\lambda, \phi, u) = gm/\varepsilon \operatorname{arccot}(\frac{u}{\varepsilon})$. We have to mention that in *Box 1-19* we have gone up to *second order* directional derivatives. Finally, under the assumption $w(\lambda, \phi, u) = U(\lambda, \phi, u) = gm/\varepsilon \operatorname{arccot}(\frac{u}{\varepsilon})$ we have proceeded to the *non-linear ellipsoidal Bruns transformation formula* of *Box 1-22*. One may now ask what is the relation between the surface normal height h of the reference equipotential surface appearing in Taylor series expansion (3.39) and the Jacobi ellipsoidal height u. To answer this question we start with the following Taylor expansion of geoid's potential

w_0, over the expansion point $w(u=b)$. $w(u=b)$ is the actual potential at point any point $\mathbf{X}$ on the surface of the reference ellipsoid $u=b$.

$$\begin{aligned} w_0 &= w(u=b) + \frac{1}{1!}\mathrm{D}_u w(\mathbf{X})u \\ &+ \frac{1}{2!}\mathrm{D}_u(\mathrm{D}_u w(\mathbf{X}))u^2 + \cdots =: W(\mathbf{X}) \end{aligned} \tag{3.50}$$

The partial derivative $\mathrm{D}_u := \partial / \partial u$ is related to the directional derivative along the coordinate line of u as follows.

$$\mathrm{D}_u = \sqrt{g_{uu}}\nabla_u \tag{3.51}$$

Therefore, (3.50) can be written as

$$\begin{aligned} w_0 &= w(u=b) + \frac{1}{1!}\nabla_u w(\mathbf{X})\sqrt{g_{uu}}u \\ &+ \frac{1}{2!}\nabla_u(\nabla_u w(\mathbf{X}))g_{uu}u^2 + \cdots =: W(\mathbf{X}) \end{aligned} \tag{3.52}$$

According to *A. Eringen* (1962, page 437) $h = \sqrt{g_{uu}}u$ is the physical component of the Jacobi ellipsoidal coordinate u. $h = \sqrt{g_{uu}}u$ is an invariant parameter and is indeed the quantity that we need to present the height of geoid with respect to the reference ellipsoid of WGD2000. $h = \sqrt{g_{uu}}u$ can be called the *geoidal height* or *geoidal undulation* (see also *Appendix F*, *page 236*).

Box 3-1: Gradient of a scalar function $U(\lambda,\phi,u)$

(i) General definition of the gradient of a scalar function in terms of a curvilinear coordinate system

$$\begin{aligned} \mathrm{grad}U &= \mathbf{m}^{\mu}D_{\mu}U = g^{\mu\nu}\mathbf{m}_{\nu}D_{\mu}U \\ &= g^{\mu\nu}\|\mathbf{m}_{\nu}\|\mathbf{e}_{\nu}D_{\mu}U = g^{\mu\nu}\sqrt{g_{\nu\nu}}\mathbf{e}_{\nu}D_{\mu}U \end{aligned} \tag{3.53}$$

(ii) Gradient of the scalar function U in terms of orthogonal Jacobi ellipsoidal coordinates $\{\lambda,\phi,u\}$

$$\mathrm{grad}U = \mathbf{E}_{\lambda}\frac{1}{\sqrt{g_{\lambda\lambda}}}D_{\lambda}U + \mathbf{E}_{\phi}\frac{1}{\sqrt{g_{\phi\phi}}}D_{\phi}U + \mathbf{E}_{u}\frac{1}{\sqrt{g_{uu}}}D_{u}U \tag{3.54}$$

$$\Rightarrow$$

$$\begin{aligned} \mathrm{grad}U &= \mathbf{E}_{\lambda}\frac{1}{\sqrt{u^2+\varepsilon^2}\cos\phi}D_{\lambda}U + \mathbf{E}_{\phi}\frac{1}{\sqrt{u^2+\varepsilon^2-\varepsilon^2\cos^2\phi}}D_{\phi}U \\ &+ \mathbf{E}_{u}\frac{\sqrt{u^2+\varepsilon^2}}{\sqrt{u^2+\varepsilon^2-\varepsilon^2\cos^2\phi}}D_{u}U \end{aligned} \tag{3.55}$$

Box 3-2: Directional derivative along the surface normal of the reference ellipsoid $\mathbb{E}^2_{a,b}$

$$\langle \text{grad } U \,|\, \mathbf{E}_u \rangle = \nabla_{\mathbf{E}_u} U = \frac{\sqrt{u^2+\varepsilon^2}}{\sqrt{u^2+\varepsilon^2-\varepsilon^2\cos^2\phi}} D_u U = \frac{1}{\sqrt{g_{uu}}} \partial_u U \tag{3.56}$$

Box 3-3: Reference ellipsoidal gravitational field and its directional derivatives along the surface normals of reference ellipsoid $\mathbb{E}^2_{a,b}$

(i) Normal ellipsoidal field of the first order

$$U(\lambda,\phi,\eta) = \frac{gm}{\varepsilon} \operatorname{arc\,cot}(\frac{u}{\varepsilon}) \tag{3.57}$$

(ii) Directional derivative along the surface normals of $\mathbb{E}^2_{a,b}$

$$\begin{aligned} \nabla_N U &= \nabla_{\mathbf{E}_u} U = \frac{1}{\sqrt{g_{uu}}} \partial_u U = \frac{\sqrt{u^2+\varepsilon^2}}{\sqrt{u^2+\varepsilon^2-\varepsilon^2\cos^2\phi}} D_u U \\ &= -\frac{gm}{\sqrt{u^2+\varepsilon^2}(u^2+\varepsilon^2-\varepsilon^2\cos^2\phi)^{1/2}} \end{aligned} \tag{3.58}$$

$$\begin{aligned} \nabla_N \nabla_N U &= \nabla_{\mathbf{E}_u} \nabla_{\mathbf{E}_u} U = \frac{1}{\sqrt{g_{\eta\eta}}} \partial_u \nabla_{\mathbf{E}_u} U = \frac{\sqrt{u^2+\varepsilon^2}}{\sqrt{u^2+\varepsilon^2-\varepsilon^2\cos^2\phi}} D_u \nabla_{\mathbf{E}_u} U \\ &= gm \frac{u\left(2\dfrac{u^2+\varepsilon^2}{\varepsilon^2} - \cos^2\phi\right)}{\varepsilon^2(u^2+\varepsilon^2)(\dfrac{u^2+\varepsilon^2}{\varepsilon^2} - \cos^2\phi)^2} \end{aligned} \tag{3.59}$$

Box 3-4: Geometrical interpretation of the reference equipotential surface

$$U(\lambda,\phi,u) = gm \,/\, \varepsilon \operatorname{arc\,cot}(\frac{u}{\varepsilon}) = w_0 .$$

from the reference equipotential surface

$$U(\lambda,\phi,\eta) = \frac{gm}{\varepsilon} \operatorname{arc\,cot}(\frac{u}{\varepsilon}) = w_0 \tag{3.60}$$

one can imply that the only varying parameter, i.e., η must be constant

$$u = u_0 \tag{3.61}$$

from the inverse transformation of Cartesian coordinates $\{x,y,z\}$ into Jacobi ellipsoidal coordinate u (cf. *Appendix A.1.3*) we have

$$\begin{aligned} u &= \{\frac{1}{2}[x^2 + y^2 + z^2 - \varepsilon^2 \\ &+\sqrt{(x^2 + y^2 + z^2 - \varepsilon^2)^2 + 4\varepsilon^2 z^2}]\}^{1/2} \\ &= u_0 \\ &\Leftrightarrow \frac{1}{2}[x^2 + y^2 + z^2 - \varepsilon^2 \\ &+\sqrt{(x^2 + y^2 + z^2 - \varepsilon^2)^2 + 4\varepsilon^2 z^2}] \\ &= u_0^2 \\ &\Leftrightarrow \sqrt{(x^2 + y^2 + z^2 - \varepsilon^2)^2 + 4\varepsilon^2 z^2} \\ &= 2u_0^2 - x^2 + y^2 + z^2 - \varepsilon^2 \\ &\Leftrightarrow (x^2 + y^2 + z^2 - \varepsilon^2)^2 + 4\varepsilon^2 z^2 \\ &= (2u_0^2 - x^2 + y^2 + z^2 - \varepsilon^2)^2 \\ &\Leftrightarrow \frac{u_0^2}{\varepsilon^2}(x^2 + y^2) + \left(\frac{u_0^2 + \varepsilon^2}{\varepsilon^2}\right) z^2 \\ &= (u_0^2 + \varepsilon^2)\frac{u_0^2}{\varepsilon^2} \\ &\Leftrightarrow \frac{x^2 + y^2}{u_0^2 + \varepsilon^2} + \frac{z^2}{u_0^2} = 1 \end{aligned} \tag{3.62}$$

which is the equation of the reference ellipsoid $\mathbb{E}^2_{\sqrt{u_0^2+\varepsilon^2},u_0}$.

Box 3-5: *Non-linear ellipsoidal Bruns transformation*

$$h = \sum_{n=1}^{\infty} b_{1n}[-\delta W(\mathbf{X})]^n$$

subject to

$$
\begin{aligned}
b_{11} &:= \frac{1}{\nabla_N w(\mathbf{X})} \doteq \frac{1}{\nabla_N U(\mathbf{X})} + \mathcal{O}(e^2) \\
&= \frac{1}{\nabla_{\mathbf{E}_u} U} + \mathcal{O}(e^2) = (\frac{1}{\sqrt{g_{uu}}}\partial_u U)^{-1} + \mathcal{O}(e^2) \\
&= (\frac{\sqrt{u^2+\varepsilon^2}}{\sqrt{u^2+\varepsilon^2-\varepsilon^2\cos^2\phi}} D_u U)^{-1} + \mathcal{O}(e^2) \\
&= -\frac{(u^2+\varepsilon^2)(\frac{u^2+\varepsilon^2}{\varepsilon^2}-\cos^2\phi)^{1/2}}{gm} + \mathcal{O}(e^2)
\end{aligned} \tag{3.64}
$$

$$
\begin{aligned}
b_{12} &:= -\frac{1}{(\nabla_N w(\mathbf{X}))^3}\left(\frac{1}{2!}\nabla_N\nabla_N w(\mathbf{X})\right) \\
&\doteq -\frac{1}{(\nabla_N U(\mathbf{X}))^3}\left(\frac{1}{2!}\nabla_N\nabla_N U(\mathbf{X})\right) + \mathcal{O}(e^2) \\
&= -(\frac{\sqrt{u^2+\varepsilon^2}(u^2+\varepsilon^2-\varepsilon^2\cos^2\phi)^{1/2}}{gm})^{-3} \\
&\times(\frac{1}{2}gm\frac{\frac{u}{\varepsilon}\left(2\frac{u^2+\varepsilon^2}{\varepsilon^2}-\cos^2\phi\right)}{\varepsilon(u^2+\varepsilon^2)(\frac{u^2+\varepsilon^2}{\varepsilon^2}-\cos^2\phi)^2}) + \mathcal{O}(e^2)
\end{aligned} \tag{3.65}
$$

$$\cdots$$

$$
\begin{aligned}
&\Rightarrow h = \delta W(\mathbf{X})\frac{(u^2+\varepsilon^2)(\frac{u^2+\varepsilon^2}{\varepsilon^2}-\cos^2\phi)^{1/2}}{gm} \\
&-\left(\delta W(\mathbf{X})\right)^2(\frac{\sqrt{u^2+\varepsilon^2}(u^2+\varepsilon^2-\varepsilon^2\cos^2\phi)^{1/2}}{gm})^{-3} \\
&\times(\frac{1}{2}gm\frac{\frac{u}{\varepsilon}\left(2\frac{u^2+\varepsilon^2}{\varepsilon^2}-\cos^2\phi\right)}{\varepsilon(u^2+\varepsilon^2)(\frac{u^2+\varepsilon^2}{\varepsilon^2}-\cos^2\phi)^2}) + \mathcal{O}(e^2) \\
&= \frac{\sqrt{b^2+\varepsilon^2}}{gm}\sqrt{b^2+\varepsilon^2\sin^2\phi}\,\delta W(\mathbf{X}_0) \\
&-\frac{1}{2}\frac{(\varepsilon^2\cos^2\phi-2\varepsilon^2-2u^2)u}{gm^2\left(\frac{u^2+\varepsilon^2-\varepsilon^2\cos^2\phi}{u^2+\varepsilon^2}\right)^{1/2}}(\delta W(\mathbf{X}_0))^2 + \mathcal{O}(e^2)
\end{aligned} \tag{3.66}
$$

3.4 Geoid computation procedure

The *generalised Bruns formula* enables us to convert the disturbing gravity potential calculated on the surface of reference equipotential surface $W(\mathbf{X}) = w_0$ into incremental geoidal height $h(\mathbf{X})$. This formula also gives a procedure for geoid determination, which is shown schematically in *Figure 3-2*, and is described bellow.

1. Determine the reference equipotential surface $W(\mathbf{X}) = w_0$.

2. Determine the actual potential $w(\mathbf{X})$ on the surface of the reference equipotential surface $W(\mathbf{X}) = w_0$ (via e.g. (i) remove, harmonic downward continuation, and restore process, or by (ii) a global geopotential model).

3. Subtract the gravity potential $w(\mathbf{X})$ from w_0 to produce the disturbing gravity potential $\delta W(\mathbf{X})$.

4. Convert the disturbing potential into geoidal height by using a version of Bruns formula, which complies with the reference equipotential surface $W(\mathbf{X}) = w_0$.

As case studies, here we are going to use this geoid determination procedure for computing a global geoid. Namely, by applying ellipsoidal harmonic expansion of degree/order 360/360 that carries only global scale information about geoid.

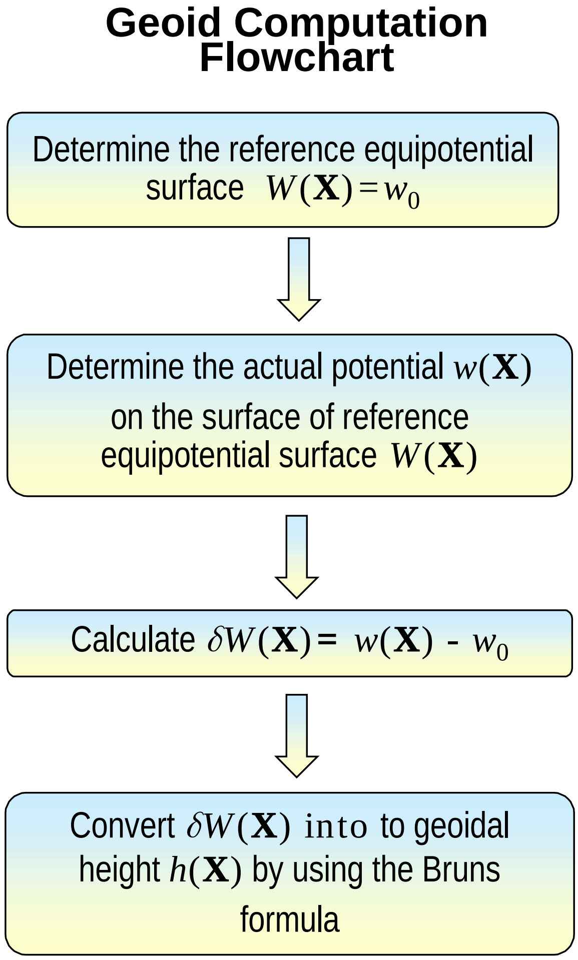

Figure 3-2: Geoid determination procedure, inferred from implicit function theorem and generalised Bruns formula.

3.5 Application of ellipsoidal harmonics

Application of spherical harmonic expansion to geoid determination problem has already been extensively studied, see for example *R. Rapp* (1971, 1992, and 1997), *D. Smith* (1998), and *C. Tscherning et al.* (1983). However, if we use spherical harmonic expansion to determine the gravitational potential on the surface of a reference equipotential surface of the type ellipsoid of rotation, the compus! It is for the reason that the spherical harmonic expansion is valid outside an international sphere $\mathbb{S}^2_{R=a}$ $\mathbb{S}^2_{R=a}$, which is inside the international reference ellipsoid $\mathbb{E}^2_{a,b}$. International reference ellipsoid $\mathbb{E}^2_{a,b}$ is actually is in global geoid computation, where we need to compute the gravity potential values.

In contrast, the ellipsoidal harmonic expansion is valid outside a rotational ellipsoid $\mathbb{E}^2_{a*,b*}$, which can be selected in a way to be smaller than international ellipsoid $\mathbb{E}^2_{a,b}$. Therefore, there will be no problem with the validity of the ellipsoidal harmonic expansion on the surface of the reference ellipsoid $\mathbb{E}^2_{a,b}$.

Given the ellipsoidal harmonics u_{nm}, and angular velocity of the earth ω, a model gravity field for the external gravity field of the earth can be derived from ellipsoidal harmonic expansion (say up to degree/order 360/360).

$$W(\mathbf{X}) = \frac{gm}{a^*}\sum_{n=0}^{360}\sum_{m=-n}^{+n} u_{nm}\frac{Q^*_{n|m|}(\frac{u}{\varepsilon})}{Q^*_{n|m|}(\frac{b}{\varepsilon})}e_{nm}(\lambda,\phi) + \frac{1}{2}\omega^2(u^2+\varepsilon^2)\cos^2\phi \tag{3.67}$$

where in (3.67) gm=3 986 004.415E+8 m^3/s^2 is the product of *Newton* gravitational constant by the mass of the earth, $Q^*_{n,|m|}(\frac{u}{\varepsilon})$ stands for numerically stabilised *associated Legendre functions of the second kind*, introduced in Appendix *C*, and $e_{nm}(\lambda,\phi)$ are surface ellipsoidal harmonics.

$$e_{nm}(\lambda,\phi) = P^*_{n|m|}(\sin\phi)\begin{bmatrix}\cos m\lambda & \forall m \geq 0\\ \sin|m|\lambda & \forall m < 0\end{bmatrix} \tag{3.68}$$

The *Equation* (3.67) converges uniformly for the points outside the ellipsoid $\mathbb{E}^2_{a*,b*}$. For the computations that will be offered later in case studies, the semi-major axis, a^* = 6 378 136.3 m, which comes from the identity $R=a$, is used. Where $r=R$ presents the sphere $\mathbb{S}^2_{R=a}$ out of which the spherical harmonic expansion is valid (i.e., converging uniformly). The semi-minor axis b^*=6 356 751.647m is determined by introducing linear eccentricity ε = 521 853.580 (m) of *WGD 2000* of *E. Grafarend and A. Ardalan* (1999b) in tide free permanent tide system.

Furthermore, since we want to present the geoidal undulations with respect to the reference ellipsoid $\mathbb{E}^2_{a,b}$ of World *Geodetic Datum 2000*, we adopt a reference gravity field, with ellipsoidal equipotential surfaces. The problem of geoid determination is then the problem of determination of the shape function of geoid with respect to the reference equipotential surface of WGD2000.

for the points $\mathbf{X} \in \mathbb{E}^2_{a,b}$, on the surface of reference equipotential surface, $W(\mathbf{X}) = w_0$, the disturbing potential $\delta W(\mathbf{X}) = w_0 - W(\mathbf{X})$ can be computed as follows.

$$
\begin{aligned}
\delta W(\mathbf{X}) &= w_0 - W(\mathbf{X}) \\
&= \sum_{n=0}^{360} \sum_{m=-n}^{+n} u_{nm} \frac{Q^*_{n|m|}(\frac{u}{\varepsilon})}{Q^*_{n|m|}(\frac{b}{\varepsilon})} e_{nm}(\lambda, \phi) \\
&+ \frac{1}{2}\omega^2(u^2 + \varepsilon^2)\cos^2\phi
\end{aligned}
\tag{3.69}
$$

According to geoid computation flowchart (*Figure 3-2*) to compute the geoidal height $h(\mathbf{X})$, one needs to supply the actual potential on the surface of reference equipotential surface. $\delta W(\mathbf{X})$ can consequently be converted to incremental heights /geoidal heights/ via Bruns formula.

3.5.1 Case study 1; geoid computations in the area bounded by *l*=7.5°-10.5° E and *b*=47.5°-50° N

Using the ellipsoidal harmonic expansion of external gravitational field of the earth and nonlinear ellipsoidal Bruns formula (*Section 1.7*, formula (1.80)) the geoidal undulations of 28800 points on a grid of $((\Delta L = 1.5') \times (\Delta B = 1'))$ in the area bounded by *Gauss ellipsoidal* coordinates *L*=7.5°-10.5° E and *B*=47.5°-50° N are computed. The calculated geoidal undulations $h = h(\lambda, \phi, w_0)$ for some few first points are given in *Table 3-5*. Column 1 and 2 of the *Table 3-5* presenting the *Gauss ellipsoidal coordinates* of the computation points which are first transferred into *Jacobi ellipsoidal coordinates* and then used for the computation of the geoidal undulations of column 3.

Table 3-5: Geoidal heights of a few grid points in the area bounded by geographical coordinates *L*=7.5°-10.5° E and *B*=47.5°-50° N. Based on ellipsoidal harmonic expansion in tide free, w_0= 62 636 855.80m^2/s^2 (*E. Grafarend and A. Ardalan*, 1997); reference ellipsoid *WGD 2000 a* = 6 378 136.572m, *b* = 6 356 751.920m in tide free system (*E. Grafarend and A. Ardalan*, 1999b).

L (degree)	*B* (degree)	$h = h(\lambda, \phi, w_0)$ (m)
7.0125E+000	4.99916666E+001	4.929709E+001
7.5125E+000	4.99916666E+001	4.936084E+001
8.0125E+000	4.99916666E+001	4.902617E+001
8.5125E+000	4.99916666E+001	4.866512E+001
9.0125E+000	4.99916666E+001	4.877286E+001

9.5125E+000	4.99916666E+001	4.895994E+001
1.0012E+001	4.99916666E+001	4.856834E+001
1.0512E+001	4.99916666E+001	4.791010E+001
7.0125E+000	4.96583333E+001	4.923508E+001
7.5125E+000	4.96583333E+001	4.945663E+001
8.0125E+000	4.96583333E+001	4.899719E+001
8.5125E+000	4.96583333E+001	4.854704E+001
9.0125E+000	4.96583333E+001	4.875500E+001
9.5125E+000	4.96583333E+001	4.911705E+001
1.0012E+001	4.96583333E+001	4.886358E+001

The calculated geoid at the 28800 test points over a 1.5’×1’ grid were compared with the *European Gravimetric Geoid EGG97* made available to us over the same grid. Summary of the statistics of this comparison is given in *Table 3-6*. *Figure 3-3* presents us with a geoid map derived from computed geoidal undulations, in equidistant conic map projection system. *Figure 3-4* presents the difference between our global geoid and *EGG97*. As the *Table 3-6* documents difference between two geoid does not accedes 0.579 m, on average, with a standard deviation of ±0.394 m. This difference is partly due to different reference ellipsoids and permanent tide systems to which the two solutions are referred.

Table 3-6: Statistical summary of the difference *h(Global) – h(EGG97)*.

Statistics of $\Delta h = h(Global) - h(EGG97)$	m
mean	0.579
minimum	–3.726
maximum	4.141
standard deviation	0.394
number of sample points	28 800

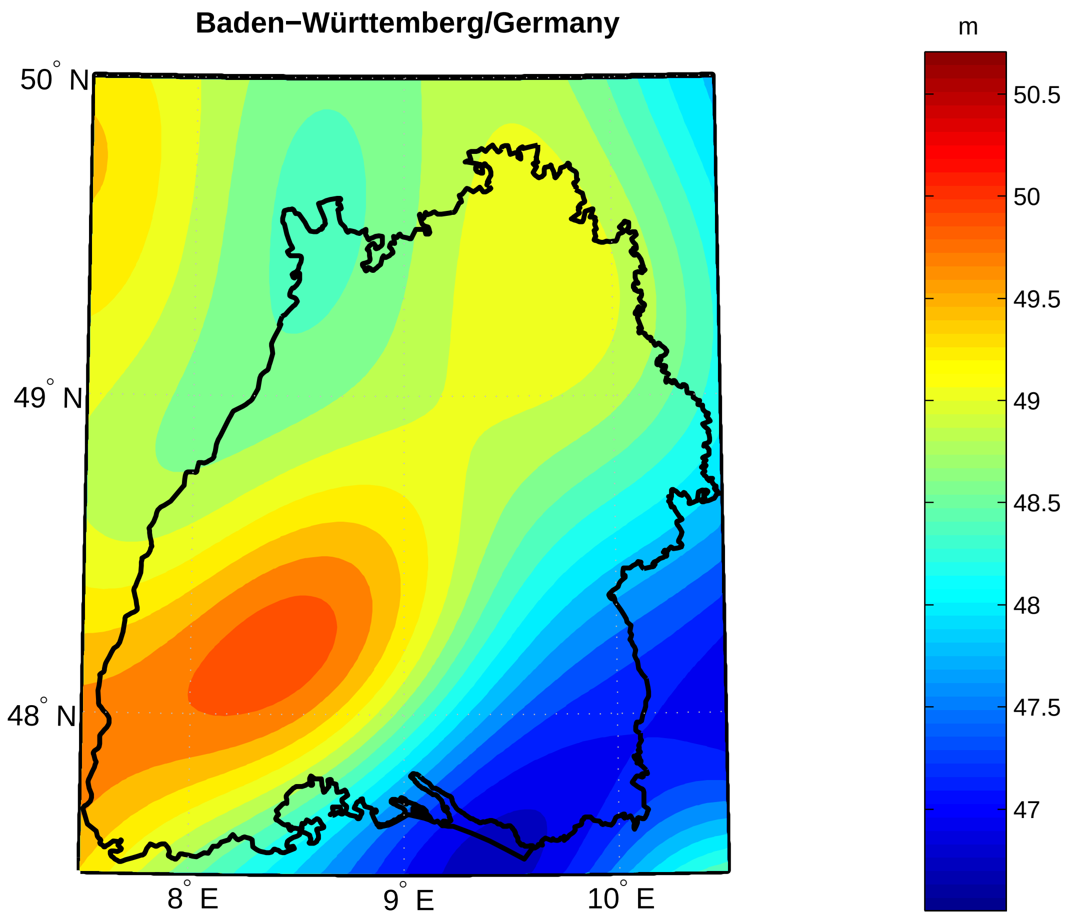

Figure 3-3: Calculated geoid based on ellipsoidal harmonic expansion in tide free system, $w_0 = 62\ 636\ 855.80\ m^2/s^2$ (*E. Grafarend and A. Ardalan*, 1997); reference ellipsoid *WGD2000* $a = 6\ 378\ 136.572$ m, $b = 6\ 356\ 751.920$ m, in tide free system (*E. Grafarend and A. Ardalan*, 1999b).

Map Projection Information:

Equidistant Conic Projection
Standard Parallels: $48^\circ N$ *and* $49^\circ N$
Reference ellipsoid: WGD2000

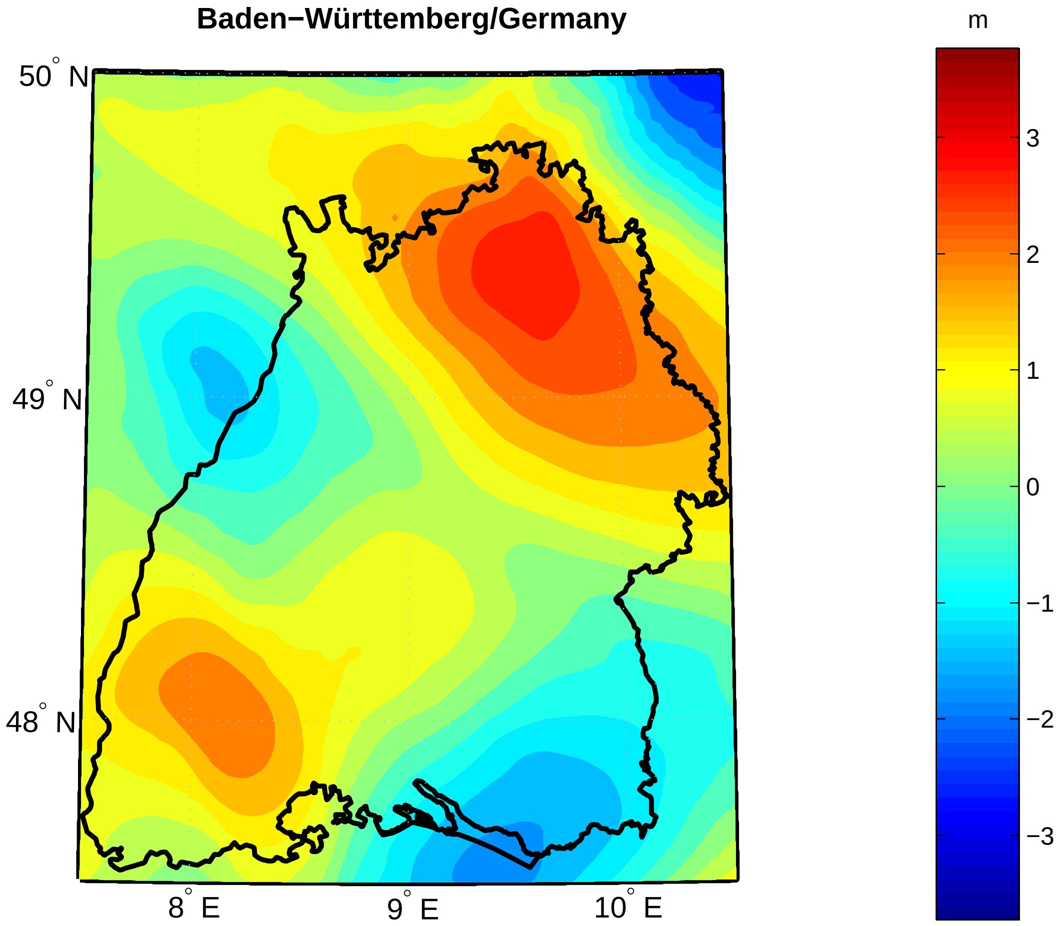

Figure 3-4: Difference between calculated geoid based on ellipsoidal harmonic expansion in tide free system, $w_0 = 62\ 636\ 855.80\, m^2/s^2$ (*E. Grafarend and A. Ardalan*, 1997); reference ellipsoid *WGD2000* $a = 6\ 378\ 136.572$m, $b = 6\ 356\ 751.920$m in tide free system (*E. Grafarend and A. Ardalan*, 1999b) and EGG97 in zero frequency tide system, with respect to ref. ellipsoid *GRS80*.

<u>Map Projection Information:</u>

Equidistant Conic Projection
Standard Parallels: $48^\circ N$ *and* $49^\circ N$
Reference ellipsoid: WGD2000

3.5.2 Case study 2; geoid computation at tide-gauge stations of Baltic Sea level project, third campaign

As the second case study we used 23 tide gauge stations of the Baltic Sea Level Project, third campaign 1997.4. Those stations can be a good benchmark for checking the computed geoid. The orthometric heights of those tide gauge stations are known very accurately by direct sea level observations. Some of the tide gauges have several hundred years of tide gauge observations behind. See *J. Kakkuri* (1995), *J. Kakkuri and M Poutanen* (1997), *M. Poutanen* (1998a, 1998b, 1998c), and *M. Vermeer* (1995) for the state-of-art of the *Baltic Sea Level Project*, and more information on the tide gauge stations. Those tide gauge stations are also equipped with precise GPS observations. *Table 3-7* presents the GPS coordinates of the tide gauge stations in terms of *Cartesian coordinates* in *ITRF 96* reference frame. In the last column of *Table 3-7* are orthometric heights of the tide gauge stations. To provide the *Jacobi ellipsoidal coordinates*, needed for the ellipsoidal harmonic expansion the *Cartesian coordinates* are converted into Jacobi ellipsoidal coordinates given in *Table 3-8*. From the *Cartesian coordinates* the *Gauss ellipsoidal height* of the tide gauge stations with respect to the international ellipsoid *WGD2000*, are computed. The computed *Gauss ellipsoidal heights*, and the known orthometric heights of the tide gauge stations led to, geoidal undulations/ geoidal heights/ of the GPS stations with respect to WGD2000, according to following formula.

$$h(Baltic) \doteq H(GPS) - H_o(Baltic) \tag{3.70}$$

where $H_0(Baltic)$ is *orthometric* height, and $H(GPS)$ *is Gauss ellipsoidal height* of the tide gauge stations. $h(Baltic)$ is the geoidal undulation of the tide gauges with respect to WGD2000. The equation (3.70) is accurate up to the curvature of plumb line, which is neglected here.

Using *ellipsoidal harmonic expansion* and non-linear ellipsoidal *Bruns formula* (see *Section 1.7*, *formula (1.80)*) the global geoidal undulations $h(Global)$ of 23 tide gauge stations of the Baltic Sea Level Project are computed and compared with the GPS derived geoidal undulations $h(Baltic)$. *Table 3-9* presents the results of this comparison. Summary of statistics of the comparison of $h(Global)$ and $h(Baltic)$ is given in *Table 3-10*. By a review of the results of *Table 3-9* and *Table 3-10* we can conclude that on average the global geoidal undulation deviates from that of the Baltic Sea Level project by (–0.0087±0.1780)m, which reflects an impressive consistency between the two sets of geoidal undulations! It is important to note that here, geoidal undulations are referred to the same ellipsoid, namely *WGD2000* (c.f. *Table 3-8*).

Table 3-7: Cartesian coordinates (ITRF 96), and orthometric heights of the GPS stations of the Baltic Sea Level Project, third campaign 1997.4

Station Name	X(m)	Y(m)	Z(m)	Ho (m)
Borkum (Ger)	3770667.9989	446076.4896	5107686.2085	4.501
Degerby (Fin)	2994064.9360	1112559.0570	5502241.3760	2.687
Furuögrund_TG (Swe)	2527022.8721	981957.2890	5753940.9920	10.861
Hamina (Fin)	2795471.2067	1435427.7930	5531682.2031	1.583
Hanko (Fin)	2959210.9709	1254679.1202	5490594.4410	5.031
Helgoland (Ger)	3706044.9443	513713.2151	5148193.4472	4.429
Helsinki (Fin)	2885137.3909	1342710.2301	5509039.1190	6.346
Kemi (Fin)	2397071.5771	1093330.3129	5789108.4470	6.874
Klagshamn (Swe)	3527585.7675	807513.8946	5234549.7020	2.053
Klaipeda (Lit)	3353590.2428	1302063.0141	5249159.4123	28.186
List/Sylt (Ger)	3625339.9221	537853.8704	5202539.0255	4.066
Mäntyluoto (Fin)	2831096.7193	1113102.7637	5587165.0458	2.303
Molas (Lit)	3358793.3811	1294907.4149	5247584.4010	4.554
Ölands N. Udde.(Swe)	3295551.5710	1012564.9063	5348113.6687	4.146
Raahe (Fin)	2494035.0244	1131370.9936	5740955.4096	3.287
Ratan (Swe)	2620087.6160	1000008.2649	5709322.5771	1.433
Spikarna (Swe)	2828573.4638	893623.7288	5627447.0693	1.788
Stockholm (Swe)	3101008.8620	1013021.0372	5462373.3830	11.927
Swinoujscie (Pol)	3649458.3681	927709.9794	5130741.6420	2.184
Ustka (Pol)	3545014.3300	1073939.7720	5174949.9470	1.454
Vaasa (Fin)	2691307.2541	1063691.5238	5664806.3799	0.917
Visby (Swe)	3249304.4375	1073624.8912	5364363.0732	2.014
Warnemuende (Ger)	3658217.6419	783004.6986	5148504.3041	21.171
Ger: Germany, Fin: Finland, Swe: Sweden, Lit: Lithuania, Pol: Poland				

Table 3-8: *Gauss ellipsoidal coordinates* of the GPS stations of the Baltic Sea Level Project, third campaign 1997.4, with respect to the reference ellipsoid *WGD 2000* (a = 6 378 136.572m, b = 6 356 751.920m in tide free system (*E. Grafarend and A. Ardalan*, 1999b))

Station Name	*L (degrees)*	*B (degrees)*	*H (meters)*
Borkum (Ger)	6.74683093901	53.55763277178	45.0936
Degerby (Fin)	20.38446961960	60.03134814035	22.0658
Furuögrund_TG (Swe)	21.23526361253	64.91950300777	33.2520
Hamina (Fin)	27.17974139926	60.56471648855	17.1284
Hanko (Fin)	22.97651236414	59.82267871268	25.2759
Helgoland (Ger)	7.89176332880	54.17483199363	44.0129
Helsinki (Fin)	24.95673461689	60.15367752700	24.5952
Kemi (Fin)	24.51824268792	65.67436132063	26.5358
Klagshamn (Swe)	12.89365547340	55.52231343765	38.3139
Klaipeda (Lit)	21.21917098867	55.75460902512	53.3124
List/Sylt (Ger)	8.43882205649	55.01752680208	45.0711
Mäntyluoto (Fin)	21.46327159076	61.59426465421	21.5889
Molas (Lit)	21.08302585169	55.72978961516	29.7446
Ölands N. Udde.(Swe)	17.07968171596	57.36762447842	31.7890

Raahe (Fin)	24.40050548601	64.64634248642	21.7134
Ratan (Swe)	20.89034421363	63.99155313921	23.1852
Spikarna (Swe)	17.53275165792	62.36354502846	27.5791
Stockholm (Swe)	18.09090355205	59.32233411275	35.5029
Swinoujscie (Pol)	14.26276599922	53.90788921075	38.2916
Ustka (Pol)	16.85385420680	54.58768995293	34.2772
Vaasa (Fin)	21.56553183992	63.09523250642	19.5395
Visby (Swe)	18.28442477487	57.63926280096	27.5974
Warnemuende (Ger)	12.08129300662	54.17940436931	60.0204

Ger: Germany, Fin: Finland, Swe: Sweden, Lit: Lithuania, Pol: Poland

Table 3-9: Geodetic longitude *L*, geodetic latitude *B*, geoidal undulations $h(Global)$, and difference Δh between the calculated geoidal heights and that of the tide gauge stations of the Baltic Sea Level Project, Third campaign 1997.4. Based on ellipsoidal harmonic expansion in tide free tide system, w_0= 62 636 855.80 m^2/s^2 (*E. Grafarend and A. Ardalan*, 1997); reference ellipsoid *WGD 2000 a* = 6 378 136.572m, *b* = 6 356 751.920m in tide free permanent tide system (*E. Grafarend and A. Ardalan*, 1999b).

Station Name	*L (degrees)*	*B (degrees)*	*h(Global)*	Δh
Borkum (Ger)	6.746830939	53.557632771	40.6641	0.0715
Degerby (Fin)	20.384469619	60.031348140	19.0611	–0.3177
Furuögrund_TG (Swe)	21.235263612	64.919503007	22.4812	0.0902
Hamina (Fin)	27.179741399	60.564716488	15.6561	0.1106
Hanko (Fin)	22.976512364	59.822678712	20.0588	–0.1861
Helgoland (Ger)	7.891763328	54.174831993	39.6885	0.1046
Helsinki (Fin)	24.956734616	60.153677527	18.3905	0.1413
Kemi (Fin)	24.518242687	65.674361320	19.6509	–0.0109
Klagshamn (Swe)	12.893655473	55.522313437	36.1692	–0.0917
Klaipeda (Lit)	21.219170988	55.754609025	25.1266	0.0002
List/Sylt (Ger)	8.438822056	55.017526802	41.1569	0.1518
Mäntyluoto (Fin)	21.463271590	61.594264654	19.3383	0.0524
Molas (Lit)	21.083025851	55.729789615	25.1627	–0.0279
Ölands N. Udde.(Swe)	17.079681715	57.367624478	27.9441	0.3010
Raahe (Fin)	24.400505486	64.646342486	18.2121	–0.2143
Ratan (Swe)	20.890344213	63.991553139	21.9975	0.2453
Spikarna (Swe)	17.532751657	62.363545028	25.8072	0.0161
Stockholm (Swe)	18.090903552	59.322334112	23.6516	0.0757
Swinoujscie (Pol)	14.262765999	53.907889210	36.0640	–0.0436
Ustka (Pol)	16.853854206	54.587689952	32.3518	–0.4714
Vaasa (Fin)	21.565531839	63.095232506	18.5281	–0.0944
Visby (Swe)	18.284424774	57.639262800	25.6559	0.0725
Warnemuende (Ger)	12.081293006	54.179404369	38.6743	–0.1751

Ger: Germany, Fin: Finland, Swe: Sweden, Lit: Lithuania, Pol: Poland

Table 3-10: Statistical Summary of the difference *h(Global) – h(Baltic)*, geoid at tide-gauge stations of Baltic Sea Level Project and calculated geoid based on ellipsoidal harmonic expansion.

Statistics of $\Delta h = h(Global) - h(Baltic)$	m
mean	–0.0087
minimum	–0.4714
maximum	0.3010

standard deviation	0.1780
number of sample points	23

3.6 Conclusions

Form the results of the two case studies we can conclude that our rigours method for global geoid determination based on the application of *implicit function theorem,* and *nonlinear ellipsoidal harmonic expansion* is accuracy up to *decimetre* level! In summary, the achievements are as follows.

- *Surface normal mapping* of geoid with respect to the reference ellipsoid $\mathbb{E}^2_{a,b}$, based on the *implicit function theorem*, through (3.14).
- *Generalised Bruns formula* (3.42) as a realisation of implicit function theorem.
- A general procedure for geoid computation, according to *Figure 3-2*, based on *generalised Bruns formula* and *implicit function theorem.*
- A *rigorous* method for *global geoid computation* based on *ellipsoidal harmonic expansion* and *nonlinear ellipsoidal Bruns formula*.

At the end, we have to emphasise that:

1. Spherical harmonic expansion *should not* be used for determination of gravitational potential on the surface of a reference ellipsoid, namely for the reason that the reference ellipsoid $\mathbb{E}^2_{a,b}$ is partially *inside* the sphere $\mathbb{S}^2_{R=a}$. The spherical harmonic expansion is only valid at the *outer* space of $\mathbb{S}^2_{R=a}$.
2. The traditional Bruns formula $\delta r = \frac{\delta w(R)}{GM\,/\,R^2}$ is only true for a geoid mapping with respect to the *reference sphere* $\mathbb{S}^2_R$. Therefore *cannot* be used to presents the geoidal heights with respect to the reference ellipsoid $\mathbb{E}^2_{a,b}$.

4 Minimum distance mapping of the surface of the earth onto the telluroid

In this chapter, a potential type *Molodensky telluroid* based upon minimum distance mapping is formulated. With respect to the *reference potential* field of *Somigliana-Pizzetti type* it is shown that a point-wise minimum distance mapping of the topographical surface of the Earth onto the telluroid surface, constrained to the *gauge* $W(P) = u(p)$, leads to a system of four nonlinear normal equations. Those normal equations are solved by a fast *Newton-Raphson* iteration.

M. S. Molodensky in 1945 introduced the *telluroid* as the best *analytical* representation of the irregular surface of the Earth. See for example *M. S. Molodensky* 1945, 1948, and 1960. Given the placement vector of a point in *geometry space*, for instance by GPS, and reference gravity potential in *gravity space*, the telluroid can be uniquely defined by a properly chosen projection. For instance, astronomical longitude / astronomical latitude (spherical coordinates in gravity space) at the topographic point can be defined to be equal with the reference longitude / reference latitude (spherical coordinates in reference gravity space) at the telluroid point in order to establish an *isoparametric mapping* of the telluroid. Such a mapping procedure as was experienced by *A. Bode and E. Grafarend* (1982) for a reference gravity field generated by (i) the zero order coefficient of a spherical harmonic expansion of the gravitational potential *and* (ii) the centrifugal potential. Here we aim at an *ellipsoidal telluroid mapping*, which is set-up as following:

Let us suppose that the *Jacobi* ellipsoidal / spheroidal coordinates $\{\lambda_p, \phi_p, u_p\}$ of a point p on the topographic surface of the Earth be given. Such a triple which parameterise the geometry space can be obtained by converting the GPS positions into Jacobi ellipsoidal coordinates. In addition, let as assume that the actual gravity potential w_p, which parameterise the gravity space, at p be *given* by means of *gravimetric levelling*. Now the problem of mapping the points on the surface of the earth onto *Molodensky telluroid* can be stated as follows. *Find* the point P on the telluroid whose reference gravity potential W_P is equal to the actual gravity potential w_p at point p under a *mapping procedure*. The telluroid derived from such a definition is called a *potential telluroid* in contrast to case where the *modulus of gravity acceleration/ gravity intensity* at p is considered equal to the modulus of *reference gravity acceleration* at P . In such a case, we would refer to a *gravity telluroid*, a proposal which was materialised by *E. Grafarend* (1978a, 1978b, and 1980). Here we have chosen the reference gravity field of a level ellipsoid which coincides with the *World Geodetic Datum* (*E. Grafarend and A. Ardalan* 1999) and is known as *Somigliana-Pizzetti gravity potential field*. (*C. Somigliana* 1930, and *P. Pizzetti* 1894). We may therefore call the related telluroid, "the *Somigliana-Pizzetti telluroid*". Besides, our mapping procedure is based on minimisation of the distance between the points on the surface of the earth and potential telluroid. Therefore, we are going to formulate a *minimum distance Somigliana-Pizzetti potential telluroid*.

In the next section, we introduce the minimum distance mapping of a topographic point p to the corresponding point P on the telluroid with a proper potential gauge. In particular / we present the *Somigliana-Pizzetti gravity potential field*, both in an explicit form and in a form of ellipsoidal orthonormal functions. Then we present two case studies, namely we compute the *Somigliana-Pizzetti potential telluroid* and *quasi-geoid* from position and potential data for the state Baden Württemberg and *East Germany*.

4.1 Formulation of the problem

In the introduction, we presented a general definition for the mapping of the Earth surface onto the telluroid. Here we are going to specify that definition to the *Somigliana-Pizzetti* reference field and the minimum distance mapping. We call such a mapping, *minimum-distance Somigliana-Pizzetti telluroid-mapping*.

The *minimum-distance Somigliana-Pizzetti telluroid-mapping* can be defined as follows:

> Given the actual gravity potential value $w(\mathbf{x})$, at the known point $p(\mathbf{x})$ on the surface of the Earth $\mathbb{M}_h^2$,
> find the point $P(\mathbf{X})$ such that;
> (i) the reference *Somigliana-Pizzetti* potential field $W_P = W(\mathbf{X})$ at point $P(\mathbf{X}) \in \mathbb{M}_H^2$ be equal to the actual potential at $p(\mathbf{x}) \in \mathbb{M}_h^2$,

(ii) the point $P(\mathbf{X}) \in \mathbb{M}_H^2$ be at minimum (*Euclidean*) distance from the point $p(\mathbf{x}) \in \mathbb{M}_h^2$.on the physical surface of the Earth.

By definition, the surface $\mathbb{M}_H^2$ is called *Molodensky telluroid*, or specifically in our case, the *Molodensky telluroid of Somigliana-Pizzetti type*. *Figure 4-1* shows the point $p(\mathbf{x})$ on the Earth's surface and its minimum distance projection $P(\mathbf{X})$ onto telluroid.

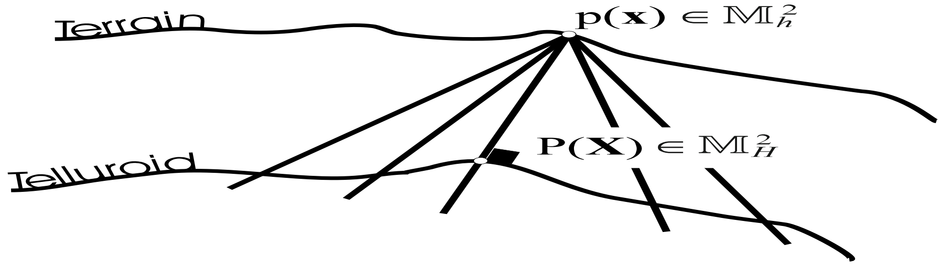

Figure 4-1: Point $p(\mathbf{x}) \in \mathbb{M}_h^2$ on the topographic surface and its minimum distance mapping onto the surface of telluroid $\mathbb{M}_H^2$: Various projections, but one orthogonal projection of $\mathbb{M}_h^2$ onto $\mathbb{M}_H^2$.

Analytically we can formulate the above stated optimisation problem by minimising the *constraint Lagrangean*:

$$\begin{aligned}\mathbb{L}(x_1,x_2,x_3,x_4) &:= \|\mathbf{x}-\mathbf{X}\|^2 + x_4(W_P - w_p) \\ &= [x - X(x_1,x_2,x_3)]^2 + [y - Y(x_1,x_2,x_3)]^2 \\ &\quad +[z - Z(x_1,x_2,x_3)]^2 + x_4[W(x_1,x_2,x_3) - w_p] \\ &= \min_{x_1,x_2,x_3,x_4}\end{aligned} \tag{4.1}$$

$$(\hat{x}_1,\hat{x}_2,\hat{x}_3,\hat{x}_4) = \min_{x_1,x_2,x_3,x_4} \mathbb{L}(x_1,x_2,x_3,x_4) \tag{4.2}$$

where $(x_1,x_2,x_3) = (\Lambda,\Phi,U)$ are *Jacobi ellipsoidal coordinates of the point* $P \sim \mathbf{X} \in \mathbb{M}_H^2$ on the telluroid, and x_4 is the unknown *Lagrange multiplier*. For the definition of *Jacobi ellipsoidal coordinates* we refer to *Appendix A*.

Since the most suitable coordinate system for formulation of the *Somigliana-Pizzetti field* is ellipsoidal coordinates, we formulate our minimisation problem in terms of *Jacobi ellipsoidal coordinates* $\{\lambda,\phi,u\}$. *Definition 4-1* presents the *Somigliana-Pizzetti* gravity potential field in terms of *Jacobi- ellipsoidal* coordinates $\{\lambda,\phi,u\}$. *Somigliana-Pizzetti* field has been developed by *P. Pizzetti* (1894) and *C. Somigliana* (1930) and recently extensively analysed by *E. Grafarend and A. Ardalan* (1999) in functional analytical terms.

Definition 4-1: *Somigliana-Pizzetti* field as the gravity potential field of an ellipsoid of revolution.

(i) Explicit form in terms of fundamental geodetic parameters $\{a, b, W_0, \Omega\}$ (according to E. Grafarend and A. Ardalan 1999)

$$
\begin{aligned}
W(\phi, u) = \quad & (W_0 - \frac{1}{3}\Omega^2 a^2)\frac{\cot^{-1}(\frac{u}{\varepsilon})}{\cot^{-1}(\frac{b}{\varepsilon})} + \frac{1}{3}\Omega^2(u^2 + \varepsilon^2) \\
& + \left\{ \frac{1}{3\sqrt{5}}\Omega^2 a^2 \frac{(3\frac{u^2}{\varepsilon^2} + 1)\cot^{-1}(\frac{u}{\varepsilon}) - 3\frac{u}{\varepsilon}}{(3\frac{b^2}{\varepsilon^2} + 1)\cot^{-1}(\frac{b}{\varepsilon}) - 3\frac{b}{\varepsilon}} - \right. \\
& \left. - \frac{1}{3\sqrt{5}}\Omega^2(u^2 + \varepsilon^2) \right\} \frac{\sqrt{5}}{2}(3\sin^2\phi - 1).
\end{aligned} \tag{4.3}
$$

(ii) Explicit form in terms of fundamental geodetic parameters $\{a, b, GM, \Omega\}$

$$
\begin{aligned}
W(\phi, u) = & \frac{GM}{\varepsilon}\operatorname{arc}\cot(\frac{u}{\varepsilon}) \\
& + \frac{1}{6}\Omega^2 a^2 \frac{(3\frac{u^2}{\varepsilon^2} + 1)\operatorname{arc}\cot(\frac{u}{\varepsilon}) - 3\frac{u}{\varepsilon}}{(3\frac{b^2}{\varepsilon^2} + 1)\operatorname{arc}\cot(\frac{b}{\varepsilon}) - 3\frac{b}{\varepsilon}}(3\sin^2\phi - 1) \\
& + \frac{1}{2}\Omega^2(u^2 + \varepsilon^2)\cos^2\phi
\end{aligned} \tag{4.4}
$$

(iii) Functional analytical form (according to Grafarend et al. 1999)

$$
\begin{aligned}
W(\phi, u) = & \frac{GM}{\varepsilon}Q^*_{00}(\frac{u}{\varepsilon})e_{00} \\
& + \frac{1}{3}\Omega^2 a^2 \frac{2P^*_2(\frac{u}{\varepsilon})Q^*_{00}(\frac{u}{\varepsilon}) - 3P^*_1(\frac{u}{\varepsilon})}{2P^*_2(\frac{b}{\varepsilon})Q^*_{00}(\frac{b}{\varepsilon}) - 3P^*_1(\frac{b}{\varepsilon})}\frac{1}{\sqrt{5}}e_{20}(\phi) \\
& + \frac{2}{9}\Omega^2\varepsilon^2[1 + P^*_2(\frac{u}{\varepsilon})]e_{00} \\
& - \frac{2}{9\sqrt{5}}\Omega^2\varepsilon^2[1 + P^*_2(\frac{u}{\varepsilon})]e_{20}(\phi)
\end{aligned} \tag{4.5}
$$

Where $e_{n0}(\lambda, \phi) = P^*_{n0}(\sin\phi)$ are orthogonal base functions of Legendre type, $P^*_{nm}(\sin\phi)$, and $P^*_{nm}(\frac{u}{\varepsilon})$ are normalised associated Legendre functions of the first kind, and $Q^*_{nm}(\frac{u}{\varepsilon})$ are associated Legendre functions of the second kind as shortly reviewed by *Table 4-1*.□

Table 4-1: Normalised associated Legendre functions of the first kind $P^*_{nm}(\sin\phi)$, $P^*_{nm}(\frac{u}{\varepsilon})$, and the associated Legendre functions of the second kind $Q^*_{nm}(\frac{u}{\varepsilon})$

n	m	$P^*_{nm}(\sin\phi)$	$P^*_{nm}(\frac{u}{\varepsilon})$	$Q^*_{nm}(\frac{u}{\varepsilon})$
0	0	1	1	$\operatorname{arc}\cot(\frac{u}{\varepsilon})$
1	0	$\sqrt{3}\sin\phi$	$\frac{u}{\varepsilon}$	$1-\frac{u}{\varepsilon}\operatorname{arc}\cot(\frac{u}{\varepsilon})$
2	0	$\frac{\sqrt{5}}{2}(3\sin^2\phi-1)$	$\frac{1}{2}(3\frac{u^2}{\varepsilon^2}+1)$	$\frac{1}{2}[(3\frac{u^2}{\varepsilon^2}+1)\operatorname{arc}\cot(\frac{u}{\varepsilon})-3\frac{u}{\varepsilon}]$
n	m	$\frac{\sqrt{4n^2-1}}{\sqrt{n^2-m^2}}\sin\phi\, P^*_{n-1,m}$ $-\frac{\sqrt{(2n+1)(n+m-1)(n-m-1)}}{\sqrt{(n^2-m^2)(2n-3)}}$ $\times P^*_{n-2,m}\ \forall n\in[3,\infty)$ and $m\in[0,n-2]$	$\frac{(n+m)!}{\pi n!}$ $\times\int_0^{\pi}(\frac{u}{\varepsilon}+\sqrt{\frac{u^2}{\varepsilon^2}+1}\cos\tau)^n$ $\times\cos m\tau\, d\tau$	$(-1)^m\frac{2^n(n+m)!\,m!}{(n-m)!(2m)!}$ $\times\int_0^{\infty}\frac{\sinh^{2m}\tau\, d\tau}{(\frac{u}{\varepsilon}+\sqrt{\frac{u^2}{\varepsilon^2}+1}\cosh\tau)^{n+m+1}}$

Using the forward transformation relations of *Jacobi ellipsoidal coordinates* $\{\lambda,\phi,u\}$ into *Cartesian coordinates* $\{x,y,z\}$ as summarised in *Appendix A* (*Section A.1.3*, *page 212*) the functional $\mathbb{L}(x_1,x_2,x_3,x_4)$ can be written as

$$\begin{aligned}\mathbb{L}(\Lambda_P,\Phi_{P2},U_P,\lambda):=&(x_p-\sqrt{U_P{}^2+\varepsilon^2}\cos\Phi_P\cos\Lambda_P)^2\\&+(y_p-\sqrt{U_P{}^2+\varepsilon^2}\cos\Phi_P\sin\Lambda_P)^2\\&+(z_p+U_P\sin\Phi_P)^2\\&+x_4(W(\Phi_P,U_P)-w_p)\end{aligned}\tag{4.6}$$

or

$$\begin{aligned}\mathbb{L}(x_1,x_2,x_3,x_4):=&(x_p-\sqrt{x_3{}^2+\varepsilon^2}\cos x_2\cos x_1)^2\\&+(y_p-\sqrt{x_3{}^2+\varepsilon^2}\cos x_2\sin x_1)^2\\&+(z_p+x_3\sin x_2)^2\\&+x_4(W(x_2,x_3)-w_p)\end{aligned}\tag{4.7}$$

where $\{x_1,x_2,x_3\}$ are unknown *Jacobi ellipsoidal coordinates* of the point $P(\Lambda,\Phi,U)=P(x_1,x_2,x_3)$ on the telluroid ($P(\mathbf{X})\in\mathbb{M}_H^2$), $W(\Phi,U)=W(x_2,x_3)$ corresponds to *Somigliana-Pizzetti* potential field at point $P(\Lambda,\Phi,U)\in\mathbb{M}_H^2$ (c.f. Equation (4.4)), and w_p refers to actual gravity potential at point $p\{x,y,z\}$ on the surface of the Earth.

The functional $\mathbb{L}(x_1,x_2,x_3,x_4)$ is minimal if and only if following two conditions hold:

$$f_1:=\frac{\partial\mathbb{L}}{\partial x_1}(\hat{x}_1,\hat{x}_2,\hat{x}_3,\hat{x}_4)=2\sqrt{\hat{x}_3^2+\varepsilon^2}\cos\hat{x}_2(x_p\sin\hat{x}_1-y_p\cos\hat{x}_1)=0$$

$$\begin{aligned}f_2:=\frac{\partial\mathbb{L}}{\partial x_2}(\hat{x}_1,\hat{x}_2,\hat{x}_3,\hat{x}_4)=&\,2(x_p-\sqrt{\hat{x}_3^2+\varepsilon^2}\cos\hat{x}_2\cos\hat{x}_1)\sqrt{\hat{x}_3^2+\varepsilon^2}\sin\hat{x}_2\cos\hat{x}_1\\&+2(y_p-\sqrt{\hat{x}_3^2+\varepsilon^2}\cos\hat{x}_2\sin\hat{x}_1)\sqrt{\hat{x}_3^2+\varepsilon^2}\sin\hat{x}_2\sin\hat{x}_1\\&-2(z_p-\hat{x}_3\sin\hat{x}_2)\hat{x}_3\cos\hat{x}_2+\hat{x}_4(\frac{\partial W}{\partial x_2}(\hat{x}_2,\hat{x}_3))=0\end{aligned}$$

$$f_3 := \frac{\partial \mathbb{L}}{\partial x_3}(\hat{x}_1,\hat{x}_2,\hat{x}_3,\hat{x}_4) = -2\frac{(x_p - \sqrt{\hat{x}_3{}^2+\varepsilon^2}\cos\hat{x}_2\cos\hat{x}_1)\hat{x}_3\cos\hat{x}_2\cos\hat{x}_1}{\sqrt{\hat{x}_3{}^2+\varepsilon^2}}$$
$$-2\frac{(y_p - \sqrt{\hat{x}_3{}^2+\varepsilon^2}\cos\hat{x}_2\sin\hat{x}_1)\hat{x}_3\cos\hat{x}_2\sin\hat{x}_1}{\sqrt{\hat{x}_3{}^2+\varepsilon^2}}$$
$$-2(z_p - \hat{x}_3\sin\hat{x}_2)\sin\hat{x}_2 + \hat{x}_4\frac{\partial W}{\partial x_3}(\hat{x}_2,\hat{x}_3) = 0$$
$$f_4 := \frac{\partial \mathbb{L}}{\partial x_4}(\hat{x}_1,\hat{x}_2,\hat{x}_3,\hat{x}_4) = W(\hat{x}_2,\hat{x}_3) - w_p = 0 \tag{4.8}$$

$$\frac{\partial^2 L}{\partial x_i \partial x_j}(\hat{x}_1,\hat{x}_2,\hat{x}_3) \text{ be positive-semi-definite for } i,j \in \{1,2,3\} \tag{4.9}$$

Partial derivatives $\partial W / \partial\phi$ and $\partial W / \partial u$ of (4.8) can be readily derive from (4.4) as follows

$$\frac{\partial W}{\partial \phi} = \frac{\partial W}{\partial x_2} = a^2\Omega^2\frac{(3x_3{}^2+\varepsilon^2)\operatorname{arc}\cot(\frac{x_3}{\varepsilon}) - 3x_3\varepsilon}{[(3b^2+\varepsilon^2)\operatorname{arc}\cot(\frac{b}{\varepsilon}) - b\varepsilon]}\sin x_2\cos x_2 \tag{4.10}$$
$$-\Omega^2(x_3{}^2+\varepsilon^2)\sin x_2\cos x_2$$

$$\frac{\partial W}{\partial u} = \frac{\partial W}{\partial x_3} = -\frac{GM}{x_3{}^2+\varepsilon^2}$$
$$-\frac{1}{3}\Omega^2 a^2\frac{\varepsilon(3x_3{}^2+2\varepsilon^2) + (-3x_3{}^3 - 3x_3\varepsilon^2)\operatorname{arc}\cot(\frac{x_3}{\varepsilon})}{(x_3{}^2+\varepsilon^2)[\operatorname{arc}\cot(\frac{b}{\varepsilon})\varepsilon^2 + (-3\varepsilon + 3\operatorname{arc}\cot(\frac{b}{\varepsilon})b)b]}(3\sin^2 x_2 - 1)$$
$$+\Omega^2 x_3\cos^2 x_2 \tag{4.11}$$

Equations (4.8) build up the variational equations of the optimisation problem (4.2). System of equations (4.8) is a nonlinear system and its *Brook Taylor* expansion reads

$$\mathbf{F}(\mathbf{x}) = \mathbf{F}(\mathbf{x}_0) + \frac{1}{1!}\mathbf{F}'(\mathbf{x}_0)(\mathbf{x}-\mathbf{x}_0)$$
$$+\frac{1}{2!}\mathbf{F}''(\mathbf{x}_0)(\mathbf{x}-\mathbf{x}_0)\otimes(\mathbf{x}-\mathbf{x}_0) + \mathcal{O}_3\left((\mathbf{x}-\mathbf{x}_0)\otimes(\mathbf{x}-\mathbf{x}_0)\otimes(\mathbf{x}-\mathbf{x}_0)\right)$$
$$= \mathbf{F}_0 + \mathbf{J}_0(\mathbf{x}-\mathbf{x}_0) + \frac{1}{2}\mathbf{H}_0(\mathbf{x}-\mathbf{x}_0)\otimes(\mathbf{x}-\mathbf{x}_0) + \mathcal{O}_3 \tag{4.12}$$

where

$$\mathbf{F} = \begin{bmatrix} f_1(x_1,x_2,x_3,x_4) \\ f_2(x_1,x_2,x_3,x_4) \\ f_3(x_1,x_2,x_3,x_4) \\ f_4(x_1,x_2,x_3,x_4) \end{bmatrix}, \ \mathbf{x} = \begin{bmatrix} x_1 \\ x_2 \\ x_3 \\ x_4 \end{bmatrix}, \ \mathbf{F}' := \mathbf{J} = \begin{bmatrix} \frac{\partial f_1}{\partial x_1} & \frac{\partial f_1}{\partial x_2} & \frac{\partial f_1}{\partial x_3} & \frac{\partial f_1}{\partial x_4} \\ \frac{\partial f_2}{\partial x_1} & \frac{\partial f_2}{\partial x_2} & \frac{\partial f_2}{\partial x_3} & \frac{\partial f_2}{\partial x_4} \\ \frac{\partial f_3}{\partial x_1} & \frac{\partial f_3}{\partial x_2} & \frac{\partial f_3}{\partial x_3} & \frac{\partial f_3}{\partial x_4} \\ \frac{\partial f_4}{\partial x_1} & \frac{\partial f_4}{\partial x_2} & \frac{\partial f_4}{\partial x_3} & \frac{\partial f_4}{\partial x_4} \end{bmatrix},$$

$\mathbf{F}'' := \mathbf{H} =$

$$\begin{bmatrix}
\frac{\partial^2 f_1}{\partial x_1^2} & \frac{\partial^2 f_1}{\partial x_1 x_2} & \frac{\partial^2 f_1}{\partial x_1 x_3} & \frac{\partial^2 f_1}{\partial x_1 x_4} & \frac{\partial^2 f_1}{\partial x_2 x_1} & \frac{\partial^2 f_1}{\partial x_2^2} & \frac{\partial^2 f_1}{\partial x_2 x_3} & \frac{\partial^2 f_1}{\partial x_2 x_4} & \frac{\partial^2 f_1}{\partial x_3 x_1} & \frac{\partial^2 f_1}{\partial x_3 x_2} & \frac{\partial^2 f_1}{\partial x_3^2} & \frac{\partial^2 f_1}{\partial x_3 x_4} & \frac{\partial^2 f_1}{\partial x_4 x_1} & \frac{\partial^2 f_1}{\partial x_4 x_2} & \frac{\partial^2 f_1}{\partial x_4 x_3} & \frac{\partial^2 f_1}{\partial x_4^2} \\
\frac{\partial^2 f_2}{\partial x_1^2} & \frac{\partial^2 f_2}{\partial x_1 x_2} & \frac{\partial^2 f_2}{\partial x_1 x_3} & \frac{\partial^2 f_2}{\partial x_1 x_4} & \frac{\partial^2 f_2}{\partial x_2 x_1} & \frac{\partial^2 f_2}{\partial x_2^2} & \frac{\partial^2 f_2}{\partial x_2 x_3} & \frac{\partial^2 f_2}{\partial x_2 x_4} & \frac{\partial^2 f_2}{\partial x_3 x_1} & \frac{\partial^2 f_2}{\partial x_3 x_2} & \frac{\partial^2 f_2}{\partial x_3^2} & \frac{\partial^2 f_2}{\partial x_3 x_4} & \frac{\partial^2 f_2}{\partial x_4 x_1} & \frac{\partial^2 f_2}{\partial x_4 x_2} & \frac{\partial^2 f_2}{\partial x_4 x_3} & \frac{\partial^2 f_2}{\partial x_4^2} \\
\frac{\partial^2 f_3}{\partial x_1^2} & \frac{\partial^2 f_3}{\partial x_1 x_2} & \frac{\partial^2 f_3}{\partial x_1 x_3} & \frac{\partial^2 f_3}{\partial x_1 x_4} & \frac{\partial^2 f_3}{\partial x_2 x_1} & \frac{\partial^2 f_3}{\partial x_2^2} & \frac{\partial^2 f_3}{\partial x_2 x_3} & \frac{\partial^2 f_3}{\partial x_2 x_4} & \frac{\partial^2 f_3}{\partial x_3 x_1} & \frac{\partial^2 f_3}{\partial x_3 x_2} & \frac{\partial^2 f_3}{\partial x_3^2} & \frac{\partial^2 f_3}{\partial x_3 x_4} & \frac{\partial^2 f_3}{\partial x_4 x_1} & \frac{\partial^2 f_3}{\partial x_4 x_2} & \frac{\partial^2 f_3}{\partial x_4 x_3} & \frac{\partial^2 f_3}{\partial x_4^2} \\
\frac{\partial^2 f_4}{\partial x_1^2} & \frac{\partial^2 f_4}{\partial x_1 x_2} & \frac{\partial^2 f_4}{\partial x_1 x_3} & \frac{\partial^2 f_4}{\partial x_1 x_4} & \frac{\partial^2 f_4}{\partial x_2 x_1} & \frac{\partial^2 f_4}{\partial x_2^2} & \frac{\partial^2 f_4}{\partial x_2 x_3} & \frac{\partial^2 f_4}{\partial x_2 x_4} & \frac{\partial^2 f_4}{\partial x_3 x_1} & \frac{\partial^2 f_4}{\partial x_3 x_2} & \frac{\partial^2 f_4}{\partial x_3^2} & \frac{\partial^2 f_4}{\partial x_3 x_4} & \frac{\partial^2 f_4}{\partial x_4 x_1} & \frac{\partial^2 f_4}{\partial x_4 x_2} & \frac{\partial^2 f_4}{\partial x_4 x_3} & \frac{\partial^2 f_4}{\partial x_4^2}
\end{bmatrix}$$

and $\otimes$ is the symbol for the *Kronecker* tensor product.

Newton iteration solution (*X. Chen et al.* (1997)) can be performed by the n-sequence

$$\mathbf{x} - \mathbf{x}_0 = \Delta\mathbf{x} = \mathbf{J}_0^{-1}(\mathbf{F} - \mathbf{F}_0) = (\mathbf{J}(\mathbf{x}_0))^{-1}(\mathbf{F} - \mathbf{F}_0) \qquad (4.13)$$

$$\mathbf{x} - \mathbf{x}_0 = +\mathbf{J}^{-1}(\mathbf{F} - \mathbf{F}_0)$$

$$\Rightarrow \mathbf{x}_1 = \mathbf{x}_0 + \mathbf{J}_0^{-1}(\mathbf{F} - \mathbf{F}_0) \qquad (4.14)$$

$$\Rightarrow \mathbf{x}_2 = \mathbf{x}_1 + \mathbf{J}_1^{-1}(\mathbf{F} - \mathbf{F}_1) \qquad (4.15)$$

$$\Rightarrow \quad \cdots \quad \Rightarrow \mathbf{x}_n = \mathbf{x}_{n-1} \qquad (4.16)$$

where Jacobean matrix of linearized form of the variational equations (4.13) is as follows.

$$\mathbf{J} := \begin{bmatrix} \frac{\partial f_1}{\partial x_1} & \frac{\partial f_1}{\partial x_2} & \frac{\partial f_1}{\partial x_3} & \frac{\partial f_1}{\partial x_4} \\ \frac{\partial f_2}{\partial x_1} & \frac{\partial f_2}{\partial x_2} & \frac{\partial f_2}{\partial x_3} & \frac{\partial f_2}{\partial x_4} \\ \frac{\partial f_3}{\partial x_1} & \frac{\partial f_3}{\partial x_2} & \frac{\partial f_3}{\partial x_3} & \frac{\partial f_3}{\partial x_4} \\ \frac{\partial f_4}{\partial x_1} & \frac{\partial f_4}{\partial x_2} & \frac{\partial f_4}{\partial x_3} & \frac{\partial f_4}{\partial x_4} \end{bmatrix} \qquad (4.17)$$

$$\frac{\partial f_1}{\partial x_1} = 2(x_3{}^2 + \varepsilon^2)^{1/2} \cos x_2 (x_p \cos x_1 + y_p \sin x_1)$$

$$\frac{\partial f_1}{\partial x_2} = 2(x_3{}^2 + \varepsilon^2)^{1/2} \sin x_2 (- x_p \sin x_1 + y_p \cos x_1)$$

$$\frac{\partial f_1}{\partial x_3} = -2 \frac{\cos x_2 (- x_p \sin x_1 + y_p \cos x_1) x_3}{(x_3{}^2 + \varepsilon^2)^{1/2}}$$

$$\frac{\partial f_1}{\partial x_4} = 0$$

$$\frac{\partial f_2}{\partial x_1} = -2(x_3{}^2 + \varepsilon^2)^{1/2} \sin x_2 (x_p \sin\ x_1 - y_p \cos x_1)$$

$$\frac{\partial f_2}{\partial x_2} = 2(x_3{}^2 + \varepsilon^2)(\sin x_2)^2 (\cos x_1)^2 + 2(x_p - (x_3{}^2 + \varepsilon^2)^{1/2} \cos(x_2) \cos x_1)(x_3{}^2$$
$$+ \varepsilon^2)^{1/2} \cos x_2 \cos x_1 + 2(x_3{}^2 + \varepsilon^2)(\sin x_2)^2 (\sin x_1)^2 + 2(y_p$$
$$-(x_3{}^2 + \varepsilon^2)^{1/2} \cos x_2 \sin x_1)(x_3{}^2 + \varepsilon^2)^{1/2} \cos x_2 \sin x_1 + 2x_3{}^2 (\cos x_2)^2$$
$$+2(z_p - x_3 \sin x_2) x_3 \sin x_2 + x_4 (\Omega^2 a^2 ((3x_3{}^2/\varepsilon^2 + 1) \mathrm{acot}(x_3/\varepsilon)$$
$$-3x_3/\varepsilon)/((3b^2/\varepsilon^2 + 1) \mathrm{acot}(b/\varepsilon) - 3b/\varepsilon) \cos(x_2)^2 - \Omega^2 a^2 ((3x_3{}^2/\varepsilon^2$$
$$+1) \mathrm{acot}(x_3/\varepsilon) - 3x_3/\varepsilon)/((3b^2/\varepsilon^2 + 1) \mathrm{acot}(b/\varepsilon) - 3b/\varepsilon)(\sin x_2)^2$$
$$+\Omega^2 (\mathrm{x}_3{}^2 + \varepsilon^2)(\sin x_2)^2 - \Omega^2 (x_3{}^2 + \varepsilon^2)(\cos x_2)^2)$$

$$\frac{\partial f_2}{\partial x_3} = -2 \sin x_2 (\cos x_1)^2 \cos(x_2) x_3 + 2(x_p - (x_3{}^2 + \varepsilon^2)^{1/2} \cos x_2 \cos x_1)$$
$$/(x_3{}^2 + \varepsilon^2)^{1/2} \sin x_2 \cos x_1 (x_3) - 2 \sin x_2 (\sin x_1)^2 \cos x_2 (x_3)$$
$$+2(y_p - (x_3{}^2 + \varepsilon^2)^{1/2} \cos x_2 \sin x_1)/(x_3{}^2 + \varepsilon^2)^{1/2} \sin x_2 \sin x_1 (x_3)$$
$$+2x_3 \cos x_2 \sin x_2 - 2(z_p - x_3 \sin x_2) \cos x_2 + x_4 (\Omega^2 a^2 (6x_3 \varepsilon^2 \mathrm{acot}(x_3/\varepsilon)$$
$$-(3x_3{}^2/\varepsilon^2 + 1)/\varepsilon/(1 + x_3{}^2/\varepsilon^2) - 3/\varepsilon)/((3b^2/\varepsilon^2 + 1) \mathrm{acot}(b/\varepsilon) - 3b/\varepsilon) \sin x_2 \cos x_2$$
$$-2\Omega^2 x_3 \cos x_2 \sin x_2)$$

$$\frac{\partial f_2}{\partial x_4} = \Omega^2 a^2 ((3x_3{}^2/\varepsilon^2 + 1) \mathrm{acot}(x_3/\varepsilon) - 3x_3/\varepsilon)/((3b^2/\varepsilon^2 + 1) \mathrm{acot}(b/\varepsilon)$$
$$-3b/\varepsilon) \sin x_2 \cos x_2 - \Omega^2 (x_3{}^2 + \varepsilon^2) \cos x_2 \sin x_2$$

$$\frac{\partial f_3}{\partial x_1} = 2 \frac{\cos x_2 x_3 (\sin x_1 x_p - \cos x_1 y_p)}{(x_3{}^2 + \varepsilon^2)^{1/2}}$$

$$\frac{\partial f_3}{\partial x_2} = -2\sin x_2(\cos x_1)^2\cos(x_2)x_3+2(x_p-(x_3{}^2$$
$$+\varepsilon^2)^{1/2}\cos x_2\cos x_1)/(x_3{}^2+\varepsilon^2)^{1/2}\sin x_2\cos(x_1)x_3$$
$$-2\sin x_2(\sin x_1)^2\cos(x_2)x_3+2(y_p-(x_3{}^2+\varepsilon^2)^{1/2}\cos x_2\sin x_1)/(x_3{}^2$$
$$+\varepsilon^2)^{1/2}\sin x_2\sin(x_1)x_3+2x_3\cos x_2\sin x_2-2(z_p$$
$$-x_3\sin x_2\cos x_2+x_4(\Omega^2a^2(6x_3/\varepsilon^2\,\mathrm{acot}(x_3/\varepsilon)$$
$$-(3x_3{}^2/\varepsilon^2+1)/\varepsilon/(1+x_3{}^2/\varepsilon^2)-3/\varepsilon)/((3b^2/\varepsilon^2$$
$$+1)\mathrm{acot}(b/\varepsilon)-3b/\varepsilon)\sin x_2\cos x_2-2\Omega^2x_3\cos x_2\sin x_2)$$

$$\frac{\partial f_3}{\partial x_3}=2/(x_3{}^2+\varepsilon^2)(\cos x_2)^2(\cos x_1)^2x_3{}^2+2(x_p$$
$$-(x_3{}^2+\varepsilon^2)^{1/2}\cos x_2\cos x_1)/(x_3{}^2+\varepsilon^2)^{3/2}\cos x_2\cos(x_1)x_3{}^2$$
$$-2(x_p-(x_3{}^2+\varepsilon^2)^{1/2}\cos x_2\cos x_1)/(x_3{}^2+\varepsilon^2)^{1/2}\cos x_2\cos x_1$$
$$+2/(x_3{}^2+\varepsilon^2)(\cos x_2)^2\sin(x_1)^2x_3{}^2+2(y_p-(x_3{}^2$$
$$+\varepsilon^2)^{1/2}\cos x_2\sin x_1)/(x_3{}^2+\varepsilon^2)^{3/2}\cos x_2\sin x_1x_3{}^2$$
$$-2(y_p-(x_3{}^2+\varepsilon^2)^{1/2}\cos x_2\sin x_1)/(x_3{}^2+\varepsilon^2)^{1/2}\cos x_2\sin x_1$$
$$+2\sin x_2{}^2+x_4(2\mathrm{GM}/\varepsilon^4/(1+x_3{}^2/\varepsilon^2)^2x_3+1/6\Omega^2a^2(6/\varepsilon^2\,\mathrm{acot}(x_3/\varepsilon)$$
$$-12x_3/\varepsilon^3/(1+x_3{}^2/\varepsilon^2)+2(3x_3{}^2/\varepsilon^2+1)/\varepsilon^3/(1+x_3{}^2/\varepsilon^2)^2x_3)$$
$$/((3b^2/\varepsilon^2+1)\mathrm{acot}(b/\varepsilon)-3b/\varepsilon)(3\sin(x_2)^2-1)+\Omega^2(\cos x_2)^2)$$
$$\frac{\partial f_3}{\partial x_4} = -\mathrm{GM}/\varepsilon^2/(1+x_3{}^2/\varepsilon^2)+1/6\Omega^2a^2(6x_3/\varepsilon^2\,\mathrm{acot}(x_3/\varepsilon)$$
$$-(3x_3{}^2/\varepsilon^2+1)/\varepsilon/(1+x_3{}^2/\varepsilon^2)-3/\varepsilon)/((3b^2/\varepsilon^2+1)\mathrm{acot}(b/\varepsilon)$$
$$-3b/\varepsilon)(3(\sin x_2)^2-1)+\Omega^2x_3(\cos x_2)^2$$
$$\frac{\partial f_4}{\partial x_1}=0$$
$$\frac{\partial f_4}{\partial x_2}=\Omega^2a^2((3x_3{}^2/\varepsilon^2+1)\mathrm{acot}(x_3/\varepsilon)-3x_3/\varepsilon)/((3b^2/\varepsilon^2+1)\mathrm{acot}(b/\varepsilon)$$
$$-3b/\varepsilon)\sin x_2\cos x_2-\Omega^2(x_3{}^2+\varepsilon^2)\cos(x_2)\sin(x_2)$$
$$\frac{\partial f_4}{\partial x_3} = -\mathrm{GM}/\varepsilon^2/(1+x_3{}^2/\varepsilon^2)+1/6\Omega^2a^2(6x_3/\varepsilon^2\,\mathrm{acot}(x_3/\varepsilon)$$
$$-(3x_3{}^2/\varepsilon^2+1)/\varepsilon/(1+x_3{}^2/\varepsilon^2)-3/\varepsilon)/((3b^2/\varepsilon^2+1)\mathrm{acot}(b/\varepsilon)-3b/\varepsilon)(3(\sin x_2)^2$$
$$-1)+\Omega^2x_3(\cos x_2)^2$$
$$\frac{\partial f_4}{\partial x_4}=0$$

The solution set $(\hat{x}_1, \hat{x}_2, \hat{x}_3, \hat{x}_4)$ derived from final step of *Newton iteration* (4.16) provides the necessary condition (4.8) of a minimal solution. This extremal solution is minimal if condition (4.9) is also satisfied. Indeed, we must show that *Hesse matrix* $\mathbf{H}_{\mathbb{L}}$ of second derivatives is *positive semi-definite*, i.e. the characteristic polynomials of $|\mathbf{H}_{\mathbb{L}} - \lambda \mathbf{I}| = 0$ are all *non-negative*. The *Hesse matrix* $\mathbf{H}_{\mathbb{L}}$ of second derivatives is given in *Appendix E*. We proved the *positive-definiteness* of the *Hesse-matrix* $H_{\mathbb{L}}$ of second derivatives by a numerical test.

4.2 Case study 1: Quasi-geoid map of Baden-Württemberg

Here, we shall present the results of the minimum distance mapping of the *physical surface of the earth* $\mathbb{M}_h^2$ onto the *Somigliana-Pizzetti telluroid* $\mathbb{M}_H^2$ for 157 GPS stations in the state Baden-Württemberg/Germany. *Table 4-2* shows the first ten GPS points of the GPS file of Baden-Württemberg. The coordinates are given in terms of *Gauss ellipsoidal coordinates* $\{l, b, h\}$ with respect to the GRS80 reference ellipsoid. This set of points constitute the Baden-Württemberg part (BWREF) of the German GPS network (DREF) which itself is part to European GPS network (EUREF).

Table 4-2: Part of the GPS file of the state Baden-Württemberg/Germany

Point ID Number	Longitude (l_P) (deg)	Latitude (b_P) (deg)	Ellipsoidal height (h_P) (m)	Geopotential Number (m^2/s^2)
621707001	8.62383367	49.71395228	218.6128	2148.9295
631805402	8.81299339	49.60717789	587.0355	5785.3299
632000110	9.06549094	49.65066941	590.7425	5811.1345
632107425	9.21517069	49.65909479	234.5042	2305.4354
632302808	9.57513953	49.67395950	379.2613	3733.6137
632400308	9.80809056	49.64845024	412.8049	4058.8965
641400308	8.15923636	49.59699675	349.7134	3434.9047
641600108	8.47034288	49.59000986	136.4937	1339.6896
641701308	8.62851323	49.52709190	143.9359	1415.1545
642100208	9.25086269	49.55034041	523.2340	5160.5154

The *Gauss ellipsoidal coordinates* $\{l, b, h\}$ of 157 GPS stations are converted to *Jacobi* ellipsoidal coordinates $\{\lambda, \phi, u\}$ according to forward transformation equations (A.47)-(A.49). *Table 4-3* presents the *Jacobi* ellipsoidal coordinates of the sample stations of *Table 4-2*.

Table 4-3: Transferred *Jacobi* ellipsoidal coordinates $\{\lambda, \phi, u\}_p$ of *Table 4-2*

Point ID Number	λ_p	ϕ_p	u_p
621707001	9.617432869327	49.60898966016	6356968.4504330
631805402	9.549475653403	49.60842348799	6356966.7368298
632000110	9.552776702951	49.61342803807	6356955.3539607
632107425	9.518509890067	49.66515664873	6356940.4330151
632302808	9.584526828221	49.60509389361	6356960.5466633
632400308	9.535064264303	49.62428053013	6356953.7623961
641400308	9.526483136723	49.63746430741	6356947.9810204
641600108	9.525534139567	49.64979432997	6356958.1832061
641701308	9.512823290742	49.65372897068	6356948.4890495
642100208	9.544545338174	49.62132133267	6356961.9798826

Newton Raphson iteration solution of the normal equations (4.8) led to point-wise *telluroid mapping* of all GPS stations in the state of *Baden-Württemberg*. A portion of the results for first ten GPS stations is presented in *Table 4-4*. Columns 2-4 are referring to *Jacobi* ellipsoidal coordinates of telluroid projection points. Column 5 presents the difference between u component of the GPS stations and their telluroid projection. Finally, column 6 shows the projection of $u_p - U_p$ along the unit vector $\mathbf{E}_u$. The geometrical height $H = (u - U_p)\sqrt{G_{33}}$ presents the separation between the surface of the earth and *Molodensky telluroid*, specifically the minimum distance mapping of the physical surface of the earth to the *Somigliana-Pizzetti* telluroid. If we consider H as the height above the *reference ellipsoid*, by definition, we have a presentation of the *quasi-geoid*. *Figure 4-2* is the result of the *minimum distance mapping* described here for *Baden-Württemberg* in the form of a *quasi-geoid* map.

Finally, the calculated quasi-geoid is compared with new *European Gravimetric Quasi-Geoid* (*EGG97*) (*H. Denker and W. Torge*, 1998). The summary of statistics of this comparison is given in *Table 4-4*.

Table 4-4: Telluroid mapping of the sample GPS stations of *Table 4-2*

Point ID Number	Λ_P	Φ_P	U_P	$u_P - U_P$	$(u - U_P)\sqrt{G}$ (m)
621707001	8.623833	49.61901	6356923.6746	47.10590	47.0396
631805402	8.812993	49.51218	6357295.0294	44.69613	44.6330
632000110	9.065490	49.55569	6357297.6868	45.74952	45.6850
632107425	9.215170	49.56412	6356939.7418	46.95325	46.8870
632302808	9.575139	49.57899	6357085.8037	45.85237	45.7878
632400308	9.808090	49.55347	6357118.3259	46.92168	46.8555
641400308	8.159236	49.50199	6357054.1765	47.89158	47.8239
641600108	8.470342	49.49500	6356840.8091	47.73767	47.6702
641701308	8.628513	49.43205	6356848.6787	47.32132	47.2542
642100208	9.250862	49.45531	6357231.6235	44.21203	44.1494

Table 4-5: Statistics of the comparison between calculated height anomalies at 157 GPS station in Baden-Württemberg and EGG97

Statistics of $N_{EGG97} - \zeta$	(m)
Mean	0.995
Std	1.322
Max	7.402
Min	–0.921
number of sample points	157

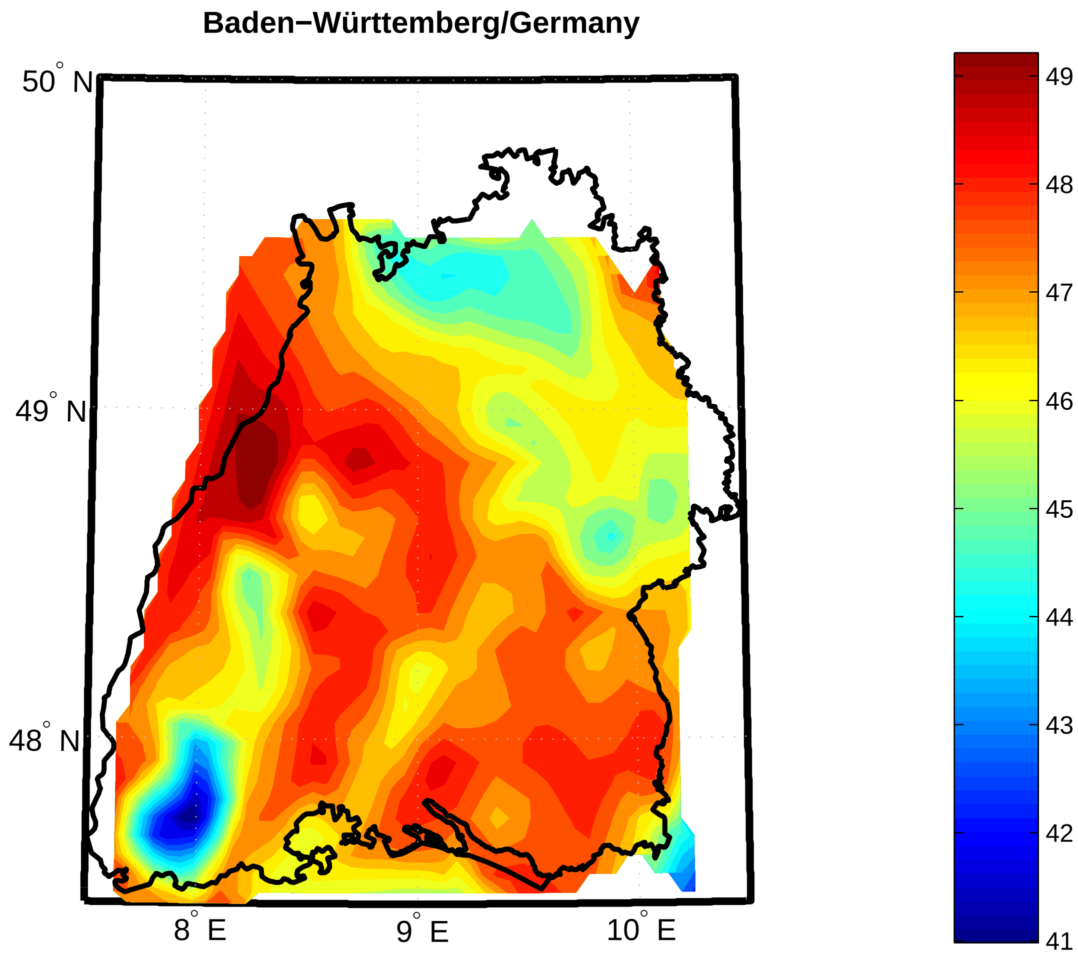

Figure 4-2: Quasi-geoid map of Baden-Württemberg, based on the minimum-distance mapping of the physical surface of the earth to the *Somigliana-Pizzetti* telluroid.

Range of variations: 40.653-49.722m.

Map Projection Information:
Equidistant Conic Projection
Standard Parallels: $48^\circ N$ *and* $49^\circ N$
Reference ellipsoid: WGD2000

4.2.1 Remarks and conclusions

From a review of *Table 4-2 to Table 4-5* the following conclusions can be made: (i) $\{\Lambda_P, \Phi_P\}$ of the telluroid point *P* is very close to $\{\lambda_p, \phi_p\}$ of point *p* on the surface of the earth. This reveals the fact that the minimum distance mapping of the physical surface of the earth to the *Somigliana-Pizzetti* telluroid is very close to the mapping along the coordinate line of *u*. (ii) The calculated quasi-geoid for GPS station based on minimum distance mapping of the physical surface of the earth to the *Somigliana-Pizzetti* deviates from *EGG97* by (0.995 ± 1.322778)(m) on average. This difference can be mainly due to the interpolations process involved in providing the GPS stations with geopotential numbers. Indeed, since the present GPS stations of *Baden-Württemberg* are not identical with the first order level stations, where we have the geopotential numbers, such an interpolation is unavoidable. However, the present results, which are based on a very simple interpolation process, are indicating the minimum distance mapping of the physical surface of the earth to the *Somigliana-Pizzetti* telluroid is an optimal method in quasi-geoid calculations. This is especially valid if the GPS stations are identical with first order levelling stations, which we recommend for the future national GPS campaigns.

4.3 Case study 2: Quasi-geoid map of East Germany

Next, we shall present the results of the minimum distance mapping of the *physical surface of the earth* $\mathbb{M}_h^2$ onto the *Somigliana-Pizzetti telluroid* $\mathbb{M}_H^2$ for 196 GPS stations in eastern part of Germany. *Figure 4-3* shows the geographical distribution of the GPS stations while *Table 4-6* lists the first ten GPS records of the GPS file of East Germany. The coordinates are given in terms of *Gauss ellipsoidal coordinates* $\{l, b, h\}$ with respect to the GRS80 reference ellipsoid.

Table 4-6: Part of the GPS file of the East Germany

Longitude (l_p) (deg)	Latitude (b_p) (deg)	Ellipsoidal height (h_p) (m)	Geopotential Number (m^2/s^2)
13.4363	54.6772	82.295	455.75
13.6433	54.5136	68.192	318.76
12.5016	54.4716	39.663	21.20
13.0076	54.4256	48.669	115.93
13.4252	54.4172	92.697	553.89
13.2909	54.3508	42.444	58.39
12.7371	54.2981	50.352	127.90
13.6586	54.2971	101.363	641.58
13.0796	54.2511	55.762	185.67
12.4053	54.2495	40.304	23.93

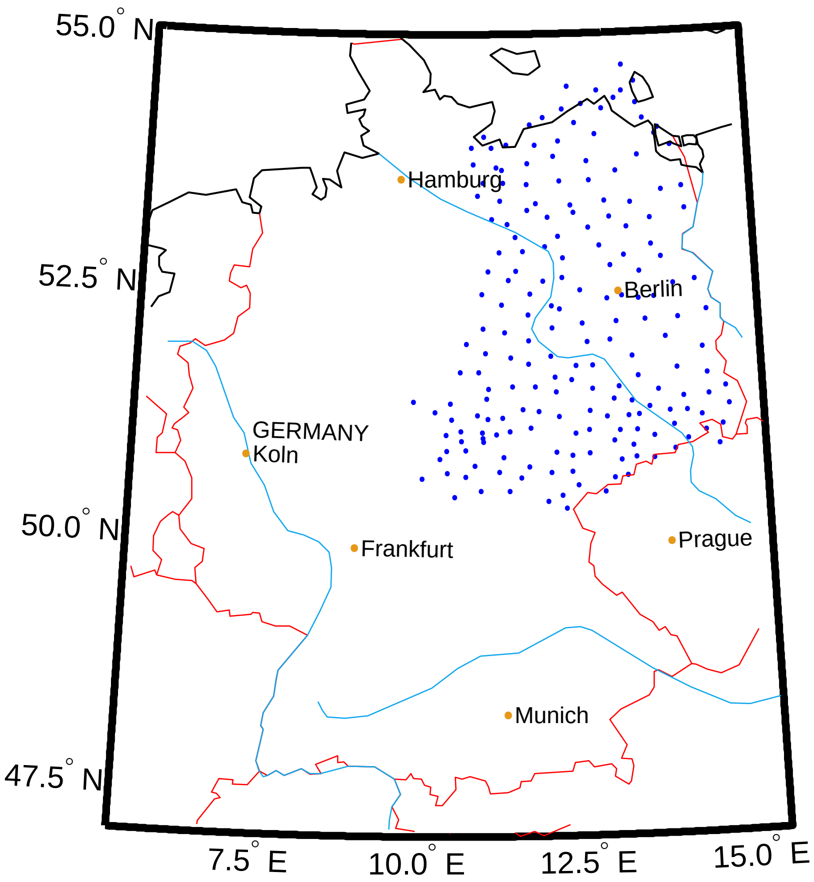

Figure 4-3: The 196 GPS stations in East Germany.

<u>Map Projection Information:</u>
Equidistant Conic Projection
Standard Parallels: 50° *N and* 52.5° *N*
Reference ellipsoid: WGD2000

The *Gauss ellipsoidal coordinates* $\{l,b,h\}$ of 196 GPS stations are converted to *Jacobi* ellipsoidal coordinates $\{\lambda,\phi,u\}$ according to forward transformation equations (A.47)-(A.49). *Table 4-7* presents the *Jacobi* ellipsoidal coordinates of the sample stations of *Table 4-6*.

Table 4-7: Transferred *Jacobi* ellipsoidal coordinates $\{\lambda,\phi,u\}_p$ of *Table 4-6*

λ_p	ϕ_p	u_p
13.4363	54.5864	6356834.2477
13.6433	54.4226	6356820.1294
12.5016	54.3805	6356791.5681
13.0076	54.3345	6356800.5844
13.4252	54.3261	6356844.6627
13.2909	54.2596	6356794.3526
12.7371	54.2069	6356802.2698
13.6586	54.2059	6356853.3393
13.0796	54.1598	6356807.6861
12.4053	54.1582	6356792.2103

Newton Raphson iteration solution of the normal equations led to point-wise *telluroid mapping* of all GPS stations in the state of *East Germany*. The geometrical height $H = (u - U_p)\sqrt{G_{33}}$ presenting the separation between the surface of the earth and *Molodensky telluroid* is considered as the height above the *reference ellipsoid*, to produce the *quasi-geoid map* shown in *Figure 4-4*. A part of *European Gravimetric Quasi-Geoid* (*EGG97*) (*H. Denker and W. Torge*, 1998) covering the East Germany is also shown in *Figure 4-5*.

Finally, the calculated quasi-geoid is compared with new *European Gravimetric Quasi-Geoid* (*EGG97*). The summary of statistics of this comparison is given in *Table 4-8*, while *Figure 4-6* shows the contour map of the difference.

Table 4-8: Statistics of Quasi-geoid height of EGG97 minus the calculated quasi geoid based on minimum distance mapping of physical surface of the earth on to the telluroid at 196 GPS station in eastern part of Germany.

Statistics of $N_{EGG97} - \zeta$	(m)
Mean	-0.05496
Std	0.0389
Max	0.0299
Min	-0.1446
number of sample points	196

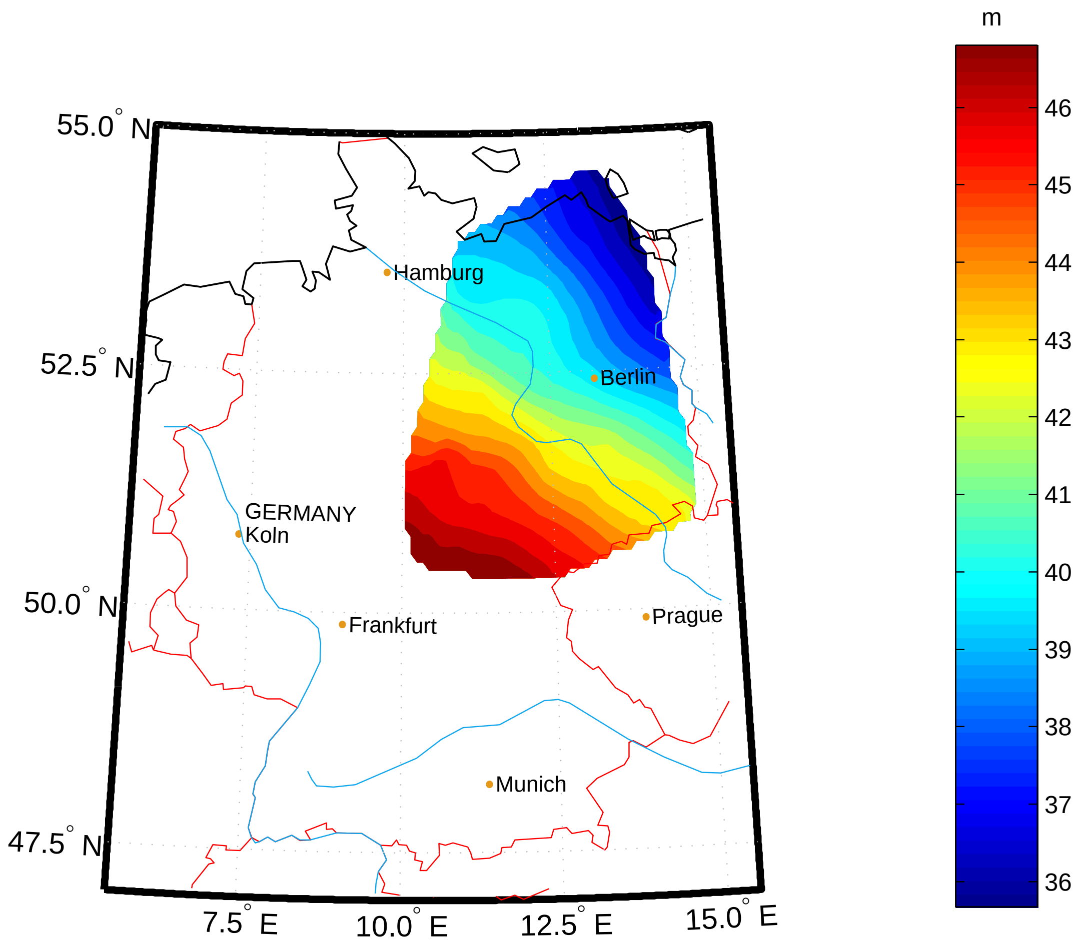

Figure 4-4: Quasi-geoid map of eastern part of Germany, based on the minimum-distance mapping of the physical surface of the earth to the *Somigliana-Pizzetti* telluroid. The quasi-geoid undulations are in the interval [35.609m-47.501m].

<u>Map Projection Information:</u>
Equidistant Conic Projection
Standard Parallels: $50^\circ N$ *and* $52.5^\circ N$
Reference ellipsoid: WGD2000

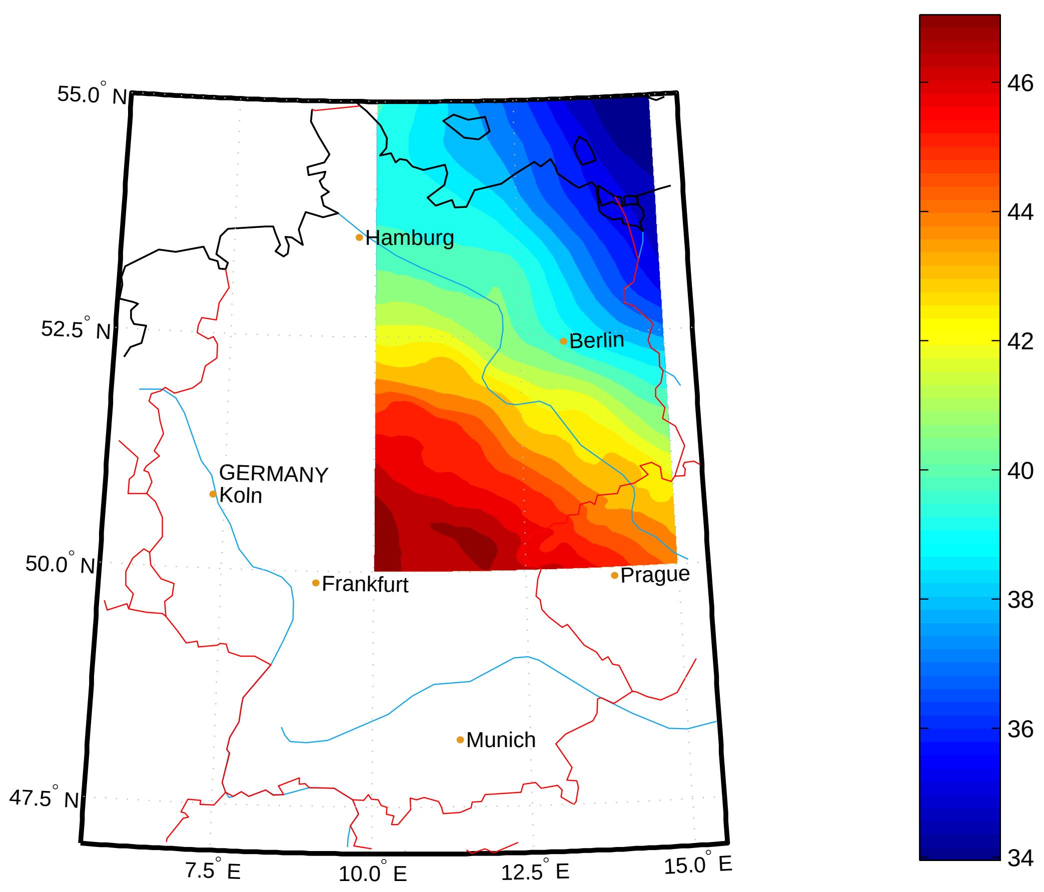

Figure 4-5: Quasi-geoid height of EGG97 over the East Germany.

<u>Map Projection Information:</u>
Equidistant Conic Projection
Standard Parallels: $50^{\circ} N$ *and* $52.5^{\circ} N$
Reference ellipsoid: WGD2000

4.3.1 Conclusions and remarks

A review of *Table 4-6 - Table 4-8* reveals that *(i)* the Jacobi ellipsoidal coordinates $\{\Lambda_P, \Phi_P\}$ of the telluroid point P are very close to *Jacobi* ellipsoidal coordinates $\{\lambda_p, \phi_p\}$ of point p on the surface of the Earth. An indication to the fact that the minimum distance mapping of the physical surface of the Earth to the *Somigliana-Pizzetti* telluroid is very close to the alternative mapping along the coordinate line of u. Such a result can be analysed in *Figure A-1-Figure A-3* in terms of the curvatures of the coordinate line of u. As one can deduce from *Figure A-1-Figure A-3* the curvature of the coordinate line of u approaches zero very fast as one goes away from the centre of the coordinate system. According to *Figure A-2* for $u \geq 2000000m$ coordinate line of u has practically *no curvature*. *(ii)* The calculated quasi-geoid for GPS station based on minimum distance mapping of the physical surface of the Earth to the *Somigliana-Pizzetti* telluroid deviates from *EGG97* by $(-0.05496 \pm 0.0389)m$ on average. Considering the speed of our calculations as compared to classical *Molodensky quasi-geoid* computation, we can concluded that the minimum distance mapping of the physical surface of the Earth to the *Somigliana-Pizzetti* telluroid is an optimal method for quasi-geoid determination. Therefore, we recommend the GPS observations along the first-order levelling stations, for the future national GPS campaigns, which can open the door to the quasi-geoid calculation based on *Somigliana-Pizzetti telluroid mapping*.

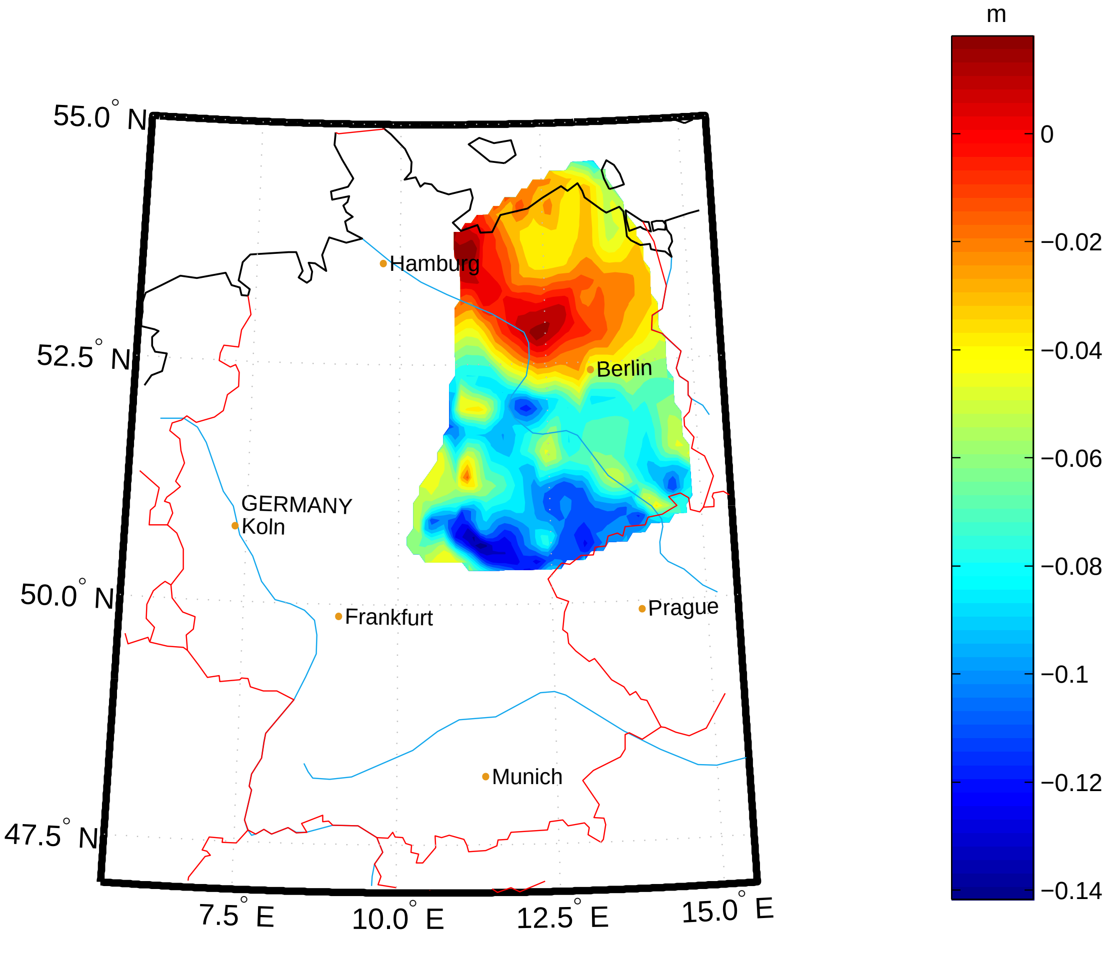

Figure 4-6: Quasi-geoid height of EGG97 minus the calculated quasi geoid based on minimum distance mapping of physical surface of the earth on to the telluroid. The difference is in the range of -0.1446m to 0.0299m.

<u>Map Projection Information:</u>
Equidistant Conic Projection
Standard Parallels: $50^\circ N$ and $52.5^\circ N$
Reference ellipsoid: WGD2000

References:

Abd-Elmotaal H (1995) Attraction of the topographic masses. Bulletin Geodesique 69: 304-307.

Ardalan AA, and Grafarend EW (2000) Reference ellipsoidal gravity potential field and gravity intensity field of degree/order 360/360 (Manual of using ellipsoidal harmonic coefficients "ellipfree.dat" and ellipmean.dat"). http:// www.uni-stuttgart.de / gi / research / index.html # Projects.

Ardalan A. A., and Grafarend E.W. (1999) The first test for $\dot{W}_0$ the time variation of W_0 based on three GPS campaigns of the Baltic Sea Level Project. Reports of the Finnish Geodetic Institute 99:4

Arfken, G. (1985) Hilbert-Schmidt Theory. §16.4 in Mathematical Methods for Physicists, 3rd ed. Orlando, FL: Academic Press, pp. 890-897, 1985.

Baker C. (1977) The numerical treatment of integral equations. Oxford University press 1977.

Baker C., and G. Miller (1982) Treatment of integral equations by numerical methods. Eds., proceedings of the workshop and symposium on the numerical treatment of integral equations, Durham University 19^{th}-29^{th} July 1982.

Bjerhammar A. (1974) Discrete approach to the solution of the boundary value problem in physical geodesy. International School of Geodesy, Eriche 1974.

Bode A., and E. W. Grafarend (1982) The telluroid mapping based on a normal gravity potential including the centrifugal term. Bolletino di Geodesia e Scienze Affini 41: 21-56.

Borkowski K.M. (1989) Accurate algorithms to transform geocentric to geodetic coordinates. Bull. Géod. 63: 50-56.

Bruns H. (1878) Die Figur der Erde. Ein Beitrag zur Europäischen Gradmessung. Publ. kgl. preuß. geod. Inst., Berlin 1878.

Burša M., Kouba J., Radej K., True S. A., Vatrt V., and Vojtíšková M. (1997a) Monitoring geoidal potential on the basis of TOPEX/POSEIDON altimeter data and EGM96. Paper presented at scientific assembly of IAG, Rio de Janeiro 1997.

Burša M., Radej K., Šíma Z., True S. A., and Vatrt V. (1997b) Determination of the geopotential scale factor from TOPEX/POSEIDON satellite altimetry. Stud Geoph et Geod 14: 203-216.

Burša M. (1995a) Primary and derived parameters of common relevance of astronomy, geodesy, and geodynamics. Earth, Moon, and Planets, 69: 51-63.

Burša M. (1995b) Report of special commission SC3§, Fundamental Constants. Travoux de L' Association Internationale de Geodesie. Reports Generaux et Rapports Technique, IAG, 140 rue de Grenelle, 75700 Paris, 1995.

Burša M. (1995c) Geoidal potential free of zero-frequency tidal distortion. Earth, Moon and Planets 71: 59-64.

Burša M., Bystrzycká B., Radej K., and Vatrt V. (1995) Estimation of the accuracy of geopotential models. Studia geoph. et geod. 4:39 365-374.

Chambers, D.P., Tapley B.D. and Stewart R.H. (1998) Reduction of geoid gradient error in ocean variability from satellite altimetry. Mar. Geod. 21: 25-39.

Čadek O. and Martinec Z. (1991) Spherical harmonic expansion of the earth's crustal thickness up to degree and order 30. Studia geoph. Et geod. 35: 151-165

Chen R., and Kakkuri J. (1995) Results of the Baltic Sea Level 1993 GPS Campaign, in: Final results of the Baltic Sea Level 1993 GPS Campaign. Report 95:2, Finnish Geodetic Institute, ed. J. Kakkuri, pages 21-30, Helsinki 1995.

Chen X., Nashed Z., and Qi L. (1997) Convergence of Newton's method for singular smooth and nonsmooth equations using adaptive outer inverses. SIAM J. Optim. 7: 445-462.

Corduneanu C. (1991) Integral Equations and Applications. Cambridge, England: Cambridge University Press, 1991.

Davis H. T. (1962) Introduction to Nonlinear Differential and Integral Equations. New York: Dover, 1962.

Defence Mapping Agency, Department of Defence (1991) World Geodetic System 1984. DMA Technical Report 8350.2, second edition, September 1, 1991.

Denker H., and Torge W. (1998) The European gravimetric quasi-geoid EGG97 -an IAG supported continental enterprise, In: R. Forsberg el al. (eds.) IAG symp. proceed. 119: 249-254, Springer, Berlin-Heidelberg-New-York.

Eitschberger B., and Grafarend E. W. (1974) World geodetic datum WD 1 and WD 2 from satellite and terrestrial observations. Bulletin Géodésique 114: 364-385.

Ekman M. (1979) The stationary effect of moon and sun upon the gravity of the earth, and some aspects of the definition of gravity. Uppsala University, Geodetic Institute, Report 5.

Ekman M. (1981) On the definition of gravity. Bulletin Géodésique, 55:2

Ekman M. (1989) Impacts of Geodynamic phenomena on systems of height and gravity. Bulletin Géodésique 63: 281-296.

Ekman M. (1996) The permanent problem of the permanent tide: What to do with it in geodetic reference systems. Marees Terrestres 125: 9508-9513.

Engels J., and Grafarend E.W. (1993) The gravitational field of topographic-isostatic and the hypothesis of mass condensation, Surveys in Geophysics, 140: 495-524.

Engels, J., Grafarend, E., Keller, W., Martinec, Z., Sansò, F. and Vaniček P. (1993): The geoid as an inverse problem to be regularized, in: Inverse Problems: Principles and Applications in Geophysics, Technology and Medicine, eds. G. Anger, R. Gorenfol, H. Jochmann, H. Moritz and W. Webers, Akademie-Verlag, Berlin 1993, 122-167.

Eringen AC (1962) Nonlinear theory of contiuous media. McGraw-Hill Bookd Company, New York, 1962.

Euler H. J., Groten E., Hausch W., and Kling Th. (1986) New results obtained for detailed geoid approximations. Boll. Di Geodesia e Scienze Affini 4: 429-452.

Feistritzer M. (1998) Geoidbestimmung mit geopotentiellen Koten. Deutsche Geodätische Kommission, der Bayerischen Akademie der Wissenschaften, Report C486, München 1997.

Forsberg R. (1984) A study of terrain reductions, density anomalies and geophysical inversion methods in gravity field modelling, Reports of the Department of Geodetic Science and Surveying, No. 355,The Ohio State University, Columbus, Ohio.

Forsberg R. (1985) Gravity field terrain effect computations by FFT. Bulletin Geodesique. 59: 342-360.

Forsberg R. (1994) Terrain effects in geoid computations. In Lecture Notes, Int. school for deter. and use of geoid. Milano, Oct. 1994 pp: 101-134. IGeS, Milano.

Frommer A., and Maass P. (1999) Fast cg-based methods for Tikhonov-Phillips regularization. SIAM J. Sci. Comput. 20: 1831-1850.

Gauss C. F. (1828) Bestimmung des Breitenunterschiedes zwischen den Sternwarten von Göttingen und Altona. Vandenhoek und Ruprecht, Göttingen 1828.

Gleason D. M. (1989) Some notes on the evaluation of ellipsoidal and ellipsoidal harmonic expansions. manuscripta geodaetica 14: 110-116.

Gleason D. M. (1988) Comparing corrections to the transformation between the geopotential's spherical and ellipsoidal spectrum. manuscripta geodaetica 13: 114-129.

Grafarend E.W., and Eitschberger B. (1974) World geodetic datum WD 1 and WD 2 from satellite and terrestrial observations. Bulletin Géodésique 114*:* 364-385.

Grafarend E. W., and Schaffrin B. (1993) Ausgleichungsrechnung in linearen Modellen. B.I. Wissenschaftsverlag, Manheim.

Grafarend E. W. (1978) The definition of the telluroid. Bull. Geod. 52: 25-37.

Grafarend E. W. (1988) Azimuth transport and the problem of orientation within geodetic traverses and geodetic networks. Zeitschrift für Vermessung, Photogrammetric, Kultur (schweiz) 86: 314-332.

Grafarend E. W. (1989) The geoid and the gravimetric boundary value problem, The Royal Institute of Technology Stockholm Department of Geodesy, Report 18, Trita. Geod. 1018, Stockholm 1989.

Grafarend E. W. (1991) Application of geodesy to engineering, Symposium No 108. Eds. K. Linkwitz, V. Eisele, H. J. Mönicke, Springer-Verlag, Berlin, Heidelberg, New York.

Grafarend E. W., and Ardalan A. A. (1997) W_0 – an estimate in the Finnish Height Datum N60, epoch 1993.4, from twenty-five GPS points of the Baltic Sea Level Project. J Geod 71: 673-679.

Grafarend E. W., and Ardalan A. A. (1999a) World Geodetic Datum 2000. in: R. Rummel (ed.), Towards and integrated global geodetic observing system, Munich 5-9 October 1998.

Grafarend E. W., and Ardalan A. A. (1999b) World Geodetic Datum 2000, Journal of Geodesy 73: 611-623.

Grafarend E. W., and Hanke S. (2000) The terrain correction in a moving tangent space. Submitted to Journal of Geodesy.

Grafarend E. W., and Schaffrin B. (1993) Ausgleichungsrechnung in linearen Modellen. B.I. Wissenschaftsverlag, Manheim.

Grafarend E. W., and Lohse P. (1991) The minimal distance mapping of the topographic surface onto the (reference) ellipsoid of revolution. manuscripta geodaetica 16: 92-110.

Grafarend E.W., and Sanso F. (1984) The multibody space-time geodetic boundary value problem and the Honkasalo term. Geophys. J.R. astr. Soc 78: 255-275.

Grafarend E. W., Niemeier W. (1971) The free nonlinear boundary value problem of physical geodesy. Bull. Géodésique 101: 243-262.

Grafarend E. W., Ardalan A. A., and Sideris M. (1999) The ellipsoidal fixed-free two-boundary value problem for geoid determination (the ellipsoidal Bruns transform). Journal of Geodesy 73:513-533.

Grafarend, E. W., Schaffrin B. (1993): Ausgleichungsrechnung in linearen Modellen. Brockhaus, Mannheim 1993.

Grafarend E. W., Krarup T., and Syffus R. (1996) An algorithm for the inverse of a multivariate homogeneous polynomial of degree n. Journal of Geodesy 70: 276-286.

Grafarend E. W., Syffus R. and You R. (1995) Projective heights in geometry and gravity space. Allgemeine Vermessungs Nachrichten 10: 382-403.

Grafarend E. W., Heidenreich E. D., and Schaffrin B. (1977) A representation of the standard gravity field. manuscripta geodaetica 2: 135-174.

Greenberg J. L. (1995) The problem of the earth's shape from Newton to Clairaunt. Cambridge University Press USA, 1995.

Groten E. (1979/80) Geodesy and the earth's gravity field, vol. I and II. Dümmler Verlog, Bonn.

Groten (1980) A remark on M. Heikkinen's paper:"On the Honkasalo term in tidal corrections to gravimetric observations". Bulletin Géodésique, 54:2

Groten E. (1984) Local and global gravity field representation. In: Advances in Geodesy (ed. By E.W. Grafarend and R. H. Rapp), Reviews of Geophysics and Space Physics, 19, No. 2: 101-108.

Groten E. (1996a) Vertical datum unification: Implications and use of results. Proceedings of second Intern. Conference Denpasar "Geodetic Aspects of the Law of the Sea" Bali, 1-4 July 1996.

Groten E. (1996b) Vertical datum unification problems and their solution. Proceedings of the first workshop of the subcommission IAG SSC 8.1 "Studies of the Baltic Sea" Riga, Latvia, March 28-29, P. 33.

Groten E. (1996c) High precision geoid evaluation for Germany-geoid and quasigeoid. Pres. At Fifth Winter Seminar Sopron on Geodynamics (WSS 96) "Gravity in Time and Space", Acta Geodaetica et Geophysica Hungarica, Vol. 31, 3-4: 293-303.

Groten E. (1997) Current best estimates of the parameters of common relevance to astronomy, geodesy, and geodynamics. Internal Communications of IAG/IUGG Special Commission 3, Darmstadt 1997.

Hankasalo (1964) On the tidal gravity correction. Bollettino di Geofisica Teorica ed Applicata, VI/21.

Hansen P. C. (1996) Rank-deficient and discrete ill-posed problems. Christian Hansen and Polyteknisk Forlag, Denmark 1996.

Heikkinen M. (1979) On the Honkasalo term in tidal corrections to gravimetric observations. Bulletin Gédésique. 53/3.

Heikkinen M. (1982) Geschlossene Formeln zur Berechnung räumlicher geodätischer Koordinaten aus rechtwinkligen Koordinaten. ZfV 5: 207-211.

Heiskanen W. (1951) On the world geodetic system. Publ. Isostotic Institute, Geodeetinen Laitos, Helsinki 1951.

Heiskanen W., and Moritz H. (1967) Physical Geodesy. W.H. Freeman and Co., San Francisco, 1967.

Helmert F. R. (1880) Die mathematischen und physikalischen Theorien der höheren Geodäsie. B.G. Teubner, Leipzip 1880.

Hirvonen R. A. (1960) New theory of the gravimetric geodesy. Pobl. Isostatic Institute, Annales Academiae Sci. Fennicae, A3: 1-50.

Hobson E. W. (1965) The theory of spherical and ellipsoidal harmonics. Chelsea Publishing company, New York.

Hotine, M. (1969) Mathematical geodesy. Washington 1969.

International Association of Geodesy (1974) The international gravity standardization net 1971. Special Publication No.4, Paris, France.

Jekeli C. (1981) The downward continuation to the earth's surface of truncated spherical and ellipsoidal harmonic series of the gravity and height anomalies. Report 323, Ohio State University Department of Geodetic Science and Surveying, Columbus Ohio 1981.

Jekeli C. (1988) The exact transformation between ellipsoidal and spherical harmonic expansions. Manuscr Geod 13: 106-113.

Kakkuri J. (1995) The Baltic Sea Level Project. Allgemeine Vermessungs-Nachrichten 8-9: 331-336.

Kakkuri J., and Poutanen M. (1997) Geodetic Determination of the surface topography of the Baltic Sea. Marine Geodesy, 20: 307-316.

Kakkuri J., T. J. Kukkamäki, J. J. Levallois, and H. Moritz (1986) Le 250[E] Anniversaire de la Mesure de L'Arc du Meridien en Laponie. Publication of the Finnish Geodetic Institute, Report 103, Helsinki 1986.

Kakkuri J. (1995) The Baltic Sea Level Project. Allg. Vermessungsnachrichten 102: 331-336.

Kakkuri J., and Poutanen M. (1996) Geodetic determination of the surface topography of the Baltic Sea. accepted for publ. Marine Geodesy.

Kling T. M., Becker H., Euler J., and Groten E. (1987) Studien zur detaillierten Geoidberechnung. Deutsche Geodät. Komm., B. 285, München.

Kondo J. (1992) Integral Equations. Oxford, England: Clarendon Press, 1992.

Lambert W. D. (1961) The gravity field of an ellipsoid of revolution as a level surface. Annales Academiae Sci. Fennicae, A57: 1-42.

Lemoine F. G., Smith D. E., Kunz L., Smith R., Pavlis E. C., Pavlis N. K., Klosko S. M., Chinn D. S., Torrence M. H., Williamson R. G., Cox C. M., Rachlin K. E., Wang Y. M. Kenyon S. C., Salman R., Trimmer R., Rapp R. H., and Nerem, R. S. (1996) The development of the NASA GSFC and NIMA joint geopotential model. In: J. Segawa, H. Fujimoto, and S. Okubo (eds), Gravity, Geoid and Marine Geodesy, International Association of Geodesy Symposia, Vol. 117, Springer Berlin Heidelberg pp 461-469.

Lemoine F. G., Smith D. E., Kunz L., Smith R., Pavlis E. C., Pavlis N. K., Klosko S. M., Chinn D. S., Torrence M. H., Williamson R. G., Cox C. M., Rachlin K. E., Wang Y. M., Kenyon S. C., Salman R., Trimmer R., Rapp R. H., and Nerem, R. S. (1998) The development of the NASA GSFC and NIMA joint geopotential model. NASA, technical report No. 206861.

Li Y.C., and Sideris M. G. (1992) The fast Hartley transform and its application in Physical Geodesy. Manuscr. Geod. 17: 381-387.

Li Y.C., and Sideris M. G. (1994) Improved gravimetric terrain corrections, Geophys. J. Int. 119: 740-752.

Listing, J.B. (1873) Über unsere jetzige Kenntnis der Gestalt und Größe der Erde. Dietrichsche Verlagsbuchhandlung, Göttingen 1873.

Lovitt W. V. (1950) Linear Integral Equations. New York: Dover, 1950.

Malys S. (1996) The WGS84 Reference Frame. National Imagery and Mapping Agency, November 7, 1996.

Marti J. T. (1978) An algorithm for computing minimum norm solution of Fredholm integral equations of the first kind. SIAM J: Numer. Anal. 15: 1071-1076.

Marti J. T. (1980) On the convergence of an algorithm for computing minimum norm solutions of ill-posed problems. Maths. Comp. 34: 521-527.

Martinec Z. (1998a) Boundary-value problem for gravimetric determination of a precise geoid. Springer Verlag, Berlin 1998.

Martinec Z. (1998b) Construction of Green's function for the Stokes boundary-value problem with ellipsoidal corrections in the boundary condition. Journal of Geodesy, 7/8: 460-472.

Martinec Z. (1991) On the accuracy of the method of condensation of the Earth's topography. manuscripta geodaetica 16: 288-294.

Martinec Z., and Grafarend E. W. (1997a) Solution of the Stokes boundary-value problem on an ellipsoid of revolution. Stud Geoph Geod 41: 103-129.

Martinec Z., and Grafarend E. W. (1997b) Construction of Green's functions to the external Dirichlet boundary-value problem for the Laplace equation on an ellipsoid of revolution. Journal of Geodesy 71: 562-570.

McCarthy D. (1996) IERS Technical Note 21. Observatioire de Paris 1996.

Mihelcic M. (1972) Über eine Theorie zur Simultanauswertung von fluggravimetrischen und terrestrisch-gravimetrischen Messungsdaten, Deutsche Geodätische Kommission, Bayerische Akademie der Wissenschaften, Heft C172, München 1972

Mikhlin S. G. (1961) Linear Integral Equations. New York: Gordon & Breach, 1961.

Mikhlin S. G. (1964) Integral Equations and Their Applications to Certain Problems in Mechanics, Mathematical Physics and Technology, 2nd rev. ed. New York: Macmillan, 1964.

Moon P., and Spencer D. E. (1953) Recent investigations of the separation of Laplace's equation. Ann. Math. Soc. Proc. 4: 302-307.

Moon P., and Spencer D. E. (1961) Field theory handbook. Springer-Verlog, New York, Heidelberg, Berlin, 1961.

Moritz H. (2000) Geodetic Reference System 1980. Journal of Geodesy 74: 128-133.

Nahavandchi H (1998) On some methods of downward continuation of mean free-air gravity anomaly. IGeS Bulletin 8: 1-16

Nahavandchi H, LE Sjoeberg (1998) Terrain correction to power 3 in gravimetric geoid determination. Journal of Geodesy 3:124-135

Natterer F. (1977) The finite element method for ill-posed problems. RAIRO-Analyse Numerique 11: 271-278.

Nesvorný D., and Šíma Z. (1994) Refinement of the geopotential scale factor R_0 on the satellite altimetry basis. Earth, Moon, and Planets 65: 79-88.

Neumann J. (1848) Entwicklung der in elliptischen Koordinaten ausgedruckten reziproken Entfernung zweier Punkte in Reihen. Journal für die reine und angewandte Mathematik 37: 21-50.

Paul M. K. (1973) A note on computation of geodetic coordinates from geocentric (Cartesian) coordinates. Bull. Géod. 108: 135-139.

Peng M., Li Y. C., and Sideris M. G. (1994) First results on the computation of terrain corrections by the 3D-FFt method. manuscripta geodaetica 6: 475-488

Phillips D. L. (1962) A technique for the numerical solution of certain integral equations of the first kind. J. Ass. comput. Mach. 9: 84-96.

Pipkin A. C. (1991) A Course on Integral Equations. New York: Springer-Verlag, 1991.

Pizzetti P. (1894) Geodesia--Sulla espressione della gravita alla superficie del geoide, supposto ellissoidico. Atti Reale Accademia dei Lincei 3: 166-172.

Porter D., and Stirling D. S. G. (1990) Integral Equations: A Practical Treatment, from Spectral Theory to Applications. Cambridge, England: Cambridge University Press, 1990.

Papp G., and Benedek J. (2000) Numerical modelling of gravitational field lines—the effect of mass attraction on horizontal coordinates. Journal of Geodesy, 73: 648-659.

Poutanen M. (1998a) Results of the Baltic Sea Level 1997 GPS Campaign. Presented at the 13th General Meeting of the Nordic Geodetic Commission, Gävle, Sweden, 25-29 May 1998.

Poutanen M. (1998b) Towards the unification of vertical datums in the Baltic Sea region. Presented at the 13th General Meeting of the Nordic Geodetic Commission, Gävle, Sweden, 25-29 May 1998.

Poutanen M. (1998c) The FGI computation of the EUVN/BSL 1997 GPS Campaign.. Report on the results of the European Vertical Reference Network GPS Campaign 97 (EUVN97) pp 151-160.

Press W. H., Flannery B. P., Teukolsky S. A., and Vetterling W. T. (1992) Integral Equations and Inverse Theory. Ch. 18 in Numerical Recipes in FORTRAN: The Art of Scientific Computing, 2nd ed. Cambridge, England: Cambridge University Press, pp. 779-817, 1992.

Rapp R. (1971) Methods for the computation of geoid undulations from potential coefficients. Bulletin Géodésique 101:283-297.

Rapp R. (1992) Global geoid solutions. In: Geophysical interpretations of the geoid, ed. Vaníček and Christou. CRC Press, Boca Raton, FL, pp 57-76.

Rapp R. (1997) Use of potential coefficients models for geoid undulation determinations using a spherical harmonic representation of the height anomaly/geoid undulation difference. Journal of Geodesy 71: 282-289.

Rapp R. H., Wang Y. M., and Pavlis N. K. (1991) The Ohio State 1991 geopotential and sea surface topography harmonic coefficient models. Report 410, Ohio State University Department of Geodetic Science and Surveying, Columbus, Ohio.

Ries J. C., Eanes R. J., Shum C. K., and Watkins M. M. (1992) Progress in the determination of the gravitational coefficient of the Earth. Geophys Res Lett 19: 529-531.

Rummel R. Rapp R.H., Suenkel H., and Tscherning C. C. (1988) Comparison of global topographic/isostatic models to the earth's observed gravity field. Report of the Dep. Of Geodetic Science and Surveying, No 388, The Ohio State University.

Sansó F. (1995) The long road from measurements to boundary value problems in physical geodesy. Manuscripta geodaetica 20: 34-45.

Saupe D. (1988) Discrete versus continuous Newton's method: a case study. Acta Appl. Math. 13: 59-80.

Schaffrin B., Heidenreich E., and Grafarend E. W. (1977) A representation of the standard gravity field. Manuscripta geodaetica 2: 135-174.

Schwarz K. P., Sideris M. G., and Forsberg R. (1990) The use of FFT techniques in physical geodesy. Geophys. J. Int. 100: 485-514.

Sideris M. G., and Li Y. C. (1993) Gravity field convolutions without windowing and edge effects. Bulletin Géodésique 2: 107-118

Sideris M. G. (1995) Fourier geoid determination with irregular data. Journal of Geodesy 1: 2-12

Sjoeberg L. E. (1998) The external Airy/Heiskanen topographic-isostatic gravity potential, anomaly and the effect of analytical continuation. Journal of Geodesy 11: 654-662

Sjoeberg L. E. (2000) Topographic effect by the Stiokes-Helmert method of geoid and quai-geoid determinations. Hournal of Geodesy 74: 255-268.

Smith D. (1998) There is no such thing as "The" EGM96 geoid: Subtle points on the use of a global geopotential model. IGeS Bulletin 8: 17-28.

Smith J. R. (1986) From plane to spheroid, Landmark Enterprises,.Rancho Cordova, USA 1986.

Smith J. R. (1987) The beginning of modern geodesy 250 years ago. Survey Review 29: 105-119.

Somigliana C. (1930) Geofisica--Sul campo gravitazionale esterno del geoide ellissoidico. Atti della Reale Academia Nazionale dei Lincei Rendiconti 6: 237-243.

Sona G. (1996) Numerical problems in the computation of ellipsoidal harmonics. Journal of Geodesy 70: 117-126.

Sun W., and Vaníček P. (1996) On the discrete problem of downward continuation of Helmert's gravity. Proceedings of Session G7 (Techniques for local geoid determination), Annual meeting of European Geophysical Society. The Hague, May 6-10, Reports of the Finnish Geodetic Institute, 96:2, pp. 29-34.

Tapley B. D., Watkins M. M., Ries J. C., Davis G. W., Eanes R. J., Poole S. R., Rim H. J., Schutz B. E., Shum C. K., Nerem R. S., Lerch F. J., Marshall J. A., Klosko S. M., Pavlis N. K., and Williamson R.G. (1996) The JGM3 gravity model. J Geophys Res 101: 28029-28049.

Thong N.C. (1989) Simulation of gradiometry using the ellipsoidal harmonic model of the gravitational field. manuscripta geodaetica 14: 404-417.

Thong N. C. (1993) Untersuchen zur Lösung der fixen gravimetrischen Randwertprobleme mittels sphäroidaler und Greenscher Funktionen. Deutsche Geodätische Kommision, Bayerische Akademie der Wissenschaften, Reihe C: 399, München 1993.

Thong N. C., and Grafarend E. W. (1989) An ellipsoidal model of the terrestrial gravitational field. Manuscr Geod 14: 285-304.

Tikhonov A. N. (1963) The regularization of incorrectly posed problems. Soviet Math. Doklady 4: 1624-1627.

Tobé E. (1986) Fransysk visit i Tornedalen. 1736-1737, I-Tryck AB, Lulea 1966.

Torge W. (1994) Development, state of the art and problems at large scale geoid determinations. International Geoid Service, Bulletin 3: 47-66.

Tricomi F. G. (1957) Integral Equations. New York: Dover, 1957.

Tscherning C. C., Rapp R. H., and Goad C. (1983) A comparison of methods for computing gravimetric quantities from high degree spherical harmonic expansions. Manuscripta geodaetica 8: 249-272.

Vermeer M. (1995) Two new geoids determined at the FGI. Reports of Finnish Geodetic Institute), 95:5.

Vermeer M., and Poutanen M. (1997) A modified GRS-80 normal field including permanent tide and atmosphere. In: Proc. IAG Symposium Tokyo/Japan, J. Segawa, H Fujimoto and S Okubo (Eds.).

Vermeer M., and Poutanen P. (1997) International Symposium. IAG symposia No. 117. Eds. J. Sagawa, H. Fujimoto, ans S. Okubo. Springer-Verlag, Berlin, Heidelberg, New York.

Wenzel H. G. (1998) Ultra hochauflösende Kugelfunktionsmodelle GPM98A und GPM98B des Erdschwerefeldes. In: Progress in Geodetic Science, W. Freeden (ed.) pp. 323-331, Shaker Verlag, Aachen 1998.

Whittaker E. T., and Robinson G. (1967) The Numerical Solution of Integral Equations." §183 in The Calculus of Observations: A Treatise on Numerical Mathematics, 4th ed. New York: Dover, pp. 376-381, 1967.

Yu J, Cao H (1996) Elliptic harmonic series and original Stokes problem with the boundary of the reference ellipsoid. J Geod 70: 431±439

Appendices A: Ellipsoidal coordinates

In this appendix, six different ellipsoidal coordinates will be introduced. Among these six, there are two, which we have used in various chapters. Therefore, for these two we will present the eigenvalue/eigenfunction solution of 3-D Laplace differential equation of gravitational field of the earth in *Appendix B*, and external *Dirichlet* problem of *Laplace* equation with boundary data on the ellipsoid of revolution in *Appendix D*. These two coordinates are *Jacobi ellipsoidal coordinates* $\{\lambda, \phi, \eta\}$ and $\{\lambda, \phi, u\}$. *N. Thong and E. Grafarend* (1989) have given an extensive review to four different types of ellipsoidal coordinates *and* the ellipsoidal eigenvalues/eigenfunctions which span the three-dimensional *Laplace* partial differential equation for the external gravity field of the *earth*.

Box A-1 presents six different ellipsoidal coordinates, which will be introduced in detail in the following sections of this appendix.

Box A-1: Different types of ellipsoidal coordinates

- *Jacobi ellipsoidal coordinates*

  1st variant, elliptic coordinates $\{\lambda, \mu, \nu\}$

  2nd variant, trigonometric elliptic coordinates $\{\lambda, \phi, \eta\}$

  3rd variant, mixed elliptic-trigonometric elliptic coordinates $\{\lambda, \phi, u\}$

  4th variant, mixed elliptic-trigonometric elliptic coordinates $\{\lambda, v, \eta\}$

- *Gauss ellipsoidal coordinates*

  First variant, geodetic coordinates $\{l, b, h\}$ (geodetic longitude, geodetic latitude, and ellipsoidal height)

  Second variant, normal-geodetic coordinates $\{l, b, h_N\}$ (geodetic longitude, geodetic latitude, and normal height)

A.1 Jacobi ellipsoidal coordinates

In this section, we will briefly review the ellipsoidal coordinates of Jacobi type. This brief review covers all the backgrounds that one may need in different chapters of the thesis. For more on ellipsoidal coordinates, one can refer for example to *P. Moon and E. Spencer* (1961), *W. Heiskanen and H. Moritz* (1967), *and N. Thong and E. Grafarend* (1989).

A.1.1 First variant: Elliptic coordinates $\{\lambda, \mu, \nu\}$

In terms of ellipsoidal coordinates $\{\lambda, \mu, \nu\}$, a point in space can be located as intersection of three coordinate surfaces. In *Jacobi ellipsoidal coordinate system* the coordinate surfaces are corresponding to three families the type *(i)* confocal oblate spheroids, *(ii)* confocal half hyperboloids, and *(iii)* planes. These families of surfaces are defined as follows. For the variant $\{\lambda, \mu, \nu\}$ of Jacobi ellipsoidal coordinates these families are as follows

(i) the family of confocal, oblate spheroids

$$\mathbb{E}^2_{\sqrt{a^2-\mu},\sqrt{b^2-\mu}} := \left\{ \mathbf{x} \in \mathbb{R}^3 \mid \frac{x^2+y^2}{a^2-\mu} + \frac{z^2}{b^2-\mu} = 1,\ \mu < b^2 < a^2 \right\} \quad \text{(A.1)}$$

(ii) the family of confocal half hyperboloids

$$\mathbb{H}^2_{\sqrt{a^2-\nu},\sqrt{\nu-b^2}} := \left\{ \mathbf{x} \in \mathbb{R}^3 \mid \frac{x^2+y^2}{a^2-\nu} + \frac{z^2}{b^2-\nu} = 1,\ b^2 < \nu < a^2 \right\} \quad \text{(A.2)}$$

(iii) the family of half planes

$$\mathbb{P}^2_{\cos\lambda,\sin\lambda} := \left\{ \mathbf{x} \in \mathbb{R}^3 \mid y = x \tan\lambda,\ \lambda \in [0, 2\pi] \right\} \quad \text{(A.3)}$$

According to *Figure A-4 page 222*, the longitude λ gives *orientation* to the half planes. The elliptic coordinate ν is related to the *inclination* ϕ of the asymptotes of confocal half hyperboloids through $\nu = a^2 - \varepsilon^2 \cos^2\phi$, the elliptic coordinate μ in the form of $a^2 - \mu$ defines the *semi-major axis* of confocal oblate spheroids (confocal, oblate ellipsoids of revolution).

The forward and backward transformations of ellipsoidal coordinates $\{\lambda, \mu, \nu\}$ into Cartesian coordinates are collected in *Box A-2*, while and the *Jacobi* matrix of the forward transformation is reviewed in *Definition A-2*.

Box A-2: Conversion of Cartesian coordinates $\{x, y, z\}$ into ellipsoidal coordinates $\{\lambda, \mu, \nu\}$:

(i) Forward transformation from ellipsoidal coordinates $\{\lambda, \mu, \nu\}$ into Cartesian coordinates $\{x, y, z\}$

$$\begin{aligned} x &= \sqrt{\frac{(a^2-\mu)(a^2-\nu)}{a^2-b^2}}\cos\lambda \\ y &= \sqrt{\frac{(a^2-\mu)(a^2-\nu)}{a^2-b^2}}\sin\lambda \\ z &= \pm\sqrt{\frac{(b^2-\mu)(\nu-b^2)}{a^2-b^2}}\cos\lambda \end{aligned} \tag{A.4}$$

(ii) Backward transformation of Cartesian coordinates $\{x, y, z\}$ into ellipsoidal coordinates $\{\lambda, \mu, \nu\}$

$$\lambda = \begin{cases} \arctan\frac{y}{x} & \text{for } x > 0 \text{ and } y \geq 0 \\ \arctan\frac{y}{x} + \pi & \text{for } x < 0 \text{ and } y \neq 0 \\ \arctan\frac{y}{x} + 2\pi & \text{for } x > 0 \text{ and } y < 0 \\ \frac{\pi}{2} & \text{for } x = 0 \text{ and } y > 0 \\ 3\frac{\pi}{2} & \text{for } x = 0 \text{ and } y < 0 \end{cases} \tag{A.5}$$

$$\begin{aligned} \mu = &\frac{1}{2}(a^2+b^2-(x^2+y^2+z^2)) \\ &-\frac{1}{2}\sqrt{(a^2-b^2-x^2-y^2+z^2)^2+4(x^2+y^2)z^2} \end{aligned} \tag{A.6}$$

$$\begin{aligned} \nu = &\frac{1}{2}(a^2+b^2-(x^2+y^2+z^2)) \\ &+\frac{1}{2}\sqrt{(a^2-b^2-x^2-y^2+z^2)^2+4(x^2+y^2)z^2} \end{aligned} \tag{A.7}$$

Definition A-1: Basic geometry of ellipsoidal coordinates $\{\lambda, \mu, \nu\}$

(i) Jacobi matrix of the transformation from *ellipsoidal coordinates* $\{\lambda, \mu, \nu\}$ into *Cartesian coordinates* $\{x, y, z\}$

From equation (A.4) the *Jacobi matrix* "J " of the transformation from *ellipsoidal coordinates* $\{\lambda, \mu, \nu\}$ into *Cartesian coordinates* $\{x, y, z\}$ can be constructed as follows.

$$J := \begin{bmatrix} X_\lambda & X_\mu & X_\nu \\ Y_\lambda & Y_\mu & Y_\nu \\ Z_\lambda & Z_\mu & Z_\nu \end{bmatrix} \tag{A.8}$$

The partial derivatives involved in (A.8) reads as follows

$$\begin{gathered}
X_\lambda = D_\lambda X = -\sqrt{(a^2\text{-}\mu)(a^2\text{-}\nu)/(a^2\text{-}b^2)}\sin\lambda \\
Y_\lambda = D_\lambda Y = \sqrt{(a^2-\mu)(a^2-\nu)/(a^2-b^2)}\cos\lambda \\
Z_\lambda = D_\lambda Z = 0 \\
X_\mu = D_\mu X = -1/2\sqrt{(a^2-\nu)/[(a^2-\mu)(a^2-b^2)]}\cos\lambda \\
Y_\mu = D_\mu Y = -1/2\sqrt{(a^2-\nu)/[(a^2-\mu)(a^2-b^2)]}\sin\lambda \\
Z_\mu = D_\mu Z = -1/2\sqrt{(b^2-\nu)/[(b^2-\mu)(a^2-b^2)]} \\
X_\nu = D_\nu X = -1/2\sqrt{(a^2-\mu)/[(a^2-\nu)(a^2-b^2)]}\cos\lambda \\
Y_\nu = D_\nu Y = -1/2\sqrt{(a^2-\mu)/[(a^2-\nu)(a^2-b^2)]}\sin\lambda \\
Z_\nu = D_\nu Z = -1/2\sqrt{(b^2-\mu)/[(b^2-\nu)(a^2-b^2)]}.
\end{gathered}$$

(ii) The metric tensor of the ellipsoidal geometry space $\{\lambda, \mu, \nu\}$ *is given by*

$$dS^2 = [d\lambda, d\mu, d\nu]J^* J \begin{bmatrix} d\lambda \\ d\mu \\ d\nu \end{bmatrix} \tag{A.9}$$

$$G := J^* J$$

$$= \begin{bmatrix} (a^2-\mu)(a^2-\nu)/(a^2-b^2) & 0 & 0 \\ 0 & 1/4(\mu\text{-}\nu)/[(a^2\text{-}\mu)(b^2\text{-}\nu)] & 0 \\ 0 & 0 & \text{-}1/4(\mu\text{-}\nu)/[(b^2\text{-}\mu)(\mathrm{a}^2\text{-}\mu)] \end{bmatrix}$$

$$:= g_{nm} \qquad \forall \qquad n,m = 1,2,3 \tag{A.10}$$

(iii) The Laplacian read as follows

$$\begin{aligned} \Delta &= \frac{1}{\sqrt{g}}\left\{\frac{\partial}{\partial\lambda}(\frac{\sqrt{g}}{g_{11}}\frac{\partial}{\partial\lambda}) + \frac{\partial}{\partial\mu}(\frac{\sqrt{g}}{g_{22}}\frac{\partial}{\partial\mu}) + \frac{\partial}{\partial\nu}(\frac{\sqrt{g}}{g_{33}}\frac{\partial}{\partial\nu})\right\} \\ &= \frac{1}{\nu-\mu}\left\{\frac{(a^2-b^2)(\mu-\nu)}{(a^2-\mu)(a^2-\nu)}\frac{\partial^2}{\partial\lambda^2} - 2(-3\mu+a^2+b^2)\frac{\partial}{\partial\mu}\right. \\ &\quad +4(b^2-\mu)(a^2-\mu)\frac{\partial^2}{\partial\mu^2} + 2(-3\nu+a^2+2b^2)\frac{\partial}{\partial\nu} \\ &\quad \left. +4(\nu-b^2)(a^2-\nu)\frac{\partial^2}{\partial\eta^2}\right\} \end{aligned} \tag{A.11}$$

■

A.1.2 Second variant: Trigonometric elliptic coordinates $\{\lambda,\phi,\eta\}$

In terms of *ellipsoidal coordinates* $\{\lambda,\phi,\eta\}$, a point in space can be located as the intersection of three coordinate surfaces. The coordinate surfaces are corresponding to three families of surfaces of the type *(i)* confocal oblate spheroids, *(ii)* confocal half hyperboloids, and *(iii)* planes. These families of surfaces are defined as follows.

(i) The family of confocal oblate spheroids

$$\begin{aligned} \mathbb{E}^2_{\varepsilon\cosh\eta,\varepsilon\sinh\eta} := \Big\{\mathbf{x}\in\mathbb{R}^3 \,|\, \frac{x^2+y^2}{\varepsilon^2\cosh^2\eta} + \frac{z^2}{\varepsilon^2\sinh^2\eta} = 1, \\ \eta\in(0,+\infty),\ \varepsilon^2 := a^2-b^2\Big\} \end{aligned} \tag{A.12}$$

(ii) The family of confocal half hyperboloids

$$\mathbb{H}^2_{\varepsilon\cos\phi,\varepsilon\sin\phi} := \left\{ \mathbf{x} \in \mathbb{R}^3 \,|\, \frac{x^2+y^2}{\varepsilon^2\cos^2\phi} - \frac{z^2}{\varepsilon^2\sin^2\phi} = 1, \right.$$
$$\left. \phi \in [-\frac{\pi}{2}, \frac{\pi}{2}],\ \phi \neq 0 \right\} \tag{A.13}$$

(iii) The family of half planes

$$\mathbb{P}^2_{\cos\lambda,\sin\lambda} := \left\{ \mathbf{x} \in \mathbb{R}^3 \,|\, y = x\tan\lambda,\ \lambda \in [0, 2\pi] \right\} \tag{A.14}$$

■

According to *Figure A-4 page 222*, the longitude λ gives *orientation* to the half planes. The latitude ϕ is related to the *inclination* of the asymptotes of confocal half hyperboloids; the elliptic coordinate η in the form of $\varepsilon\cosh\eta$ defines the *semi-minor axis* of confocal oblate spheroids (confocal, oblate ellipsoids of revolution).

The forward and backward transformations of ellipsoidal coordinates $\{\lambda, \phi, \eta\}$ into Cartesian coordinates are collected in *Box A-3*. The *Jacobi* matrix of the forward transformation is reviewed in *Definition A-2*.

Box A-3: Conversion of Cartesian coordinates $\{x, y, z\}$ into ellipsoidal coordinates $\{\lambda, \phi, \eta\}$

Forward transformation of ellipsoidal coordinates $\{\lambda, \phi, \eta\}$ into Cartesian coordinates $\{x, y, z\}$

$$\begin{aligned} x &= \varepsilon\cosh\eta\cos\phi\cos\lambda \\ y &= \varepsilon\cosh\eta\cos\phi\sin\lambda \\ z &= \varepsilon\sinh\eta\sin\phi \end{aligned} \tag{A.15}$$

Backward transformation of Cartesian coordinates $\{x, y, z\}$ into ellipsoidal coordinates $\{\lambda, \phi, \eta\}$

$$\lambda = \begin{cases} \arctan\frac{y}{x} & \text{for } x > 0 \text{ and } y \geq 0 \\ \arctan\frac{y}{x} + \pi & \text{for } x < 0 \text{ and } y \neq 0 \\ \arctan\frac{y}{x} + 2\pi & \text{for } x > 0 \text{ and } y < 0 \\ \frac{\pi}{2} & \text{for } x = 0 \text{ and } y > 0 \\ 3\frac{\pi}{2} & \text{for } x = 0 \text{ and } y < 0 \end{cases} \tag{A.16}$$

$$\phi = (\operatorname{sgn} z)\arcsin\left\{\frac{1}{2\varepsilon^2}[\varepsilon^2 - (x^2 + y^2 + z^2) + \sqrt{(x^2 + y^2 + z^2 - \varepsilon^2)^2 + 4\varepsilon^2 z^2}]\right\}^{1/2} \tag{A.17}$$

$$\eta = \operatorname{arccosh}\left\{\frac{1}{2\varepsilon^2}[x^2 + y^2 + z^2 + \varepsilon^2 + \sqrt{(x^2 + y^2 + z^2 + \varepsilon^2)^2 - 4\varepsilon^2(x^2 + y^2)}]\right\}^{1/2} \tag{A.18}$$

Valid for

$$\begin{gathered} \lambda \in \{\lambda \in \mathbb{R} \mid 0 < \lambda < 2\pi\} \\ \phi \in \{\phi \in \mathbb{R} \mid -\frac{\pi}{2} < \phi < +\frac{\pi}{2}\} \\ \eta \in \{\eta \in \mathbb{R} \mid \eta > 0\} \end{gathered} \tag{A.19}$$

Definition A-2: Basic geometry of *ellipsoidal coordinates* $\{\lambda, \phi, \eta\}$

(i) Jacobi matrix of transformation from the ellipsoidal coordinates $\{\lambda, \phi, \eta\}$ *into Cartesian coordinates* $\{x, y, z\}$

From equation (A.15) Jacobi matrix "J" of the transformation from ellipsoidal coordinates $\{\lambda, \phi, \eta\}$ into Cartesian coordinates $\{x, y, z\}$ can be constructed as follows

$$J := \begin{bmatrix} X_\lambda & X_\phi & X_\eta \\ Y_\lambda & Y_\phi & Y_\eta \\ Z_\lambda & Z_\phi & Z_\eta \end{bmatrix} \tag{A.20}$$

(ii) The partial derivatives involved in (A.20) *read as*

$$\begin{gathered} X_\lambda = D_\lambda X = -\varepsilon \cosh\eta \cos\phi \sin\lambda \\ Y_\lambda = D_\lambda Y = \varepsilon \cosh\eta \cos\phi \cos\lambda \\ Z_\lambda = D_\lambda Z = 0 \\ X_\phi = D_\phi X = -\varepsilon \cosh\eta \sin\phi \cos\lambda \\ Y_\phi = D_\phi Y = -\varepsilon \cosh\eta \sin\phi \sin\lambda \\ Z_\phi = D_\phi Z = \varepsilon \sinh\eta \cos\phi \\ X_\eta = D_\eta X = \varepsilon \sinh\eta \cos\phi \cos\lambda \\ Y_\eta = D_\eta Y = \varepsilon \sinh\eta \cos\phi \sin\lambda \\ Z_\eta = D_\eta Z = \varepsilon \cosh\eta \sin\phi. \end{gathered}$$

(iii) The metric tensor

$G := J^*J$

$$= \begin{bmatrix} \varepsilon^2 \cosh^2\eta \cos^2\phi & 0 & 0 \\ 0 & \varepsilon^2(\cosh^2\eta - \cos^2\phi) & 0 \\ 0 & 0 & \varepsilon^2(\cosh^2\eta - \cos^2\phi) \end{bmatrix}$$

$$= \begin{bmatrix} (g_{\lambda\lambda})^2 & 0 & 0 \\ 0 & (g_{\phi\phi})^2 & 0 \\ 0 & 0 & (g_{\eta\eta})^2 \end{bmatrix} \tag{A.21}$$

(iv) The Laplacian

$$\Delta = \frac{1}{\sqrt{g}}\left\{\frac{\partial}{\partial\lambda}(\frac{\sqrt{g}}{g_{11}}\frac{\partial}{\partial\lambda}) + \frac{\partial}{\partial\phi}(\frac{\sqrt{g}}{g_{22}}\frac{\partial}{\partial\phi}) + \frac{\partial}{\partial\eta}(\frac{\sqrt{g}}{g_{33}}\frac{\partial}{\partial\eta})\right\}$$

$$= \frac{1}{\varepsilon^2(\sin^2\phi + \sinh^2\eta)}\left\{\frac{\sin^2\phi + \sinh^2\eta}{\cos^2\phi\cosh^2\eta}\frac{\partial^2}{\partial\lambda^2} - \tan\phi\frac{\partial}{\partial\phi}\right. \tag{A.22}$$

$$\left. + \frac{\partial^2}{\partial\phi^2} + \tanh\eta\frac{\partial}{\partial\eta} + \frac{\partial^2}{\partial\eta^2}\right\}$$

■

A.1.3 Third variant: Mixed elliptic-trigonometric elliptic coordinates $\{\lambda, \phi, u\}$

In terms of *ellipsoidal coordinates* $\{\lambda, \phi, u\}$, a point in space can be located as the intersection of following family of surfaces.

(i) the family of confocal, oblate spheroids

$$\mathbb{E}^2_{\sqrt{u^2+\varepsilon^2},u} := \left\{\mathbf{x}\in\mathbb{R}^3 \mid \frac{x^2+y^2}{u^2+\varepsilon^2} + \frac{z^2}{u^2} = 1,\ u \in (0, +\infty),\ \varepsilon^2 := a^2 - b^2\right\} \tag{A.23}$$

(ii) the family of confocal half hyperboloids

$$\mathbb{H}^2_{\varepsilon\cos\phi,\varepsilon\sin\phi} := \left\{\mathbf{x}\in\mathbb{R}^3 \mid \frac{x^2+y^2}{\varepsilon^2\cos^2\phi} - \frac{z^2}{\varepsilon^2\sin^2\phi} = 1,\ \phi \in [-\frac{\pi}{2}, \frac{\pi}{2}],\ \phi \neq 0\right\} \tag{A.24}$$

(iii) the family of half planes

$$\mathbb{P}^2_{\cos\lambda,\sin\lambda} := \left\{\mathbf{x}\in\mathbb{R}^3 \mid y = x\tan\lambda,\ \lambda \in [0, 2\pi]\right\} \tag{A.25}$$

According to *Figure A-4 page 222*, the longitude λ gives *orientation* to the half planes. The latitude ϕ is related to the *inclination* of the asymptotes of confocal half hyperboloids; the elliptic coordinate *u* coincides with the *semi-minor axis* of confocal oblate spheroids (confocal, oblate ellipsoids of revolution).

Box A-4: Conversion of Cartesian coordinates $\{x, y, z\}$ into ellipsoidal coordinates $\{\lambda, \phi, u\}$

(i) Forward transformation from ellipsoidal coordinates $\{\lambda, \phi, u\}$ into Cartesian coordinates $\{x, y, z\}$

$$\begin{aligned} x &= \sqrt{u^2 + \varepsilon^2}\cos\phi\cos\lambda \\ y &= \sqrt{u^2 + \varepsilon^2}\cos\phi\sin\lambda \\ z &= u\sin\phi \end{aligned} \tag{A.26}$$

(ii) Backward transformation of Cartesian coordinates $\{x, y, z\}$ into ellipsoidal coordinates

$$\lambda = \begin{cases} \arctan\dfrac{y}{x} & \text{for } x > 0 \text{ and } y \geq 0 \\ \arctan\dfrac{y}{x} + \pi & \text{for } x < 0 \text{ and } y \neq 0 \\ \arctan\dfrac{y}{x} + 2\pi & \text{for } x > 0 \text{ and } y < 0 \\ \dfrac{\pi}{2} & \text{for } x = 0 \text{ and } y > 0 \\ 3\dfrac{\pi}{2} & \text{for } x = 0 \text{ and } y < 0 \end{cases} \tag{A.27}$$

$$\begin{aligned} \phi = (\operatorname{sgn} z)\arcsin\Bigg\{ & \frac{1}{2\varepsilon^2}[\varepsilon^2 - (x^2 + y^2 + z^2) \\ & + \sqrt{(x^2 + y^2 + z^2 - \varepsilon^2)^2 + 4\varepsilon^2 z^2}]\Bigg\}^{1/2} \end{aligned} \tag{A.28}$$

$$\begin{aligned} u = \{ & \frac{1}{2}[x^2 + y^2 + z^2 - \varepsilon^2 \\ & + \sqrt{(x^2 + y^2 + z^2 - \varepsilon^2)^2 + 4\varepsilon^2 z^2}]\}^{1/2} \end{aligned} \tag{A.29}$$

Figure A-1 illustrates the coordinate lines u and ϕ in the plane $\lambda = 0°$. This configuration, because of the rotational symmetry of the system is the same for any plane $\lambda = const$. As one can see the coordinate line of ϕ for $u = b = 6{,}356{,}751.860$ m, with linear eccentricity $\varepsilon := \sqrt{a^2 + b^2}$ $= 521{,}854.677$ m is very close to a circle. Besides, the coordinate lines u ($(\lambda, \phi) = const.$) for $u > 2000{,}000m$ tend to become straight lines. This can be very well seen in terms of variations of curvature of coordinate line

$\phi = const.$ in $\lambda = 0^\circ$ plane verses *Jacobi ellipsoidal coordinate* u as shown in *Figure A-2* and *Figure A-3*.

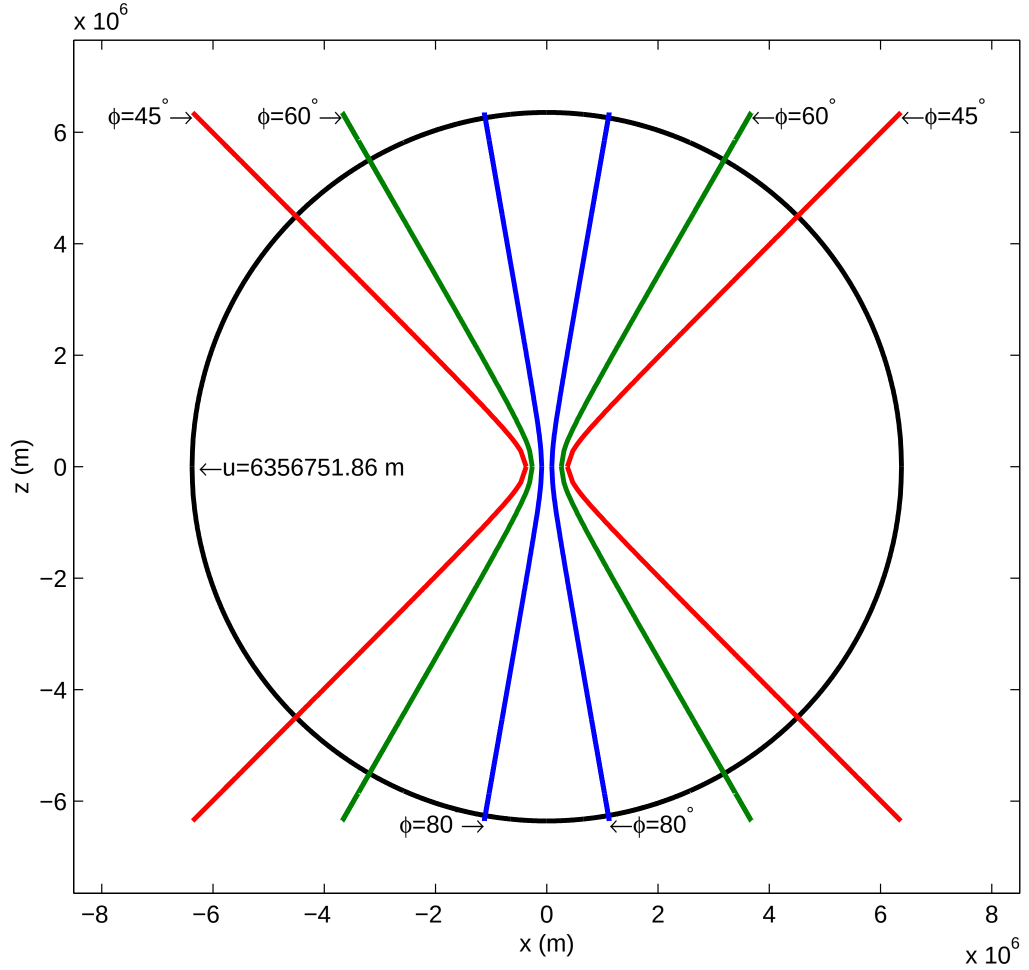

Figure A-1: Jacobi ellipsoidal coordinates $\{\lambda, \phi, u\}$. Coordinate lines $\phi = \{45^\circ, 60^\circ, 80^\circ\}$, and $u = b = 6,356,751.860(m)$ with linear eccentricity $\varepsilon = \sqrt{a^2 - b^2} = 521854.677(m)$, in the plane $\lambda = 0^\circ$.

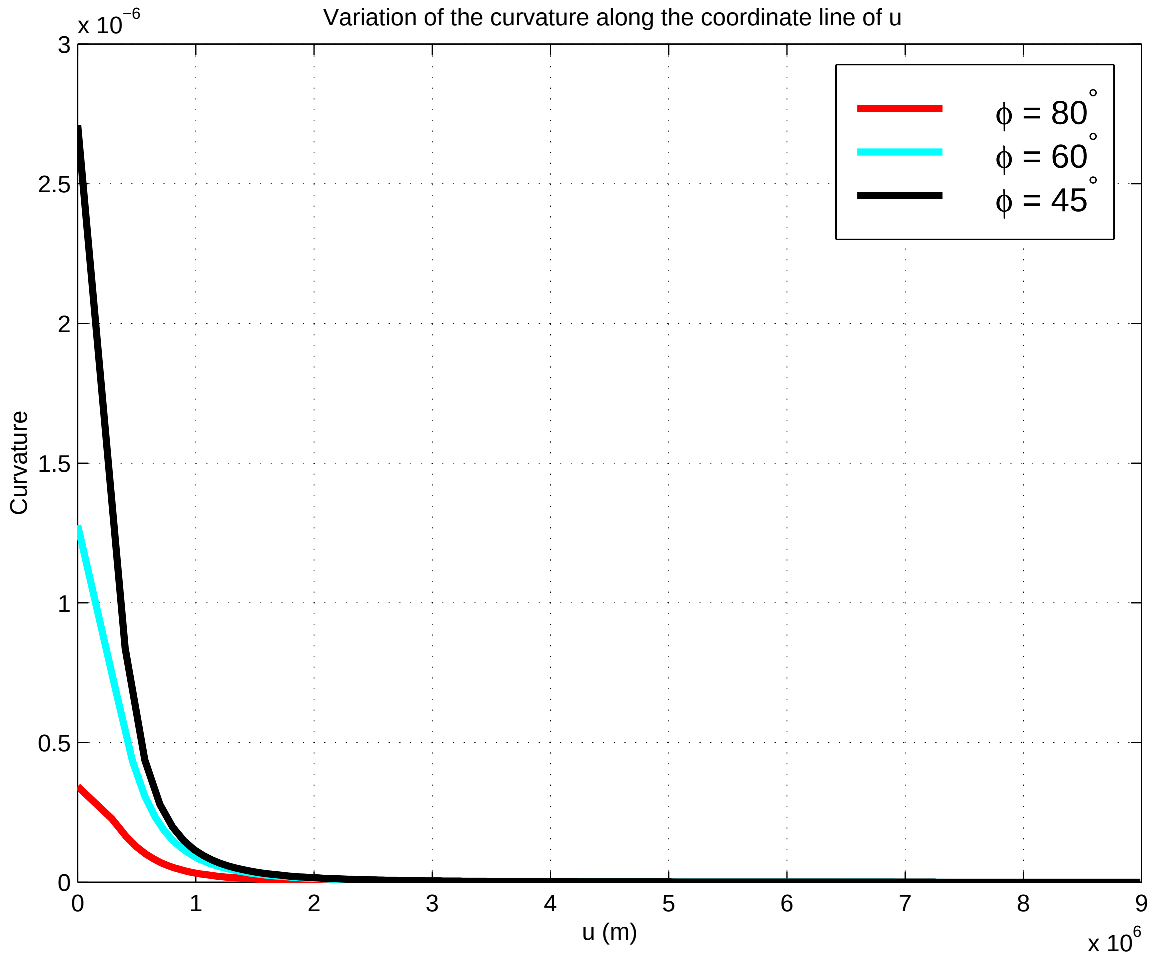

Figure A-2: Variation of the curvature of the coordinate lines $\phi = \{45^\circ, 60^\circ, 80^\circ\}$ in the plane $\lambda = 0^\circ$ verses the *Jacobi ellipsoidal coordinate u* .

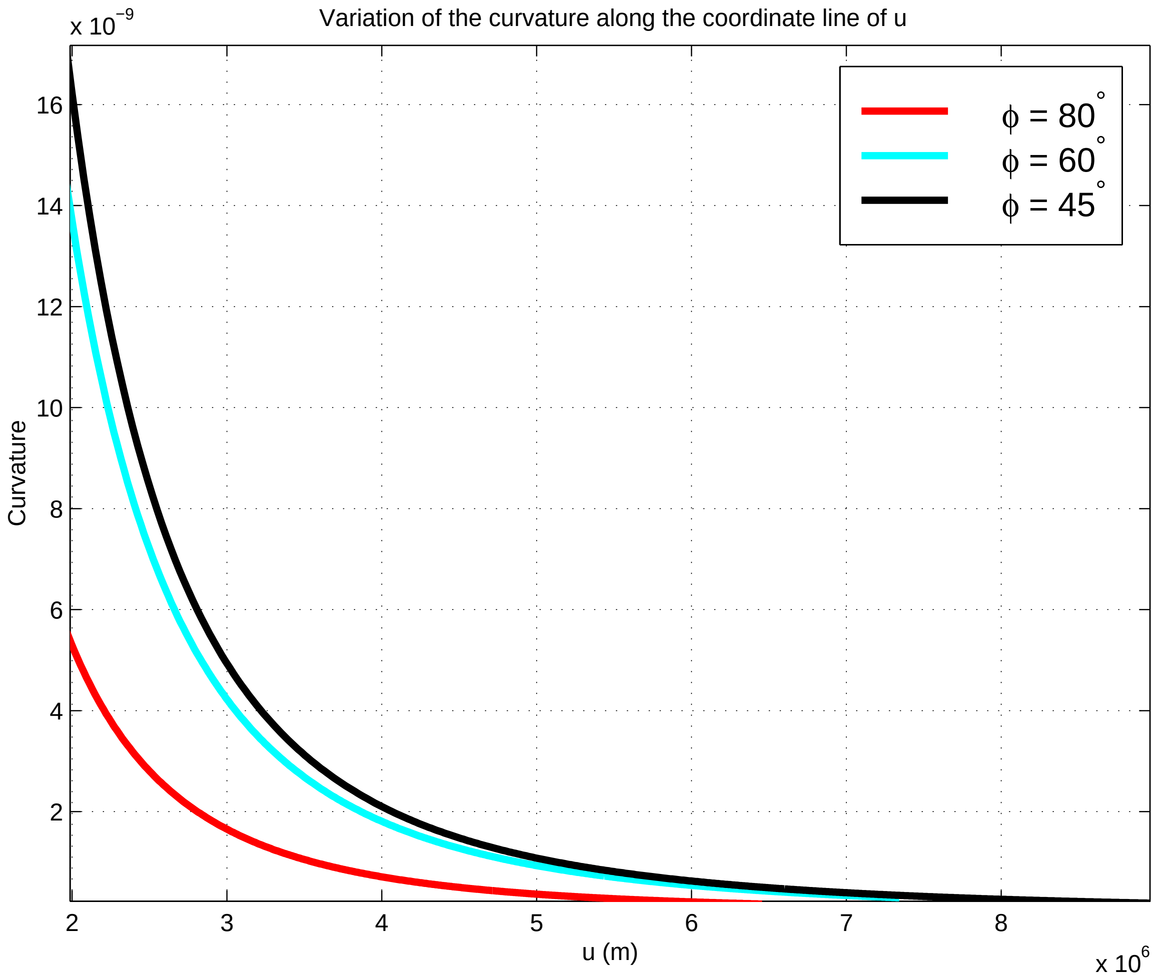

Figure A-3: Variation of the curvature of the coordinate lines $\phi = \{45^\circ, 60^\circ, 80^\circ\}$ in the plane $\lambda = 0^\circ$ verses the *Jacobi ellipsoidal coordinate* zoomed in for $u \geq 2\,000\,000\,m$.

Definition A-3: Basic geometry of *ellipsoidal coordinates* $\{\lambda, \phi, u\}$

(i) Jacobi matrix of the transformation from ellipsoidal coordinates $\{\lambda, \phi, u\}$ *into Cartesian coordinates* $\{x, y, z\}$

From equation (A.26) Jacobi matrix "J" of the transformation from ellipsoidal coordinates $\{\lambda, \phi, u\}$ into Cartesian coordinates $\{x, y, z\}$ can be constructed

$$J := \begin{bmatrix} X_\lambda & X_\phi & X_u \\ Y_\lambda & Y_\phi & Y_u \\ Z_\lambda & Z_\phi & Z_u \end{bmatrix} \tag{A.30}$$

The partial derivatives involved in (A.30) are as follows

$$\begin{gathered}
X_\lambda = D_\lambda X = -\sqrt{u^2 + \varepsilon^2} \cos\phi \sin\lambda \\
Y_\lambda = D_\lambda Y = \sqrt{u^2 + \varepsilon^2} \cos\phi \cos\lambda \\
Z_\lambda = D_\lambda Z = 0 \\
X_\phi = D_\phi X = -\sqrt{u^2 + \varepsilon^2} \sin\phi \cos\lambda \\
Y_\phi = D_\phi Y = -\sqrt{u^2 + \varepsilon^2} \sin\phi \sin\lambda \\
Z_\phi = D_\phi Z = u \cos\phi \\
X_u = D_u X = \frac{u}{\sqrt{u^2 + \varepsilon^2}} \cos\phi \cos\lambda \\
Y_u = D_u Y = \frac{u}{\sqrt{u^2 + \varepsilon^2}} \cos\phi \sin\lambda \\
Z_u = D_u Z = \sin\phi .
\end{gathered}$$

(ii) The metric tensor

$$dS^2 = [d\lambda, d\phi, du] J^* J \begin{bmatrix} d\lambda \\ d\phi \\ du \end{bmatrix} \tag{A.31}$$

$$G := J^* J \begin{bmatrix} (u^2 + \varepsilon^2)\cos^2\phi & 0 & 0 \\ 0 & u^2 + \varepsilon^2 \sin^2\phi & 0 \\ 0 & 0 & (u^2 + \varepsilon^2 \sin^2\phi)/(u^2 + \varepsilon^2) \end{bmatrix}$$

$$:= g_{nm} \quad \forall \quad n, m = 1, 2, 3 \tag{A.32}$$

(iii) Laplacian

$$\Delta = \frac{1}{\sqrt{g}}\left\{\frac{\partial}{\partial\lambda}(\frac{\sqrt{g}}{g_{11}}\frac{\partial}{\partial\lambda}) + \frac{\partial}{\partial\phi}(\frac{\sqrt{g}}{g_{22}}\frac{\partial}{\partial\phi}) + \frac{\partial}{\partial u}(\frac{\sqrt{g}}{g_{33}}\frac{\partial}{\partial u})\right\}$$

$$= \frac{1}{u^2 + \varepsilon^2 \sin^2\phi}\left\{\frac{u^2 + \varepsilon^2\sin^2\phi}{(u^2+\varepsilon^2)\cos^2\phi}\frac{\partial^2}{\partial\lambda^2} - \tan\phi\frac{\partial}{\partial\phi} \right. \tag{A.33}$$

$$\left. + \frac{\partial^2}{\partial\phi^2} + 2u\frac{\partial}{\partial u} + (u^2+\varepsilon^2)\frac{\partial^2}{\partial u^2}\right\}$$

A.1.4 Fourth variant: Mixed elliptic-trigonometric elliptic coordinates $\{\lambda, \mathrm{v}, \eta\}$

In terms of *ellipsoidal coordinates* $\{\lambda, \nu, \eta\}$, a point in space can be located as the intersection point of family of surfaces.

(i) the family of confocal, oblate spheroids

$$\mathbb{E}^2_{\varepsilon\cosh\varepsilon,\varepsilon\sinh\eta} := \left\{\mathbf{x}\in\mathbb{R}^3 \mid \frac{x^2+y^2}{\varepsilon^2\cosh^2\eta} + \frac{z^2}{\varepsilon^2\sinh^2\eta} = 1,\ \eta\in(0,+\infty),\ \varepsilon^2 := a^2-b^2\right\} \tag{A.34}$$

(ii) the family of confocal half hyperboloids

$$\mathbb{H}^2_{v,\sqrt{\varepsilon^2-v^2}} := \left\{\mathbf{x}\in\mathbb{R}^3 \mid \frac{x^2+y^2}{\mathrm{v}^2} - \frac{z^2}{\varepsilon^2-\mathrm{v}^2} = 1,\ 0<\mathrm{v}<a^2-b^2\right\} \tag{A.35}$$

(iii) the family of half planes

$$\mathbb{P}^2_{\cos\lambda,\sin\lambda} := \left\{\mathbf{x}\in\mathbb{R}^3 \mid y = x\tan\lambda,\ \lambda\in[0,2\pi]\right\} \tag{A.36}$$

According to *Figure A-4 page 222*, the longitude λ gives *orientation* to the half planes. The elliptic coordinate v is related to the *inclination* ϕ of the asymptotes of confocal half hyperboloids through $\mathrm{v} = \varepsilon\cos\phi$; the elliptic coordinate η defines the *semi-minor axis* of confocal oblate spheroids via $\varepsilon^2\cosh^2\eta$ (confocal, oblate ellipsoids of revolution).

Box A-5: Conversion of Cartesian coordinates $\{x, y, z\}$ into ellipsoidal coordinates $\{\lambda, \mathrm{v}, \eta\}$

(i) Forward transformation from ellipsoidal coordinates $\{\lambda, \mathrm{v}, \eta\}$ into Cartesian coordinates $\{x, y, z\}$

$$\begin{aligned} x &= \mathrm{v}\cosh\eta\cos\lambda \\ y &= \mathrm{v}\cosh\eta\sin\lambda \\ z &= \pm\sqrt{\varepsilon^2 - \mathrm{v}^2}\,\sinh\eta \end{aligned} \tag{A.37}$$

(ii) Backward transformation of Cartesian coordinates $\{x, y, z\}$ into ellipsoidal coordinates $\{\lambda, \mathrm{v}, \eta\}$

$$\lambda = \begin{cases} \arctan\dfrac{y}{x} & \text{for } x > 0 \text{ and } y \geq 0 \\ \arctan\dfrac{y}{x} + \pi & \text{for } x < 0 \text{ and } y \neq 0 \\ \arctan\dfrac{y}{x} + 2\pi & \text{for } x > 0 \text{ and } y < 0 \\ \dfrac{\pi}{2} & \text{for } x = 0 \text{ and } y > 0 \\ 3\dfrac{\pi}{2} & \text{for } x = 0 \text{ and } y < 0 \end{cases} \tag{A.38}$$

$$\begin{aligned} \eta = \operatorname{arccosh}\Bigg\{ & \frac{1}{2\varepsilon^2}[x^2 + y^2 + z^2 + \varepsilon^2 \\ & + \sqrt{(x^2 + y^2 + z^2 + \varepsilon^2)^2 - 4\varepsilon^2(x^2 + y^2)^2}\,]\Bigg\}^{1/2} \end{aligned} \tag{A.39}$$

$$\mathrm{v} = \sqrt{\frac{1}{2}(\varepsilon^2 + x^2 + y^2 + z^2) - \frac{1}{2}\sqrt{(\varepsilon^2 + x^2 + y^2 + z^2)^2 - 4\varepsilon^2(x^2 + y^2)}} \tag{A.40}$$

Definition A-4: Geometry of ellipsoidal coordinates $\{\lambda, \mathrm{v}, \eta\}$

(i) *Jacobi matrix of the transformation of ellipsoidal coordinates* $\{\lambda, \mathrm{v}, \eta\}$ *into Cartesian coordinates* $\{x, y, z\}$

From equation (A.37) Jacobi matrix "J" of the transformation of ellipsoidal coordinates $\{\lambda, \mathrm{v}, \eta\}$ into Cartesian coordinates $\{x, y, z\}$ can be constructed

$$J := \begin{bmatrix} X_\lambda & X_{\mathrm{v}} & X_\eta \\ Y_\lambda & Y_{\mathrm{v}} & Y_\eta \\ Z_\lambda & Z_{\mathrm{v}} & Z_\eta \end{bmatrix} \tag{A.41}$$

The partial derivatives involved in (A.41) are as bellows

$$X_\lambda = D_\lambda X = -\mathrm{v} \cosh\eta \sin\lambda$$
$$Y_\lambda = D_\lambda Y = \mathrm{v} \cosh\eta \cos\lambda$$
$$Z_\lambda = D_\lambda Z = 0$$
$$X_{\mathrm{v}} = D_{\mathrm{v}} X = \cosh\eta \cos\lambda$$
$$Y_{\mathrm{v}} = D_{\mathrm{v}} Y = \cosh\eta \sin\lambda$$
$$Z_{\mathrm{v}} = D_{\mathrm{v}} Z = -1/\sqrt{e^2 \text{-} \mathrm{v}^2}\, \mathrm{v} \sinh\eta$$
$$X_\eta = D_\eta X = \mathrm{v} \sinh\eta \cos\lambda$$
$$Y_\eta = D_\eta Y = \mathrm{v} \sinh\eta \sin\lambda$$
$$Z_\eta = D_\eta Z = \sqrt{\varepsilon^2 - \mathrm{v}^2} \cosh\eta\,.$$

(ii) The metric tensor

$$dS^2 = [d\lambda, d\mathrm{v}, d\eta] J^* J \begin{bmatrix} d\lambda \\ d\mathrm{v} \\ d\eta \end{bmatrix} \tag{A.42}$$

$$G := J^* J = \begin{bmatrix} \mathrm{v}^2 \cosh^2\eta & 0 & 0 \\ 0 & (-\mathrm{v}^2 + \varepsilon^2 \cosh^2\eta)/(\varepsilon^2 - \mathrm{v}^2) & 0 \\ 0 & 0 & -\mathrm{v}^2 + \varepsilon^2 \cosh^2\eta \end{bmatrix}$$

$$:= g_{nm} \quad \forall \quad n, m = 1, 2, 3 \tag{A.43}$$

(iii) The Laplacian

$$\Delta = \frac{1}{\sqrt{g}} \left\{ \frac{\partial}{\partial\lambda}\left(\frac{\sqrt{g}}{g_{11}} \frac{\partial}{\partial\lambda}\right) + \frac{\partial}{\partial\mathrm{v}}\left(\frac{\sqrt{g}}{g_{22}} \frac{\partial}{\partial\mathrm{v}}\right) + \frac{\partial}{\partial\eta}\left(\frac{\sqrt{g}}{g_{33}} \frac{\partial}{\partial\eta}\right) \right\}$$

$$\begin{aligned} &= \frac{1}{(\varepsilon^2 \cosh^2\eta - \mathrm{v}^2)\, \mathrm{v} \cosh\eta} \left\{ \frac{\varepsilon^2 \cosh^2\eta - \mathrm{v}^2}{\mathrm{v} \cosh\eta} \frac{\partial^2}{\partial\lambda^2} \right. \\ &\quad + (\varepsilon^2 - 2\mathrm{v}^2) \cosh\eta \frac{\partial}{\partial\mathrm{v}} + (\varepsilon^2 - \mathrm{v}^2)\, \mathrm{v} \cosh\eta \frac{\partial^2}{\partial\mathrm{v}^2} \\ &\quad \left. + \mathrm{v} \sinh\eta \frac{\partial}{\partial\eta} + \mathrm{v} \cosh\eta \frac{\partial^2}{\partial\eta^2} \right\} \end{aligned} \tag{A.44}$$

Figure A-4: Ellipsoidal Coordinates $\{\lambda, \mu, \nu\}$, characterised by the coordinate surfaces of the type: *(i)* Spheroids (μ = const.), *(ii)* half hyperboloids of one sheet (ν = cost.) and, *(iii)* half planes (λ = const.).

Ellipsoidal Coordinates $\{\lambda, \phi, \eta\}$, characterised by the coordinate surfaces of the type: *(i)* Spheroids (η = const.), *(ii)* half hyperboloids of one sheet (ϕ = cost.) and, *(iii)* half planes (λ = const.).

Ellipsoidal Coordinates $\{\lambda, \phi, u\}$, characterised by the coordinate surfaces of the type: *(i)* Spheroids (u = const.), *(ii)* half hyperboloids of one sheet (ϕ = const.) and, *(iii)* half planes (λ = const.).

Ellipsoidal Coordinates $\{\lambda, \mathrm{v}, \eta\}$, characterised by the coordinate surfaces of the type: *(i)* Spheroids (η = const.), *(ii)* half hyperboloids of one sheet (v = const.) and, *(iii)* half planes (λ = const.).

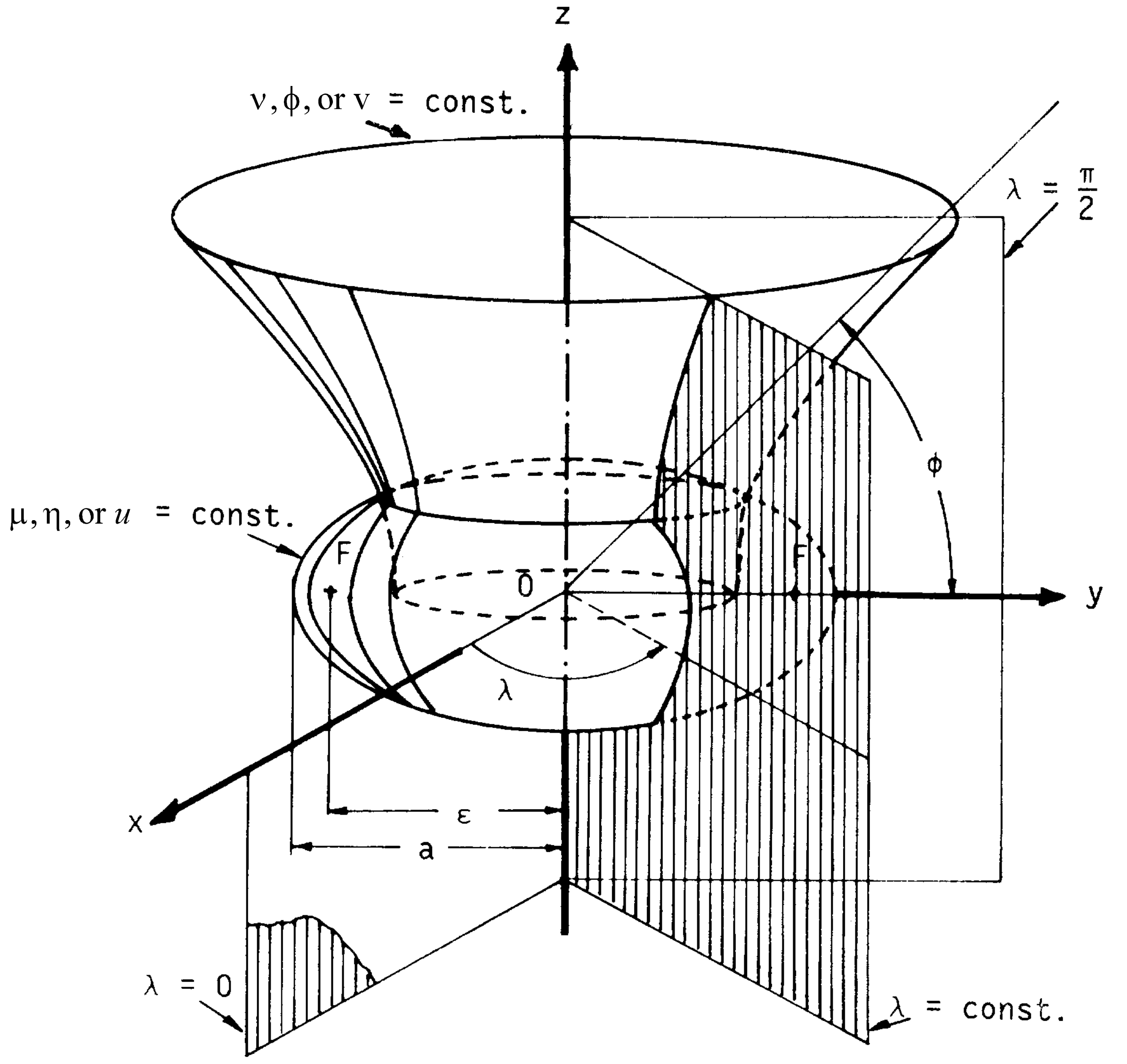

A.2 Gauss ellipsoidal coordinates

A.2.1 1st variant: Geodetic coordinates {L, B, H}

In terms of *Gauss ellipsoidal coordinates,* a point in 3-D space is identified by intersection of a plane and a reference ellipsoid and a vertical distance from the reference ellipsoid $\mathbb{E}^2_{a,b}$. *Box A-6* defines the *Gauss* ellipsoidal coordinates through their relation with the Cartesian coordinates $\{x, y, z\}$.

Box A-6: forward and backward transformation of *Gauss ellipsoidal coordinates* $\{L, B, H\}$ into Cartesian coordinates $\{x, y, z\}$

"Forward transformation"

$$\begin{cases} x = [\dfrac{a}{\sqrt{1-e^2\sin^2 B}} + H(L,B)]\cos B\cos L \\ y = [\dfrac{a}{\sqrt{1-e^2\sin^2 B}} + H(L,B)]\cos B\sin L \\ z = [\dfrac{a(1-e^2)}{\sqrt{1-e^2\sin^2 B}} + H(L,B)]\sin B \end{cases} \tag{A.45}$$

In (A.45) $e := \sqrt{a^2 - b^2}/a$ is the relative eccentricity.

"Backward transformation"

$$L = \arctan Y/X \begin{cases} \operatorname{sgn} X = +, \operatorname{sgn} Y = + : 0 \le L < \pi/2 \\ \operatorname{sgn} X = -, \operatorname{sgn} Y = + : \pi/2 \le L < \pi \\ \operatorname{sgn} X = -, \operatorname{sgn} Y = - : \pi \le L < 3\pi/2 \\ \operatorname{sgn} X = +, \operatorname{sgn} Y = - : 3\pi/2 \le L < 2\pi \end{cases} \tag{A.46}$$

The other two components i.e. B, H can be derived either by Newton iteration *or* by solution of a system of algebraic equations *or* using closed formulae of *M. Heikkinen* (1982). *E. Grafarend and J. Engels* (1992a, 1992b) have developed series expansion for the height function *H (L, B)* in terms of a set of orthonormal functions on $\mathbb{E}^2_{a,b}$.

A.2.2 2nd variant: Normal-geodetic coordinates {L, B, H_N}

The normal geodetic coordinates $\{L, B, H_N\}$ are the same as geodetic coordinates $\{L, B, H\}$ except that the height component H_N here refers to reference gravity field. In fact, in terms of normal geodetic coordinates $\{L, B, H_N\}$, in contrast to geodetic coordinates, the height component H_N is measured along the normal plumb line down to the surface of quasi-geod (see *Figure A-5*).

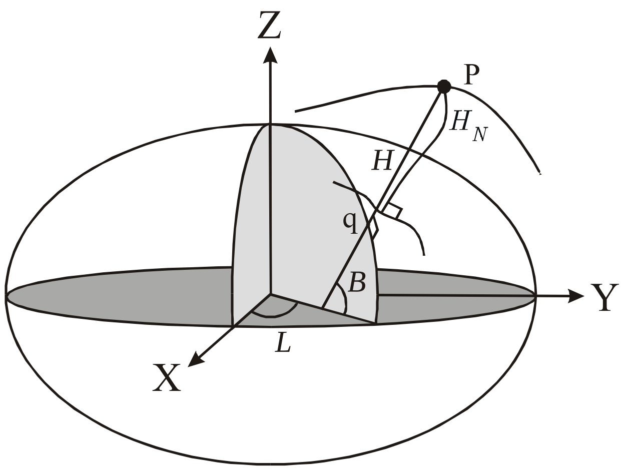

Figure A-5: Geodetic coordinates $\{L, B, H\}$ versus normal-geodetic coordinates $\{L, B, H_N\}$. H is measured along the ellipsoidal normal while H_N is a length along normal plumb line down to the surface of quasi-geoid.

A.3 Direct transformation between Gauss ellipsoidal coordinates and Jacobi ellipsoidal coordinates

According to *E. Grafarend et al.* (1999), following relations between *Gauss ellipsoidal coordinates* $\{L, B, H\}$ and *Jacobi ellipsoidal coordinates* $\{\lambda, \phi, u\}$ exists.

(i) *Forward transformation* $\{\lambda, \phi, u\} \mapsto \{L, B, H\}$

$$\lambda = L \tag{A.47}$$

$$\phi = \arctan(\sqrt{1-e^2}\tan B) \tag{A.48}$$

$$u = \frac{1}{\sqrt{1-e^2}} \cos B \left[\frac{a(1-e^2)}{(1-e^2 \sin^2 B)^{1/2}} + H \right] \left[1 + (1-e^2) \tan^2 B \right]^{1/2} \tag{A.49}$$

(ii) Backward transformation $\{\lambda, \phi, u\} \mapsto \{L, B, H\}$

$$L = \lambda \tag{A.50}$$

$$B = \arctan\left(\frac{1}{\sqrt{1-e^2}} \tan \phi\right) \tag{A.51}$$

$$H = \sqrt{1-e^2} u \cos(\phi)[1 + \frac{1}{1-e^2} \tan^2 \phi]^{1/2} - a(1-e^2) \left[1 - e^2 \frac{\tan^2 \phi}{1-e^2 + \tan^2 \phi} \right]^{-1/2} \tag{A.52}$$

Appendix B: Eigenspace solution of 3-D Laplace differential equation of gravitational field of the earth

Jacobi ellipsoidal coordinates enjoy the property of decomposing the three-dimensional *Laplace* partial differential equation into separable functions. In the next sections, a summary of the ellipsoidal eigenvalue/eigenfunction solution of *Laplace* differential equation for Jacobi ellipsoidal coordinates of the types $\{\lambda, \phi, \eta\}$ and $\{\lambda, \phi, u\}$ will be presented.

B.1 In terms of Jacobi ellipsoidal coordinates $\{\lambda, \phi, \eta\}$

(i) Laplace differential equation

$$\begin{aligned} \Delta U(\lambda, \phi, \eta) = \frac{1}{\varepsilon^2(\sin^2 \phi + \sinh^2 \eta)} \left\{ \frac{\sin^2 \phi + \sinh^2 \eta}{\cos^2 \phi \cosh^2 \eta} \frac{\partial^2}{\partial \lambda^2} - \tan \phi \frac{\partial}{\partial \phi} \right. \\ \left. + \frac{\partial^2}{\partial \phi^2} + \tanh \eta \frac{\partial}{\partial \eta} + \frac{\partial^2}{\partial \eta^2} \right\} U = 0 \end{aligned} \tag{B.1}$$

(ii) Multiplicative decomposition

$$U(\lambda, \phi, \eta) = \Lambda(\lambda)\Phi(\phi)H(\eta) \tag{B.2}$$

(iii) Separated ordinary differential equations

$$\begin{cases} \dfrac{d^2\Lambda}{d\lambda^2} + \alpha_1\Lambda = 0 \\ \dfrac{d^2\Phi}{d\phi^2} - \tan\phi\dfrac{d\Phi}{d\phi} + (-\dfrac{\alpha_1}{\cos^2\phi} + \alpha_2)\Phi = 0 \\ \dfrac{d^2H}{d\eta^2} + \tanh\eta\dfrac{dH}{d\eta} + (\dfrac{\alpha_1}{\cosh^2\eta} - \alpha_2)H = 0 \end{cases} \tag{B.3}$$

(iv) Eigen-conditions

$$\begin{cases} U(2\pi,\phi,\eta) = U(0,\phi,\eta) \\ \left|U(\lambda,\phi,\eta)\right| < \infty \\ \lim\limits_{\eta\to\infty} U(\lambda,\phi,\eta) = 0 \end{cases} \tag{B.4}$$

Or equivalently

$$\begin{cases} \Lambda(2\pi) = \Lambda(0) \\ \left|\Lambda(\lambda)\right| < \infty \\ \left|\Phi(\phi)\right| < \infty \\ \left|H(\eta)\right| < \infty \\ \lim\limits_{\eta\to\infty} H(\eta) = 0 \end{cases} \tag{B.5}$$

(v) Eigenvalue-eigenfunction solutions

$$\begin{cases} \Lambda(\lambda) = \sum\limits_{m=0}^{\infty}(u_m \cos m\lambda + v_m \sin m\lambda) \quad \forall\ m = \sqrt{\alpha_1} \ \wedge\ m \in \mathbb{N} \\ \Phi(\sin\phi) = \sum\limits_{n=0}^{\infty}\sum\limits_{m=0}^{n} u_{nm}\, P_{nm}(\sin\phi) \qquad \forall\ n(n+1) = \alpha_2 \ \wedge\ n,m \in \mathbb{N}_0 \\ H(\eta) = \sum\limits_{n=0}^{\infty}\sum\limits_{m=0}^{n} u_{nm} Q_{nm}(i\sinh\eta) \end{cases} \tag{B.6}$$

(vi) General eigenvalue-eigenfunction solution

$$U(\lambda,\phi,\eta) = \sum_{n=0}^{\infty}\sum_{m=-n}^{n} u_{nm} Q_{n|m|}(i\sinh\eta) e_{nm}(\lambda,\phi) \tag{B.7}$$

Where the surface ellipsoidal harmonics $e_{nm}(\lambda,\phi)$ are defined as

$$e_{nm}(\lambda,\phi) = P^{*}_{n|m|}(\sin\phi)\begin{bmatrix} \cos m\lambda & \forall m \geq 0 \\ \sin|m|\lambda & \forall m < 0 \end{bmatrix} \tag{B.8}$$

B.2 In terms of Jacobi ellipsoidal coordinates $\{\lambda,\phi,u\}$

(i) Laplace differential equation

$$\Delta U(\lambda,\phi,u) = \frac{1}{u^2+\varepsilon^2\sin^2\phi}\left\{\frac{u^2+\varepsilon^2\sin^2\phi}{(u^2+\varepsilon^2)\cos^2\phi}\frac{\partial^2}{\partial\lambda^2} - \tan\phi\frac{\partial}{\partial\phi} + \frac{\partial^2}{\partial\phi^2}\right.$$
$$\left. +2u\frac{\partial}{\partial u} + (u^2+\varepsilon^2)\frac{\partial^2}{\partial u^2}\right\}U = 0 \tag{B.9}$$

(ii) Multiplicative decomposition

$$U(\lambda,\phi,u) = \Lambda(\lambda)\Phi(\phi)H(u) \tag{B.10}$$

(iii) Separated ordinary differential equations

$$\begin{cases} \dfrac{d^2\Lambda}{d\lambda^2} + \alpha_1\Lambda = 0 \\ \dfrac{d^2\Phi}{d\phi^2} - \tan\phi\dfrac{d\Phi}{d\phi} + (-\dfrac{\alpha_1}{\cos^2\phi} + \alpha_2)\Phi = 0 \\ (u^2+\varepsilon^2)\dfrac{d^2H}{du^2} + 2u\dfrac{dH}{du} + (\dfrac{\varepsilon^2\alpha_1}{u^2+\varepsilon^2} - \alpha_2)H = 0 \end{cases} \tag{B.11}$$

(iv) Eigen-conditions

$$\begin{cases} U(2\pi,\phi,u) = U(0,\phi,u) \\ |U(\lambda,\phi,u)| < \infty \\ \lim\limits_{u\to\infty} U(\lambda,\phi,u) = 0 \end{cases} \tag{B.12}$$

Or equivalently

$$\begin{cases} \Lambda(2\pi) = \Lambda(0) \\ |\Lambda(\lambda)| < \infty \\ |\Phi(\phi)| < \infty \\ |H(u)| < \infty \\ \lim\limits_{u\to\infty} H(u) = 0 \end{cases} \tag{B.13}$$

(v) Eigenvalue-eigenfunction solutions

$$\begin{cases} \Lambda(\lambda) = \sum_{m=0}^{\infty} (u_m \cos m\lambda + v_m \sin m\lambda) & \forall\ m = \sqrt{\alpha_1} \ \wedge \ m \in \mathbb{N} \\ \Phi(\sin\phi) = \sum_{n=0}^{\infty} \sum_{m=0}^{n} u_{nm} P_{nm}(\sin\phi) & \forall\ n(n+1) = \alpha_2 \ \wedge \ n,m \in \mathbb{N}_0 \\ H(u) = \sum_{n=0}^{\infty} \sum_{m=0}^{n} u_{nm} Q_{nm}(i\frac{u}{\varepsilon}) & \end{cases} \tag{B.14}$$

(vi) General eigenvalue-eigenfunction solution

$$U(\lambda,\phi,u) = \sum_{n=0}^{\infty} \sum_{m=-n}^{n} u_{nm} Q_{n|m|}(i\frac{u}{\varepsilon}) e_{nm}(\lambda,\phi) \tag{B.15}$$

Where the surface ellipsoidal harmonics $e_{nm}(\lambda,\phi)$ are defined as

$$e_{nm}(\lambda,\phi) = P^*_{n|m|}(\sin\phi) \begin{bmatrix} \cos m\lambda & \forall m \geq 0 \\ \sin|m|\lambda & \forall m < 0 \end{bmatrix} \tag{B.16}$$

The normalised associated *Legendre* functions of the first kind $P^*_{nm}(\sin\phi)$, as well as of the second kind $Q^*_{nm}(\sinh\eta)$as they appear in (B.7), (B.8), (B.15)and (B.16) will be defined in the next section.

Appendix C: Normalised associated Legendre functions of the first and second kind

We define the normalised *associated Legendre functions of the first kind* $P^*_{nm}(\sin\phi)$ by the recurrence relations

$$P^*_{nn}(\sin\phi) = \frac{\sqrt{2n+1}}{\sqrt{2n}} \cos\phi \, P^*_{n-1,n-1}(\sin\phi) \tag{C.1}$$

$$P^*_{n,n-1}(\sin\phi) = \frac{\sqrt{2n+1}}{\sqrt{2(n-1)}} \cos\phi \, P^*_{n-1,n-2}(\sin\phi) \tag{C.2}$$

$$\begin{aligned} P^*_{nm}(\sin\phi) = {} & \frac{\sqrt{4n^2-1}}{\sqrt{n^2-m^2}} \sin\phi \, P^*_{n-1,m}(\sin\phi) \\ & - \frac{\sqrt{(2n+1)(n+m-1)(n-m-1)}}{\sqrt{(n^2-m^2)(2n-3)}} P^*_{n-2,m}(\sin\phi) \end{aligned} \tag{C.3}$$

subject to

$$\forall n \in [3, \infty) \text{ and } m \in [0, n-2]$$

with start up values

$$P_{00}^*(\sin\phi) = 1 \tag{C.4}$$

$$P_{10}^*(\sin\phi) = \sqrt{3}\sin\phi \tag{C.5}$$

$$P_{11}^*(\sin\phi) = \sqrt{3}\cos\phi \tag{C.6}$$

$$P_{20}^*(\sin\phi) = \frac{\sqrt{5}}{2}(3\sin^2\phi - 1) \tag{C.7}$$

$$P_{21}^*(\sin\phi) = \sqrt{15}\sin\phi\cos\phi \tag{C.8}$$

$$P_{22}^*(\sin\phi) = \frac{\sqrt{15}}{2}\cos^2\phi \tag{C.9}$$

Let us define the normalised *associated Legendre functions of the first kind* $P_{nm}^*(\sinh\eta)$ through an integral equation

$$P_{nm}^*(\sinh\eta) := i^{-n} P_{nm}(i\sinh\eta) \tag{C.10}$$

$$P_{nm}(i\sinh\eta) = i^n \frac{(n+m)!}{\pi n!} \int_0^\pi (\sinh\eta + \cosh\eta\cos\phi)^n \cos m\phi\, d\phi \tag{C.11}$$

where $i = \sqrt{-1}$ is the imaginary unit. First few normalised *associated Legendre functions of the first kind* $P_{nm}^*(\sinh\eta)$ for $n = 0, 1, 2$ and $m = 0$ are as follows.

$$P_0^*(\sinh\eta) = 1 \tag{C.12}$$

$$P_1^*(\sinh\eta) = \sinh\eta \tag{C.13}$$

$$P_2^*(\sinh\eta) = \frac{1}{2}(3\sinh^2\eta + 1) \tag{C.14}$$

The *associated Legendre functions of the second kind* can be defined by an integral relation of the type

$$Q_{nm}^*(\sinh\eta) = i^{n+1} Q_{nm}(i\sinh\eta) \tag{C.15}$$

$$Q_{nm}(i\sinh\eta) = \frac{(-1)^m 2^n (n+m)!\, m!}{i^{n+1}(n-m)!(2m)!}(\cosh\eta)^m \cdot \int_0^\infty \frac{\sinh^{2m}\tau\, d\tau}{(\sinh\eta + \cosh\eta\cosh\tau)^{n+m+1}} \tag{C.16}$$

with starting values for $n = 0, 1, 2$ and $m = 0$

$$Q_0^*(\sinh\eta) = \operatorname{arc\,cot}(\sinh\eta) \tag{C.17}$$

$$Q_1^*(\sinh\eta) = 1 - \sinh\eta\, \operatorname{arc\,cot}(\sinh\eta) \tag{C.18}$$

$$Q_2^*(\sinh\eta) = \frac{1}{2}[(3\sinh^2\eta + 1)\operatorname{arc\,cot}(\sinh\eta) - 3\sinh\eta] \tag{C.19}$$

■

Instead of the above integral formulas, in practice the associated Legendre functions of the second kind are better to be calculated via the recursive relations which enjoy the numerical stable, especially for the higher degree and order functions (*N. Thong and E. Grafarend*, 1989, *G. Sona*, 1996)

$$Q^*_{n|m|}(\sinh\eta) = \sum_{k=0}^{k_{\max}} Q^*_{n|m|k}(\eta) \tag{C.20}$$

$$Q^*_{n|m|k}(\eta) = \frac{(1-n-|m|-2k)(n+|m|+2k)}{2k(2n+2k+1)\sinh^2\eta} Q^*_{n|m|k-1}(\eta) \qquad \forall\, k \geq 1 \tag{C.21}$$

$$Q^*_{n|m|0}(\eta) = \cosh^{|m|}\eta\left(\frac{\cosh\eta_0}{\sinh\eta}\right)^{n+1} \qquad \forall\, n \in \mathcal{N},\, m \in [-n,n] \subset \mathbb{Z} \tag{C.22}$$

The summation (C.20) is continued until

$$Q^*_{n|m|k_{\max}}(\eta) - Q^*_{n|m|k_{\max-1}}(\eta) < \sigma \tag{C.23}$$

where σ indicates the numerical accuracy limit. For double precision accuracy, σ =1E–16 may be adopted.

Appendix D: External Dirichlet problem of Laplace equation with boundary data on the ellipsoid of revolution

D.1 In terms of Jacobi ellipsoidal coordinates $\{\lambda,\phi,\eta\}$

Definition of the problem:

(i) Field differential equation

$$\Delta U(\mathbf{x}) = 0 \;\; \forall \mathbf{x} \in \mathbb{R}^3 / \mathbb{E}^2_{a\,b} \tag{D.1}$$

(i.e., $\forall \mathbf{x} \in$ external points of the reference ellipsoid $\mathbb{E}^2_{a,b}$)

(ii) Eigen-conditions

$$\begin{cases} U(2\pi, \phi, \eta) = U(0, \phi, \eta) \\ |U(\lambda, \phi, \eta)| < \infty \\ \lim\limits_{u \to \infty} U(\lambda, \phi, \eta) = 0 \end{cases} \tag{D.2}$$

(iii) Boundary values

$$U(\mathbf{X}) = f(\lambda, \phi) \qquad \forall \mathbf{X} \in \mathbb{E}^2_{a,b} \tag{D.3}$$

Solution steps:

(i) Eigenvalue/eigenfunction solution of external gravitational field of the earth, in terms of ellipsoidal coordinates $\{\lambda, \phi, \eta\}$ according to

$$U(\lambda, \phi, \eta) = \sum_{n=0}^{\infty} \sum_{m=-n}^{n} u_{nm} Q_{n|m|}(i \sinh \eta) e_{nm}(\lambda, \phi) \tag{D.4}$$

(ii) At the surface of reference ellipsoid $\mathbb{E}^2_{a,b}$

$$\sum_{n=0}^{\infty} \sum_{m=-n}^{n} u_{nm} Q_{n|m|}(i \sinh \eta_0) e_{nm}(\lambda, \phi) = f(\lambda, \phi) \tag{D.5}$$

(iii) Using the weighted orthonormality of ellipsoidal harmonics

$$u_{nm} = \frac{1}{Q_{n|m|}(i \sinh \eta_0)} \frac{1}{S} \int_{\mathbb{E}^2_{a,b}} w(\phi') f(\lambda', \phi') e_{nm}(\lambda', \phi') dS' \tag{D.6}$$

where the local area element

$$dS' = d\{\text{area } (\mathbb{E}^2_{a,b})\} = a \cdot \sqrt{b^2 + \varepsilon^2 \sin^2 \phi'} \cos \phi' d\lambda' d\phi' \tag{D.7}$$

global area element

$$S = \text{area } (\mathbb{E}^2_{a,b}) = 4\pi a \cdot \left\{ \frac{1}{2} + \frac{1}{4} \frac{b^2}{a\varepsilon} \ln \frac{a + \varepsilon}{a - \varepsilon} \right\} \tag{D.8}$$

and the weight function

$$w(\phi) := \frac{a}{\sqrt{b^2 + \varepsilon^2 \sin^2 \phi}} \left(\frac{1}{2} + \frac{1}{4} \frac{b^2}{a\varepsilon} \cdot \ln \frac{a + \varepsilon}{a - \varepsilon} \right) \tag{D.9}$$

(iv) Solution of the ellipsoidal Dirichlet boundary value problem

$$U(\lambda, \phi, \eta) = \sum_{n=0}^{\infty} \sum_{m=-n}^{n} \frac{Q_{n|m|}(i \sinh \eta)}{Q_{n|m|}(i \sinh \eta_0)} \frac{1}{S} \int_{\mathbb{E}^2_{a,b}} dS' w(\phi') f(\lambda', \phi') e_{nm}(\lambda', \phi') e_{nm}(\lambda, \phi) \tag{D.10}$$

(v) Ellipsoidal Abel-Poisson integral

$$U(\lambda,\phi,\eta) = \int_{\mathbb{E}^2_{a,b}} dS' \frac{w(\phi')}{S} \sum_{n=0}^{\infty} \sum_{m=-n}^{n} \frac{Q_{n|m|}(i\sinh\eta)}{Q_{n|m|}(i\sinh\eta_0)}$$
$$\times e_{nm}(\lambda',\phi')e_{nm}(\lambda,\phi)f(\lambda',\phi') \quad \text{(D.11)}$$
$$= \int_{\mathbb{E}^2_{a,b}} dS' K(\lambda,\phi,\eta;\lambda',\phi',\eta_0)f(\lambda',\phi')$$

Where to reach (D.11) from (D.10) we have interchanged the integral and summation signs which is justified by the uniform convergent property of the series (D.4) in the domain $\mathbb{R}^3/\mathbb{E}^2_{a\,b}$.

(vi) Abel-Poisson Kernel

$$K(\lambda,\phi,\eta;\lambda',\phi',\eta_0) = \frac{w(\phi')}{S} \sum_{n=0}^{\infty} \sum_{m=-n}^{n} \frac{Q_{n|m|}(i\sinh\eta)}{Q_{n|m|}(i\sinh\eta_0)} e_{nm}(\lambda',\phi')e_{nm}(\lambda,\phi)$$
(D.12)

D.2 In terms of Jacobi ellipsoidal coordinates $\{\lambda,\phi,u\}$

Definition of the problem:

(i) Field differential equation

$$\Delta U(\mathbf{x}) = 0 \quad \forall \mathbf{x} \in \mathbb{R}^3/\mathbb{E}^2_{a\,b} \quad \text{(D.13)}$$

(i.e., $\mathbf{x} \in$ external space of the reference ellipsoid $\mathbb{E}^2_{a,b}$)

(ii) Eigen-conditions

$$\begin{cases} U(2\pi,\phi,u) = U(0,\phi,u) \\ |U(\lambda,\phi,u)| < \infty \\ \lim\limits_{u\to\infty} U(\lambda,\phi,u) = 0 \end{cases} \quad \text{(D.14)}$$

(iii) Boundary values

$$U(\mathbf{X}) = f(\lambda,\phi) \qquad \forall \mathbf{X} \in \mathbb{E}^2_{a,b} \quad \text{(D.15)}$$

Solution steps:

(i) Eigenvalue/eigenfunction solution of external gravitational field of the earth, in terms of ellipsoidal coordinates $\{\lambda,\phi,u\}$ according to

$$U(\lambda,\phi,u) = \sum_{n=0}^{\infty}\sum_{m=-n}^{n} u_{nm} Q_{n|m|}(i\frac{u}{\varepsilon}) e_{nm}(\lambda,\phi) \tag{D.16}$$

(ii) At the surface of reference ellipsoid $\mathbb{E}^2_{a,b}$

$$\sum_{n=0}^{\infty}\sum_{m=-n}^{n} u_{nm} Q_{n|m|}(i\frac{b}{\varepsilon}) e_{nm}(\lambda,\phi) = f(\lambda,\phi) \tag{D.17}$$

(iii) Using the weighted orthonormality of ellipsoidal harmonics we have

$$u_{nm} = \frac{1}{Q_{n|m|}(i\frac{b}{\varepsilon})}\frac{1}{S}\int_{\mathbb{E}^2_{a,b}} w(\phi')f(\lambda',\phi')e_{nm}(\lambda',\phi')dS' \tag{D.18}$$

where the local area element

$$dS' = d\{\text{area } (\mathbb{E}^2_{a,b})\} = a\cdot\sqrt{b^2+\varepsilon^2\sin^2\phi'}\cos\phi' d\lambda' d\phi' \tag{D.19}$$

global area element

$$S = \text{area } (\mathbb{E}^2_{a,b}) = 4\pi a\cdot\left\{\frac{1}{2}+\frac{1}{4}\frac{b^2}{a\varepsilon}\ln\frac{a+\varepsilon}{a-\varepsilon}\right\} \tag{D.20}$$

and the weight function

$$w(\phi) := \frac{a}{\sqrt{b^2+\varepsilon^2\sin^2\phi}}\left(\frac{1}{2}+\frac{1}{4}\frac{b^2}{a\varepsilon}\cdot\ln\frac{a+\varepsilon}{a-\varepsilon}\right) \tag{D.21}$$

(iv) Solution of the ellipsoidal Dirichlet boundary value problem

$$U(\lambda,\phi,u) = \sum_{n=0}^{\infty}\sum_{m=-n}^{n} \frac{Q_{n|m|}(i\frac{u}{\varepsilon})}{Q_{n|m|}(i\frac{b}{\varepsilon})}\frac{1}{S}\int_{\mathbb{E}^2_{a,b}} dS' w(\phi')f(\lambda',\phi')e_{nm}(\lambda',\phi')e_{nm}(\lambda,\phi) \tag{D.22}$$

(v) Ellipsoidal Abel-Poisson integral

$$\begin{aligned} U(\lambda,\phi,u) &= \int_{\mathbb{E}^2_{a,b}} dS'\left(\frac{w(\phi')}{S}\sum_{n=0}^{\infty}\sum_{m=-n}^{n}\frac{Q_{n|m|}(i\frac{u}{\varepsilon})}{Q_{n|m|}(i\frac{b}{\varepsilon})}e_{nm}(\lambda',\phi')e_{nm}(\lambda,\phi)\right)f(\lambda',\phi') \\ &= \int_{\mathbb{E}^2_{a,b}} dS' K(\lambda,\phi,u;\lambda',\phi',b)f(\lambda',\phi') \end{aligned} \tag{D.23}$$

Where to reach (D.23) from (D.22) we have interchanged the integral and summation signs which is justified by the uniform convergent property of the series (D.4) in the domain $\mathbb{R}^3/\mathbb{E}^2_{a,b}$.

(iv) Abel-Poisson Kernel

$$K(\lambda,\phi,u;\lambda',\phi',b) = \frac{w(\phi')}{S}\sum_{n=0}^{\infty}\sum_{m=-n}^{n} \frac{Q_{n|m|}(i\frac{u}{\varepsilon})}{Q_{n|m|}(i\frac{b}{\varepsilon})} e_{nm}(\lambda',\phi') e_{nm}(\lambda,\phi) \quad \text{(D.24)}$$

Appendix E: The Hesse matrix of minimum distance mapping of the surface of the earth onto the telluroid

Here we shall present the *Hesse matrix* $\mathbf{H}_{\mathbb{L}}$ of second derivatives of the minimisation problem (4.1) as follows.

$$\mathbf{H}_{\mathbb{L}} = \frac{\partial^2 L}{\partial x_i \partial x_j} = \begin{bmatrix} \frac{\partial^2 L}{\partial x_1{}^2} & \frac{\partial^2 L}{\partial x_1 x_2} & \frac{\partial^2 L}{\partial x_1 x_3} \\ \frac{\partial^2 L}{\partial x_2 x_1} & \frac{\partial^2 L}{\partial x_2{}^2} & \frac{\partial^2 L}{\partial x_2 x_3} \\ \frac{\partial^2 L}{\partial x_3 x_1} & \frac{\partial^2 L}{\partial x_3 x_2} & \frac{\partial^2 L}{\partial x_3{}^2} \end{bmatrix} \quad \text{(E.1)}$$

where

$$\frac{\partial^2 L}{\partial x_1{}^2} = 2(x_3{}^2 + \varepsilon^2)^{1/2} \cos x_2 (x_p \cos x_1 + y_p \sin x_1)$$

$$\frac{\partial^2 L}{\partial x_1 x_2} = 2(x_3{}^2 + \varepsilon^2)^{1/2} \sin x_2 (- x_p \sin x_1 + y_p \cos x_1)$$

$$\frac{\partial^2 L}{\partial x_1 x_3} = -2x_3 \cos x_2 (- x_p \sin x_1 + y_p \cos x_1) / (x_3{}^2 + \varepsilon^2)^{1/2}$$

$$\frac{\partial^2 L}{\partial x_2 x_1} = \frac{\partial^2 L}{\partial x_1 x_2}$$

$$\frac{\partial^2 L}{\partial {x_2}^2}=2({x_3}^2+\varepsilon^2)(\sin x_2)x_3{}^2(\cos x_1)^2+2(x_p$$
$$-({x_3}^2+\varepsilon^2)^{1/2}\cos x_2\cos x_1)({x_3}^2+\varepsilon^2)^{1/2}\cos x_2\cos x_1$$
$$+2({x_3}^2+\varepsilon^2)(\sin x_2)^2(\sin x_1)^2$$
$$+2(y_p-({x_3}^2+\varepsilon^2)^{1/2}\cos x_2\sin x_1)({x_3}^2+\varepsilon^2)^{1/2}\cos x_2\sin x_1$$
$$+2{x_3}^2\cos {x_2}^2+2(z_p-x_3\sin(x_2)x_3\sin x_2$$
$$+x_4(\Omega^2a^2((3{x_3}^2/\varepsilon^2+1)\mathrm{acot}(x_3/\varepsilon)$$
$$-3x_3/\varepsilon)/((3b^2/\varepsilon^2+1)\mathrm{acot}(b/\varepsilon)-3b/\varepsilon)(\cos x_2)^2$$
$$-\Omega^2a^2((3{x_3}^2/\varepsilon^2+1)\mathrm{acot}(x_3/\varepsilon)$$
$$-3x_3/\varepsilon)/((3b^2/\varepsilon^2+1)\mathrm{acot}(b/\varepsilon)-3b/\varepsilon)(\sin x_2)^2$$
$$+\Omega^2({x_3}^2+\varepsilon^2)(\sin x_2)^2$$
$$-\Omega^2({x_3}^2+\varepsilon^2)(\cos x_2)^2)$$
$$\frac{\partial^2 L}{\partial x_2 x_3}=-2\cos x_2(\cos x_1)^2x_3\sin x_2$$
$$+2(x_p-({x_3}^2+\varepsilon^2)^{1/2}\cos x_2\cos x_1)/({x_3}^2+\varepsilon^2)^{1/2}\sin x_2\cos(x_1)x_3$$
$$-2\cos x_2(\sin x_1)^2x_3\sin x_2+2(y_p-({x_3}^2+\varepsilon^2)^{1/2}\cos x_2\sin x_1)/({x_3}^2$$
$$+\varepsilon^2)^{1/2}\sin x_2\sin(x_1)x_3+2\sin(x_2)x_3\cos x_2-2(z_p-x_3\sin x_2)\cos x_2$$
$$+x_4(\Omega^2a^2(6x_3/\varepsilon^2\mathrm{acot}(x_3/\varepsilon)-(3{x_3}^2/\varepsilon^2+1)/\varepsilon/(1+{x_3}^2/\mathrm{e}^2)$$
$$-3/\varepsilon)/((3b^2/\varepsilon^2+1)\mathrm{acot}(b/\varepsilon)-3b/\varepsilon)\sin x_2\cos x_2-2\Omega^2x_3\cos x_2\sin x_2)$$
$$\frac{\partial^2 L}{\partial x_3 x_1}=\frac{\partial^2 L}{\partial x_1 x_3}$$
$$\frac{\partial^2 L}{\partial x_3 x_2}=\frac{\partial^2 L}{\partial x_2 x_3}$$
$$\frac{\partial^2 L}{\partial {x_3}^2}=2/({x_3}^2+\varepsilon^2)(\cos x_2)^2(\cos x_1)^2{x_3}^2$$
$$+2(x_p-({x_3}^2+\varepsilon^2)^{1/2}\cos x_2\cos x_1)/({x_3}^2+\varepsilon^2)^{3/2}\cos x_2\cos(x_1){x_3}^2$$
$$-2(x_p-({x_3}^2+\varepsilon^2)^{1/2}\cos x_2\cos x_1)/({x_3}^2+\varepsilon^2)^{1/2}\cos x_2\cos x_1$$
$$+2/({x_3}^2+\varepsilon^2)(\cos x_2)^2(\sin x_1)^2{x_3}^2+2(y_p-({x_3}^2+\varepsilon^2)^{1/2}\cos x_2\sin x_1)/({x_3}^2$$
$$+\varepsilon^2)^{3/2}\cos x_2\sin(x_1){x_3}^2-2(y_p-({x_3}^2+\varepsilon^2)^{1/2}\cos x_2\sin x_1)/({x_3}^2$$
$$+\varepsilon^2)^{1/2}\cos x_2\sin x_1+2(\sin x_2)^2+x_4(2\mathrm{GM}/\varepsilon^4/(1+{x_3}^2/\varepsilon^2)^2x_3$$
$$+1/6\Omega^2a^2(6/\varepsilon^2\mathrm{acot}(x_3/\varepsilon)-12x_3/\varepsilon^3/(1+{x_3}^2/\varepsilon^2)$$
$$+2(3{x_3}^2/\varepsilon^2+1)/\varepsilon^3/(1+{x_3}^2/\varepsilon^2)^2x_3)/((3b^2/\varepsilon^2+1)\mathrm{acot}(b/\varepsilon)$$
$$-3b/\varepsilon)(3(\sin x_2)^2-1)$$
$$+\Omega^2(\cos x_2)^2)$$

Appendix F: Taylor series expansion in terms of invariant / physical components

Suppose $F(u,v,w)$ is a scalar function of orthogonal curvilinear coordinates $\{u,v,w\}$. The *B. Taylor* expansion of $F(u,v,w)$ with respect to the curvilinear component u around the point u_0 by definition is as follows.

$$\begin{aligned} F(u,v,w) &= F(u_0,v,w) + \frac{1}{1!}\frac{\partial F}{\partial u}\bigg|_{u=u_0} du + \frac{1}{2!}\frac{\partial^2 F}{\partial u^2}\bigg|_{u=u_0} du^2 + \cdots \\ &= F(u_0,v,w) + \frac{1}{1!}\mathrm{D}_u\big|_{u=u_0} du + \frac{1}{2!}\mathrm{D}_u^2\big|_{u=u_0} du^2 + \cdots \end{aligned} \tag{F.1}$$

du in (F.1) is the differential form of the curvilinear coordinate u, and as such depends on the definition of the curvilinear coordinates $\{u,v,w\}$. However, when dealing with physical quantities it is advantageous to present the *Taylor* series expansions in terms of invariant quantities, which do not depend on the coordinate systems. It is for the reason that natural / physical quantities indeed, do not depend on any coordinate system. According to *A. Eringen* (1962) the physical / invariant form of du is as follows.

$$du^{(1)} = \sqrt{g_{uu}}du \tag{F.2}$$

where g_{uu} is the metric tensor of the u component of the curvilinear coordinates $\{u,v,w\}$. The metric tensor of the orthogonal curvilinear coordinates $\{u,v,w\}$, i.e. $\{g_{uu},g_{vv},g_{ww}\}$, can be derived from the transformation relations of the curvilinear coordinates $\{u,v,w\}$ into Cartesian coordinates $\{x,y,z\}$ as follows.

$$\begin{cases} x = x(u,v,w) \\ y = y(u,v,w) \\ z = z(u,v,w) \end{cases} \tag{F.3}$$

or in short

$$\mathbf{x} = \mathbf{x}(u,v,w) \tag{F.4}$$

where

$$\mathbf{x} = \begin{bmatrix} x(u,v,w) \\ y(u,v,w) \\ z(u,v,w) \end{bmatrix} \tag{F.5}$$

$$g_{uu} := \left\langle \frac{\partial \mathbf{x}}{\partial u} \mid \frac{\partial \mathbf{x}}{\partial u} \right\rangle = \langle \mathbf{t}_u \mid \mathbf{t}_u \rangle = (\frac{\partial x}{\partial u})^2 + (\frac{\partial y}{\partial u})^2 + (\frac{\partial z}{\partial u})^2 \tag{F.6}$$

$$g_{vv} := \left\langle \frac{\partial \mathbf{x}}{\partial v} \mid \frac{\partial \mathbf{x}}{\partial v} \right\rangle = (\frac{\partial x}{\partial v})^2 + (\frac{\partial y}{\partial v})^2 + (\frac{\partial z}{\partial v})^2 \tag{F.7}$$

$$g_{ww} := \left\langle \frac{\partial \mathbf{x}}{\partial w} \mid \frac{\partial \mathbf{x}}{\partial w} \right\rangle = \langle \mathbf{t}_w \mid \mathbf{t}_w \rangle = (\frac{\partial x}{\partial w})^2 + (\frac{\partial y}{\partial w})^2 + (\frac{\partial z}{\partial w})^2 \tag{F.8}$$

$\mathbf{t}_u := \partial \mathbf{x} / \partial u$, $\mathbf{t}_v := \partial \mathbf{x} / \partial v$, and $\mathbf{t}_w := \partial \mathbf{x} / \partial w$ are the local tangent vectors of the coordinate line of u, v, and w, respectively. Accordingly, the normalised local tangent vectors $\{\mathbf{e}_u, \mathbf{e}_v, \mathbf{e}_w\}$ can be defined as follows.

$$\mathbf{e}_u := \frac{\mathbf{t}_u}{\sqrt{g_{uu}}} \tag{F.9}$$

$$\mathbf{e}_v := \frac{\mathbf{t}_v}{\sqrt{g_{vv}}} \tag{F.10}$$

$$\mathbf{e}_w := \frac{\mathbf{t}_w}{\sqrt{g_{ww}}} \tag{F.11}$$

By definition, the directional derivative of $F(u,v,w)$ along the coordinate line of u is as follows.

$$\nabla_{\mathbf{e}_u} F(u,v,w) = \langle \operatorname{grad} F(u,v,w) \mid \mathbf{e}_u \rangle \tag{F.12}$$

The gradient of $F(u,v,w)$, $\operatorname{grad} F(u,v,w)$, in terms of orthogonal coordinates $\{u,v,w\}$ is given by

$$\begin{aligned} \operatorname{grad} F(u,v,w) = {} & \frac{1}{\sqrt{g_{uu}}} \frac{\partial F(u,v,w)}{\partial u} \mathbf{e}_u \\ & + \frac{1}{\sqrt{g_{vv}}} \frac{\partial F(u,v,w)}{\partial v} \mathbf{e}_v \\ & + \frac{1}{\sqrt{g_{ww}}} \frac{\partial F(u,v,w)}{\partial w} \mathbf{e}_w \end{aligned} \tag{F.13}$$

Substitution of (F.13) in to (F.12) results in

$$\begin{aligned} \nabla_{\mathbf{e}_u} F(u,v,w) &= \langle \operatorname{grad} F \mid \mathbf{e}_u \rangle \\ &= \frac{1}{\sqrt{g_{uu}}} \frac{\partial F}{\partial u} \\ &= \frac{1}{\sqrt{g_{uu}}} \mathrm{D}_u F \end{aligned} \tag{F.14}$$

From (F.14) one may conclude that

$$D_u F = \sqrt{g_{uu}} \nabla_{\mathbf{e}_u} F(u,v,w). \tag{F.15}$$

Now, let us return to the *Taylor* series expansion (F.1). By using the definition (F.2) and (F.15) now we can offer an alternative presentation for the *Taylor* expansion (F.1), which depends on the physical component $du^{(1)}$.

$$F(u,v,w) = F(u_0,v,w) + \frac{1}{1!}\nabla_{\mathbf{e}_u} F du^{(1)} + \frac{1}{2!}\nabla_{\mathbf{e}_u}(\nabla_{\mathbf{e}_u} F)(du^{(1)})^2 + \cdots \tag{F.16}$$

CURRICULUM VITAE (Date: 23/07/00)

13.04.1962:	Born in Mashhad/Iran
1969 - 1974:	Primary Education, Noor Primary School, Tabriz/Iran
1974 - 1977:	Secondary School Education Jahane-Danesh Secondary School, Mashhad/Iran.
1977 - 1981:	High School Education,. Kharazmi High School, Tehran/Iran.
1981 – 1983:	Military Service, Ghale-Morghi Airbase Tehran/Iran
9.1984 - 7.1987:	Bachelor of Science (BSc.) in Surveying, K.N. Toosi University of Technology, Tehran/Iran.
9.1988 - 7.1994:	Master of Science (M. Sc.) in Geodesy, K.N. Toosi University of Technology, Tehran/Iran.
1989 - 1995:	Teaching assistant at the Survey Engineering Department of K.N. Toosi University of Technology, Tehran/Iran, and Survey Engineering Department of Tehran University, Tehran/Iran.
1.1995 - 7.1996:	Fulfilment of Ph.D. conditions in order to commence the Ph.D. studies at the Department of Geodesy and GeoInformatics, University of Stuttgart; Germany. The conditions included writing a Masters thesis, attending some courses and writing two examinations.
8.1996 - 12.1999:	Ph.D. Studies at the Department of Geodesy and GeoInformatics, University of Stuttgart/Germany.
1.2000 – 3.2000:	Research assistance at the Department of Geodesy and GeoInformatics, University of Stuttgart/Germany.

ISBN: 3-00-006457-5